Western Graduate&PostdoctoralStudies

Western University
Scholarship@Western

Electronic Thesis and Dissertation Repository

11-5-2020 1:45 PM

Molecular Mechanisms Regulating the Platelet Thrombin Receptor PAR4

Pierre E. Thibeault, *The University of Western Ontario*

Supervisor: Ramachandran, Rithwik, *The University of Western Ontario*

A thesis submitted in partial fulfillment of the requirements for the Doctor of Philosophy degree in Physiology and Pharmacology

© Pierre E. Thibeault 2020

Follow this and additional works at: https://ir.lib.uwo.ca/etd

 Part of the Pharmacology Commons

Recommended Citation

Thibeault, Pierre E., "Molecular Mechanisms Regulating the Platelet Thrombin Receptor PAR4" (2020). *Electronic Thesis and Dissertation Repository*. 7479.
https://ir.lib.uwo.ca/etd/7479

This Dissertation/Thesis is brought to you for free and open access by Scholarship@Western. It has been accepted for inclusion in Electronic Thesis and Dissertation Repository by an authorized administrator of Scholarship@Western. For more information, please contact wlswadmin@uwo.ca.

Abstract

Proteinase activated receptor 4 (PAR4) is a G-protein-coupled receptor with an important role in the platelet response to vascular injury. In platelets, PAR4 activation, by thrombin-cleavage of its N-terminus and unmasking of a tethered ligand, leads to G-protein- and β-arrestin-mediated intracellular signalling pathways which result in platelet activation, shape change, and ultimately, platelet aggregation. As an important platelet thrombin receptor, PAR4 is an interesting target for the development of anti-platelet therapeutics. However, molecular determinants of PAR4 activation, signalling, and signal regulation remain poorly understood. In this thesis, mechanisms of PAR4 activation and signalling were studied through determination of the molecular basis of agonist binding at the extracellular surface of the receptor that result in G-protein signalling and β-arrestin recruitment and evaluation of the role of Helix-8 and C-terminal tail residues on effector interaction and signalling. In our first series of experiments, we evaluated the impact of single amino acid substitutions to the parental PAR4 agonist peptide, AYPGKF-NH_2, in an effort to understand the chemical characteristics enabling activity at the PAR4 receptor. We identified key residue characteristics contributing to agonist peptide activation of PAR4. We further showed that different chemical modifications affect G-protein and β-arrestin signalling through PAR4, providing leads for further development of biased ligands of PAR4. Additionally, using *in silico* receptor modelling and peptide docking, we identify a key residue in the ECL2 of the receptor that is required for receptor activation by either peptide or enzyme-revealed tethered ligand. Subsequent studies evaluated the role of the Helix-8 and C-terminal tail motifs in PAR4 and the related receptor, PAR2, on intracellular effector interaction and signalling. PAR4 was compared to PAR2 since several key Class A GPCR regulatory sites are missing in PAR4 and are retained in PAR2. These studies have revealed residues and structural features that are involved in PAR4 interaction with $G\alpha_{q/11}$ and β-arrestin. Importantly we also identified key differences in residues that are important for signalling following enzyme- versus peptide- activation of PARs. Taken together, this body of work enhances our

understanding of how PAR4 engages and is activated by agonists to promote signalling and cellular function.

Keywords

G-protein-coupled receptor (GPCR), proteinase activated receptor 4 (PAR4), G-protein, β-arrestin, platelet, biased signalling, peptide, Helix-8, C-terminal tail, signalling

Summary for Lay Audience

This thesis studies the molecular basis of signalling from Proteinase activated Receptor-4 (PAR4), a thrombin-activated GPCR that is an important regulator of the innate immune response to injury or infection. When blood vessels become damaged, they release signals to communicate with blood cells, called platelets. Proteins expressed on the surface of the platelet, called receptors, receive the signals from the damaged blood vessel and signal platelets to become active and change shape – making them sticky and forming a blood clot. This is the first step in repairing a damaged vessel. Sometimes this clotting response becomes overactive when a person is at significant risk of heart attacks or stroke, thus, a lot of drug discovery efforts have gone into blocking this process. A group of these cellular receptors, called G-protein-coupled receptors (GPCRs), become activated by signals sent from the damaged blood vessel leading to platelets becoming activated. Thus, studies investigating how this process happens and how to therapeutically block it have been very important for drug development. In recent years, a GPCR named Proteinase Activated Receptor 4 (PAR4) has become an increasingly attractive target for blocking platelet activation. It is believed that blocking PAR4 activation will allow for appropriate blood clotting to occur through other receptors (such as PAR1) but will block the formation of larger, more dangerous, blood clots. Unfortunately, there is a lot we do not know about how PAR4 becomes activated and how it communicates these signals in the platelet. In a series of studies, we investigated how the receptor becomes activated through drug binding (receiving the signal) and interaction with proteins inside the cell (how it communicates the signal into the cell). We have identified properties of drugs that can selectively target PAR4. We have also identified key parts of the PAR4 receptor that control PAR4 signalling. Together, these studies uncover new insights into PAR4 signalling and aid development of therapies targeting PAR4.

Co-Authorship Statement

All studies presented in this thesis were designed, completed, and analyzed by Pierre E. Thibeault in the laboratory of Dr. Rithwik Ramachandran, with experimental contributions from co-authors listed below. Pierre E. Thibeault also prepared manuscripts of all chapters. Dr. Rithwik Ramachandran contributed to design, analysis, interpretation, and manuscript preparation for all chapters.

Chapter 1:

Chapter 1 contains components of a review paper published by Pierre E. Thibeault and Dr. Rithwik Ramachandran. Pierre E. Thibeault contributed to manuscript text and prepared the table and all figures.

Thibeault, P. E., and Ramachandran, R. (2020) Biased signalling in platelet G-protein-coupled receptors. *Can. J. Physiol. Pharmacol.* 10.1139/cjpp-2020-0149

Chapter 2:

Jordan Cole LeSarge and Michaela Fernandes completed all peptide synthesis and design, with direction from Dr. Leonard G. Luyt. Jordan Cole LeSarge and D'Arcy Arends assisted Pierre E. Thibeault with collection of bioluminescence resonance energy transfer and calcium experiments for some of the peptides described. Dr. Peter B. Stathopulos contributed his expertise to interpretation and presentation of peptide docking and solution NMR data. Jordan Cole LeSarge wrote all methods related to peptide synthesis. Dr. Peter Chidiac, Dr. Peter B. Stathopulos, Dr. Leonard G. Luyt, and Jordan Cole LeSarge assisted with manuscript editing.

Thibeault, P. E., LeSarge, J. C., Arends, D., Fernandes, M., Chidiac, P., Stathopulos, P. B., Luyt, L. G., and Ramachandran, R. (2019) Molecular basis for activation and biased signaling at the thrombin-activated GPCR Proteinase Activated Receptor-4 (PAR4). J. Biol. Chem. 10.1074/jbc.RA119.011461

Chapter 3:

All data collection and analyses were conducted by Pierre E. Thibeault. Manuscript preparation was conducted by Pierre E. Thibeault and Dr. Rithwik Ramachandran.

Thibeault, P. E., and Ramachandran, R. (2020) Role of the Helix-8 and C-Terminal Tail in Regulating Proteinase Activated Receptor 2 Signaling. *ACS Pharmacol. Transl. Sci.* 10.1021/acsptsci.0c00039

Chapter 4:

All data collection and analyses were conducted by Pierre E. Thibeault. Manuscript preparation was conducted by Pierre E. Thibeault and Dr. Rithwik Ramachandran.

Acknowledgments

I would like to begin by acknowledging my supervisor and mentor, Dr. Rithwik Ramachandran, for giving me the opportunity to learn from him. Dr. Ramachandran's support, patience, and willingness to let me dig into the science and follow my interests have been fundamental in my training and development as a scientist. Thank you for allowing me the autonomy to grow and explore the field, even when it took us away from our original project ideas. Together our combined research interests have led to exciting new data, trips around the world, and numerous collaborations. Thank you for modelling for me the value of collaboration, taking every opportunity to share data, and fearlessly venturing into unknown areas of the field. You've provided me a once in a lifetime opportunity to see firsthand how a research program is developed which I hope one day to utilize in a lab of my own. You've given me the freedom to explore my scientific and academic interests and have always shown faith in my ability to conquer them. Without your support and example, I am confident I would not be the researcher I am becoming. As your first PhD student at Western of many to come, I want to thank you for being everything I have needed in a mentor. Five years after we began this journey, I am confident I have found a collaborator, mentor, and colleague for life and I am very grateful.

I would like to thank Dr. Peter Chidiac who helped to co-supervise my thesis work and has always made me feel like a colleague with a valued insight. You have taught me what it means to be a kind and supportive mentor. For all the times you built me up when I doubted myself, whether you knew it or not, I thank you. I must also thank Dr. Peter B. Stathopulos. Without your contributions and mentorship, I would never have been able to realize my passion for structural biology. You have remained an exemplar of what it means to mentor, collaborate, and assist trainees in realizing potential they didn't know they possessed. I consider myself immensely fortunate to have had the opportunity to learn and grow from both of you.

I would also like to thank Dr. Christina Vanderboor, who taught me my very first cell cultures and experimental approaches. Dr. Vanderboor has become a trusted voice of reason, a confidant, and friend. I am forever grateful for having you there during my first

PhD years, for discussing the science with me, and sharing your passion for all things GPCR. I would be remiss if I also did not thank you for teaching me how to crochet – a skill I still use to this day to manage the stresses of PhD life. Thank you for always being a colleague and a friend – and for frequently reminding me that balance is important.

Thank you to all of my Ramachandran lab colleagues and collaborators, past and present, who have always treated me as a valued colleague. I would also like to thank to thank my advisory committee Drs. Peter Chidiac, Peter B. Stathopulos, Lina Dagnino, and Qingping Feng for their contributions to my thesis and development. I'd like to thank Tom Stavraky, Dr. Christine Bell, and Dr. Nicole Campbell, all of whom have helped foster my ever-growing love for teaching.

As I reflect, there have been so many friends and colleagues on campus who have truly enriched my experience at Western. I truly wish I could list and thank you all personally – you all have truly made my time at Western so warm and welcoming. I have to thank Patrick Hill, Tyler Cooper, and Tyler Lalonde for always being there for me and never making me feel like I was alone in this journey - I value your friendships greatly and could not have done this without you. I'd also like to thank one of my best friends, Nick Riddick, who is currently finishing his PhD at McMaster University. Going through this experience alongside you has been a joy and a privilege and I look forward to all of the amazing things you are going to accomplish.

To my partner, Stephen – here we are, we made it. It is impossible to try and find all the words necessary to describe how much your love and support means to me. Every experiment and word contained in this thesis represents 5 years of our sacrifice and hard work. You are the best friend I've ever had, and I cannot express to you how much your dedication, love, and support have meant to me while I've been on this path. Thank you for all the phone calls, patience, drives between Niagara and London every weekend, silly selfies, laughs, and putting up with my endless scientific conversations. Truly, none of this would have been possible without you by my side. I am looking forward to the next chapter of our lives together, along with our little Hypatia.

To my beautiful mother, Marie Kinghorn, I love you with all my heart. Since my earliest memories you have always told me I could do anything that I set my heart to. Thank you for always believing in me, supporting me, and being there for me. You are truly the best friend a son could ask for. Thank you for always seeing the positive in me and for never letting me give up when things got tough. Thank you for fostering my academic development and curiosity from a young age.

To my father, Ghislain Thibeault, I love you so much. Thank you for being there for me and everything you've taught me. Thank you for never letting me forget the value of hard work and always pushing me to keep going. Thank you for never letting me believe that any challenge was too much for me. You've always had my back and been in my corner – I've never felt small knowing you were there. To my step-mother Diane, thank you for your joy and love. I've always considered myself so fortunate to have you in my life.

To my siblings, I thank you for putting up with me through the "chicken" and "little Napoleon" phases. While we may not be related by blood, I've never felt like an only child. To my brothers, Patrick and Daniel, you showed me the love of big brothers and I've always been better for it. To my beautiful sister Julie, thank you for being one of the best friends I could ask for. Thank you, Julie and Marcus, for being there for me – there were some pretty tough times that I made through because I knew how much you care. To my beautiful nieces, Celine and Scarlett – you make your uncle Pierre so proud! Thank you to my sister-in-law Julie for always reminding me to be grateful for every moment. To my partner's family – Zeljka, JP, and Ashley thank you for all the love and kindness you've shown me in welcoming me into your lives.

Thank you to the sources of research funding that have made this work possible including the Canadian Institutes of Health Research (grant 376560), Natural Sciences and Engineering Research Council (Aim #1 Luyt and Stathopulos laboratories), Ontario Graduate Scholarships, and Western Graduate Research Scholarship.

Finally, I would like to thank everyone involved in getting me to this moment. It has truly been my privilege and joy to learn from all of you.

"May there never develop in me the notion that my education is complete but give me the strength and leisure and zeal continually to enlarge my knowledge." -Maimonides

Table of Contents

List of Tables

List of Figures

List of Supplementary Tables

List of Supplementary Figures

List of Appendices

List of Abbreviations

β-Arr	β-Arrestin
1Nal	(1-naphthyl)-L-alanine
2Nal	(2-naphthyl)-L-alanine
ADP	Adenosine diphosphate
Aib	2-aminoisobutyric acid
AKT	Protein kinase B
ANOVA	Analysis of variance
AP2	Adaptor protein 2
ATP	Adenosine triphosphate
BAK	Bcl-associated killer
BAX	Bcl-2-associated X-protein
BCA	Bicinchoninic acid assay
BCL2	B-cell lymphoma 2
BetaAla	Beta-alanine, βAla
BMS	Bristol Myers Squib
BRET	Bioluminescence resonance energy transfer
cAMP	Cyclic adenosine monophosphate
Cas9	CRISPR-associated protein 9
Cit	Citrulline
CRISPR	Clustered regularly interspaced short palindromic repeats
DAG	1,2,-diacylglycerol
DAPI	4′,6-diamidino-2-phenylindole dihydrochloride
DCM	Dichloromethane
DIPEA	Diisopropylethylamine
DMEM	Dulbecco's Modified Eagle Medium

DMF	N-Dimethylformamide
DMSO	Dimethyl sulfoxide
DNA	Deoxyribonucleic acid
DOPE	Discrete optimized protein energy
EC_{50}	Half maximal effective concentration
ECL	Extracellular loop
EDTA	Ethylenediaminetetraacetic acid
EGTA	Ethylene glycol-bis(β-aminoethyl ether)-N,N,N′,N′-tetraacetic acid
ERK	Extracellular signal-regulated kinases
ESI-MS	Electrospray Ionization mass spectrometry
F(4-fluoro)	4-fluoro-L-phenylalaine
F(4-Me)	4-methyl-L-phenylalanine
F2R	Thrombin-like receptor
F2RL1	Thrombin-like receptor 1, PAR2
F2RL2	Thrombin-like receptor 2, PAR3
F2RL3	Thrombin-like receptor 3, PAR4
FBS	Fetal bovine serum
FCHO2	FCH And Mu Domain Containing Endocytic Adaptor 2
FIJI	FIJI is just image J
Fmoc	fluorenylmethoxycarbonyl
G418	Geneticin
GDP	Guanosine diphosphosphate
GEF	Guanine nucleotide exchange factor
GFP	Green fluorescent protein
GMP	Guanosine monophosphate
GPCR	G-protein-coupled receptor
GRK	G-protein receptor kinase

GTP	Guanosine triphosphate
HATU	*O*-(7-azabenzotriazol-1-yl)-*N*,*N*,*N*′,*N*′-tetramethyluronium hexafluorophosphate
HBSS	Hank's balanced salt solution
HCTU	*O*-(1*H*-6-chlorobenzotriazole-1-yl)-1,1,3,3-tetramethyluronium hexafluorophosphate
HEK	Human embrionic kidney cell
HEPES	4-(2-hydroxyethyl)-1-piperazineethanesulfonic acid
HPLC	High performance liquid chromatography
IC_{50}	Half maximal inhibitory concentration
ICL	Intracellular loop
Inp	Isonipecotic acid
IP_3	1,4, 5-trisphosphate
KCl	Potassium chloride
MAPK	Mitogen-activated protein kinase
MBHA	4-(2′,4′-Dimethoxyphenyl-Fmoc-aminomethyl)-phenoxyacetamido-norleucyl-MBHA resin
MS	Mass spectrometry
Nip	Nipecotic acid
Nle	Norleucine
NMP	N-methylpyrrolidone
NP-40	Nonidet P-40
PAR	Proteinase activated receptor (PAR1-PAR4)
PAR2-AP	PAR2 agonist peptide, SLIGRL-NH_2
PAR4-AP	PAR4 agonist peptide, AYPGKF-NH_2
PBS	Phosphate-buffered saline
PDB	Protein data bank
PI3K	Phosphoinositide 3-kinase

Pip	pipecolic acid
PKA	Protein kinase A
PKC	Protein kinase C
PLC	Phospholipase C
PPP	Platelet-poor plasma
PRP	Platelet-rich plasma
RGS	Regulators of G-protein signalling protein
Rluc	Renilla luciferase
ROCK	Rho-associated protein kinase
RP-HPLC	Reverse-phase high-performance liquid chromatography
SAR	Structure activity relationship
Sar	Sarcosine
SDS-PAGE	Sodium dodecyl sulphate-polyacrylamide gel electrophoresis
SEM/SE	Standard error of the mean (S.E.M.; S.E.)
siRNA	Small interfering ribonucleic acid
SPPS	Solid phase peptide synthesis
TBS	Tris-buffered saline
TBST	Tris-buffered Saline with 0.1% v/v Tween
TFA	Trifluoroacetic acid
THF	Tetrahydrofuran
TIPS	Triisopropylsilane
Tyr(Me)	*O*-methyl-tyrosine
UV	Ultraviolet
YFP	Yellow fluorescent protein

Chapter 1

1 Introduction[i]

1.1 G-protein-coupled receptors

1.1.1 GPCR Structure and Function

G-Protein-coupled Receptors (GPCRs) are the largest superfamily of cellular receptors in humans (over 800), which mediate many cellular responses, often through activation by neurotransmitters and hormones (1–4). Importantly, due to the wide range of physiological roles GPCRs perform and the highly tractable nature of these receptors for drug development, GPCRs are the target for approximately 35% of currently approved drugs (5, 6). GPCRs are characterized by distinct structure that includes seven transmembrane spanning domains, connected by 3 intracellular and extracellular loops.

The superfamily of GPCRs is further divided, based on sequence identity and structural similarity, into 5 subfamilies (commonly referred to as classes) – glutamate (G) rhodopsin (R, commonly referred to as 'Class A'), adhesion (A), and Frizzled/Taste2 (F), and secretin (S), (4, 7). Class A (Rhodopsin-like GPCRs) comprises the largest subfamily of GPCRs, accounting for over 85% of GPCR genes, further divided into 4 subgroups (α, β, γ, δ) based on based on phylogenetic analysis (7, 8).Class A GPCRs are known to be similar in sequence identity, structure, and activation.

GPCRs are cellular proteins with 7 α-helical transmembrane (TM) domains connected by three extracellular loops (ECL1-ECL3) and three intracellular loops (ICL1-ICL3) (Figure

---

[i]A version of this chapter has been published: Thibeault, P. E., and Ramachandran, R. (2020) Biased signalling in platelet G-protein-coupled receptors. *Can. J. Physiol. Pharmacol.* 10.1139/cjpp-2020-0149

1.1A) (1, 9). GPCRs also possess an N-terminal domain sequence (upstream of TM1) and a C-terminal tail sequence (downstream of TM7), the latter of which contains an intracellular helical domain, often referred to as the eighth helix (Helix-8), which is a common site important for interaction with intracellular effectors, both structurally and through direct binding, along with the remainder of the C-tail (Figure 1.1A & B) (9–11). The transmembrane domains interact with one another to arrange the protein into a tertiary, barrel-like, structure which creates an extracellular solvent exposed cavity where the GPCR binds its ligand(s); and an intracellular solvent exposed cavity wherein effectors can bind the activated GPCR (Figure 1.1B) (12, 13). The seven transmembrane (7TM) core of Class A GPCRs is common and highly conserved, while the extracellular and intracellular regions have high levels of heterogeneity in sequence, structure, and function – enabling specificity in targeting by agonists and G-protein/effector sub-type selectivity (3, 7, 14).

Class A GPCRs are most commonly activated by the binding of an extracellular, soluble, hormone ligand which enables activation of the receptor and engagement of the GPCR with intracellular effectors to stimulate intracellular signalling (9, 10, 12). GPCR ligands bind to the GPCR orthosteric site leading to large-scale conformational rearrangements transmitted through the transmembrane domains. These conformational rearrangements are transmitted through the TM bundle and prompt important changes in the intracellular face of the receptor, thus enabling interaction with the heterotrimeric G-proteins and other intracellular effectors, such as β-arrestins and small G-proteins (9, 10, 12). The most prominent of these rearrangements is an outward movement of helix VI (TM6), accompanied by helix V (TM5) movement towards helix VI (9, 15). Additionally, helix VII (TM7) moves inward towards the middle axis of the transmembrane bundle and helix III moves upwards and laterally (9, 15). While crystallography and cryo-EM structures have revealed variance in the magnitude to which each helix moves in a given agonist-bound receptor, rearrangement in helix V and VI have been consistently observed in G-protein-bound structures, and thus are key rearrangements in effector binding, independent of the GPCR studied (9, 15).

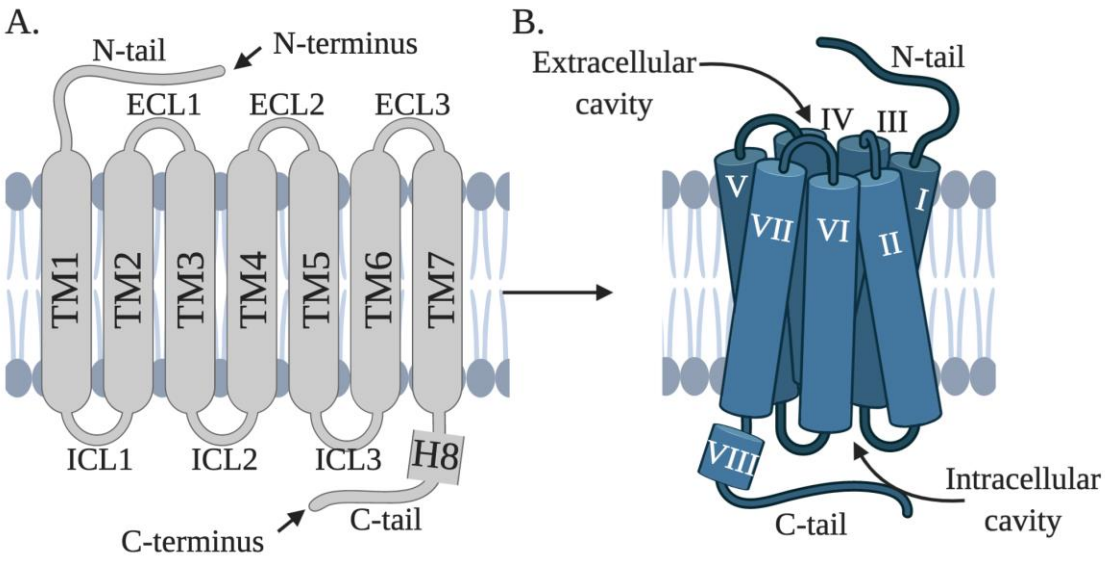

Figure 1.1 General structure of G-protein-coupled receptors (Class A). (A) Linear structure of Class A GPCRs showing N-tail, transmembrane helices (TM1-7), extracellular loops (ECL1-3), intracellular loops (ICL1-3), and C-terminal tail including Helix-8 (H8). (B) Three-dimensional model of Class A GPCRs showing the barrel-like, tertiary-structure adopted through interactions of the transmembrane domains (I-VII) with solvent exposed extracellular and intracellular cavities. (Created with BioRender.com)

1.1.2 GPCR Signalling Mechanisms

GPCRs form a large family of cell surface receptors that respond to a diversity of activators (16). Upon ligand binding, GPCRs trigger activation of intracellular second messenger signalling pathways by engaging one of four major class of guanine nucleotide binding proteins (G-proteins) – $G\alpha_{i/o}$ (inhibition of adenylyl cyclase-mediated cAMP production), $G\alpha_s$ (stimulation of adenylyl cyclase-mediated cAMP production), $G\alpha_{q/11}$ (stimulates membrane-bound PLCβ-mediated production of IP_3 and DAG), and $G\alpha_{12/13}$ (activation of Rho family GTPase signalling) (17, 18). In the inactive state, the heterotrimeric G-proteins consist of a guanosine diphosphate (GDP) bound α subunit that is associated with β and γ subunits. Ligand-bound GPCRs act as a guanine nucleotide exchange factor (GEF) and trigger guanine nucleotide exchange at the G-protein α subunit (19, 20). The release of GDP and subsequent binding of GTP in G-protein α subunits leads to the release and/or conformational remodeling of the βγ subunits, and allows the G-protein α and βγ subunits to activate effectors, produce second messengers, and propagate intracellular signals (21–23).

G-protein signalling is terminated by the intrinsic GTPase activity of the G-protein α subunits, which can be further accelerated by interactions with Regulators of G-protein Signalling (RGS) proteins (24). The activated GPCR is rapidly phosphorylated by GPCR kinases (GRKs), often at serine and threonine residues on the receptor C-terminal tail, enabling binding with β-arrestins (25). The initial docking of β-arrestins on the phosphorylated GPCR C-terminal tail is followed by interactions with the intracellular core of the GPCR transmembrane bundle, which sterically block Gα interaction, thus terminating G-protein-mediated signalling (26–28). β-arrestins also scaffold the activated receptors to cellular endocytic proteins and promote receptor internalization (29–31). Depending on the strength of receptor interaction with β-arrestins, receptors can either be recycled back to cell membrane (weak binders) or traffic to the lysosomes for degradation (strong binders) (32–35).

In addition to the classical role in terminating GPCR signalling, β-arrestins are now recognized as mediators of G-protein-independent signalling from GPCRs by scaffolding

other signalling mediators (32, 36, 37). For a number of different GPCRs it has been proposed that both G-protein- and β-arrestin-mediated signalling lead to distinct cellular responses, some being beneficial and others being pathological (31, 38). This extends the now well accepted idea that a single receptor can/may couple to multiple G-protein subtypes, and further, adds β-arrestins to the list of GPCR interacting signalling effectors. The ability of a single receptor to activate multiple signalling effectors has also provided the stimulus for seeking ligands that are able to stabilize different GPCR conformations which enable the receptor to selectively engage different signalling pathways (39–41). This paradigm, variously termed as functional selectivity, biased agonism, or biased signalling, has opened up a novel strategy for therapeutically targeting GPCRs, that goes beyond simply blocking or activating receptor signalling.

1.1.3 Biased Agonism of GPCRs

There is significant interest in the emerging field of GPCR pharmacology referred to as *biased agonism*. Classically, it was thought that each GPCR had a physiological agonist(s) that would activate the receptor to accomplish a defined signalling paradigm (Figure 1.2A). Thus, it was believed that for therapeutic targeting of the receptor drug therapies were aiming at turning “on” the receptor (Figure 1.2A) through agonism; or inhibiting activation and signalling by turning “off” the receptor through antagonism (Figure 1.2B). The concept of biased agonism was formally proposed in the 1990s and involves the phenomenon that some receptor agonists can induce differential signalling through the same receptor in order to accomplish varied physiological outcomes (Figure 1.2C) (42–49). The discovery of biased agonism has many potential applications and challenges the classical signalling model. Furthermore, investigation of biased agonism is leading to the development of new receptor agonists that selectively avoid or inhibit activation of signalling cascades that may contribute to pathology, while leaving non-pathogenic, homeostatic signalling intact (48). Currently, the consensus among experts is that this process is mediated through differences in receptor conformational changes dependent on the activating agonist (50–52). It is widely debated whether the differential signalling is due to agonist binding to, and thus stabilizing, receptor conformations favoring one signalling pathway over another (i.e. a biased agonist has high affinity for a

conformation favouring biased signalling) or whether the conformational requirement for biased signalling is facilitated by transmembrane reorganization induced by agonist binding. Irrespective of this debate, it is hypothesized that subtle differences in receptor conformation can lead to diverse interactions with key intracellular proteins, including G-proteins and β-arrestins. Understanding the distinct signalling signatures that may exist between agonists for the same receptor provides valuable insight into the development of pharmaceuticals that selectively activate or inhibit various signalling processes. Additionally, dissection of signalling pathway contributions through preferential activation of a pathway versus another provides insight into which pathways are responsible for signalling in health and disease.

An example of the importance of biased agonism can be observed with the μ-opioid receptor (μOR). Through various knockout studies, the μOR receptor agonist, morphine, was revealed to signal both beneficial and deleterious signalling pathways simultaneously. Bohn et al. found that activation of μOR with morphine displayed differential signalling in β-arrestin-2 knockout mice compared to wild-type mice (53). In this study, wild-type mice showed pain relief, as expected; however, these benefits were accompanied by unwanted side effects, including antinociceptive tolerance. Interestingly, β-arrestin-2-knockout mice failed to develop tolerance and thus continued to have the antinociceptive benefits of morphine (53). β-arrestins are an important desensitization and internalization protein. Recall that phosphorylation of GPCRs causes the recruitment of β-arrestins in many GPCRs, leading to cessation of receptor/G-protein coupling (1.1.2). Additionally, β-arrestins function as scaffolding proteins for endocytic machinery, such as adaptor protein 2 (AP2) during clathrin-mediated endocytosis. Bohn and colleagues concluded that β-arrestin-2 appears to have an important modulatory effect on μ-OR, mainly in decreasing receptor desensitization, which could have important implications on treating pain and narcotic tolerance through manipulation of β-arrestin-2 in a vulnerable patient subset (53). Discovery of the importance of β-arrestin-2 in inhibiting the analgesic effect of morphine (an unwanted side effect) has provoked many studies to investigate other endogenous μOR agonists and has led to the development of several new drugs that selectively do not engage β-arrestin-2 and

therefore may be more efficacious in analgesic applications (54). One such biased ligand, oliceridine (TRV130), activates μOR-mediated G-protein signalling while mitigating β-arrestin recruitment; thus, maintaining analgesic properties while reducing deleterious side effects (55, 56). From this example, it is apparent that the study of downstream effecters and receptor-protein interactions can lead to discovery of potential therapeutic targets. The discovery of biased agonism by design can also be shown with 5-HT, serotonin, receptors. Some studies have shown biased agonism with 5-HT receptors where striking differences are reported between physiological agonists- each engaging very different signalling cascades after receptor activation (57). Understanding the ways in which these various agonists activate the receptor and induce differential signalling has led to more targeted design of small molecules capable of eliciting similar signalling biases.

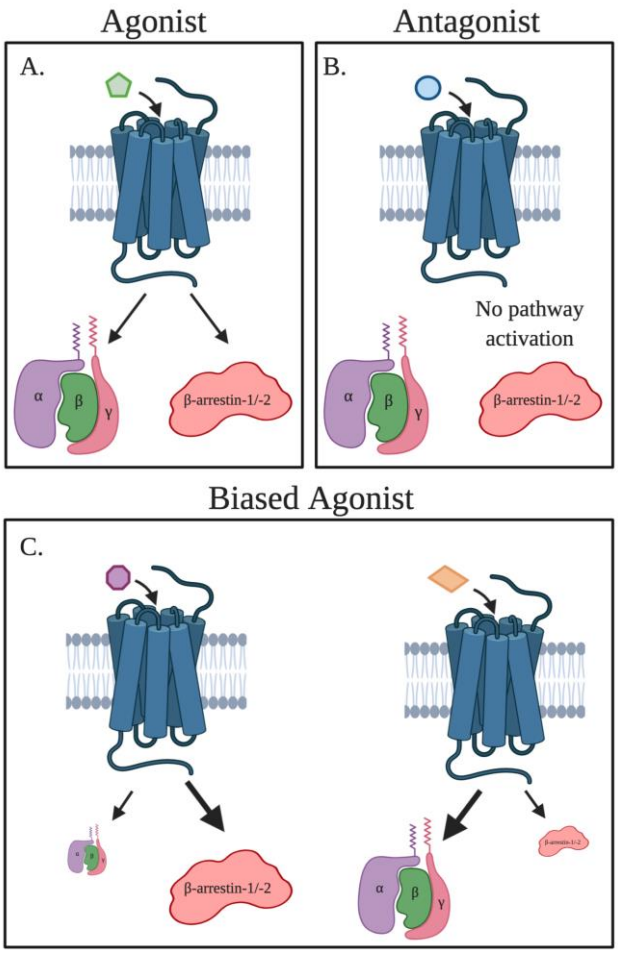

Figure 1.2 Ligand-receptor signalling paradigms (A) Schematic of classical Class A GPCR signalling wherein, a GPCR is activated by its endogenous ligand and signals to all of its effector partners. (B) Schematic of classical therapeutic approach of an orthosteric, neutral, antagonist that blocks GPCR activation by binding to the orthosteric site of the receptor without having any signalling activity at the receptor. (C) Schematic of biased agonism, wherein, one ligand (purple hexagon, left) is able to activate the GPCR in a biased manner and initiate signalling to β-arrestins but not G-protein signalling pathways; the other ligand (orange rhombus, right) has the opposite activity and is able to bias signalling to the G-protein-dependent signalling pathways while effectively blocking or disengaging β-arrestin-dependent signalling (similar to what is observed with oliceridine for μOR). (Created with BioRender.com)

1.2 Platelet physiology and a role for selected targeting of GPCRs in anti-platelet therapeutics

1.2.1 Platelet physiology

1.2.1.1 Platelet biogenesis and elimination

Platelets were first described in the scientific literature in the mid to late 1800's by a number of scientists, including William Osler and George Hayem, who recognized them as small anucleate disk-like structures in blood (58). At this time, platelets were believed to be fragments of disintegrated leukocytes, clots of fibrin, or precursors to red blood cells. Giulio Bizzozero is widely credited with identifying platelets as a distinct morphological element in blood and for conducting the definitive studies that uncovered the critical role of platelets in haemostasis (59). Bizzozero, also credited with first describing bone marrow megakaryocytes, however failed to recognize them as the source of platelets – a finding attributed to James Wright who noted similarities between granule contents in megakaryocytes and platelets (60). The production of platelets (thrombopoiesis) occurs primarily in the bone marrow from megakaryocytes. Megakaryocytes, formed by the differentiation of hematopoietic stem cells, home to the perivascular niche where they interact with sinusoidal bone marrow endothelial cells and form dynamic transendothelial pseudopods which project into the lumen of bone marrow sinusoids. These extensions into the sinusoids elongate and are described as pro-platelets, which remain tethered to the megakaryocytes by thin cytoplasmic bridges. The release of the platelet into the blood occurs from the tip of the pro-platelets and represents the final step in the process of platelet biogenesis (61, 62).

Platelets have a short lifespan and are eliminated within days (4-6 days in mice; 5-10 days in humans) (63, 64) via seclusion in the spleen and other organs, or through deposition at sites of vascular injury. Even in the absence of such consumption, aged platelets undergo apoptosis and are removed from circulation. A shift in the balance of the pro-apoptotic (BAX-BAK) and anti-apoptotic (BCL2) proteins is believed to play an important role in this spontaneous apoptosis of ageing platelets (65). Thus, constant

production and elimination of platelets serves to maintain normal platelet count in a healthy individual at around 150,000-300,000 cells per microliter.

1.2.1.2 The delicate balance of platelet-receptor signalling in haemostasis and thrombosis

Throughout their short lifespan, platelets must perform a delicate balancing act. They must remain poised for activation in response to a disruption of vascular integrity yet remain in their inactive state within intact vessels. Platelets are aided in performing this delicate act by the endothelial cells lining the blood vessels. The intact endothelial monolayer lining the inner surface of blood vessels acts to actively suppress platelet activation by physically separating platelets from the underlying platelet-activating matrix components, such as collagen, and by constantly producing and secreting factors that prevent platelet activation (e.g. thrombomodulin, ectonucleotides, prostaglandin I_2 (PGI_2), nitric oxide (NO)).

In the event of vascular injury, platelet activation is rapid and is initially mediated by platelet glycoprotein (GP) Ib-V-IX interaction with von Willebrand factor (vWF) in the subendothelial matrix. This initial interaction slows the circulating platelets and enables further interaction between platelet adhesion receptors/integrins and their counter receptors; and/or adhesive matrix components (e.g. GPVI-Collagen or αIIbβ3-Fibronectin). At the cellular level, these signals also trigger a cytoskeletal rearrangement in the platelets and cause platelet spreading which increases their attachment to subendothelial surfaces at the sites of injury. The initial activation of platelets further involves signalling mediated by factors released from the damaged cells in an injured blood vessel (e.g. ADP) and produced during coagulation (e.g. thrombin). The inflammatory response accompanying the injury may also produce factors (e.g. platelet-activating factor) that further activate platelets. Crucially, these signals from the injured vascular cells are amplified dramatically by the release of platelet granule contents including thromboxane A_2 (TXA_2), adenosine diphosphate (ADP), and serotonin which further amplify platelet activation and serve to recruit additional platelets to the site of a growing thrombus. The release of platelet granules involves cytoskeletal rearrangement, fusion of granules with the open-canalicular system, and release of granule contents (66,

67). Activated platelets also provide a surface on which additional thrombin is generated and fibrin can accumulate (68).

Many of the factors that contribute to platelet activation in response to injury are also engaged in the inappropriate activation of platelets, which occurs within blood vessels in disease. Endothelial dysfunction, resulting from diseases such as diabetes, leads to a loss of molecules that are beneficial to maintenance of a healthy endothelium, like prostaglandin I2 and nitric oxide (PGI_2 and NO, respectively), and thus is an important driver of platelet activation in disease (69–71). Factors that are produced in vessel injury can also be generated in unhealthy blood vessels, as a result of inappropriate endothelial signalling. For example, lysophosphatidic acid (LPA), in atherosclerotic plaques, can trigger platelet activation that in turn causes the release of factors such as ADP and TXA_2 from platelets, which trigger inappropriate platelet aggregation and thrombosis.

Many of these important mediators of platelet activation act on platelet cell surface GPCRs to mediate the various phases of platelet activation. In the following sections, I will discuss the major, receptor-proximal, signalling pathways engaged by GPCRs, provide a brief overview of the different GPCRs expressed in human platelets, and discuss whether selective targeting of signalling pathways downstream of these different platelet GPCRs might provide a route to safer and more efficacious anti-platelet agents.

Platelets express many GPCRs that respond to soluble mediators produced at the site of injury or in diseases to initiate the platelet aggregation sequalae. As such, GPCR signalling in platelets is an attractive therapeutic target that may allow some level of platelet activation while concurrently preventing the amplification that occurs through autocrine and paracrine signalling. Indeed, GPCRs have proven to be highly tractable drug targets and a number of anti-platelet agents are currently in clinical use target platelet GPCRs (72). In the following subsections, the primary platelet-expressed GPCRs are outlined and contextualized within the currently available literature on their engagement with different G-protein-mediated and G-protein-independent signalling pathways and their contribution to different aspects of platelet activation.

1.2.2 Proteinase activated receptors

Human platelets express both PAR1 and PAR4, while murine (mouse and rat) platelets express PAR3 and PAR4 (73–77). PAR1 and PAR4 are two of over 30 GPCRs expressed in human platelets. Since thrombin is the most potent stimulus for platelet activation, considerable research has been conducted to investigate the role of these platelet thrombin receptors on platelet activation and aggregation. This section serves as an introduction to signalling and therapeutic targeting of PAR1 and PAR4 specifically in the platelet context. In the following sections (1.3-1.5), PAR discovery (1.3.1), expression profile (1.3.2), activation (1.3.3), therapeutic targeting (1.4), and regulation (1.5) will be discussed in greater detail.

Upon activation, both PAR1 and PAR4 signal through common G-protein pathways including coupling and activation of $G\alpha_{q/11}$ and $G\alpha_{12/13}$ (78–80). Although coupling to $G\alpha_{i/o}$ has been reported for PAR1 and PAR4, in some instances this coupling may require crosstalk with certain purinergic receptors (Table 1.1; Figure 1.3 & 1.5) (81, 82). While PAR1 and PAR4 signal through common G-proteins, there are reported differences in the kinetics of PAR1- and PAR4-dependent G-protein signalling, with PAR4 causing a slower and more sustained calcium signalling compared to PAR1 (83). Coupling to other intracellular effectors, such as β-arrestins, has also been demonstrated for both PAR1 and PAR4. β-arrestin-mediated scaffolding of signalling effectors can occur downstream of both PAR1 and PAR4, though a role for PAR1 coupling to β-arrestin in platelets has not yet been established (84–87). Previously, we have shown that PAR4-mediated activation of β-arrestins is involved in the Akt signalling pathway and may in fact synergize with $G\alpha_{q/11}$-mediated signalling to activate platelets (85). Association of PAR4 with the purinergic $P2Y_{12}$ receptor in platelets is also proposed to support β-arrestin-mediated sustained signalling to Akt and aid in recruitment of β-arrestins, as well as appropriate cellular trafficking of PAR4 (82, 88–90).

Given the important roles for PAR1 and PAR4 activation downstream of their activation, considerable research has focused on these receptors for anti-platelet therapies. As the higher affinity thrombin receptor, much research has focused on antagonism of PAR1

which is thought to initiate PAR-mediated platelet activation. Potent and selective small molecule antagonists of PAR1, including the clinically approved ligand vorapaxar, have been described (91, 92). Vorapaxar potently inhibits PAR1 signalling and is able to effectively inhibit thrombin-mediated platelet activation downstream of PAR1 activation (Figure 1.3) (91). The United States Food and Drug Administration (FDA) approved vorapaxar (brand name Zontivity™) for use as an anti-platelet therapeutic, however, incidence of bleeding including intracranial bleeds have limited its use (Fala, 2015). The bleeding diatheses might stem from the role of PAR1 in maintaining the vascular endothelial barrier, which may be similarly disrupted upon PAR1 antagonism (95). Therefore, indications for the use of vorapaxar have been limited to individuals with prior myocardial infarction or peripheral artery disease (PAD) (95, 100).

By comparison to PAR1, PAR4 has more restricted cellular expression and tissue distribution (see 1.3.2) therefore attention has been turned to targeting this receptor as a better antiplatelet drug target (101, 102). Early efforts to develop anti-platelet antagonists yielded the compound YC-1, a broad spectrum inhibitor of platelet activation (103). Structure activity relationship (SAR) studies of YC-1 yielded the first PAR4-specific antagonist, YD-3 (104). It was determined that YD-3 selectively inhibited PAR4 peptide-(GYPGQV) stimulated platelet activation. In a further SAR, it was shown that the 4"-ethoxycarbonyl group of YD-3 is the major contributing functional group for antiplatelet activity. Further, it was demonstrated that YD-3 was able to prevent GYPGKF peptide-stimulated platelet activation and aggregation, however was unable to inhibit platelet aggregation stimulated by thrombin, thromboxane A2 mimetic U46610, collagen, or SFLLRN (PAR1 agonist peptide) (105). Inhibition was observed with an IC_{50} of 0.13 µM, however, potency of inhibition was found to have a high degree of variability. In addition to variable *in vitro* and *ex vivo* inhibition of platelet activation, YD-3 has a lengthy synthesis route and is highly lipophilic and these limitations prevented use *in vivo*. An additional study sought to modify these limiting chemical characteristics through replacement of an indazole ring with an indole ring, enabling easier synthesis, higher-yield, and improved physical characteristics including decreased hydrophobicity (106). This yielded the compound ML354 which was found to inhibit PAR4 stimulated platelet activation and aggregation, however, was also found to have some limited

activity at PAR1 (106). A promising PAR4-specific antagonist, BMS-986120, has been demonstrated to block thrombin-stimulated G-protein signalling and β-arrestin recruitment to PAR4, *ex vivo* thrombus formation, and platelet aggregation (Figure 1.3) (107–109). BMS-98120 has completed Phase I clinical trials (108).

Despite these promising advances with PAR4 as an anti-platelet target, there remains the question of whether a complete inhibition of PAR4 will also lead to deleterious side effects as observed with the PAR1 anti-platelet therapeutic voropaxar. PAR4 can activate multiple signalling pathways through coupling to $G\alpha_{q/11}$, $G\alpha_{12/13}$, and β-arrestin (Figure 1.3) (85, 110, 111). In previous work, we demonstrated that a pepducin targeting different intracellular motifs in PAR4 could be employed to inhibit platelet activation by blocking G-protein-coupled or β-arrestin-dependent signalling (85). The ability to selectively block GPCRs in a biased manner is of great interest and has been proposed as a strategy for obtaining therapeutically superior drugs for a number of conditions. Therefore, I believe that efforts should be focused on examining the potential to exploit biased PAR4 signalling as a therapeutic approach, which will be further explored in section 1.4 and chapter 2.

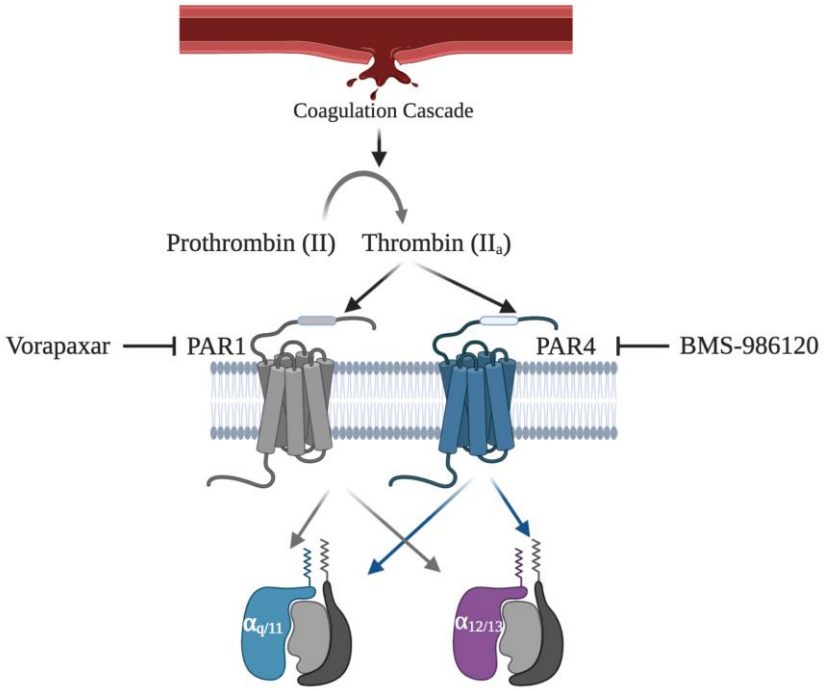

Figure 1.3 PAR G-protein-coupling and signalling pathways in platelets. At the site of vascular injury tissue-derived and coagulation cascade-generated thrombin can act on two platelet thrombin receptors, PAR1 and PAR4. Thrombin, produced in low concentrations locally at the site of injury, activates the high-affinity PAR, PAR1 enabling signalling through $G\alpha_{q/11}$ and $G\alpha_{12/13}$, and subsequent activation of platelets. As the thrombin concentration increases locally on the growing platelet thrombus, the lower affinity thrombin receptor, PAR4, is cleaved and able to signal through shared G-protein subtypes. Importantly, while both PAR1 and PAR4 share common signalling pathways, studies have clearly demonstrated unique kinetics and signalling profiles through these common pathways, that enable PAR1 and PAR4 signalling to contribute differently to platelet activation and aggregation. Arrows indicate which cytosolic G-protein subtypes ($G\alpha_{q/11}$ - blue or $G\alpha_{12/13}$ – purple) PAR1 and PAR4 engage following receptor activation. (Created with BioRender.com)

1.2.3 Prostanoid receptors

Prostanoids, a subfamily of eicosanoids, are formed from arachidonic acid by the action of prostaglandin G/H synthase [cyclooxygenase (COX) 1 and 2, respectively] to form the common prostaglandin precursors PGG_2 and PGH_2, which are then acted upon by additional synthases to form prostaglandins (e.g., PGD_2, PGE_2, PGF_{2a}), thromboxane A_2 (TXA_2), and prostacyclin (PGI_2) (Figure 1.4). These prostanoids mediate cellular signalling through a family of Rhodopsin-like/Class A GPCRs that include IP_1 (PGI_2), TP (TXA_2), $EP_{1\text{-}4}$ (PGE_2), FP ($PGF_{2\alpha}$) and $DP_{1\text{-}2}$ (PGD_2) receptors (112, 113). The DP_1, EP_2, EP_4, and IP_1 receptors couple to $G\alpha_s$ and mediate production of cyclic adenosine monophosphate (cAMP) (Figure 1.4). EP_1, FP, and TP subfamilies couple to $G\alpha_{q/11}$ to initiate phospholipase C activation, leading to phosphatidylinositol 4,5, bisphosphate conversion to inositol 1,4, 5-trisphosphate (IP_3) and 1,2,-diacylglycerol (DAG), which results in Ca^{2+} mobilization from the endoplasmic reticulum and protein kinase C (PKC) activation (Figure 1.4). The EP_3 receptor couples largely to the pertussis toxin-sensitive $G\alpha_i$ pathway resulting in a decrease in cAMP levels (Figure 1.4). It must also be stressed that the prostanoid receptors often couple to more than one G-protein to activate second messenger signalling cascades - for example, the $G\alpha_{q/11}$-coupled EP_1, FP and TP receptor families also couple to $G\alpha_{12/13}$ to activate Rho-associated kinases (114) (Table 1.1; Figure 1.4). Generally, in platelets the activation of $G\alpha_s$-coupled prostanoid receptors result in inhibition of platelets, while $G\alpha_i$-, $G\alpha_{q/11}$-, and $G\alpha_{12/13}$-coupled receptor activation results in platelet activation and aggregation (Table 1.1, Figure 1.4).

Prostacyclin (PGI_2) is the major product of cyclooxygenase (COX) and prostaglandin I synthase-catalyzed metabolism of arachidonic acid in the macrovascular endothelium (115, 116) and is a key endothelium-derived inhibitor of platelet activation. PGI_2 stimulates the $G\alpha_s$-coupled IP_1 receptor to activate adenylyl cyclase and elevate levels of cAMP. Nitric oxide, the other negative regulator of platelets produced by endothelial cells, acts directly on guanylyl cyclase to elevate levels of cyclic guanosine monophosphate (cGMP) (117). cGMP, in turn, activates protein kinase A (PKA) which can blunt multiple aspects of platelet function including Ca^{2+} mobilization, integrin activation, secretion (at least in part through inhibition of RhoA signalling), and myosin

light chain phosphorylation (118, 119). Further evidence for IP_1 receptor-mediated signalling as an inhibitor of platelets comes from knockout mouse studies. IP-knockout mice do not develop spontaneous thrombosis, however, are more susceptible to thrombotic stimuli than their wild-type littermates (120). Like PGI_2, TXA_2 is produced by the cyclooxygenase pathway and the action of thromboxane synthase on PGH_2. TXA_2 acts on the TP receptor on platelets and is a potent activator of platelets. Platelets from TP-deficient mice are unresponsive to TXA_2 and exhibit a mild bleeding tendency and are unable to form stable thrombi (121).

G-protein-mediated signalling, through agonist-activated GPCRs, is temporally restricted by second messenger or GPCR kinase-mediated (GRK) phosphorylation of the receptor and β-arrestin recruitment. It is now well established that β-arrestin recruitment can also serve as a scaffold that regulates GPCR-mediated signalling, independent of G-protein activation. It is challenging to directly examine a role for β-arrestins in the regulation of GPCR mediated platelet function because of embryonic lethality in β-arrestin-1 and -2 double knockout mice and the significant redundancy in function of the two arrestin isoforms. Platelets are also not amenable to other genetic methods such as siRNA and CRISPR/Cas9 mediated target methods that are frequently employed to study β-arrestin regulation of GPCRs. Thus, the role of β-arrestins in regulating prostanoid receptor in platelets has not been extensively studied. In other cell types, EP_2 and EP_4 receptor interaction with β-arrestins form scaffolds with Src-Kinase, which results in transactivation of the epidermal growth factor receptor (EGFR) and AKT activation (122–125). AKT signalling can play important roles in platelets (126) and whether such β-arrestin-mediated AKT activation downstream of prostanoid receptors is important in platelets remains to be established.

As described above, prostanoid receptor-mediated signalling, that results in increased cAMP production, is associated with platelet inhibition; while an inhibition of adenylyl cyclase (AC), by $G\alpha_I$ activation, leads to decreased cAMP which promotes platelet aggregation induced by calcium mobilization (Table 1.1). This balance is reflected in the cardioprotective effects seen with aspirin, which is in large-part, attributed to its

irreversible inactivation of platelet COX enzymes – resulting in a reduction in the pro-aggregating effects of TXA_2. The inherent lack of significant transcriptional activity, in the anuclear platelets, results in a long-lasting inhibition of TXA_2 production for the duration of the platelet lifespan. Aspirin and other traditional non-steroidal anti-inflammatory drugs (NSAIDS) also inhibit endothelial production of PGI_2 which is largely derived from endothelial cell COX-2 enzymes. The development of the COX-2-selective inhibitors (Coxibs), which was driven by a quest for NSAIDS with greater gastro-intestinal safety, unfortunately resulted in an increase in myocardial infarctions resultant from the incorrect assumption that PGI_2 was derived from the constitutively expressed COX-1 and endothelial specific expression of PGI synthase, while platelet expression of thromboxane synthase was believed to underlie the predominant production of thromboxane by platelets (127, 128). The levels of PGI_2 in the healthy endothelium is now established to be produced by COX-2 which is induced by shear forces generated by normal blood flow (129–132). Overall, synthetic prostacyclins, thromboxane synthase inhibitors, and thromboxane receptor antagonists are likely to be useful agents for inhibiting platelet function, often though they are thought to be mechanistically too similar to their inexpensive counterpart, aspirin, limiting their development and use except in cases where aspirin is contraindicated (133).

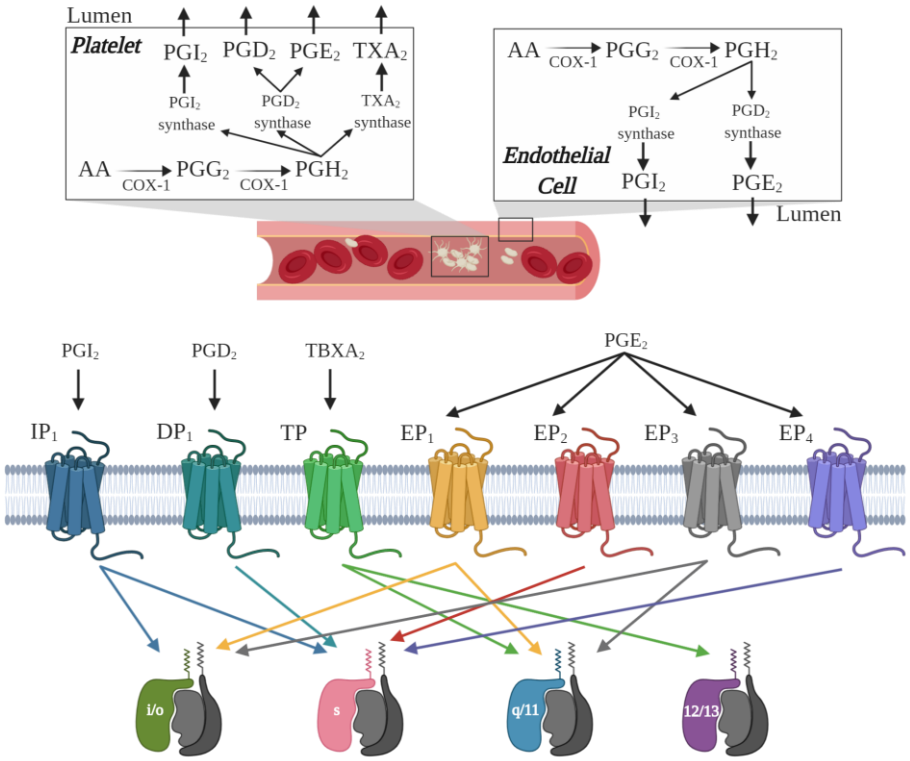

Figure 1.4 Synthesis of prostanoids (top) and their known receptor targets and G-protein-coupling effectors expressed in human platelets (bottom). Synthesis of prostanoids occurs through biochemical conversion of arachidonic acid (AA) by cyclooxygenase 1 (COX-1) to PGH_2 which then can be acted on by prostanoid synthases to generate active prostanoid receptor ligands. Prostanoid biosynthesis occurs in both the endothelium as well as through synthesis and release following of platelet activation. Arrows indicate which cytosolic G-protein subtypes ($G\alpha_{i/o}$ - green, $G\alpha_{s}$ - pink, $G\alpha_{q/11}$ - blue, or $G\alpha_{12/13}$ – purple) each prostanoid GPCR engages following receptor activation. (Created with BioRender.com)

1.2.4 Purinergic receptors

ADP is stored in platelet dense granules and released upon platelet activation. ADP is also released from damaged cells, at sites of vascular injury, acting in both an autocrine and paracrine manner for recruiting platelets and stabilizing the hemostatic plug. (134, 135). Platelets express two receptors for ADP, the $G\alpha_{q/11}$-coupled $P2Y_1$ receptor and the $G\alpha_i$-coupled $P2Y_{12}$ receptor (Table 1.1; Figure 1.5) (136, 137). Activation of both of these receptors is required for ADP to exert its maximal effect on platelets (138) however, $P2Y_1$ deficient mice do not show significant increases in bleeding tendency or protection from thromboembolic mortality and platelets from these mice still aggregate in response to ADP. Conversely, $P2Y_{12}$-deficient mouse platelets do not aggregate in response to ADP stimulation (139, 140), suggesting that ADP-meditated activation of the $G\alpha_i$ signalling pathway is the predominant stimulus from ADP, synergizing with $G\alpha_{q/11}$ activation by $P2Y_1$ and other $G\alpha_{q/11}$- or $G\alpha_{12/13}$-coupled GPCRs in platelets (81, 141).

As with the other receptors described above, few studies have directly studied β-arrestin mediated signalling downstream of P2Y receptors in platelets. A role for GRKs and second messenger kinases in regulating $P2Y_1$ and $P2Y_{12}$ receptor desensitization has been examined (142). This study showed that platelets express GRK2 and GRK6 and overexpression of these kinases (in non-platelet cells) was able to increase desensitization of the $P2Y_{12}$ receptor. Similarly GRK6 deletion resulted in increased signalling through $P2Y_{12}$ (and PAR1/4 receptors) while this deletion was without effect on TXA_2 responses (143). GRK and second messenger mediated phosphorylation of the P2Y receptors would enable β-arrestin recruitment and these desensitization responses can indirectly infer β-arrestin interaction with the respective receptors. Whether β-arrestin interaction with these receptors mediates signalling that is relevant to platelet function remains unclear. As described above it has been proposed that PAR4 stabilization of platelet thrombi is dependent on $P2Y_{12}$ signalling and formation of PAR4/$P2Y_{12}$ complex with β-arrestin, allowing the scaffolding of Lyn and PI3K to phosphorylate and activate AKT. Further studies are necessary, but lack of pharmacological modulators of β-arrestins remains a limitation.

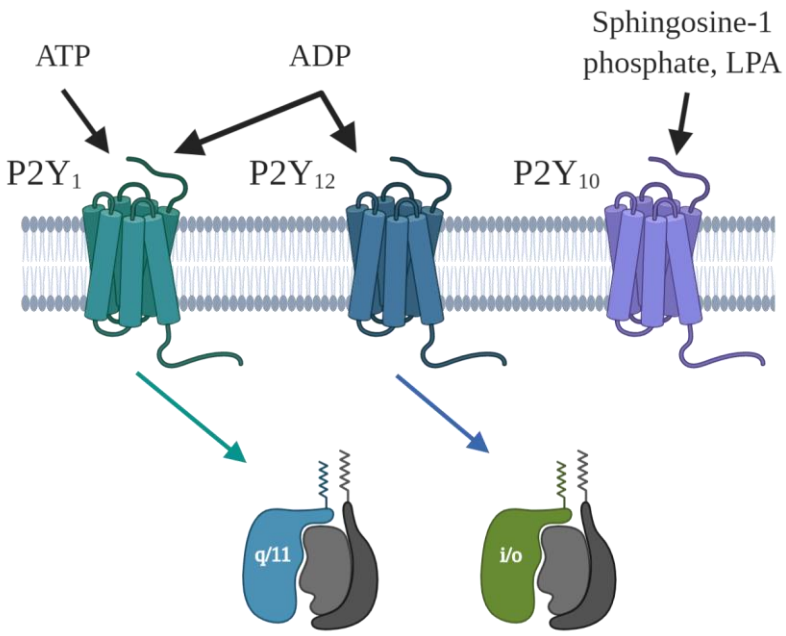

Figure 1.5 Purinergic receptor signalling following activation by ATP ($P2Y_1$), ADP ($P2Y_1$ and $P2Y_{12}$), and lipids (sphingosine-1 phosphate, LPA; $P2Y_{10}$). ADP and ATP are released by the injured endothelium but importantly serve as a major feed forward mechanism in platelet activation when they are released from platelet dense granules following initial priming of platelet by other stimuli. Activation of $P2Y_1$ by ATP or ADP leads to $G\alpha_{q/11}$-mediated shape change and platelet aggregation while activation of $P2Y_{12}$ by ADP engages $G\alpha_i$ signalling and inhibition of cAMP. Full platelet activation of platelets by ADP is thought to require signalling from both receptors. Role of the $P2Y_{10}$ receptor in platelets remains unclear. Arrows indicate which cytosolic G-protein subtypes ($G\alpha_{i/o}$ – green or $G\alpha_{q/11}$ - blue) each of the purinergic GPCRs engage following receptor activation. (Created with BioRender.com)

1.2.5 Other platelet-expressed GPCRs

As described above the thrombin receptors, prostanoid receptors, and purinergic receptors are the major GPCR activators of platelets, with profound effects on platelet responsiveness seen when these receptors are genetically or pharmacologically blocked. While these are primarily the targets of interest in platelet studies and for the purpose of therapeutic design, proteomic and functional studies have established the expression of a number of other GPCRs on platelets that have more modest effects on platelet function (Table 1.1). While these receptors do not act by themselves to affect full platelet activation, they interact with the three major platelet activating receptor families to influence platelet reactivity. Broadly these include the adenosine receptors (A_{2A}>A_{2B}), α_{2A}-adrenergic receptor, lysophosphatidic acid (LPA) receptors (LPA_{1-3}), serotonin receptors, cysteinyl leukotriene receptors, and others (Table 1.1) (144–149). Functional studies with the α_{2A}-adrenergic and serotonin receptors which couple to $G\alpha_i$ or $G\alpha_{q/11}$ show synergy with the strong platelet activating receptors to enhance platelet activation while activation of the $G\alpha_s$ coupled A_{2A} receptor inhibits platelet aggregation (146, 147). Overall the involvement of these receptors in platelet regulation is likely context specific (tissue, pathology, etc.) and considering these signals may be important in understanding platelet function in conditions such as stress, inflammation or atherosclerosis (150–152). Further, the implications of alterations to signalling from these receptors on platelet haemostasis, which may be accomplished through therapeutic interventions or in pathology, remains poorly understood and warrant prioritization in order to understanding the full interplay of platelet expressed GPCRs.

Thus, GPCRs are important regulators of platelet function. GPCRs also couple to multiple receptor proximal signalling effectors to effect platelet activation. A deeper understanding of specific pathways engaged by each GPCR in the context of a specific platelet response is critical to determining the pathways that have to be selectively targeted in order to prevent inappropriate platelet activation in disease.

Table 1.1 Summary of platelet expressed G-protein-coupled receptors identified by functional and/or proteomic approaches.[ii]

Receptor	Endogenous Agonists	G-protein effectors	Coupling to /Signalling through β-Arrestins	Role in human platelets
PAR1	Thrombin (153), APC, MMP1, MMP13 (154)	$G\alpha_{q/11}$, $G\alpha_{12/13}$, $G\alpha_{i/o}$ (79, 155, 156)	Yes (157)	Shape change, aggregation (74, 83, 158)
PAR4	Thrombin, cathepsin G, serine proteases	$G\alpha_{q/11}$, $G\alpha_{12/13}$ (159, 160)	Yes (84, 88, 89)	Aggregation (161), stabilization (85), shape change (161), granule secretion (74, 83, 158)
$P2Y_1$	ADP, ATP	$G\alpha_{q/11}$ (162–164)	Yes (165)	Shape change (137), aggregation (166)
$P2Y_{12}$	ADP	$G\alpha_{i2}$ (164, 167)	Yes (88, 89)	Aggregation, stabilization, granule secretion (168–170)
$P2Y_{10}$	Sphingosine-1 phosphate, LPA	- (171, 172)	-	-
IP_1	PGI_2	$G\alpha_s$, $G\alpha_{i/o}$ (173)	-	Inhibition of aggregation (174, 175)

[ii]Where possible, the primary endogenous agonist, G-protein subtypes, known interaction with β-Arrestins (known interaction denoted by "Yes"; known not to couple denoted by "No"; unknown denoted by "-"), and known role in human platelets is described.

DP_1	PGD_2	$G\alpha_s$ (176)	-	Inhibition of aggregation (177, 178)
TP	TBXA2	$G\alpha_{q/11}$, $G\alpha_{12/13}$	-	Aggregation (179, 180)
EP1	PGE_2	$G\alpha_{q/11}$, $G\alpha_{i/o}$ (173, 181, 182)	-	Aggregation
EP2	PGE_2	$G\alpha_s$ (173)	Yes (123)	Inhibition of aggregation (183, 184)
EP3	PGE_2	$G\alpha_{i/o}$, $G\alpha_{q/11}$ (171, 185–187)	Yes (188)	Aggregation (183, 189–191)
EP4	PGE_2	$G\alpha_s$ (192)	Yes (193)	Inhibition of aggregation (184, 194)
A_1	Adenosine	$G\alpha_{i/o}$, $G\alpha_s$, $G\alpha_{q/11}$ (171, 195, 196)	Yes (197)	-
A_{2A}	Adenosine	$G\alpha_z$, $G\alpha_s$, $G\alpha_{q/11}$ (198, 199)	Yes (197)	Inhibition of aggregation (200, 201)
A_{2B}	Adenosine	$G\alpha_s$, $G\alpha_{q/11}$ (198, 199)	Yes (197)	Inhibition of aggregation (202)
α_{2A}-adrenergic	Epinephrine, norepinephrine	$G\alpha_{i/o}$, $G\alpha_s$ (203–206)	No (207, 208)	Aggregation (209)
V_{1A}	Arginine, vasopressin	$G\alpha_{q/11}$ (171, 210)	Yes (211)	Aggregation (212, 213)
LPA_1	LPA	$G\alpha_{q/11}$, $G\alpha_{12/13,}$ $G\alpha_{i/o}$ (149, 171, 214)	Yes (215, 216)	Shape change (149)
LPA_2	farnesyl diphosphate, farnesyl monophosphate, LPA	$G\alpha_{i/o}$, $G\alpha_{q/11}$, $G\alpha_{12/13}$ (217)	Yes (216)	Shape change (149)
LPA_3	farnesyl diphosphate, farnesyl	$G\alpha_{q/11}$ (149, 171)	Yes (216)	Shape change (149)

	monophosphate, LPA			
LPA_4 (GPR23)	farnesyl diphosphate, LPA	$G\alpha_s$, $G\alpha_{q/11}$, $G\alpha_{i/o}$ (149, 171, 218, 219)	Yes (220)	Inhibition of aggregation (149, 221)
LPA_5 (GPR92)	farnesyl diphosphate, farnesyl monophosphate, LPA, N-arachidonoylglycine	$G\alpha_{q/11}$, $G\alpha_{12/13}$ (149, 171, 222)	Yes (220)	Shape change, activation (149)
$5HT_{2A}$	Serotonin	$G\alpha_{q/11}$, $G\alpha_{i/o}$ (223)	Yes (224, 225)	Modulator of ADP and thrombin induced aggregation (226–228)
$5HT_{1F}$	Serotonin	$G\alpha_{i/o}$ (171, 229)	-	-
$5HT_4$	Serotonin	$G\alpha_s$, $G\alpha_{12/13}$ (171, 230, 231)	Yes (232)	-
$mGlu_3$	L-glutamate	$G\alpha_{i/o}$ (171, 233)	Yes (234)	-
$mGlu_4$	L-glutamate	$G\alpha_{i/o}$, $G\alpha_{q/11}$ (171, 235)	-	-
OT	Oxytocin	$G\alpha_{q/11}$, $G\alpha_{i/o}$ (171, 236)	Yes (237)	-
Succinate receptor 1	Succinate	$G\alpha_{i/o}$ (171, 238)	Yes (239)	Aggregation (238)
$CX3CR_1$	Fractalkine	$G\alpha_{i/o}$ (171, 240)	Yes (241, 242)	-
CMKOR1 (CXCR7, ACKR3)	Adrenomedullin, CXCL11, CXCL12a	- (171, 243, 244)	Yes (245)	-
$CysLT_1$	Cysteinyl leukotrienes	$G\alpha_{q/11}$, $G\alpha_{i/o}$ (171, 246)	Yes (247)	Secretion (144)
$CysLT_2$	Cysteinyl leukotrienes	$G\alpha_{q/11}$, $G\alpha_{i/o}$ (246, 248, 249)	Yes (250)	-

Epstein-Barr virus induced gene 2 (EIB2)	Oxysterols	$G\alpha_{i/o}$ (171, 251)	Yes (252)	-
GPR1	Chemerin	(171, 253)	Yes (254)	-
GPR133	Unknown	$G\alpha_{s}$ (171, 255)	-	-

1.3 Proteinase Activated Receptors (PARs)

1.3.1 Discovery and expression of proteinase activated receptors

Proteinase Activated Receptors (PARs) are a family of four GPCRs (PAR1-PAR4), expressed throughout the human body which are important regulators of the innate immune response to injury or infection (155). The action of thrombin as a coagulation cascade-derived enzyme, that converts fibrinogen to fibrin, has been recognized as far back as the late 1800's, when it was described by Schmidt and others as *fibrinferment* (256, 257). However it was recognized that in addition to its role in the coagulation cascade, thrombin had concentration-dependent ability to activate platelets, stimulate mitogenesis, regulate vascular tone, and affect neuronal cell functions and this led to the idea that there existed so called 'thrombin receptors' (258–264). Initial studies to identify the thrombin receptor employed radiolabeled thrombin, however, these studies were unsuccessful in identifying the target receptor of thrombin (258, 265). Finally, in 1991, two landmark studies employed expression cloning approaches using *xenopus* oocytes, and were successfully able to identify the thrombin receptor (now known as Proteinase Activated Receptor 1) (Figure 1.6 and 1.7) (75, 76). These studies lead to the discovery of a unique mechanism of activation, wherein, cleavage of the human PAR1 receptor N-terminus, at the canonical serine-protease site, Arg^{41}/Ser^{42}, is required for receptor activation which reveals a tethered ligand "SFLLR…" (266, 267). Shortly thereafter, PAR1 activation by a synthetic tethered-ligand mimicking peptide, SFLLRN, was reported which was capable of activating the receptor in the absence of cleavage by thrombin (268, 269).

Following the discovery of PAR1, a second receptor sequence was identified in the mouse genome resembling PAR1 but with a varied sequence (270). Due to differences in receptor sequence and poor thrombin cleavage (except at very high thrombin concentrations), it was observed that while the cleavage site of the receptor was similar to that observed in PAR1, the enzyme-recognition sites were disparate between PAR1 and this newly cloned receptor. This second receptor was termed the thrombin-like receptor 1 (F2RL1), also known as PAR2, and was determined to be activated by trypsin cleavage at

the putative serine-protease site (Arg^{36}/Ser^{37}) (Figure 1.6 and 1.7) (270). Further, it was found that PAR2 could also be activated by a tethered ligand-mimicking peptide, SLIGRL, as well as, the PAR1 tethered ligand-mimicking peptide, SFLLRN (270–272). It was further determined that SFLLRN activity at PAR2 was due to ligand cross-reactivity (271, 272). These data supported the finding that this was a distinct receptor to PAR1, with a similar mechanism of activation, and further, a unique endogenous protease target. In the same year, the human PAR2 sequence was also cloned and reported to respond to both trypsin-cleavage and peptide stimulation of the receptor with the peptide based on the murine PAR2 tethered ligand sequence (SLIGRL-NH_2) (273).

Using a polymerase chain reaction approach, a third human thrombin-like receptor was cloned, with 27% sequence identity to PAR1, and 28% sequence identity to PAR2 (274). Thrombin-like receptor 2 (F2RL2), also known as proteinase activated receptor 3 (PAR3), was found to be a second thrombin substrate, similar to PAR1 (Figure 1.6). Thrombin-cleavage of PAR3 occurs at Lys^{38}/Thr^{39}, which reveals "TFRGAP…" as the tethered ligand (Figure 1.7). Interestingly, PAR3, unlike PAR1 and PAR2, fails to signal following activation by proteolysis. Additionally, PAR3 activation by its tethered ligand-mimicking peptide, TFRGAP or TFRGAPPNS, does not lead to intracellular signalling (274).

Finally, a fourth human thrombin-like receptor, F2RL3 (a.k.a. PAR4), was identified in an expression sequence tag database (Figure 1.6) (77). PAR4 was identified to be a substrate for both thrombin and trypsin cleavage-activation. Cleavage of the human PAR4 receptor occurs at the canonical serine-protease Arg^{47}/Gly^{48} site, revealing the tethered ligand "GYPGQV…", for both thrombin and trypsin cleavage of the receptor (Figure 1.7). Similar to the activity observed with PAR1 and PAR2 tethered ligand-mimicking peptides, PAR4 can be activated by a synthetic tethered ligand-mimicking peptide, GYPGQV, to stimulate downstream G-protein signalling (77).

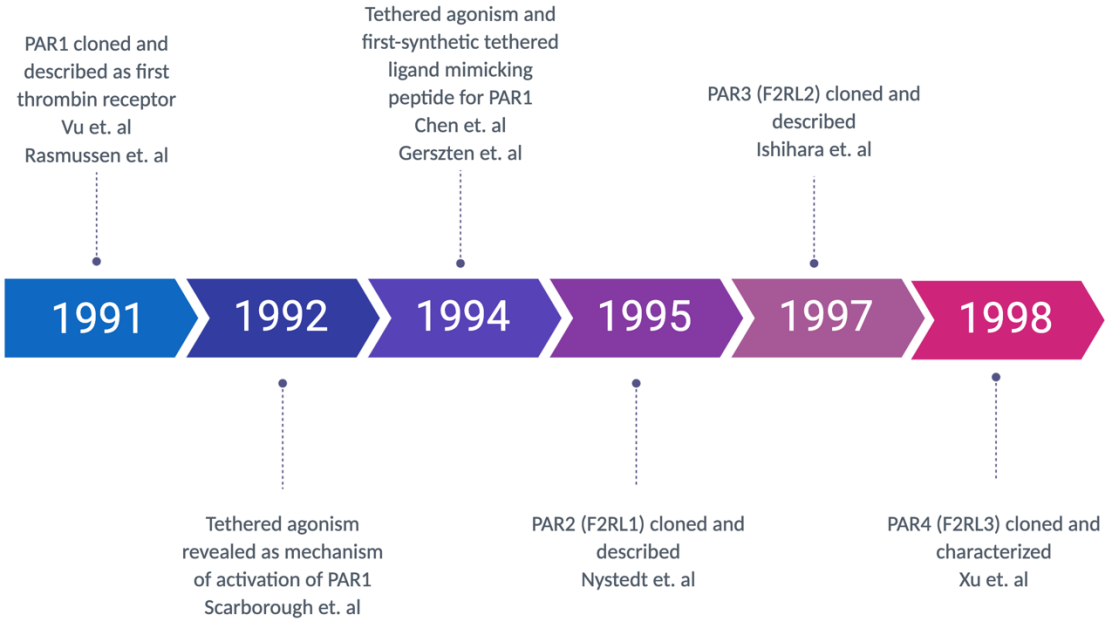

Figure 1.6 Timeline of proteinase activated receptor (PAR) discovery and cloning. (Created with BioRender.com)

1.3.2 PAR expression profile

PARs are expressed throughout the body, enabling many roles in both regulatory and pathogenic processes; thus, understanding and targeting this subfamily of GPCRs has potential therapeutic benefit. Table 1.2 summarizes the tissue distribution and cellular expression of PARs throughout the human body. PARs have known physiological roles in endothelial (PAR1) and epithelial (PAR1 and PAR2) barrier permeability, hypertension (PAR1) and hypotension (PAR2 and PAR4), nociception, inflammation, platelet activation and aggregation (PAR1 and PAR4), CNS neuronal and astrocyte function, placental development and function (PAR1, PAR2, and PAR4), and many pathogenic processes (summary on Figure 1.7) (275–281). There is a growing body of literature demonstrating the diverse pathologies resultant from PAR signalling dysregulation. The discovery of PARs and their unique mechanism of action has also led to a shift in the way that we must investigate and target GPCRs that are non-canonically activated (102). Additionally, PARs have been shown to be important receptors in the transduction of pain making them interesting targets for the development of anti-pain therapeutics.

Table 1.2 Tissue distribution and cellular expression profile of proteinase activated receptors.[iii]

	Tissue	Cell
PAR1/F2R	Brain, lung, heart, stomach, colon, kidney, testis	Platelets, endothelium, vascular smooth muscle, leukocytes, GI tract epithelium, fibroblasts, neurons, mast cells
PAR2/F2RL1	Prostate, small intestine, colon, liver, kidney, pancreas, trachea	Endothelium, leukocytes, GI tract epithelium and lung, airway and vascular smooth muscle, neurons, mast cells, keratinocytes, lung fibroblasts, renal tubular cells
PAR3/F2RL2	Heart, kidney, pancreas, thymus, small intestine, stomach, lymph node, trachea	Airway smooth muscle, platelets
PAR4/F2RL3	Lung, pancreas, thyroid, testis, small intestine, placenta, skeletal muscle, lymph node, adrenal gland, prostate, uterus, colon	Platelets, megakaryocytes

[iii]Adapted from Thibeault, P. E., Hollenberg, M. D., & Ramachandran, R. (2020), Proteinase Activated Receptors. Encyclopedia of Biological Chemistry, Elsevier

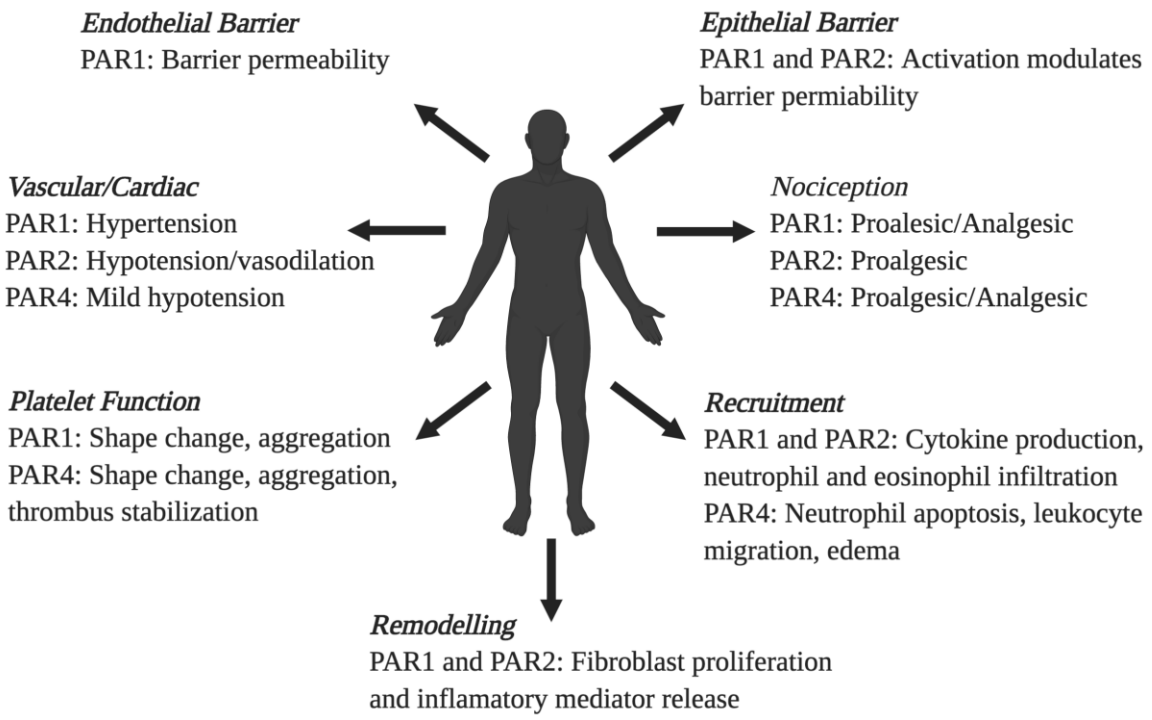

Figure 1.7 Summary of select roles for PARs in human physiology. (Created with BioRender.com)

1.3.3 Activation of PARs

1.3.3.1 Proteolytically-revealed tethered ligand activation

Most GPCRs which are activated through binding of a soluble ligand, however, PAR activation occurs irreversibly through proteolytic cleavage of a pro-peptide N-terminal sequence by enzymes, such as thrombin and trypsin, unmasking an activating tethered motif (282). The revealed motif, termed the tethered ligand, then binds intramolecularly to the receptor causing activation (282). This unique mechanism of activation irreversibly activates the receptor, likely leading to mechanisms of signalling and regulation through internalization and vesicular trafficking that are distinctive from other canonically-activated GPCRs. The tethered ligand that is revealed following cleavage is dependent on which enzyme cleaves the receptor. Some enzymes cleave at the canonical serine-protease cleavage sites revealing the classical PAR tethered ligands, while other upon cleavage may inactivate or "disarm" the receptor. Soluble endogenous agonists of PARs have not been identified to date.

PAR1 is the high-affinity thrombin receptor. The high-affinity observed with PAR1 activation by thrombin has been determined to be to a thrombin-exosite I-binding hirudin-like motif in the PAR1 N-terminus ($K^{51}YEPF^{55}$) which facilitates more efficient PAR1 cleavage (283–288). This enables high-affinity binding of thrombin to PAR1 and subsequent cleavage at the putative serine-protease site (Arg^{41}/Ser^{42}) to reveal the tethered ligand ($S^{42}FLLRN^{47}$…) and activate the receptor. Like PAR1, human PAR3 is a high-affinity thrombin receptor (due to its hirudin-like binding site) and is cleaved by thrombin at Lys^{38}/Thr^{39} to reveal the tethered ligand "$T^{39}FRGAP^{44}$…" (274). PAR4 lacks this hirudin-like binding motif therefore activation typically requires much higher concentrations of thrombin to be present (77). Instead, PAR4 interactions with thrombin occur through weaker interactions with an anionic motif that slows the dissociation of PAR4 from the cationic thrombin (285, 289). Thrombin cleaves PAR4 at the Arg^{47}/Gly^{48} site to reveal the receptor-activating tethered ligand ($G^{48}YPGQV^{53}$…) (77, 290, 291). PAR2 resists thrombin cleavage however can be activated at very high concentrations of thrombin [100-500 nM; 1 international unit (IU)/mL is approximately 10 nM] (290, 292–294). Instead, PAR2 is typically activated by trypsin cleavage at the canonical serine-

protease Arg^{36}/Ser^{37} cleavage site, revealing the PAR2 tethered ligand, "S^{46}LIGKV^{53}…" (273). A summary of PAR cleavage sites is shown in Figure 1.8.

There are multiple serine proteinases, apart from thrombin and trypsin, that have been shown to target PARs to activate or inactivate the receptors including: plasmin, granzymes (A, B, and K), cathepsin G and S, factors VIIa/X/Xa/TF, activated protein C (APC), chymase, mast-cell tryptase, tissue kallikreins (hK4, hK14, hK5, and hK6), dust mite proteinases (Der p3 and Der p9) (295), cysteine proteases (Calpain-1and Calpain-2), and the matrix metalloproteinase/MMP family (MMP-1, MMP-2, MMP-13) (295). Other sources of non-endogenous PAR-activating proteases also include bacterial, amoebic, reptilian, insect, fungal, and plant sources (295). Thus, PARs are of importance not only for sensing endogenous proteinases in the tissue microenvironment but also for responding to pathogen invasion. Importantly, proteases that do not cleave at the canonical serine-protease cleavage sites will reveal novel tethered ligands which may induce differential signalling and regulation of the PARs (296).

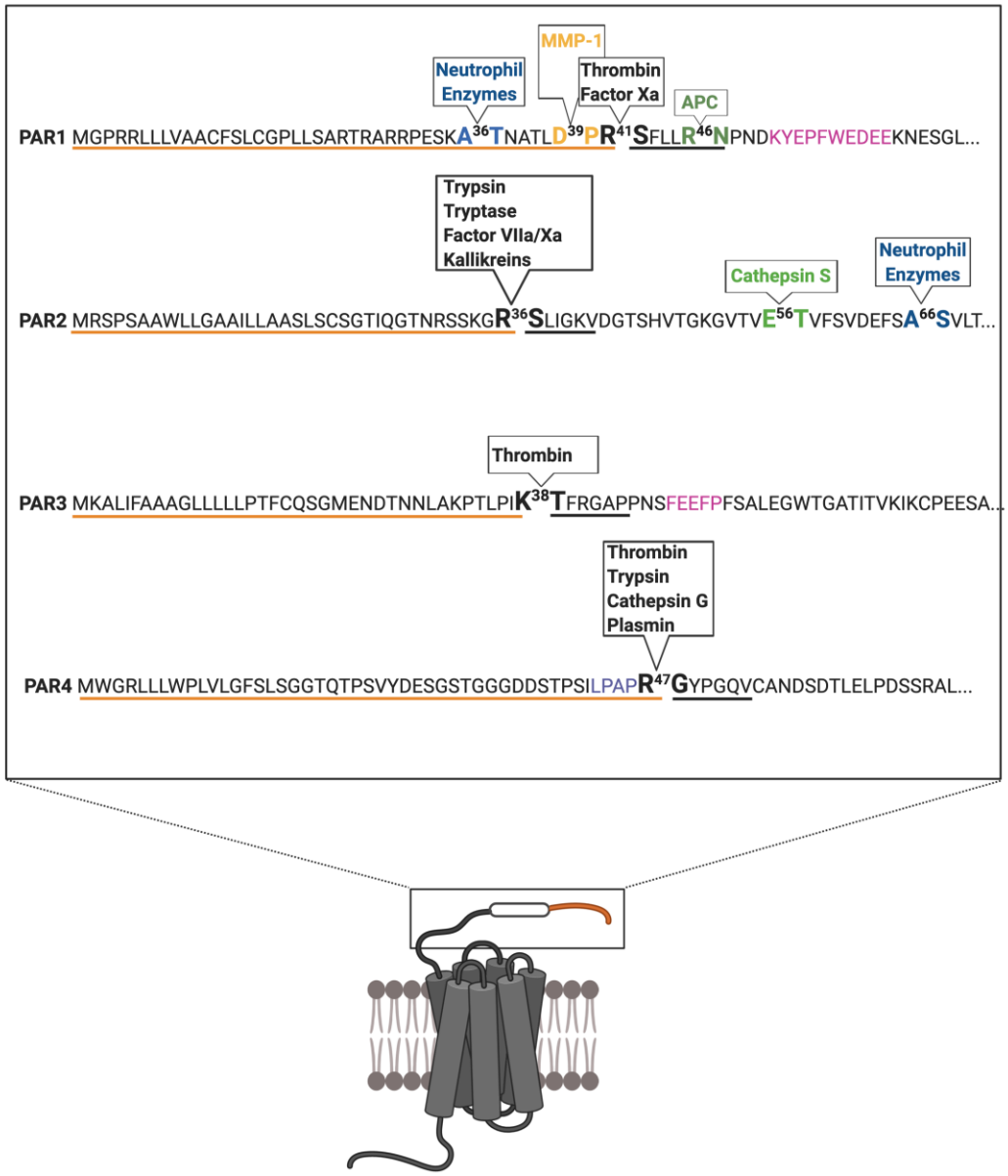

Figure 1.8 Common sites of PAR1, PAR2, PAR3, and PAR4 cleavage. Cleavage sites for PAR1, 2, 3, and 4 are shown with the common proteases that activate them. The sequence of the N-terminus (up to TM1) is shown, including the tethered ligand sequence (underlined, black) revealed by the common PAR-activating serine-proteases (thrombin, trypsin) activation. The portion of the N-tail that is cleaved from the receptor is underlined (orange). Hirundin-like binding motif of PAR1 and PAR3, which facilitate high-affinity binding of thrombin, are shown in pink. Known PAR4 binding site of thrombin is shown in purple. [Adapted from Thibeault, P. E., Hollenberg, M. D., &

Ramachandran, R. (2020), Proteinase Activated Receptors. Encyclopedia of Biological Chemistry, Elsevier] (Created with BioRender.com)

1.3.3.2 Tethered ligand-mimicking peptide activation

In addition to endogenous enzymatic cleavage, PARs can be activated by synthetic peptide sequences that mimic the tethered ligand. This mechanism of activation does not require cleavage of the receptor and is a useful tool in studying each receptor individually when a cell expresses multiple PARs that are cleaved by the same enzyme such as thrombin (PAR1 and PAR4) and trypsin (PAR2 and PAR4). The tethered ligand sequence, $S^{42}FLLRN^{47}$…, was described to activate PAR1 receptor as revealed by thrombin cleavage (268, 269). The impetus for generation of synthetic peptide sequences mimicking the tethered ligand followed an important study that confirmed the tethered ligand mechanism of PAR1 activation, as well as which residues comprised the agonist (267). Mutational studies probed the first eight residues downstream of the putative serine-protease cleavage site, SFLLRNPN, and evaluated calcium signalling in response to a saturating concentration of thrombin. This approach revealed residues 2 and 4 of the sequence (Phe and Leu, respectively) were necessary for signalling. Therefore, the native sequence, as well as tolerated receptor tethered ligand mutations, were explored to generate receptor activating peptides. Peptides mimicking the first 4-14 receptor residues downstream of thrombin cleavage ($S^{42}FLLRNPNDKYEPF^{55}$…) were generated and evaluated for their ability to induce platelet aggregation. Of the peptides tested, a C-terminally amidated hexapeptide of the first six residues (SFLLRN-NH_2) was identified to have the most potent activity at the receptor. Finally, it was found that substitution of the tethered ligand-mimicking peptide Ser with Thr residue enhanced binding and potency at the PAR1 receptor (297).

Soon after the discovery of the receptor, and its cloning from the mouse genome, the hexapeptide SLIGRL-NH_2 was identified as an agonist peptide of PAR2 (270). As with the strategy for generating the PAR1 agonist peptide, the PAR2 activating peptide, SLIGRL, is a direct mimic of the six amino acid sequence revealed by N-terminal cleavage of the murine PAR2 receptor with trypsin (270). Further, upon cloning of the human PAR2 receptor it was determined that the receptor could be activated by synthetic peptides mimicking both the human (SLIGKV) and murine (SLIGRL) tethered ligands

(271). Ultimately, it was observed that the amidated peptide of the murine tethered ligand was more selective and potent activator of PAR2-mediated calcium signalling (271).

With the successful generation of PAR1 and PAR2 tethered ligand-mimicking peptides a similar strategy was employed following the cloning of the PAR3 receptor. As previously noted, little to no activity is observed downstream of PAR3 activation either with the thrombin-revealed tethered ligand or with the tethered ligand peptide mimicking the human PAR3 sequence revealed by thrombin activation (274). No PAR3 activation is observed with either the hexapeptide (TFRGAP) or the nonapeptide (TFRGAPPNS) (274, 298). In fact, it was observed that the tethered ligand revealed by thrombin cleavage of PAR3 has activity at the PAR1 receptor, thus it is widely believed that PAR3 activation enables co-receptor signalling through cross-activation (298). Additionally, it has been demonstrated that PAR3, as a high-affinity thrombin receptor (due to its hirudin-like binding site) can function as a co-receptor for PAR4, facilitating more efficient cleavage and activation of PAR4 (299).

When cleaved by either thrombin or trypsin, the N-terminal tethered ligand revealed in human PAR4 is $G^{48}YPGQV^{53}$… (77). The tethered ligand peptide was identified based on sequence identity with PAR1 and PAR2 and confirmed through mutation of the putative serine-protease cleavage site Arg^{47}/Gly^{48} (77). When human PAR4 with an Arg^{47}Ala mutation was expressed in COS cells (fibroblast), activation with thrombin was lost confirming that this is indeed the site for receptor cleavage with thrombin. In support of this finding, a hexapeptide of the revealed sequence, G^{48}YPGQV, has full activity at both the wild-type receptor and the Arg^{47}Ala mutant PAR4 in this cell system (77). Shortly after this discovery, a full SAR study was undertaken by Coughlin and colleagues to find PAR4 activating peptides with increased potency and activity at the receptor. Much like the finding that the murine PAR2 tethered ligand had enhanced activity at human PAR2 compared to the human sequence tethered ligand mimicking peptide, the study investigated potency of the murine PAR4 tethered ligand sequence, GYPGKF, and found that it had more activity at the receptor than the peptide derived from the human PAR4 tethered ligand (291). Further, in SAR studies substitution of the first Gly residue with Ala (AYPGKF-NH_2) enhanced both potency and efficacy at the PAR4 receptor

compared to both murine (GYPGKF, 2-fold increase with alanine substitution) and human (GYPGQV, 10-fold increased potency with $Gly^{1}Ala$, $Gln^{5}Lys$, and $Val^{6}Phe$ substitutions) tethered ligand sequences (291).

1.4 Therapeutic targeting of G-protein-coupled receptor signalling for the development of improved anti-platelet therapeutics

Anti-platelet therapy is the cornerstone of current cardiovascular disease management and has significantly reduced mortality and morbidity due to coronary artery thrombosis (300). Yet significant limitations exist in current therapies, be it due to weak inhibition of platelet aggregation (e.g. with aspirin), lack of efficacy due to inter-patient pharmacogenomic differences (e.g. clopidogrel) or due to side effects such as clinically significant bleeding (e.g. PAR1 inhibition with voropaxar) and GI ulceration and bleeding with chronic use (100, 301–303). While all of these limitations cannot be resolved by biased ligands that target selected platelet pathways, in some instances the side effect profile can likely be improved with such strategies. It is now accepted that activated GPCRs seldom couple to a single downstream signalling pathway. Depending on the ligand interacting with a given receptor, GPCRs can stabilize to multiple active conformations, each of which may favour interaction with one or more intracellular effectors – translating into different cellular responses (30, 304–306). The ability of different ligands to stabilize distinct receptor conformations has been experimentally demonstrated with a number of techniques revealing that structural basis for such differences stems from favorable orientation of different amino acids that are critical for engaging different G-proteins or β-arrestins (307, 308). Most often, biased signalling is examined by monitoring the engagement of different G-protein subtypes and the recruitment of β-arrestins as the major receptor proximal effectors.

As described above, platelet aggregation involves integration of signalling inputs from multiple receptors, which are activated by multiple agonists (some of which act on more than one receptor), and frequently can couple to multiple intracellular signalling effectors

(which can be triggered downstream of multiple receptors). Layered on top of this, the variation in abundance of and temporal release of agonists adds further complexity. This staggering array of interactions, which has gradually become evident over the last decades, presents an extremely challenging framework for the study of individual signalling pathways. Knocking out or inhibiting specific effectors has provided some indication of how biased signalling may be exploited for therapeutic targeting, however, deletion of any given effector has an impact of multiple signalling pathways. Disruption of multiple signalling pathways through receptor knockout further complicates the interpretation of findings and obscures analysis of the roles individual GPCR-coupled G-protein-mediated and β-arrestin-mediated signalling pathways play in platelet activation.

Further dissection of the individual signalling pathways downstream of receptor activation requires the development of biased ligands that not only retain specificity to individual GPCRs, but also selectively engage specific signalling effectors subtypes. Development of such agents is ongoing for a number of GPCRs (309) but studies focused on platelet GPCRs are sparse. In the case of the major prostanoid and purinergic receptors discussed above, I was unable to identify studies that have systematically tested the efficacy of ligands at individual G-protein- and β-arrestin-mediated pathways in the platelets. It could however be hypothesized that ligands biasing prostanoid receptors towards the $G\alpha_s$ pathway and away from the $G\alpha_i$ pathway are likely to be beneficial. The TP receptor couples to both $G\alpha_{q/11}$ and $G\alpha_{12/13}$ signalling. While TP-dependent $G\alpha_q$ activation is necessary for triggering platelet aggregation by this receptor, TP mediated $G\alpha_{12/13}$ activation induces shape change (310). Thus, a drug that prevents TP coupling to $G\alpha_q$ might be sufficient to provide anti-platelet action. Similarly, in the case of the thrombin receptor PAR1, which can couple to $G\alpha_{q/11}$, $G\alpha_{12/13}$ and $G\alpha_i$, it could be postulated that compounds that stabilize this receptor in a conformation that prevents activation of the $G\alpha_{q/11}$ pathway in the platelets would be desirable as anti-platelet agents. In the case of PAR1, additional inhibition of the $G\alpha_{12/13}$ pathway may also be desirable since activation of this pathway by thrombin leads to endothelial barrier disruption (311, 312), while sparing $G\alpha_i$ (313) and β-arrestin (86) pathways will be desirable since these signals protect the endothelial barrier (314). Purinergic receptor signalling might be more

tractable given that $P2Y_1$ and $P2Y_{12}$ receptor-coupling to G-protein pathways is more selective and seeking G-protein vs β-arrestin activating ligands may be informative.

1.4.1 Biased signalling of PAR4 as an anti-platelet therapeutic target

As previously mentioned, PAR4 is activated by several different proteases throughout the body (trypsin, thrombin, Cathepsin-G) and thus it is reasonable that biased agonism may exist at PAR4, as has been reported with other GPCRs with several physiological agonists. Unfortunately, due to a limitation in molecular probes with the sensitivity required to flesh out differential signalling there has been a lack of investigation in this area with PAR4. However, technological and methodological advances have now enabled a detailed study of the signalling downstream of PAR4 and other GPCRs. Understanding the downstream signalling and trafficking of PAR4 in response to each agonist may uncover bias that can be therapeutically targeted. Subsequently, an investigation of the tethered ligands produced by cleavage with these various proteases may enable design of peptide and small molecule ligands that can recapitulate signalling biases observed with proteolytic cleavage. To exploit this information will require investigation of the binding sites of these ligands and well as their distinct chemical or structural characteristics to determine a molecular basis for differential signalling following agonist activation of PAR4. Further development of compounds that are able to selectively engage $G\alpha_{q/11}$, $G\alpha_{12/13}$, $G\alpha_{i}$, or β-arrestin recruitment to PAR1 and $G\alpha_{q/11}$, $G\alpha_{12/13}$ or β-arrestin recruitment to PAR4 will help to further clarify the relative contribution of each of these pathways in thrombin receptor-mediated platelet aggregation. The variety of G-proteins that can be engaged by PAR receptors and the significant cross-reactivity observed with the endogenous ligands for the platelet-expressed prostanoid receptor subtypes receptors poses a significant challenge in dissecting signalling bias.

1.5 GPCR signalling, regulation, and trafficking

1.5.1 Helix- 8 and the C-terminal tail in signalling and regulation

With recent advances in GPCR structural biology including crystallography, cryo-electron microscopy (Cryo-EM), and F^{19} nuclear magnetic resonance spectroscopy (NMR) our understanding of how effectors interact with GPCRs has increased greatly. Structures combined with mutational studies have identified many transmembrane residues/motifs involved in activation of GPCRs and effector interactions. Further, distinct roles for Helix-8 and the C-terminal tail have been demonstrated for many GPCRs, highlighting the importance of these receptor domains in effector engagement, signalling, and regulation. In order to compare important sites within GPCRs, a numbering system known as the Ballesteros-Weinstein number, will be used throughout the following text. This number identifies the α-helix the residue is found in followed by its relation to the most conserved residue in that domain. Within this numbering system, residues upstream (< x.50, wherein "x" denotes the α-helix) and downstream (> x.50) from the most conserved residue (x.50, wherein "50" denotes the most conserved residue) are used to make comparisons between GPCRs (315). For example, the highly conserved Helix-8 phenylalanine residue would be denoted as $Phe^{8.50}$.

Helix-8 is a structurally conserved, amphipathic, helical motif in class A GPCRs, immediately downstream of TM7 and preceding the C-terminal tail sequence. Helix-8 has been shown for many GPCRs to regulate G-protein interaction and signalling, β-arrestin recruitment and G-protein-independent signalling, PDZ interaction, receptor expression, and internalization (316–319). One particularly important Helix-8 residue, a cysteine residue present in many class A GPCRs, undergoes palmitoylation allowing for stabilization of Helix-8 through insertion into the cell membrane (320–325). This important palmitoylation site is present in both PAR1 and PAR2, however, is absent in PAR4 (326–329). Given the lack of a Helix-8 cysteine, and therefore by extension palmitoylation and membrane-anchoring of Helix-8, it is reasonable to expect that there are other mechanism(s) contributing to PAR4 effector interaction, signalling, and trafficking.

Previously, our laboratory has demonstrated that deletion of an 8-amino acid Helix-8 sequence, which contains Gln^{357} (8.60, Ballesteros-Weinstein numbering) in the position occupied by the palmitoylated Cys^{361} (8.60) of PAR2, yields an interesting loss of protein interaction in PAR4 (85, 315). This receptor, termed dRS-PAR4 (ΔRAGLFQRS) does not recruit certain G-proteins and has significantly diminished capacity to recruit β-arrestins. This discovery has enabled the development of a pepducin peptide targeting this motif with exciting activity in inhibiting thrombin- and peptide-stimulated activation of platelet aggregation (85). Additionally, mutation of Gln^{357} to Cys (analogous to the palmitoylated Helix-8 PAR2 Cys^{361}) enhanced β-arrestin recruitment to PAR4 (85). Therefore, while it is plausible that there may be several mechanisms by which G-proteins and β-arrestins interact with PAR4, it is expected that more residues/motifs will play a role in signalling and signal desensitization which can be further explored through systematic mutational studies of these residues. Whether the whole $R^{352}AGLFQRS^{359}$ motif, or a subset of these residues (such as Gln^{357}), are necessary for these interactions had yet to be determined.

In addition to the structural elements constituted by Helix-8 residues (such as membrane anchoring via palmitoylated Helix-8 cysteine), there are key receptor-effector interactions that are observed to occur in GPCRs, as revealed by various structural biology techniques. One highly important motif is $E/DRY^{3.49/3.50/3.51}$ which forms an ionic lock that bridges TM3 and TM6, stabilizing the inactive conformation of class A GPCRs (330–334). Typically, the ionic lock is constituted by interactions between $Asp/Glu^{3.49}$ and $Arg^{3.50}$ as well as $Arg^{3.50}$ and a TM6 $Glu^{6.30}$, however other TM6 residues are observed in class A GPCRs. Mutational studies of the $Glu/Asp^{3.49}$ residue has been shown with numerous receptors to increase agonist-independent basal activity of the receptor (334). The TM3 of PAR4 contains this important motif at Asp^{173}, Arg^{174}, and Tyr^{175}, however, lacks the $Glu^{6.30}$ observed in about 25% of class A GPCRs. An alternative mechanism is proposed for class A GPCRs lacking $Glu^{6.30}$, wherein, the salt bridge formed between $Asp/Glu^{3.49}$ and $Arg^{3.50}$ is the inactive state conformation becomes disrupted allowing $Arg^{3.50}$ to instead interact with TM5 $Tyr^{5.58}$ (which PAR4

possesses) as well as the α5-helix of the G-protein, as is observed with activated opsin and $G\alpha_t$ (334, 335).

Another key GPCR receptor motif is the $NPxxY(x)_{5,6}F$ TM7/Helix-8 sequence which allows interactions between $Tyr^{7.53}$ and Helix-8 $Phe^{8.50}$ to stabilize the helix-loop-helix conformation of this region in the inactive conformation of the receptor. Further, interaction of the $NPxxY(x)_{5,6}F$ motif has been demonstrated to interact with a core of water molecule interactions that further stabilize the inactive conformation of the receptor (336–338). Additionally, this site is a reported site of G-protein interaction (317, 339, 340). PARs contain a non-canonical sequence, wherein, $Asn^{7.49}$ is occupied by Asp, and $(x)_{5,6}$ is a sequence of 6 residues from $Tyr^{7.53}$ to $Phe^{8.50}$ (PAR1 – $DP^{7.50}LIY^{7.53}YYASSEC^{8.50}$; PAR2 – $DP^{7.50}FVY^{7.53}YFVSHDF^{8.50}$; PAR4 – $DP^{7.50}FIY^{7.53}YYVSAEF^{8.50}$; sequences obtained from UniProt) (341–343). PARs additionally lack a common inactive/active "toggle switch" tryptophan (6.48), which has been demonstrated for many class A GPCRs to be a site for change from inactive to active receptor conformation. Therefore, given the unique mechanism of activation and the key differences in common GPCR mechanisms that is observed in the PARs, the molecular mechanisms by which PARs engage protein effectors and become activated is of interest.

The role of β-arrestins in the process of GPCR signal termination has been studied extensively, however, novel roles for these proteins as signalling molecules has recently gathered the interest of the field. Recently, the role of explicitly spaced C-terminal tail motifs has been shown to form a phosphorylation "barcode" motif for many GPCRs, by which, these proteins are recruited to the receptor to engage distinct G-protein-independent signalling pathways in addition to their role as internalization scaffolding equipment (344–346). Interestingly, while PARs are unlike most GPCRs in their mechanism of activation, they are similar in their expression of these β-arrestin barcodes. In particular, the C-terminal tails of PAR2 and PAR4 contain several examples of phosphorylation barcodes and are potent recruiters of β-arrestins compared to other PAR receptors (PAR1 and PAR3). The PAR2 C-terminal tail also contains the more classically studied clustering of phosphorylatable serine and threonine residues, therefore, the role of

phosphorylation barcodes has not been fully explored with this receptor (328, 347, 348). Interestingly, unlike PAR2, the C-tail of PAR4 does not contain the canonical phosphorylation clusters, however, does contain one “complete” and many “partial” barcodes and demonstrates a less robust recruitment of β-arrestins compared to PAR2. The role of β-arrestins in PAR4 signal regulation and trafficking is poorly understood, however, comparison with the more canonically expressed mixture of phosphorylation clusters and barcodes of PAR2 provides an excellent opportunity for investigation of these proteins in PAR regulation. Systematic mutation of PAR4 C-terminal tail phosphorylatable residues would enable determination of the role of this motif in receptor-β-arrestin interaction. If β-arrestin recruitment was unexpectedly unimpeded by a phosphorylation-null PAR4 C-terminal tail, other mechanisms such as phosphorylation and recruitment to ubiquinated lysine residues can be explored.

1.5.2 Internalization

Canonically, GPCR-mediated signalling involves activation of the receptor through the binding of an extracellular soluble ligand agonist with the receptor. The activated GPCR subsequently undergoes conformational changes which allows/stabilizes receptor-protein interaction with the heterotrimeric G-proteins and subsequent initiation of G-protein signalling cascades. In parallel with this process, activation of the receptor signals for the recruitment of other intracellular proteins such as G-protein receptor kinases (GRKs) and β-arrestins recruitment which initiate G-protein-dependent signal termination. Termination of the intracellular G-protein signal, even in agonist bound state, is a key feature in the regulation of this activity (349). To terminate the intracellular signal, serine and threonine residues of the C-terminal tail of the activated receptor, are rapidly phosphorylated by GRKs. Phosphorylation signals for interaction of the receptor with scaffolding proteins such as β-arrestin-1/-2, adaptor protein 2 (AP2), and FCH Domain Only 2 (FCHO2). β-arrestin-1 and -2 connect activated receptor with the recruiting protein adaptin/AP2 complex, resulting in receptor relocation into clathrin coated pits. Clathrin-coated pits are then pinched off from the membrane with the GTPase, dynamin, resulting in the formation of endosomes.

There is evidence in the literature of PAR1 and PAR2 internalizing via the clathrin endocytic pathway, however some studies suggest they may also utilize a clathrin-independent endocytosis via a caveolin-dependent endocytic pathway (347, 350). Limited studies with PAR4 have elucidated some high-level insights into the trafficking of PAR4 following activation, however, significant resolution is lacking in this important regulatory sequence (89, 351, 352) (Figure 1.9).

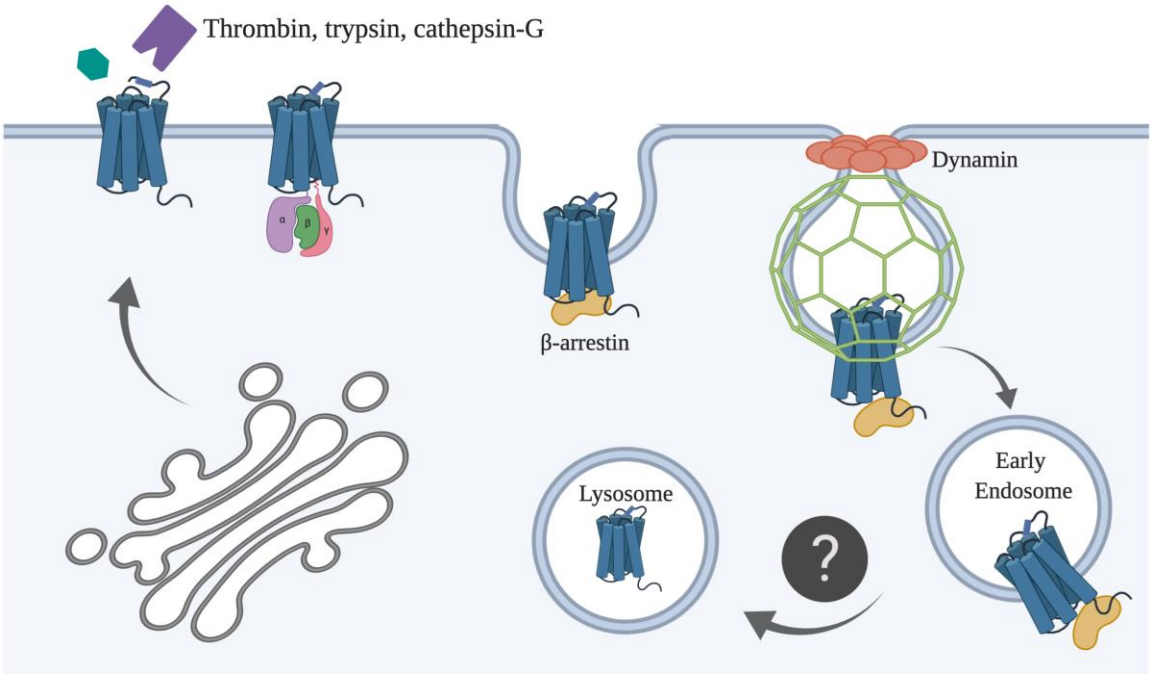

Figure 1.9 Schematic overview of PAR4 trafficking following activation.

1.6 Thesis Overview and Hypotheses

Proteinase activated receptors, PAR1 and PAR4, represent important and tractable therapeutic targets for anti-platelet therapy. However, limitations with the antagonist vorapaxar have limited the use of this clinically approved PAR1 antagonist. Drug discovery efforts have produced a PAR4 antagonist, BMS986120, which readily inhibits platelet activation and aggregation and is currently in clinical trials for human therapeutic use. Human platelets express over 30 GPCRs with signalling pathways that are convergent and, in some cases, result in the release of pro-thrombotic factors and amplification of platelet activation (e.g. PAR1/4 activation stimulates platelet granule release which contain ADP, an activator of the purinergic $P2Y_1$ receptor). Given the interest in therapeutically targeting PAR4, we have proposed that it may not be necessary to antagonize the receptor to achieve a therapeutic outcome. Biased agonism, or more finely tuned activation/inhibition of signalling pathways, may provide an advantageous anti-platelet therapeutic approach wherein pro-thrombotic signalling and granule release may be attenuated while maintaining non-pathogenic signalling. As described in this introduction, there is a dearth of information regarding the activation of PAR4 signalling pathways and their relative contribution to platelet activation, as well as other cell and tissue specific contexts. Thus, outside of the therapeutic potential, biased agonists will be useful to probe the roles of PAR4 signalling pathways in a cell/tissue specific context. Modern drug discovery efforts require certain inputs to be successful – how and where do the endogenous ligands bind, what signalling pathways are engaged, and how is this signalling regulated. Together, these data provide important inputs for rational drug discovery efforts. Therefore, we have endeavored to describe how PAR4's tethered ligand and peptide agonist interacts with and activates the receptor, how this necessarily impacts receptor-mediated signalling, and how/where effector interaction occurs downstream of receptor activation.

1.6.1 Chapter 2: Objectives and Hypothesis

1. To characterize the impact of single amino acid substitutions to the parental PAR4 agonist peptide, AYPGKF-NH_2 on PAR4 activation of $G\alpha_{q/11}$-dependent calcium signalling and β-arrestin recruitment.

2. To identify whether any of the substitutions made to the PAR4 agonist peptide result in biased agonism of PAR4.

3. To determine residues in the orthosteric binding site of PAR4 using *in silico* modelling and peptide docking. Further, to determine if AYPGKF-NH_2 adopts a defined structure in solution.

4. To assess the impact of biased agonism of PAR4 on *ex vivo* platelet preparations.

In chapter 2, *I hypothesized that single-amino acid substitutions to the PAR4 agonist peptide, AYPGKF-NH_2, would enable discovery of the chemical characteristics underscoring activity of the peptide at PAR4. Further, I hypothesized that some of the amino acid substitutions to AYPGKF-NH_2 would result in biased signalling. Next, I hypothesized that using in silico homology modeling and peptide docking we can identify residues in the PAR4 orthosteric binding site and NMR would enable solving of the peptide structure, which together with data from SAR studies has utility in rational drug discovery efforts for PAR4-targetting ligands. Finally, I hypothesized that biased ligands for PAR4 would not stimulate platelet activation and/or aggregation and therefore would provide a proof of concept that biased agonism could provide leads for novel anti-platelet therapeutics.*

1.6.2 Chapter 3: Objectives and Hypothesis

1. To determine the impact of Helix-8 Cys^{361} and C-tail serine/threonine residue mutations on β-arrestin-1/-2 recruitment to PAR2.

2. To evaluate the role of β-arrestin-1/-2 recruitment on $G\alpha_{q/11}$ calcium signalling following activation of PAR2 by either enzyme activation (trypsin) or peptide stimulation (SLIGRL-NH_2).

3. To determine the impact of Helix-8 Cys^{361} and C-tail serine/threonine residue mutations on $G\alpha_{q/11}$ calcium signalling from PAR2; and evaluate agonist-dependent differences in their contributions

In chapter 3, *I hypothesized that PAR2, which contains canonical C-tail residues (Helix-8 cysteine, clusters of serine/threonine residues), would be regulated similarly to other Class A GPCRs, with β-arrestin-1/-2 recruitment leading to desensitization of $G\alpha_{q/11}$-mediated calcium signalling. Further, specific C-tail serine and threonine residues would be responsible for β-arrestin-1/-2 recruitment to activated PAR2, dependent on the activating agonist (enzyme vs. peptide activation).*

1.6.3 Chapter 4: Objectives and Hypothesis

1. To determine the impact of Helix-8 and C-tail residue mutations on $G\alpha_{q/11}$ calcium signalling and β-arr.-1/-2 recruitment to PAR4.

2. To evaluate the role of Helix-8 residues versus C-tail residues in PAR4 signalling and signal regulation downstream of enzymatically-activated (thrombin) and peptide-activated (AYPGKF-NH_2) receptor.

3. To investigate whether the contribution of Helix-8 and C-tail reveals novel sites for $G\alpha_{q/11}$ activation and β-arr.-1/-2 recruitment.

In chapter 4, *I hypothesized that PAR4, which lacks canonical C-tail residues (Helix-8 cysteine, clusters of serine/threonine residues) when compared to other Class A GPCRs, would regulate effector interaction by different residues than more canonical GPCRs, such as PAR2. Further, regulation of PAR4 β-arrestin-1/-2 recruitment will include additional residue interactions than phosphorylatable serine/threonine residue, which has been increasingly shown for many Class A GPCRs. Finally, I hypothesized that the*

relative impact of residues would differ dependent on whether PAR4 was activated by the thrombin-revealed tethered ligand or agonist peptide (AYPGKF-NH_2).

1.7 Chapter 1 References

1. Rosenbaum, D. M., Rasmussen, S. G. F., and Kobilka, B. K. (2009) The structure and function of G-protein-coupled receptors. *Nature*. **459**, 356–363

2. Venkatakrishnan, A. J., Deupi, X., Lebon, G., Tate, C. G., Schertler, G. F., and Babu, M. M. (2013) Molecular signatures of G-protein-coupled receptors. *Nature*. **494**, 185–194

3. Lagerstrom, M. C., and Schioth, H. B. (2008) Structural diversity of G protein-coupled receptors and significance for drug discovery. *Nature reviews. Drug discovery*. **7**, 339–357

4. Fredriksson, R., Lagerström, M. C., Lundin, L.-G., and Schiöth, H. B. (2003) The G-Protein-Coupled Receptors in the Human Genome Form Five Main Families. Phylogenetic Analysis, Paralogon Groups, and Fingerprints. *Mol Pharmacol*. **63**, 1256–1272

5. Hauser, A. S., Attwood, M. M., Rask-Andersen, M., Schiöth, H. B., and Gloriam, D. E. (2017) Trends in GPCR drug discovery: new agents, targets and indications. *Nature reviews. Drug discovery*. **16**, 829–842

6. Sriram, K., and Insel, P. A. (2018) G Protein-Coupled Receptors as Targets for Approved Drugs: How Many Targets and How Many Drugs? *Mol Pharmacol*. **93**, 251–258

7. Schiöth, H. B., and Fredriksson, R. (2005) The GRAFS classification system of G-protein coupled receptors in comparative perspective. *Gen. Comp. Endocrinol.* **142**, 94–101

8. Joost, P., and Methner, A. (2002) Phylogenetic analysis of 277 human G-protein-coupled receptors as a tool for the prediction of orphan receptor ligands. *Genome Biol*. **3**, research0063.1-research0063.16

9. Weis, W. I., and Kobilka, B. K. (2018) The Molecular Basis of G Protein–Coupled Receptor Activation. *Annual review of biochemistry*. **87**, 897–919

10. Bouvier, M. (2013) Unraveling the structural basis of GPCR activation and inactivation. *Nature structural & molecular biology*. **20**, 539–541

11. Sato, T., Kawasaki, T., Mine, S., and Matsumura, H. (2016) Functional Role of the C-Terminal Amphipathic Helix 8 of Olfactory Receptors and Other G Protein-Coupled Receptors. *Int J Mol Sci*. 10.3390/ijms17111930

12. Manglik, A., and Kruse, A. C. (2017) Structural Basis for G Protein-Coupled Receptor Activation. *Biochemistry*. **56**, 5628–5634

13. Schrage, R., and Kostenis, E. (2017) Functional selectivity and dualsteric/bitopic GPCR targeting. *Current Opinion in Pharmacology*. **32**, 85–90

14. Trzaskowski, B., Latek, D., Yuan, S., Ghoshdastider, U., Debinski, A., and Filipek, S. (2012) Action of Molecular Switches in GPCRs - Theoretical and Experimental Studies. *Curr Med Chem*. **19**, 1090–1109

15. Katritch, V., Cherezov, V., and Stevens, R. C. (2013) Structure-function of the G protein-coupled receptor superfamily. *Annual Review of Pathology: Mechanisms of Disease*. **53**, 531–556

16. Lagerstrom, M. C., and Schioth, H. B. (2008) Structural diversity of G protein-coupled receptors and significance for drug discovery. *Nature reviews. Drug discovery*. **7**, 339–357

17. Cabrera-Vera, T. M., Vanhauwe, J., Thomas, T. O., Medkova, M., Preininger, A., Mazzoni, M. R., and Hamm, H. E. (2003) Insights into G protein structure, function, and regulation. *Endocr Rev*. **24**, 765–781

18. Wettschureck, N., and Offermanns, S. (2005) Mammalian G proteins and their cell type specific functions. *Physiol Rev*. **85**, 1159–1204

19. Gilman, A. G. (1987) G proteins: transducers of receptor-generated signals. *Annu Rev Biochem*. **56**, 615–649

20. Mahoney, J. P., and Sunahara, R. K. (2016) Mechanistic insights into GPCR–G protein interactions. *Current Opinion in Structural Biology*. **41**, 247–254

21. Bunemann, M., Frank, M., and Lohse, M. J. (2003) Gi protein activation in intact cells involves subunit rearrangement rather than dissociation. *Proceedings of the National Academy of Sciences*. **100**, 16077–16082

22. Galés, C., Van Durm, J. J. J., Schaak, S., Pontier, S., Percherancier, Y., Audet, M., Paris, H., and Bouvier, M. (2006) Probing the activation-promoted structural rearrangements in preassembled receptor–G protein complexes. *Nature Structural & Molecular Biology*. **13**, 778–786

23. Smrcka, A. V. (2008) G protein βγ subunits: Central mediators of G protein-coupled receptor signaling. *Cell. Mol. Life Sci.* **65**, 2191–2214

24. Berman, D. M., and Gilman, A. G. (1998) Mammalian RGS Proteins: Barbarians at the Gate. *J. Biol. Chem.* **273**, 1269–1272

25. Gurevich, V. V., and Gurevich, E. V. (2019) GPCR Signaling Regulation: The Role of GRKs and Arrestins. *Front. Pharmacol.* 10.3389/fphar.2019.00125

26. Cahill, T. J., Thomsen, A. R. B., Tarrasch, J. T., Plouffe, B., Nguyen, A. H., Yang, F., Huang, L.-Y., Kahsai, A. W., Bassoni, D. L., Gavino, B. J., Lamerdin, J. E.,

Triest, S., Shukla, A. K., Berger, B., Little, J., Antar, A., Blanc, A., Qu, C.-X., Chen, X., Kawakami, K., Inoue, A., Aoki, J., Steyaert, J., Sun, J.-P., Bouvier, M., Skiniotis, G., and Lefkowitz, R. J. (2017) Distinct conformations of GPCR–β-arrestin complexes mediate desensitization, signaling, and endocytosis. *Proceedings of the National Academy of Sciences*. **114**, 2562–2567

27. Sente, A., Peer, R., Srivastava, A., Baidya, M., Lesk, A. M., Balaji, S., Shukla, A. K., Babu, M. M., and Flock, T. (2018) Molecular mechanism of modulating arrestin conformation by GPCR phosphorylation. *Nature Structural & Molecular Biology*. **25**, 538–545

28. Shukla, A. K., Westfield, G. H., Xiao, K., Reis, R. I., Huang, L.-Y., Tripathi-Shukla, P., Qian, J., Li, S., Blanc, A., Oleskie, A. N., Dosey, A. M., Su, M., Liang, C.-R., Gu, L.-L., Shan, J.-M., Chen, X., Hanna, R., Choi, M., Yao, X. J., Klink, B. U., Kahsai, A. W., Sidhu, S. S., Koide, S., Penczek, P. A., Kossiakoff, A. A., Woods Jr, V. L., Kobilka, B. K., Skiniotis, G., and Lefkowitz, R. J. (2014) Visualization of arrestin recruitment by a G-protein-coupled receptor. *Nature*. **512**, 218–222

29. Ferguson, S. S. G., Downey, W. E., Colapietro, A.-M., Barak, L. S., Ménard, L., and Caron, M. G. (1996) Role of β-Arrestin in Mediating Agonist-Promoted G Protein-Coupled Receptor Internalization. *Science*. **271**, 363–366

30. Lefkowitz, R. J., and Shenoy, S. K. (2005) Transduction of receptor signals by beta-arrestins. *Science*. **308**, 512–517

31. Peterson, Y. K., and Luttrell, L. M. (2017) The Diverse Roles of Arrestin Scaffolds in G Protein-Coupled Receptor Signaling. *Pharmacol Rev*. **69**, 256–297

32. Jean-Charles, P.-Y., Kaur, S., and Shenoy, S. K. (2017) GPCR signaling via β-arrestin-dependent mechanisms. *J Cardiovasc Pharmacol*. **70**, 142–158

33. Oakley, R. H., Laporte, S. A., Holt, J. A., Caron, M. G., and Barak, L. S. (2000) Differential Affinities of Visual Arrestin, βArrestin1, and βArrestin2 for G Protein-coupled Receptors Delineate Two Major Classes of Receptors. *The Journal of biological chemistry*. **275**, 17201–17210

34. Thomsen, A. R. B., Plouffe, B., Cahill, T. J., Shukla, A. K., Tarrasch, J. T., Dosey, A. M., Kahsai, A. W., Strachan, R. T., Pani, B., Mahoney, J. P., Huang, L., Breton, B., Heydenreich, F. M., Sunahara, R. K., Skiniotis, G., Bouvier, M., and Lefkowitz, R. J. (2016) GPCR-G Protein-β-Arrestin Super-Complex Mediates Sustained G Protein Signaling. *Cell*. **166**, 907–919

35. Tian, X., Kang, D. S., and Benovic, J. L. (2014) β-arrestins and G Protein-Coupled Receptor Trafficking. *Handb Exp Pharmacol*. **219**, 173–186

36. Shenoy, S. K., Drake, M. T., Nelson, C. D., Houtz, D. A., Xiao, K., Madabushi, S., Reiter, E., Premont, R. T., Lichtarge, O., and Lefkowitz, R. J. (2006) beta-arrestin-

dependent, G protein-independent ERK1/2 activation by the beta2 adrenergic receptor. *The Journal of biological chemistry*. **281**, 1261–1273

37. van Gastel, J., Hendrickx, J. O., Leysen, H., Santos-Otte, P., Luttrell, L. M., Martin, B., and Maudsley, S. (2018) β-Arrestin Based Receptor Signaling Paradigms: Potential Therapeutic Targets for Complex Age-Related Disorders. *Front. Pharmacol.* 10.3389/fphar.2018.01369

38. Dewire, S. M., Ahn, S., Lefkowitz, R. J., and Shenoy, S. K. (2007) Beta-arrestins and cell signaling. *Annual review of physiology*. **69**, 483–510

39. Kenakin, T. (2019) Biased Receptor Signaling in Drug Discovery. *Pharmacol Rev*. **71**, 267–315

40. Rajagopal, S., Rajagopal, K., and Lefkowitz, R. J. (2011) Teaching old receptors new tricks: biasing seven-transmembrane receptors. *Nature reviews. Drug discovery*. **9**, 373–386

41. Seyedabadi, M., Ghahremani, M. H., and Albert, P. R. (2019) Biased signaling of G protein coupled receptors (GPCRs): Molecular determinants of GPCR/transducer selectivity and therapeutic potential. *Pharmacol. Ther.* **200**, 148–178

42. Jarpe, M. B., Knall, C., Mitchell, F. M., Buhl, A. M., Duzic, E., and Johnson, G. L. (1998) [d-Arg ^{1} ,d-Phe ^{5} ,d-Trp ^{7,9} ,Leu ^{11}]Substance P Acts as a Biased Agonist toward Neuropeptide and Chemokine Receptors. *J. Biol. Chem.* **273**, 3097–3104

43. Kenakin, T. (1995) Agonist-receptor efficacy. II. Agonist trafficking of receptor signals. *Trends in Pharmacological Sciences*. **16**, 232–238

44. Kudlacek, O., Waldhoer, M., Kassack, M. U., Nickel, P., Salmi, J. I., Freissmuth, M., and Nanoff, C. (2002) Biased inhibition by a suramin analogue of A1-adenosine receptor/G protein coupling in fused receptor/G protein tandems: the A1-adenosine receptor is predominantly coupled to Goalpha in human brain. *Naunyn Schmiedebergs Arch. Pharmacol.* **365**, 8–16

45. Manning, D. R. (2002) Measures of Efficacy Using G Proteins as Endpoints: Differential Engagement of G Proteins through Single Receptors. *Mol Pharmacol*. **62**, 451–452

46. Michel, M. C., and Alewijnse, A. E. (2007) Ligand-Directed Signaling: 50 Ways to Find a Lover. *Mol Pharmacol*. **72**, 1097–1099

47. Patel, C. B., Noor, N., and Rockman, H. A. (2010) Functional Selectivity in Adrenergic and Angiotensin Signaling Systems. *Mol Pharmacol*. **78**, 983–992

48. Rankovic, Z., Brust, T. F., and Bohn, L. M. (2016) Biased agonism: An emerging paradigm in GPCR drug discovery. *Bioorganic & Medicinal Chemistry Letters*. **26**, 241–250

49. Whistler, J. L., Chuang, H. H., Chu, P., Jan, L. Y., and von Zastrow, M. (1999) Functional dissociation of mu opioid receptor signaling and endocytosis: implications for the biology of opiate tolerance and addiction. *Neuron*. **23**, 737–746

50. Costa-Neto, C. M., Parreiras-e-Silva, L. T., and Bouvier, M. (2016) A Pluridimensional View of Biased Agonism. *Mol Pharmacol*. **90**, 587–595

51. Kenakin, T., and Miller, L. J. (2010) Seven Transmembrane Receptors as Shapeshifting Proteins: The Impact of Allosteric Modulation and Functional Selectivity on New Drug Discovery. *Pharmacological Reviews*. **62**, 265–304

52. Kenakin, T. P., and Morgan, P. H. (1989) Theoretical effects of single and multiple transducer receptor coupling proteins on estimates of the relative potency of agonists. *Molecular pharmacology*. **35**, 214–222

53. Bohn, L. M., Gainetdinov, R. R., Lin, F. T., Lefkowitz, R. J., and Caron, M. G. (2000) Mu-opioid receptor desensitization by beta-arrestin-2 determines morphine tolerance but not dependence. *Nature*. **408**, 720–723

54. Thompson, G. L., Lane, J. R., Coudrat, T., Sexton, P. M., Christopoulos, A., and Canals, M. (2015) Biased Agonism of Endogenous Opioid Peptides at the μ -Opioid Receptor. *Mol Pharmacol*. **88**, 335–346

55. Soergel, D. G., Subach, R. A., Burnham, N., Lark, M. W., James, I. E., Sadler, B. M., Skobieranda, F., Violin, J. D., and Webster, L. R. (2014) Biased agonism of the μ-opioid receptor by TRV130 increases analgesia and reduces on-target adverse effects versus morphine: A randomized, double-blind, placebo-controlled, crossover study in healthy volunteers. *PAIN*. **155**, 1829–1835

56. Fossler, M. J., Sadler, B. M., Farrell, C., Burt, D. A., Pitsiu, M., Skobieranda, F., and Soergel, D. G. (2018) Oliceridine (TRV130), a Novel G Protein-Biased Ligand at the μ-Opioid Receptor, Demonstrates a Predictable Relationship Between Plasma Concentrations and Pain Relief. I: Development of a Pharmacokinetic/Pharmacodynamic Model. *J Clin Pharmacol*. **58**, 750–761

57. Urban, J. D., Clarke, W. P., von Zastrow, M., Nichols, D. E., Kobilka, B., Weinstein, H., Javitch, J. A., Roth, B. L., Christopoulos, A., Sexton, P. M., Miller, K. J., Spedding, M., and Mailman, R. B. (2007) Functional selectivity and classical concepts of quantitative pharmacology. *The Journal of pharmacology and experimental therapeutics*. **320**, 1–13

58. Cooper, B. (2005) Osler's role in defining the third corpuscle, or "blood plates." *Proc (Bayl Univ Med Cent)*. **18**, 376–378

59. Ribatti, D., and Crivellato, E. (2007) Giulio Bizzozero and the discovery of platelets. *Leuk. Res.* **31**, 1339–1341

60. Kaushansky, K. (2008) Historical review: megakaryopoiesis and thrombopoiesis. *Blood*. **111**, 981–986

61. Machlus, K. R., and Italiano, J. E. (2013) The incredible journey: From megakaryocyte development to platelet formation. *J Cell Biol*. **201**, 785–796

62. Noetzli Leila J., French Shauna L., and Machlus Kellie R. (2019) New Insights Into the Differentiation of Megakaryocytes From Hematopoietic Progenitors. *Arteriosclerosis, Thrombosis, and Vascular Biology*. **39**, 1288–1300

63. Leeksma, C. H. W., and Cohen, J. A. (1955) Determination of the Life of Human Blood Platelets using Labelled Di iso propylfluorophosphonate. *Nature*. **175**, 552–553

64. Robinson, M., Machin, S., Mackie, I., and Harrison, P. (2000) In vivo biotinylation studies: specificity of labelling of reticulated platelets by thiazole orange and mepacrine. *British Journal of Haematology*. **108**, 859–864

65. Mason, K. D., Carpinelli, M. R., Fletcher, J. I., Collinge, J. E., Hilton, A. A., Ellis, S., Kelly, P. N., Ekert, P. G., Metcalf, D., Roberts, A. W., Huang, D. C. S., and Kile, B. T. (2007) Programmed Anuclear Cell Death Delimits Platelet Life Span. *Cell*. **128**, 1173–1186

66. Flaumenhaft Robert (2003) Molecular Basis of Platelet Granule Secretion. *Arteriosclerosis, Thrombosis, and Vascular Biology*. **23**, 1152–1160

67. Selvadurai, M. V., and Hamilton, J. R. (2018) Structure and function of the open canalicular system – the platelet's specialized internal membrane network. *Platelets*. **29**, 319–325

68. Andersen, H., Greenberg, D. L., Fujikawa, K., Xu, W., Chung, D. W., and Davie, E. W. (1999) Protease-activated receptor 1 is the primary mediator of thrombin-stimulated platelet procoagulant activity. *PNAS*. **96**, 11189–11193

69. Deanfield, J., Donald, A., Ferri, C., Giannattasio, C., Halcox, J., Halligan, S., Lerman, A., Mancia, G., Oliver, J. J., and Pessina, A. C. (2005) Endothelial function and dysfunction. Part I: Methodological issues for assessment in the different vascular beds: a statement by the Working Group on Endothelin and Endothelial Factors of the European Society of Hypertension. *Journal of hypertension*. **23**, 7–17

70. Ding, H., and Triggle, C. R. (2010) Endothelial dysfunction in diabetes: multiple targets for treatment. *Pflügers Archiv : European journal of physiology*. **459**, 977–994

71. Pober, J. S., Min, W., and Bradley, J. R. (2009) Mechanisms of Endothelial Dysfunction, Injury, and Death. *Annual Review of Pathology: Mechanisms of Disease*. **4**, 71–95

72. Dowal, L., and Flaumenhaft, R. (2011) Targeting platelet G-protein coupled receptors (GPCRs): looking beyond conventional GPCR antagonism. *Curr Vasc Pharmacol*. **8**, 140–154

73. Arachiche, A., Fuente, M. de la, and Nieman, M. T. (2014) Platelet Specific Promoters Are Insufficient to Express Protease Activated Receptor 1 (PAR1) Transgene in Mouse Platelets. *PLOS ONE*. **9**, e97724

74. Coughlin, S. R. (2005) Protease-activated receptors in hemostasis, thrombosis and vascular biology. *J Thromb Haemost*. **3**, 1800–1814

75. Rasmussen, U. B., Vouret-Craviari, V., Jallat, S., Schlesinger, Y., Pages, G., Pavirani, A., Lecocq, J. P., Pouyssegur, J., and Van Obberghen-Schilling, E. (1991) cDNA cloning and expression of a hamster alpha-thrombin receptor coupled to Ca2+ mobilization. *FEBS Lett*. **288**, 123–128

76. Vu, T. K., Hung, D. T., Wheaton, V. I., and Coughlin, S. R. (1991) Molecular cloning of a functional thrombin receptor reveals a novel proteolytic mechanism of receptor activation. *Cell*. **64**, 1057–1068

77. Xu, W. F., Andersen, H., Whitmore, T. E., Presnell, S. R., Yee, D. P., Ching, A., Gilbert, T., Davie, E. W., and Foster, D. C. (1998) Cloning and characterization of human protease-activated receptor 4. *Proceedings of the National Academy of Sciences of the United States of America*. **95**, 6642–6646

78. Hung, D. T., Wong, Y. H., Vu, T. K., and Coughlin, S. R. (1992) The cloned platelet thrombin receptor couples to at least two distinct effectors to stimulate phosphoinositide hydrolysis and inhibit adenylyl cyclase. *The Journal of biological chemistry*. **267**, 20831–20834

79. McCoy, K. L., Traynelis, S. F., and Hepler, J. R. (2010) PAR1 and PAR2 couple to overlapping and distinct sets of G proteins and linked signaling pathways to differentially regulate cell physiology. *Molecular pharmacology*. **77**, 1005–1015

80. Voss, B., McLaughlin, J. N., Holinstat, M., Zent, R., and Hamm, H. E. (2007) PAR1, but not PAR4, activates human platelets through a Gi/o/phosphoinositide-3 kinase signaling axis. *Molecular pharmacology*. **71**, 1399–1406

81. Kim, S., Foster, C., Lecchi, A., Quinton, T. M., Prosser, D. M., Jin, J., Cattaneo, M., and Kunapuli, S. P. (2002) Protease-activated receptors 1 and 4 do not stimulate G(i) signaling pathways in the absence of secreted ADP and cause human platelet aggregation independently of G(i) signaling. *Blood*. **99**, 3629–3636

82. Nylander, S., Mattsson, C., Ramström, S., and Lindahl, T. L. (2003) The relative importance of the ADP receptors, P2Y12 and P2Y1, in thrombin-induced platelet activation. *Thrombosis Research*. **111**, 65–73

83. Shapiro, M. J., Weiss, E. J., Faruqi, T. R., and Coughlin, S. R. (2000) Protease-activated receptors 1 and 4 are shut off with distinct kinetics after activation by thrombin. *The Journal of biological chemistry*. **275**, 25216–25221

84. Thibeault, P. E., LeSarge, J. C., Arends, D., Fernandes, M., Chidiac, P., Stathopulos, P. B., Luyt, L. G., and Ramachandran, R. (2019) Molecular basis for activation and biased signalling at the thrombin-activated GPCR Proteinase Activated Receptor-4 (PAR4). *J. Biol. Chem.* 10.1074/jbc.RA119.011461

85. Ramachandran, R., Mihara, K., Thibeault, P., Vanderboor, C. M., Petri, B., Saifeddine, M., Bouvier, M., and Hollenberg, M. D. (2017) Targeting a Proteinase-Activated Receptor 4 (PAR4) Carboxyl Terminal Motif to Regulate Platelet Function. *Molecular pharmacology*. **91**, 287–295

86. Soh, U. J., and Trejo, J. (2011) Activated protein C promotes protease-activated receptor-1 cytoprotective signaling through beta-arrestin and dishevelled-2 scaffolds. *Proceedings of the National Academy of Sciences of the United States of America*. **108**, E1372–80

87. Kanki, H., Sasaki, T., Matsumura, S., Yokawa, S., Yukami, T., Shimamura, M., Sakaguchi, M., Furuno, T., Suzuki, T., and Mochizuki, H. (2019) β-arrestin-2 in PAR-1-biased signaling has a crucial role in endothelial function via PDGF-β in stroke. *Cell Death & Disease*. **10**, 1–16

88. Khan, A., Li, D., Ibrahim, S., Smyth, E., and Woulfe, D. S. (2014) The Physical Association of the P2Y12 Receptor with PAR4 Regulates Arrestin-Mediated Akt Activation. *Molecular pharmacology*. **86**, 1–11

89. Smith, T. H., Li, J. G., Dores, M. R., and Trejo, J. (2017) Protease-activated receptor-4 and purinergic receptor P2Y12 dimerize, co-internalize, and activate Akt signaling via endosomal recruitment of β-arrestin. *The Journal of biological chemistry*. **292**, 13867–13878

90. Khan, A., Li, D., Ibrahim, S., Smyth, E., and Woulfe, D. (2011) Direct Association of PAR4 with P2Y12 Is Required for PAR4-Induced Recruitment of Arrestin-2: Structural and Functional Analysis of a GPCR Heterodimer,. *Blood*. **118**, 3253–3253

91. Chackalamannil, S., Wang, Y., Greenlee, W. J., Hu, Z., Xia, Y., Ahn, H.-S., Boykow, G., Hsieh, Y., Palamanda, J., Agans-Fantuzzi, J., Kurowski, S., Graziano, M., and Chintala, M. (2008) Discovery of a novel, orally active himbacine-based thrombin receptor antagonist (SCH 530348) with potent antiplatelet activity. *J. Med. Chem.* **51**, 3061–3064

92. Morrow, D. A., Braunwald, E., Bonaca, M. P., Ameriso, S. F., Dalby, A. J., Fish, M. P., Fox, K. A., Lipka, L. J., Liu, X., Nicolau, J. C., Ophuis, A. J., Paolasso, E., Scirica, B. M., Spinar, J., Theroux, P., Wiviott, S. D., Strony, J., and Murphy, S. A. (2012) Vorapaxar in the secondary prevention of atherothrombotic events. *The New England journal of medicine*. **366**, 1404–1413

93. Algahtani, F. (2017) Clinical use of vorapaxar as an emerging antithrombin agent: A literature review of current evidence. *J Appl Hematol*. **8**, 127

94. Barry, K., and Somerville, N. (2015) Vorapaxar (Zontivity) for the Prevention of Thrombotic Cardiovascular Events. *AFP*. **92**, 304–305

95. Fala, L. (2015) Zontivity (Vorapaxar), First-in-Class PAR-1 Antagonist, Receives FDA Approval for Risk Reduction of Heart Attack, Stroke, and Cardiovascular Death. *American Health & Drug Benefits*. **8**, 148

96. Kraft, W., Gilmartin, J., Chappell, D., Gheyas, F., Walker, B., Nagalla, S., Naik, U., Horrow, J., Wrishko, R., Zhang, S., and Anderson, M. (2016) Effect of Vorapaxar Alone and in Combination with Aspirin on Bleeding Time and Platelet Aggregation in Healthy Adult Subjects. *Clin Transl Sci*. **9**, 221–227

97. Morrow, D. A., Braunwald, E., Bonaca, M. P., Ameriso, S. F., Dalby, A. J., Fish, M. P., Fox, K. A., Lipka, L. J., Liu, X., Nicolau, J. C., Ophuis, A. J., Paolasso, E., Scirica, B. M., Spinar, J., Theroux, P., Wiviott, S. D., Strony, J., and Murphy, S. A. (2012) Vorapaxar in the secondary prevention of atherothrombotic events. *The New England journal of medicine*. **366**, 1404–1413

98. Morrow, D. A., Alberts, M. J., Mohr, J. P., Ameriso, S. F., Bonaca, M. P., Goto, S., Hankey, G. J., Murphy, S. A., Scirica, B. M., and Braunwald, E. (2013) Efficacy and Safety of Vorapaxar in Patients With Prior Ischemic Stroke. *Stroke*. **44**, 691–698

99. Tricoci, P., Huang, Z., Held, C., Moliterno, D. J., Armstrong, P. W., Van de Werf, F., White, H. D., Aylward, P. E., Wallentin, L., Chen, E., Lokhnygina, Y., Pei, J., Leonardi, S., Rorick, T. L., Kilian, A. M., Jennings, L. H., Ambrosio, G., Bode, C., Cequier, A., Cornel, J. H., Diaz, R., Erkan, A., Huber, K., Hudson, M. P., Jiang, L., Jukema, J. W., Lewis, B. S., Lincoff, A. M., Montalescot, G., Nicolau, J. C., Ogawa, H., Pfisterer, M., Prieto, J. C., Ruzyllo, W., Sinnaeve, P. R., Storey, R. F., Valgimigli, M., Whellan, D. J., Widimsky, P., Strony, J., Harrington, R. A., and Mahaffey, K. W. (2012) Thrombin-receptor antagonist vorapaxar in acute coronary syndromes. *The New England journal of medicine*. **366**, 20–33

100. Gryka, R. J., Buckley, L. F., and Anderson, S. M. (2017) Vorapaxar: The Current Role and Future Directions of a Novel Protease-Activated Receptor Antagonist for Risk Reduction in Atherosclerotic Disease. *Drugs R D*. **17**, 65–72

101. Han, X., and Nieman, M. T. (2017) Protease activated receptor 4: a backup receptor or a dark horse as a target in antiplatelet therapy? *Annals of Translational Medicine*. **6**, 19

102. Ramachandran, R., Noorbakhsh, F., Defea, K., and Hollenberg, M. D. (2012) Targeting proteinase-activated receptors: therapeutic potential and challenges. *Nature reviews. Drug discovery*. **11**, 69–86

103. Ko, F. N., Wu, C. C., Kuo, S. C., Lee, F. Y., and Teng, C. M. (1994) YC-1, a novel activator of platelet guanylate cyclase. *Blood*. **84**, 4226–4233

104. Lee, F.-Y., Lien, J.-C., Huang, L.-J., Huang, T.-M., Tsai, S.-C., Teng, C.-M., Wu, C.-C., Cheng, F.-C., and Kuo, S.-C. (2001) Synthesis of 1-Benzyl-3-(5‘-hydroxymethyl-2‘-furyl)indazole Analogues as Novel Antiplatelet Agents. *J. Med. Chem.* **44**, 3746–3749

105. Chen, H. S., Kuo, S. C., Teng, C. M., Lee, F. Y., Wang, J. P., Lee, Y. C., Kuo, C. W., Huang, C. C., Wu, C. C., and Huang, L. J. (2008) Synthesis and antiplatelet activity of ethyl 4-(1-benzyl-1H-indazol-3-yl)benzoate (YD-3) derivatives. *Bioorg Med Chem*. **16**, 1262–1278

106. Young, S. E., Duvernay, M. T., Schulte, M. L., Nance, K. D., Melancon, B. J., Engers, J., Wood, M. R., Hamm, H. E., and Lindsley, C. W. (2010) A Novel and Selective PAR4 Antagonist: ML354. in *Probe Reports from the NIH Molecular Libraries Program*, National Center for Biotechnology Information (US), Bethesda (MD), [online] http://www.ncbi.nlm.nih.gov/books/NBK280043/ (Accessed June 4, 2019)

107. Chen, P., Ren, S., Song, H., Chen, C., Chen, F., Xu, Q., Kong, Y., and Sun, H. (2019) Synthesis and biological evaluation of BMS-986120 and its deuterated derivatives as PAR4 antagonists. *Bioorganic & Medicinal Chemistry*. **27**, 116–124

108. Wilson, S. J., Ismat, F. A., Wang, Z., Cerra, M., Narayan, H., Raftis, J., Gray, T. J., Connell, S., Garonzik, S., Ma, X., Yang, J., and Newby, D. E. (2017) PAR4 (Protease-Activated Receptor 4) Antagonism With BMS-986120 Inhibits Human Ex Vivo Thrombus Formation. *Arteriosclerosis, Thrombosis, and Vascular Biology*. 10.1161/ATVBAHA.117.310104

109. Wong, P. C., Seiffert, D., Bird, J. E., Watson, C. A., Bostwick, J. S., Giancarli, M., Allegretto, N., Hua, J., Harden, D., Guay, J., Callejo, M., Miller, M. M., Lawrence, R. M., Banville, J., Guy, J., Maxwell, B. D., Priestley, E. S., Marinier, A., Wexler, R. R., Bouvier, M., Gordon, D. A., Schumacher, W. A., and Yang, J. (2017) Blockade of protease-activated receptor-4 (PAR4) provides robust antithrombotic activity with low bleeding. *Science translational medicine*. **9**, eaaf5294

110. Li, D., D’Angelo, L., Chavez, M., and Woulfe, D. S. (2011) Arrestin-2 Differentially Regulates PAR4 and ADP Receptor Signaling in Platelets. *J. Biol. Chem.* **286**, 3805–3814

111. Vanderboor, C. M., Thibeault, P. E., Nixon, K. C., Gros, R., Kramer, J. M., and Ramachandran, R. (2020) Proteinase-Activated Receptor 4 (PAR4) Activation Triggers Cell Membrane Blebbing through RhoA and β-arrestin. *Mol Pharmacol*. 10.1124/mol.119.118232

112. Narumiya, S., Sugimoto, Y., and Ushikubi, F. (1999) Prostanoid Receptors: Structures, Properties, and Functions. *Physiological Reviews*. **79**, 1193–1226

113. Woodward, D. F., Jones, R. L., and Narumiya, S. (2011) International Union of Basic and Clinical Pharmacology. LXXXIII: classification of prostanoid receptors, updating 15 years of progress. *Pharmacological Reviews*. **63**, 471–538

114. Offermanns, S., Laugwitz, K. L., Spicher, K., and Schultz, G. (1994) G proteins of the G12 family are activated via thromboxane A2 and thrombin receptors in human platelets. *Proceedings of the National Academy of Sciences of the United States of America*. **91**, 504–508

115. Bunting, S., Moncada, S., Vane, J. R., and Gryglewski, R. (1976) Arterial walls generate from prostaglandin endoperoxides a substance (prostaglandin X) which relaxes strips of mesenteric and coeliac arteries and inhibits platelet aggregation. *Prostaglandins*. **12**, 897–913

116. Moncada, S., Gryglewski, R., Bunting, S., and Vane, J. R. (1976) An enzyme isolated from arteries transforms prostaglandin endoperoxides to an unstable substance that inhibits platelet aggregation. *Nature*. **263**, 663–665

117. Radomski, M. W., Palmer, R. M., and Moncada, S. (1987) Endogenous nitric oxide inhibits human platelet adhesion to vascular endothelium. *The Lancet*. **2**, 1057–1058

118. Aburima, A., Walladbegi, K., Wake, J. D., and Naseem, K. M. (2017) cGMP signaling inhibits platelet shape change through regulation of the RhoA-Rho Kinase-MLC phosphatase signaling pathway. *Journal of Thrombosis and Haemostasis*. **15**, 1668–1678

119. Aburima, A., Wraith, K. S., Raslan, Z., Law, R., Magwenzi, S., and Naseem, K. M. (2013) cAMP signaling regulates platelet myosin light chain (MLC) phosphorylation and shape change through targeting the RhoA-Rho kinase-MLC phosphatase signaling pathway. *Blood*. **122**, 3533–3545

120. Murata, T., Ushikubi, F., Matsuoka, T., Hirata, M., Yamasaki, A., Sugimoto, Y., Ichikawa, A., Aze, Y., Tanaka, T., Yoshida, N., Ueno, A., Oh-ishi, S., and Narumiya, S. (1997) Altered pain perception and inflammatory response in mice lacking prostacyclin receptor. *Nature*. **388**, 678–682

121. Thomas, D. W., Mannon, R. B., Mannon, P. J., Latour, A., Oliver, J. A., Hoffman, M., Smithies, O., Koller, B. H., and Coffman, T. M. (1998) Coagulation defects

and altered hemodynamic responses in mice lacking receptors for thromboxane A2. *J Clin Invest*. **102**, 1994–2001

122. Buchanan, F. G., Gorden, D. L., Matta, P., Shi, Q., Matrisian, L. M., and DuBois, R. N. (2006) Role of β-arrestin 1 in the metastatic progression of colorectal cancer. *PNAS*. **103**, 1492–1497

123. Chu, C.-H., Chen, S.-H., Wang, Q., Langenbach, R., Li, H., Zeldin, D., Chen, S.-L., Wang, S., Gao, H., Lu, R.-B., and Hong, J.-S. (2015) PGE2 Inhibits IL-10 Production via EP2-Mediated β-Arrestin Signaling in Neuroinflammatory Condition. *Mol. Neurobiol.* **52**, 587–600

124. Chun, K.-S., Lao, H.-C., and Langenbach, R. (2010) The Prostaglandin E2 Receptor, EP2, Stimulates Keratinocyte Proliferation in Mouse Skin by G Protein-dependent and β-Arrestin1-dependent Signaling Pathways. *J. Biol. Chem.* **285**, 39672–39681

125. Kim, J. I., Lakshmikanthan, V., Frilot, N., and Daaka, Y. (2010) Prostaglandin E2 Promotes Lung Cancer Cell Migration via EP4-βArrestin1-c-Src Signalsome. *Mol Cancer Res*. **8**, 569–577

126. Woulfe, D. S. (2010) Akt signaling in platelets and thrombosis. *Expert Review of Hematology*. **3**, 81–91

127. Needleman, P., Minkes, M., and Raz, A. (1976) Thromboxanes: selective biosynthesis and distinct biological properties. *Science*. **193**, 163–165

128. Needleman, P., Moncada, S., Bunting, S., Vane, J. R., Hamberg, M., and Samuelsson, B. (1976) Identification of an enzyme in platelet microsomes which generates thromboxane A2 from prostaglandin endoperoxides. *Nature*. **261**, 558–560

129. Caughey, G. E., Cleland, L. G., Penglis, P. S., Gamble, J. R., and James, M. J. (2001) Roles of Cyclooxygenase (COX)-1 and COX-2 in Prostanoid Production by Human Endothelial Cells: Selective Up-Regulation of Prostacyclin Synthesis by COX-2. *The Journal of Immunology*. **167**, 2831–2838

130. FitzGerald, G. A. (2004) Coxibs and Cardiovascular Disease. *N Engl J Med*. **351**, 1709–1711

131. McAdam, B. F., Catella-Lawson, F., Mardini, I. A., Kapoor, S., Lawson, J. A., and FitzGerald, G. A. (1999) Systemic biosynthesis of prostacyclin by cyclooxygenase (COX)-2: The human pharmacology of a selective inhibitor of COX-2. *PNAS*. **96**, 272–277

132. Yu, Y., Ricciotti, E., Scalia, R., Tang, S. Y., Grant, G., Yu, Z., Landesberg, G., Crichton, I., Wu, W., Puré, E., Funk, C. D., and FitzGerald, G. A. (2012) Vascular

COX-2 Modulates Blood Pressure and Thrombosis in Mice. *Science Translational Medicine*. **4**, 132ra54-132ra54

133. Ritter, J. M. (2011) TP receptor antagonists (TXRAs): expensive irrelevance or wonder drugs strangled at birth? *British Journal of Clinical Pharmacology*. **71**, 801–803

134. Born, G. V. R. (1962) Aggregation of Blood Platelets by Adenosine Diphosphate and its Reversal. *Nature*. **194**, 927–929

135. Born, G. V. R., and Cross, M. J. (1963) The aggregation of blood platelets. *The Journal of Physiology*. **168**, 178–195

136. Hollopeter, G., Jantzen, H. M., Vincent, D., Li, G., England, L., Ramakrishnan, V., Yang, R. B., Nurden, P., Nurden, A., Julius, D., and Conley, P. B. (2001) Identification of the platelet ADP receptor targeted by antithrombotic drugs. *Nature*. **409**, 202–207

137. Jin, J., Daniel, J. L., and Kunapuli, S. P. (1998) Molecular basis for ADP-induced platelet activation. II. The P2Y1 receptor mediates ADP-induced intracellular calcium mobilization and shape change in platelets. *J. Biol. Chem.* **273**, 2030–2034

138. Jin, J., and Kunapuli, S. P. (1998) Coactivation of two different G protein-coupled receptors is essential for ADP-induced platelet aggregation. *PNAS*. **95**, 8070–8074

139. Foster, C. J., Prosser, D. M., Agans, J. M., Zhai, Y., Smith, M. D., Lachowicz, J. E., Zhang, F. L., Gustafson, E., Monsma, F. J., Wiekowski, M. T., Abbondanzo, S. J., Cook, D. N., Bayne, M. L., Lira, S. A., and Chintala, M. S. (2001) Molecular identification and characterization of the platelet ADP receptor targeted by thienopyridine antithrombotic drugs. *J Clin Invest*. **107**, 1591–1598

140. Woulfe, D., Yang, J., and Brass, L. (2001) ADP and platelets: the end of the beginning. *J Clin Invest*. **107**, 1503–1505

141. Dorsam, R. T., and Kunapuli, S. P. (2004) Central role of the $P2Y_{12}$ receptor in platelet activation. *J Clin Invest*. **113**, 340–345

142. Hardy, A. R., Conley, P. B., Luo, J., Benovic, J. L., Poole, A. W., and Mundell, S. J. (2005) P2Y1 and P2Y12 receptors for ADP desensitize by distinct kinase-dependent mechanisms. *Blood*. **105**, 3552–3560

143. Chen, X., Gupta, S., Cooper, M., DeHelian, D., Zhao, X., Naik, M. U., Wurtzel, J. G. T., Stalker, T. J., Goldfinger, L. E., Benovic, J., Brass, L. F., McKenzie, S. E., Naik, U. P., and Ma, P. (2020) GRK6 regulates the hemostatic response to injury through its rate-limiting effects on GPCR signaling in platelets. *Blood Advances*. **4**, 76–86

144. Hasegawa, S., Ichiyama, T., Hashimoto, K., Suzuki, Y., Hirano, R., Fukano, R., and Furukawa, S. (2010) Functional expression of cysteinyl leukotriene receptors on human platelets. *Platelets*. **21**, 253–259

145. Lopez-Vilchez, I., Diaz-Ricart, M., White, J. G., Escolar, G., and Galan, A. M. (2009) Serotonin enhances platelet procoagulant properties and their activation induced during platelet tissue factor uptake. *Cardiovasc Res*. **84**, 309–316

146. Vanags, D. M., Rodgers, S. E., Duncan, E. M., Lloyd, J. V., and Bochner, F. (1992) Potentiation of ADP-induced aggregation in human platelet-rich plasma by 5-hydroxytryptamine and adrenaline. *British Journal of Pharmacology*. **106**, 917–923

147. Johnston-Cox, H. A., and Ravid, K. (2011) Adenosine and blood platelets. *Purinergic Signal*. **7**, 357–365

148. Newman, K. D., Williams, L. T., Bishopric, N. H., and Lefkowitz, R. J. (1978) Identification of α-Adrenergic Receptors in Human Platelets by [3H]Dihydroergocryptine Binding. *J Clin Invest*. **61**, 395–402

149. Khandoga, A. L., Fujiwara, Y., Goyal, P., Pandey, D., Tsukahara, R., Bolen, A., Guo, H., Wilke, N., Liu, J., Valentine, W. J., Durgam, G. G., Miller, D. D., Jiang, G., Prestwich, G. D., Tigyi, G., and Siess, W. (2008) Lysophosphatidic Acid-Induced Platelet Shape Change Revealed Through LPA1–5 Receptor-selective Probes and Albumin. *Platelets*. **19**, 415–427

150. García-Sevilla, J. A., Ventayol, P., Pérez, V., Rubovszky, G., Puigdemont, D., Ferrer-Alcón, M., Andreoli, A., Guimón, J., and Alvarez, E. (2004) Regulation of Platelet α 2A -Adrenoceptors, Gi Proteins and Receptor Kinases in Major Depression: Effects of Mirtazapine Treatment. *Neuropsychopharmacology*. **29**, 580–588

151. Siess, W., Zangl, K. J., Essler, M., Bauer, M., Brandl, R., Corrinth, C., Bittman, R., Tigyi, G., and Aepfelbacher, M. (1999) Lysophosphatidic acid mediates the rapid activation of platelets and endothelial cells by mildly oxidized low density lipoprotein and accumulates in human atherosclerotic lesions. *PNAS*. **96**, 6931–6936

152. Wang Jong-Shyan, and Cheng Lee-Ju (1999) Effect of Strenuous, Acute Exercise on α2-Adrenergic Agonist–Potentiated Platelet Activation. *Arteriosclerosis, Thrombosis, and Vascular Biology*. **19**, 1559–1565

153. Coughlin, S. R., Vu, T. K., Hung, D. T., and Wheaton, V. I. (1992) Expression cloning and characterization of a functional thrombin receptor reveals a novel proteolytic mechanism of receptor activation. *Semin Thromb Hemost*. **18**, 161–166

154. Austin, K. M., Covic, L., and Kuliopulos, A. (2013) Matrix metalloproteases and PAR1 activation. *Blood*. **121**, 431–439

155. Macfarlane, S. R., Seatter, M. J., Kanke, T., Hunter, G. D., and Plevin, R. (2001) Proteinase-activated receptors. *Pharmacol Rev*. **53**, 245–282

156. Traynelis, S. F., and Trejo, J. (2007) Protease-activated receptor signaling: new roles and regulatory mechanisms. *Curr Opin Hematol*. **14**, 230–235

157. Paing, M. M., Stutts, A. B., Kohout, T. A., Lefkowitz, R. J., and Trejo, J. (2002) beta -Arrestins regulate protease-activated receptor-1 desensitization but not internalization or Down-regulation. *The Journal of biological chemistry*. **277**, 1292–1300

158. Kahn, M. L., Nakanishi-Matsui, M., Shapiro, M. J., Ishihara, H., and Coughlin, S. R. (1999) Protease-activated receptors 1 and 4 mediate activation of human platelets by thrombin. *The Journal of clinical investigation*. **103**, 879–887

159. Rwibasira Rudinga, G., Khan, G. J., and Kong, Y. (2018) Protease-Activated Receptor 4 (PAR4): A Promising Target for Antiplatelet Therapy. *Int J Mol Sci*. 10.3390/ijms19020573

160. Offermanns Stefan (2006) Activation of Platelet Function Through G Protein–Coupled Receptors. *Circulation Research*. **99**, 1293–1304

161. Sambrano, G. R., Weiss, E. J., Zheng, Y. W., Huang, W., and Coughlin, S. R. (2001) Role of thrombin signalling in platelets in haemostasis and thrombosis. *Nature*. **413**, 74–78

162. Ding, Z., Tuluc, F., Bandivadekar, K. R., Zhang, L., Jin, J., and Kunapuli, S. P. (2005) Arg333 and Arg334 in the COOH terminus of the human P2Y1 receptor are crucial for Gq coupling. *Am. J. Physiol., Cell Physiol.* **288**, C559-567

163. Waldo, G. L., and Harden, T. K. (2004) Agonist binding and Gq-stimulating activities of the purified human P2Y1 receptor. *Mol. Pharmacol.* **65**, 426–436

164. Hechler, B., and Gachet, C. (2011) P2 receptors and platelet function. *Purinergic Signal*. **7**, 293–303

165. Reiner, S., Ziegler, N., Leon, C., Lorenz, K., von Hayn, K., Gachet, C., Lohse, M. J., and Hoffmann, C. (2009) beta-Arrestin-2 interaction and internalization of the human P2Y1 receptor are dependent on C-terminal phosphorylation sites. *Mol. Pharmacol.* **76**, 1162–1171

166. Hechler, B., Léon, C., Vial, C., Vigne, P., Frelin, C., Cazenave, J. P., and Gachet, C. (1998) The P2Y1 receptor is necessary for adenosine 5'-diphosphate-induced platelet aggregation. *Blood*. **92**, 152–159

167. Bodor, E. T., Waldo, G. L., Hooks, S. B., Corbitt, J., Boyer, J. L., and Harden, T. K. (2003) Purification and functional reconstitution of the human P2Y12 receptor. *Mol. Pharmacol.* **64**, 1210–1216

168. Kahner, B. N., Dorsam, R. T., and Kunapuli, S. P. (2008) Role of P2Y receptor subtypes in platelet-derived microparticle generation. *Front. Biosci.* **13**, 433–439

169. Gachet, C. (2008) P2 receptors, platelet function and pharmacological implications. *Thromb. Haemost.* **99**, 466–472

170. Schoenwaelder, S. M., Ono, A., Sturgeon, S., Chan, S. M., Mangin, P., Maxwell, M. J., Turnbull, S., Mulchandani, M., Anderson, K., Kauffenstein, G., Rewcastle, G. W., Kendall, J., Gachet, C., Salem, H. H., and Jackson, S. P. (2007) Identification of a unique co-operative phosphoinositide 3-kinase signaling mechanism regulating integrin alpha IIb beta 3 adhesive function in platelets. *J. Biol. Chem.* **282**, 28648–28658

171. Amisten, S., Braun, O. Ö., Bengtsson, A., and Erlinge, D. (2008) Gene expression profiling for the identification of G-protein coupled receptors in human platelets. *Thrombosis Research*. **122**, 47–57

172. Murakami, M., Shiraishi, A., Tabata, K., and Fujita, N. (2008) Identification of the orphan GPCR, P2Y10 receptor as the sphingosine-1-phosphate and lysophosphatidic acid receptor. *Biochemical and Biophysical Research Communications*. **371**, 707–712

173. Schwaner, I., Offermanns, S., Spicher, K., Seifert, R., and Schultz, G. (1995) Differential activation of Gi and Gs proteins by E- and I-type prostaglandins in membranes from the human erythroleukaemia cell line, HEL. *Biochim. Biophys. Acta*. **1265**, 8–14

174. Seiler, S. M., Brassard, C. L., Federici, M. E., Romine, J., and Meanwell, N. A. (1997) [3-[4-(4,5-Diphenyl-2-oxazolyl)-5-oxazolyl]phenoxy]acetic acid (BMY 45778) is a potent non-prostanoid prostacyclin partial agonist: effects on platelet aggregation, adenylyl cyclase, cAMP levels, protein kinase, and iloprost binding. *Prostaglandins*. **53**, 21–35

175. Armstrong, R. A., Lawrence, R. A., Jones, R. L., Wilson, N. H., and Collier, A. (1989) Functional and ligand binding studies suggest heterogeneity of platelet prostacyclin receptors. *Br. J. Pharmacol.* **97**, 657–668

176. Sugimoto, H., Shichijo, M., Iino, T., Manabe, Y., Watanabe, A., Shimazaki, M., Gantner, F., and Bacon, K. B. (2003) An orally bioavailable small molecule antagonist of CRTH2, ramatroban (BAY u3405), inhibits prostaglandin D2-induced eosinophil migration in vitro. *J. Pharmacol. Exp. Ther.* **305**, 347–352

177. Seiler, S., Brassard, C. L., and Federici, M. E. (1990) SQ-27986 inhibition of platelet aggregation is mediated through activation of platelet prostaglandin D2 receptors. *Prostaglandins*. **40**, 119–130

178. Alvarez, R., Eglen, R. M., Chang, L. F., Bruno, J. J., Artis, D. R., Kluge, A. F., and Whiting, R. L. (1991) Stimulation of prostaglandin D2 receptors on human platelets by analogs of prostacyclin. *Prostaglandins*. **42**, 105–119

179. Gresele, P., Arnout, J., Deckmyn, H., Huybrechts, E., Pieters, G., and Vermylen, J. (1987) Role of proaggregatory and antiaggregatory prostaglandins in hemostasis. Studies with combined thromboxane synthase inhibition and thromboxane receptor antagonism. *J. Clin. Invest.* **80**, 1435–1445

180. Mais, D. E., DeHoll, D., Sightler, H., and Halushka, P. V. (1988) Different pharmacologic activities for 13-azapinane thromboxane A2 analogs in platelets and blood vessels. *Eur. J. Pharmacol.* **148**, 309–315

181. Abramovitz, M., Adam, M., Boie, Y., Carrière, M.-C., Denis, D., Godbout, C., Lamontagne, S., Rochette, C., Sawyer, N., Tremblay, N. M., Belley, M., Gallant, M., Dufresne, C., Gareau, Y., Ruel, R., Juteau, H., Labelle, M., Ouimet, N., and Metters, K. M. (2000) The utilization of recombinant prostanoid receptors to determine the affinities and selectivities of prostaglandins and related analogs. *Biochimica et Biophysica Acta (BBA) - Molecular and Cell Biology of Lipids*. **1483**, 285–293

182. Katoh, H., Watabe, A., Sugimoto, Y., Ichikawa, A., and Negishi, M. (1995) Characterization of the signal transduction of prostaglandin E receptor EP1 subtype in cDNA-transfected Chinese hamster ovary cells. *Biochim. Biophys. Acta*. **1244**, 41–48

183. Petrucci, G., De Cristofaro, R., Rutella, S., Ranelletti, F. O., Pocaterra, D., Lancellotti, S., Habib, A., Patrono, C., and Rocca, B. (2011) Prostaglandin E2 differentially modulates human platelet function through the prostanoid EP2 and EP3 receptors. *J. Pharmacol. Exp. Ther.* **336**, 391–402

184. Kuriyama, S., Kashiwagi, H., Yuhki, K., Kojima, F., Yamada, T., Fujino, T., Hara, A., Takayama, K., Maruyama, T., Yoshida, A., Narumiya, S., and Ushikubi, F. (2010) Selective activation of the prostaglandin E2 receptor subtype EP2 or EP4 leads to inhibition of platelet aggregation. *Thromb. Haemost.* **104**, 796–803

185. An, S., Yang, J., So, S. W., Zeng, L., and Goetzl, E. J. (1994) Isoforms of the EP3 subtype of human prostaglandin E2 receptor transduce both intracellular calcium and cAMP signals. *Biochemistry*. **33**, 14496–14502

186. Satoh, S., Chang, C. s, Katoh, H., Hasegawa, H., Nakamura, K., Aoki, J., Fujita, H., Ichikawa, A., and Negishi, M. (1999) The key amino acid residue of prostaglandin EP3 receptor for governing G protein association and activation steps. *Biochem. Biophys. Res. Commun.* **255**, 164–168

187. Yamaoka, K., Yano, A., Kuroiwa, K., Morimoto, K., Inazumi, T., Hatae, N., Tabata, H., Segi-Nishida, E., Tanaka, S., Ichikawa, A., and Sugimoto, Y. (2009) Prostaglandin EP3 receptor superactivates adenylyl cyclase via the Gq/PLC/Ca2+

pathway in a lipid raft-dependent manner. *Biochem. Biophys. Res. Commun.* **389**, 678–682

188. Bilson, H. A., Mitchell, D. L., and Ashby, B. (2004) Human prostaglandin EP3 receptor isoforms show different agonist-induced internalization patterns. *FEBS Lett.* **572**, 271–275

189. Singh, J., Zeller, W., Zhou, N., Hategan, G., Mishra, R. K., Polozov, A., Yu, P., Onua, E., Zhang, J., Ramírez, J. L., Sigthorsson, G., Thorsteinnsdottir, M., Kiselyov, A. S., Zembower, D. E., Andrésson, T., and Gurney, M. E. (2010) Structure-activity relationship studies leading to the identification of (2E)-3-[l-[(2,4-dichlorophenyl)methyl]-5-fluoro-3-methyl-lH-indol-7-yl]-N-[(4,5-dichloro-2-thienyl)sulfonyl]-2-propenamide (DG-041), a potent and selective prostanoid EP3 receptor antagonist, as a novel antiplatelet agent that does not prolong bleeding. *J. Med. Chem.* **53**, 18–36

190. Schober, L. J., Khandoga, A. L., Dwivedi, S., Penz, S. M., Maruyama, T., Brandl, R., and Siess, W. (2011) The role of PGE(2) in human atherosclerotic plaque on platelet EP(3) and EP(4) receptor activation and platelet function in whole blood. *J. Thromb. Thrombolysis*. **32**, 158–166

191. Fox, S. C., May, J. A., Johnson, A., Hermann, D., Strieter, D., Hartman, D., and Heptinstall, S. (2013) Effects on platelet function of an EP3 receptor antagonist used alone and in combination with a P2Y12 antagonist both in-vitro and ex-vivo in human volunteers. *Platelets*. **24**, 392–400

192. Sugimoto, Y., and Narumiya, S. (2007) Prostaglandin E Receptors. *J. Biol. Chem.* **282**, 11613–11617

193. Leduc, M., Breton, B., Galés, C., Gouill, C. L., Bouvier, M., Chemtob, S., and Heveker, N. (2009) Functional Selectivity of Natural and Synthetic Prostaglandin EP4 Receptor Ligands. *J Pharmacol Exp Ther*. **331**, 297–307

194. Philipose Sonia, Konya Viktoria, Sreckovic Ivana, Marsche Gunther, Lippe Irmgard T., Peskar Bernhard A., Heinemann Akos, and Schuligoi Rufina (2010) The Prostaglandin E2 Receptor EP4 Is Expressed by Human Platelets and Potently Inhibits Platelet Aggregation and Thrombus Formation*. *Arteriosclerosis, Thrombosis, and Vascular Biology*. **30**, 2416–2423

195. Cordeaux, Y., Ijzerman, A. P., and Hill, S. J. (2004) Coupling of the human A1 adenosine receptor to different heterotrimeric G proteins: evidence for agonist-specific G protein activation. *Br. J. Pharmacol.* **143**, 705–714

196. Jockers, R., Linder, M. E., Hohenegger, M., Nanoff, C., Bertin, B., Strosberg, A. D., Marullo, S., and Freissmuth, M. (1994) Species difference in the G protein selectivity of the human and bovine A1-adenosine receptor. *J. Biol. Chem.* **269**, 32077–32084

197. Mundell, S., and Kelly, E. (2011) Adenosine receptor desensitization and trafficking. *Biochimica et Biophysica Acta (BBA) - Biomembranes*. **1808**, 1319–1328

198. Fresco, P., Diniz, C., and Gonçalves, J. (2004) Facilitation of noradrenaline release by activation of adenosine A(2A) receptors triggers both phospholipase C and adenylate cyclase pathways in rat tail artery. *Cardiovasc. Res.* **63**, 739–746

199. Olah, M. E. (1997) Identification of A2a adenosine receptor domains involved in selective coupling to Gs. Analysis of chimeric A1/A2a adenosine receptors. *J. Biol. Chem.* **272**, 337–344

200. Varani, K., Portaluppi, F., Merighi, S., Ongini, E., Belardinelli, L., and Borea, P. A. (1999) Caffeine alters A2A adenosine receptors and their function in human platelets. *Circulation*. **99**, 2499–2502

201. Varani, K., Portaluppi, F., Gessi, S., Merighi, S., Ongini, E., Belardinelli, L., and Borea, P. A. (2000) Dose and time effects of caffeine intake on human platelet adenosine A(2A) receptors : functional and biochemical aspects. *Circulation*. **102**, 285–289

202. Yang, D., Chen, H., Koupenova, M., Carroll, S. H., Eliades, A., Freedman, J. E., Toselli, P., and Ravid, K. (2010) A new role for the A2b adenosine receptor in regulating platelet function. *Journal of Thrombosis and Haemostasis*. **8**, 817–827

203. Bylund, D. B., and Ray-Prenger, C. (1989) Alpha-2A and alpha-2B adrenergic receptor subtypes: attenuation of cyclic AMP production in cell lines containing only one receptor subtype. *J. Pharmacol. Exp. Ther.* **251**, 640–644

204. Jones, S. B., Halenda, S. P., and Bylund, D. B. (1991) Alpha 2-adrenergic receptor stimulation of phospholipase A2 and of adenylate cyclase in transfected Chinese hamster ovary cells is mediated by different mechanisms. *Mol. Pharmacol.* **39**, 239–245

205. Limbird, L. E. (1988) Receptors linked to inhibition of adenylate cyclase: additional signaling mechanisms. *FASEB J.* **2**, 2686–2695

206. Eason, M. G., Kurose, H., Holt, B. D., Raymond, J. R., and Liggett, S. B. (1992) Simultaneous coupling of alpha 2-adrenergic receptors to two G-proteins with opposing effects. Subtype-selective coupling of alpha 2C10, alpha 2C4, and alpha 2C2 adrenergic receptors to Gi and Gs. *J. Biol. Chem.* **267**, 15795–15801

207. DeGraff, J. L., Gurevich, V. V., and Benovic, J. L. (2002) The Third Intracellular Loop of α2-Adrenergic Receptors Determines Subtype Specificity of Arrestin Interaction. *J. Biol. Chem.* **277**, 43247–43252

208. DeGraff, J. L., Gagnon, A. W., Benovic, J. L., and Orsini, M. J. (1999) Role of Arrestins in Endocytosis and Signaling of α2-Adrenergic Receptor Subtypes. *J. Biol. Chem.* **274**, 11253–11259

209. Siess, W., and Lapetina, E. G. (1989) Platelet aggregation induced by alpha 2-adrenoceptor and protein kinase C activation. A novel synergism. *Biochem J.* **263**, 377–385

210. Schöneberg, T., Kostenis, E., Liu, J., Gudermann, T., and Wess, J. (1998) Molecular aspects of vasopressin receptor function. *Adv. Exp. Med. Biol.* **449**, 347–358

211. Terrillon, S., Barberis, C., and Bouvier, M. (2004) Heterodimerization of V1a and V2 vasopressin receptors determines the interaction with β-arrestin and their trafficking patterns. *Proc Natl Acad Sci U S A.* **101**, 1548–1553

212. Serradeil-Le Gal, C., Wagnon, J., Garcia, C., Lacour, C., Guiraudou, P., Christophe, B., Villanova, G., Nisato, D., Maffrand, J. P., and Le Fur, G. (1993) Biochemical and pharmacological properties of SR 49059, a new, potent, nonpeptide antagonist of rat and human vasopressin V1a receptors. *J. Clin. Invest.* **92**, 224–231

213. Hasan, K. N., Shoji, M., Tsutaya, S., Kudo, R., Matsuda, E., Saito, J., Kimura, T., and Yasujima, M. (2006) Study of V1a vasopressin receptor gene single nucleotide polymorphisms in platelet vasopressin responsiveness. *J. Clin. Lab. Anal.* **20**, 87–92

214. Fukushima, N., Kimura, Y., and Chun, J. (1998) A single receptor encoded by vzg-1/lpA1/edg-2 couples to G proteins and mediates multiple cellular responses to lysophosphatidic acid. *Proc. Natl. Acad. Sci. U.S.A.* **95**, 6151–6156

215. Urs, N. M., Jones, K. T., Salo, P. D., Severin, J. E., Trejo, J., and Radhakrishna, H. (2005) A requirement for membrane cholesterol in the β-arrestin- and clathrin-dependent endocytosis of LPA1 lysophosphatidic acid receptors. *Journal of Cell Science*. **118**, 5291–5304

216. Alcántara-Hernández, R., Hernández-Méndez, A., Campos-Martínez, G. A., Meizoso-Huesca, A., and García-Sáinz, J. A. (2015) Phosphorylation and Internalization of Lysophosphatidic Acid Receptors LPA1, LPA2, and LPA3. *PLOS ONE*. **10**, e0140583

217. Ishii, I., Contos, J. J. A., Fukushima, N., and Chun, J. (2000) Functional Comparisons of the Lysophosphatidic Acid Receptors, LPA1/VZG-1/EDG-2, LPA2/EDG-4, and LPA3/EDG-7 in Neuronal Cell Lines Using a Retrovirus Expression System. *Mol Pharmacol*. **58**, 895–902

218. Noguchi, K., Ishii, S., and Shimizu, T. (2003) Identification of p2y9/GPR23 as a Novel G Protein-coupled Receptor for Lysophosphatidic Acid, Structurally Distant from the Edg Family. *J. Biol. Chem.* **278**, 25600–25606

219. Lee, C.-W., Rivera, R., Dubin, A. E., and Chun, J. (2007) LPA4/GPR23 Is a Lysophosphatidic Acid (LPA) Receptor Utilizing Gs-, Gq/Gi-mediated Calcium Signaling and G12/13-mediated Rho Activation. *J. Biol. Chem.* **282**, 4310–4317

220. Yin, H., Chu, A., Li, W., Wang, B., Shelton, F., Otero, F., Nguyen, D. G., Caldwell, J. S., and Chen, Y. A. (2009) Lipid G Protein-coupled Receptor Ligand Identification Using β-Arrestin PathHunter™ Assay. *J Biol Chem.* **284**, 12328–12338

221. Pamuklar, Z., Lee, J. S., Cheng, H.-Y., Panchatcharam, M., Steinhubl, S., Morris, A. J., Charnigo, R., and Smyth, S. S. (2008) Individual heterogeneity in platelet response to lysophosphatidic acid: evidence for a novel inhibitory pathway. *Arterioscler. Thromb. Vasc. Biol.* **28**, 555–561

222. Lee, C.-W., Rivera, R., Gardell, S., Dubin, A. E., and Chun, J. (2006) GPR92 as a new G12/13- and Gq-coupled lysophosphatidic acid receptor that increases cAMP, LPA5. *J. Biol. Chem.* **281**, 23589–23597

223. Garnovskaya, M. N., Nebigil, C. G., Arthur, J. M., Spurney, R. F., and Raymond, J. R. (1995) 5-Hydroxytryptamine2A receptors expressed in rat renal mesangial cells inhibit cyclic AMP accumulation. *Mol. Pharmacol.* **48**, 230–237

224. Gray, J. A., and Roth, B. L. (2001) Paradoxical trafficking and regulation of 5-HT2A receptors by agonists and antagonists. *Brain Research Bulletin*. **56**, 441–451

225. Roth, B. L., Allen, J. A., and Yadav, P. N. (2008) INSIGHTS INTO THE REGULATION OF 5-HT2A RECEPTORS BY SCAFFOLDING PROTEINS AND KINASES. *Neuropharmacology*. **55**, 961–968

226. Markovitz Jerome H., Tolbert Lelland, and Winders Suzan E. (1999) Increased Serotonin Receptor Density and Platelet GPIIb/IIIa Activation Among Smokers. *Arteriosclerosis, Thrombosis, and Vascular Biology*. **19**, 762–766

227. Li, N., Wallén, N., Ladjevardi, M., and Hjemdahl, P. (1997) Effects of serotonin on platelet activation in whole blood. *Blood Coagulation & Fibrinolysis*. **8**, 517–524

228. Dale, G. L., Friese, P., Batar, P., Hamilton, S. F., Reed, G. L., Jackson, K. W., Clemetson, K. J., and Alberio, L. (2002) Stimulated platelets use serotonin to enhance their retention of procoagulant proteins on the cell surface. *Nature*. **415**, 175–179

229. Adham, N., Borden, L. A., Schechter, L. E., Gustafson, E. L., Cochran, T. L., Vaysse, P. J., Weinshank, R. L., and Branchek, T. A. (1993) Cell-specific coupling

of the cloned human 5-HT1F receptor to multiple signal transduction pathways. *Naunyn Schmiedebergs Arch. Pharmacol.* **348**, 566–575

230. Ouadid, H., Seguin, J., Dumuis, A., Bockaert, J., and Nargeot, J. (1992) Serotonin increases calcium current in human atrial myocytes via the newly described 5-hydroxytryptamine4 receptors. *Mol. Pharmacol.* **41**, 346–351

231. Ponimaskin, E. G., Profirovic, J., Vaiskunaite, R., Richter, D. W., and Voyno-Yasenetskaya, T. A. (2002) 5-Hydroxytryptamine 4(a) receptor is coupled to the Galpha subunit of heterotrimeric G13 protein. *J. Biol. Chem.* **277**, 20812–20819

232. Barthet, G., Carrat, G., Cassier, E., Barker, B., Gaven, F., Pillot, M., Framery, B., Pellissier, L. P., Augier, J., Kang, D. S., Claeysen, S., Reiter, E., Banères, J.-L., Benovic, J. L., Marin, P., Bockaert, J., and Dumuis, A. (2009) β-arrestin1 phosphorylation by GRK5 regulates G protein-independent 5-HT4 receptor signalling. *The EMBO Journal*. **28**, 2706–2718

233. Zhao, J., Ramadan, E., Cappiello, M., Wroblewska, B., Bzdega, T., and Neale, J. H. (2001) NAAG inhibits KCl-induced [(3)H]-GABA release via mGluR3, cAMP, PKA and L-type calcium conductance. *Eur. J. Neurosci.* **13**, 340–346

234. Iacovelli, L., Molinaro, G., Battaglia, G., Motolese, M., Menna, L. D., Alfiero, M., Blahos, J., Matrisciano, F., Corsi, M., Corti, C., Bruno, V., Blasi, A. D., and Nicoletti, F. (2009) Regulation of group II metabotropic glutamate receptors by G protein-coupled receptor kinases: mGlu2 receptors are resistant to homologous desensitization. *Molecular pharmacology*. **75**, 991–1003

235. Yin, S., Zamorano, R., Conn, P. J., and Niswender, C. M. (2013) Functional selectivity induced by mGlu4 receptor positive allosteric modulation and concomitant activation of Gq coupled receptors. *Neuropharmacology*. **66**, 122–132

236. Strakova, Z., Copland, J. A., Lolait, S. J., and Soloff, M. S. (1998) ERK2 mediates oxytocin-stimulated PGE2 synthesis. *American Journal of Physiology-Endocrinology and Metabolism*. **274**, E634–E641

237. Grotegut, C. A., Feng, L., Mao, L., Heine, R. P., Murtha, A. P., and Rockman, H. A. (2011) β-Arrestin mediates oxytocin receptor signaling, which regulates uterine contractility and cellular migration. *Am. J. Physiol. Endocrinol. Metab.* **300**, E468-477

238. Högberg, C., Gidlöf, O., Tan, C., Svensson, S., Nilsson-Öhman, J., Erlinge, D., and Olde, B. (2011) Succinate independently stimulates full platelet activation via cAMP and phosphoinositide 3-kinase-β signaling. *J. Thromb. Haemost.* **9**, 361–372

239. Geubelle, P., Gilissen, J., Dilly, S., Poma, L., Dupuis, N., Laschet, C., Abboud, D., Inoue, A., Jouret, F., Pirotte, B., and Hanson, J. (2017) Identification and

pharmacological characterization of succinate receptor agonists. *Br J Pharmacol*. **174**, 796–808

240. Oh, S. B., Endoh, T., Simen, A. A., Ren, D., and Miller, R. J. (2002) Regulation of calcium currents by chemokines and their receptors. *Journal of Neuroimmunology*. **123**, 66–75

241. Wakita, H., Yanagawa, T., Kuboi, Y., and Imai, T. (2017) E6130, a Novel CX3C Chemokine Receptor 1 (CX3CR1) Modulator, Attenuates Mucosal Inflammation and Reduces CX3CR1 $^{+}$ Leukocyte Trafficking in Mice with Colitis. *Mol Pharmacol*. **92**, 502–509

242. Cederblad, L., Rosengren, B., Ryberg, E., and Hermansson, N.-O. (2016) AZD8797 is an allosteric non-competitive modulator of the human CX3CR1 receptor. *Biochem. J.* **473**, 641–649

243. Kapas, S., and Clark, A. J. (1995) Identification of an orphan receptor gene as a type 1 calcitonin gene-related peptide receptor. *Biochem. Biophys. Res. Commun.* **217**, 832–838

244. Balabanian, K., Lagane, B., Infantino, S., Chow, K. Y. C., Harriague, J., Moepps, B., Arenzana-Seisdedos, F., Thelen, M., and Bachelerie, F. (2005) The chemokine SDF-1/CXCL12 binds to and signals through the orphan receptor RDC1 in T lymphocytes. *J. Biol. Chem.* **280**, 35760–35766

245. Gustavsson, M., Wang, L., van Gils, N., Stephens, B. S., Zhang, P., Schall, T. J., Yang, S., Abagyan, R., Chance, M. R., Kufareva, I., and Handel, T. M. (2017) Structural basis of ligand interaction with atypical chemokine receptor 3. *Nat Commun*. **8**, 14135

246. Capra, V., Accomazzo, M. R., Ravasi, S., Parenti, M., Macchia, M., Nicosia, S., and Rovati, G. E. (2003) Involvement of prenylated proteins in calcium signaling induced by LTD4 in differentiated U937 cells. *Prostaglandins & Other Lipid Mediators*. **71**, 235–251

247. Parhamifar, L., Sime, W., Yudina, Y., Vilhardt, F., Mörgelin, M., and Sjölander, A. (2010) Ligand-Induced Tyrosine Phosphorylation of Cysteinyl Leukotriene Receptor 1 Triggers Internalization and Signaling in Intestinal Epithelial Cells. *PLoS One*. 10.1371/journal.pone.0014439

248. Mellor, E. A., Frank, N., Soler, D., Hodge, M. R., Lora, J. M., Austen, K. F., and Boyce, J. A. (2003) Expression of the type 2 receptor for cysteinyl leukotrienes (CysLT2R) by human mast cells: Functional distinction from CysLT1R. *Proc. Natl. Acad. Sci. U.S.A.* **100**, 11589–11593

249. Heise, C. E., O'Dowd, B. F., Figueroa, D. J., Sawyer, N., Nguyen, T., Im, D. S., Stocco, R., Bellefeuille, J. N., Abramovitz, M., Cheng, R., Williams, D. L., Zeng, Z., Liu, Q., Ma, L., Clements, M. K., Coulombe, N., Liu, Y., Austin, C. P., George,

S. R., O'Neill, G. P., Metters, K. M., Lynch, K. R., and Evans, J. F. (2000) Characterization of the human cysteinyl leukotriene 2 receptor. *J. Biol. Chem.* **275**, 30531–30536

250. Ni, N. C., Yan, D., Ballantyne, L. L., Barajas-Espinosa, A., Amand, T. S., Pratt, D. A., and Funk, C. D. (2011) A Selective Cysteinyl Leukotriene Receptor 2 Antagonist Blocks Myocardial Ischemia/Reperfusion Injury and Vascular Permeability in Mice. *J Pharmacol Exp Ther*. **339**, 768–778

251. Liu, C., Yang, X. V., Wu, J., Kuei, C., Mani, N. S., Zhang, L., Yu, J., Sutton, S. W., Qin, N., Banie, H., Karlsson, L., Sun, S., and Lovenberg, T. W. (2011) Oxysterols direct B-cell migration through EBI2. *Nature*. **475**, 519–523

252. Daugvilaite, V., Madsen, C. M., Lückmann, M., Echeverria, C. C., Sailer, A. W., Frimurer, T. M., Rosenkilde, M. M., and Benned-Jensen, T. (2017) Biased agonism and allosteric modulation of G protein-coupled receptor 183 – a 7TM receptor also known as Epstein–Barr virus-induced gene 2. *British Journal of Pharmacology*. **174**, 2031

253. Barnea, G., Strapps, W., Herrada, G., Berman, Y., Ong, J., Kloss, B., Axel, R., and Lee, K. J. (2008) The genetic design of signaling cascades to record receptor activation. *Proc. Natl. Acad. Sci. U.S.A.* **105**, 64–69

254. De Henau, O., Degroot, G.-N., Imbault, V., Robert, V., De Poorter, C., Mcheik, S., Galés, C., Parmentier, M., and Springael, J.-Y. (2016) Signaling Properties of Chemerin Receptors CMKLR1, GPR1 and CCRL2. *PLoS One*. 10.1371/journal.pone.0164179

255. Bohnekamp, J., and Schöneberg, T. (2011) Cell adhesion receptor GPR133 couples to Gs protein. *J. Biol. Chem.* **286**, 41912–41916

256. Halliburton, W. D. (1888) On the Nature of Fibrin-Ferment. *The Journal of Physiology*. **9**, 229–286

257. Marcum, J. A. (1998) Defending the Priority of "Remarkable Researches": The Discovery of Fibrin Ferment. *History and Philosophy of the Life Sciences*. **20**, 51–76

258. Carney, D. H., and Cunningham, D. D. (1978) Transmembrane action of thrombin initiates chick cell division. *J Supramol Struct*. **9**, 337–350

259. Chen, L. B., and Buchanan, J. M. (1975) Mitogenic activity of blood components. I. Thrombin and prothrombin. *Proceedings of the National Academy of Sciences*. **72**, 131–135

260. De Mey, J. G., Claeys, M., and Vanhoutte, P. M. (1982) Endothelium-dependent inhibitory effects of acetylcholine, adenosine triphosphate, thrombin and

arachidonic acid in the canine femoral artery. *The Journal of pharmacology and experimental therapeutics*. **222**, 166–173

261. Gurwitz, D., and Cunningham, D. D. (1990) Neurite outgrowth activity of protease nexin-1 on neuroblastoma cells requires thrombin inhibition. *J Cell Physiol*. **142**, 155–162

262. Haver, V. M., and Namm, D. H. (1984) Characterization of the thrombin-induced contraction of vascular smooth muscle. *Blood Vessels*. **21**, 53–63

263. Schmid, H. J., Jackson, D. P., and Conley, C. L. (1962) MECHANISM OF ACTION OF THROMBIN ON PLATELETS. *J Clin Invest*. **41**, 543–553

264. Shermer, R. W., Mason, R. G., Wagner, R. H., and Brinkhous, K. M. (1961) STUDIES ON THROMBIN-INDUCED PLATELET AGGLUTINATION. *J Exp Med*. **114**, 905–920

265. Van Obberghen-Schilling, E., and Pouysségur, J. (1985) Affinity labeling of high-affinity α-thrombin binding sites on the surface of hamster fibroblasts. *Biochimica et Biophysica Acta (BBA) - Molecular Cell Research*. **847**, 335–343

266. Coughlin, S. R., Scarborough, R. M., Vu, T. K., and Hung, D. T. (1992) Thrombin receptor structure and function. *Cold Spring Harb Symp Quant Biol*. **57**, 149–154

267. Scarborough, R. M., Naughton, M. A., Teng, W., Hung, D. T., Rose, J., Vu, T. K., Wheaton, V. I., Turck, C. W., and Coughlin, S. R. (1992) Tethered ligand agonist peptides. Structural requirements for thrombin receptor activation reveal mechanism of proteolytic unmasking of agonist function. *The Journal of biological chemistry*. **267**, 13146–13149

268. Chen, J., Ishii, M., Wang, L., Ishii, K., and Coughlin, S. R. (1994) Thrombin receptor activation. Confirmation of the intramolecular tethered liganding hypothesis and discovery of an alternative intermolecular liganding mode. *The Journal of biological chemistry*. **269**, 16041–16045

269. Gerszten, R. E., Chen, J., Ishii, M., Ishii, K., Wang, L., Nanevicz, T., Turck, C. W., Vu, T. K., and Coughlin, S. R. (1994) Specificity of the thrombin receptor for agonist peptide is defined by its extracellular surface. *Nature*. **368**, 648–651

270. Nystedt, S., Larsson, A. K., Aberg, H., and Sundelin, J. (1995) The mouse proteinase-activated receptor-2 cDNA and gene. Molecular cloning and functional expression. *The Journal of biological chemistry*. **270**, 5950–5955

271. Blackhart, B. D., Emilsson, K., Nguyen, D., Teng, W., Martelli, A. J., Nystedt, S., Sundelin, J., and Scarborough, R. M. (1996) Ligand cross-reactivity within the protease-activated receptor family. *The Journal of biological chemistry*. **271**, 16466–16471

272. Hollenberg, M. D., Saifeddine, M., Al-Ani, B., and Kawabata, A. (1997) Proteinase-activated receptors: structural requirements for activity, receptor cross-reactivity, and receptor selectivity of receptor-activating peptides. *Can J Physiol Pharmacol*. **75**, 832–841

273. Nystedt, S., Emilsson, K., Larsson, A. K., Strombeck, B., and Sundelin, J. (1995) Molecular cloning and functional expression of the gene encoding the human proteinase-activated receptor 2. *Eur J Biochem*. **232**, 84–89

274. Ishihara, H., Connolly, A. J., Zeng, D., Kahn, M. L., Zheng, Y. W., Timmons, C., Tram, T., and Coughlin, S. R. (1997) Protease-activated receptor 3 is a second thrombin receptor in humans. *Nature*. **386**, 502–506

275. EREZ, O., ROMERO, R., KIM, S.-S., KIM, J.-S., KIM, Y. M., WILDMAN, D. E., THAN, N. G., MAZAKI-TOVI, S., GOTSCH, F., PINELES, B., KUSANOVIC, J. P., ESPINOZA, J., MITTAL, P., MAZOR, M., HASSAN, S. S., and KIM, C. J. (2008) OVER-EXPRESSION OF THE THROMBIN RECEPTOR (PAR-1) IN THE PLACENTA IN PREECLAMPSIA: A MECHANISM FOR THE INTERSECTION OF COAGULATION AND INFLAMMATION. *J Matern Fetal Neonatal Med*. **21**, 345–355

276. Hollenberg, M. D. (2005) Physiology and Pathophysiology of Proteinase-Activated Receptors (PARs): Proteinases as Hormone-Like Signal Messengers: PARs and More. *Journal of Pharmacological Sciences*. **97**, 8–13

277. Nieman, M. T. (2016) Protease-activated receptors in hemostasis. *Blood*. **128**, 169–177

278. Posma Jens J., Grover Steven P., Hisada Yohei, Owens A. Phillip, Antoniak Silvio, Spronk Henri M., and Mackman Nigel (2019) Roles of Coagulation Proteases and PARs (Protease-Activated Receptors) in Mouse Models of Inflammatory Diseases. *Arteriosclerosis, Thrombosis, and Vascular Biology*. **39**, 13–24

279. Szabo, R., Peters, D. E., Kosa, P., Camerer, E., and Bugge, T. H. (2014) Regulation of Feto-Maternal Barrier by Matriptase- and PAR-2-Mediated Signaling Is Required for Placental Morphogenesis and Mouse Embryonic Survival. *PLOS Genetics*. **10**, e1004470

280. Vergnolle, N. (2004) Modulation of visceral pain and inflammation by protease-activated receptors. *Br J Pharmacol*

281. Vergnolle, N. (2005) Protease-activated receptors and inflammatory hyperalgesia. *Mem Inst Oswaldo Cruz*. **100 Suppl 1**, 173–176

282. Adams, M. N., Ramachandran, R., Yau, M.-K., Suen, J. Y., Fairlie, D. P., Hollenberg, M. D., and Hooper, J. D. (2011) Structure, function and pathophysiology of protease activated receptors. *Pharmacology & therapeutics*. **130**, 248–282

283. Hayes, K. L., and Tracy, P. B. (1999) The platelet high affinity binding site for thrombin mimics hirudin, modulates thrombin-induced platelet activation, and is distinct from the glycoprotein Ib-IX-V complex. *The Journal of biological chemistry*. **274**, 972–980

284. Jacques, S. L., LeMasurier, M., Sheridan, P. J., Seeley, S. K., and Kuliopulos, A. (2000) Substrate-assisted catalysis of the PAR1 thrombin receptor. Enhancement of macromolecular association and cleavage. *The Journal of biological chemistry*. **275**, 40671–40678

285. Nieman, M. T., and Schmaier, A. H. (2007) Interaction of Thrombin with PAR1 and PAR4 at the Thrombin Cleavage Site. *Biochemistry*. **46**, 8603–8610

286. Ayala, Y. M., Cantwell, A. M., Rose, T., Bush, L. A., Arosio, D., and Di Cera, E. (2001) Molecular mapping of thrombin-receptor interactions. *Proteins*. **45**, 107–116

287. Jacques, S. L., LeMasurier, M., Sheridan, P. J., Seeley, S. K., and Kuliopulos, A. (2000) Substrate-assisted catalysis of the PAR1 thrombin receptor. Enhancement of macromolecular association and cleavage. *The Journal of biological chemistry*. **275**, 40671–40678

288. Vu, T. K., Wheaton, V. I., Hung, D. T., Charo, I., and Coughlin, S. R. (1991) Domains specifying thrombin-receptor interaction. *Nature*. **353**, 674–677

289. Jacques, S. L., and Kuliopulos, A. (2003) Protease-activated receptor-4 uses dual prolines and an anionic retention motif for thrombin recognition and cleavage. *The Biochemical journal*. **376**, 733–740

290. Kahn, M. L., Zheng, Y. W., Huang, W., Bigornia, V., Zeng, D., Moff, S., Farese, R. V. J., Tam, C., and Coughlin, S. R. (1998) A dual thrombin receptor system for platelet activation. *Nature*. **394**, 690–694

291. Faruqi, T. R., Weiss, E. J., Shapiro, M. J., Huang, W., and Coughlin, S. R. (2000) Structure-function analysis of protease-activated receptor 4 tethered ligand peptides. Determinants of specificity and utility in assays of receptor function. *The Journal of biological chemistry*. **275**, 19728–19734

292. Coughlin, S. R. (1999) How the protease thrombin talks to cells. *Proceedings of the National Academy of Sciences of the United States of America*. **96**, 11023–11027

293. Mihara, K., Ramachandran, R., Saifeddine, M., Hansen, K. K., Renaux, B., Polley, D., Gibson, S., Vanderboor, C., and Hollenberg, M. D. (2016) Thrombin-Mediated Direct Activation of Proteinase-Activated Receptor-2: Another Target for Thrombin Signaling. *Molecular pharmacology*. **89**, 606–614

294. Loew, D., Perrault, C., Morales, M., Moog, S., Ravanat, C., Schuhler, S., Arcone, R., Pietropaolo, C., Cazenave, J. P., Van Dorsselaer, A., and Lanza, F. (2000) Proteolysis of the exodomain of recombinant protease-activated receptors: prediction of receptor activation or inactivation by MALDI mass spectrometry. *Biochemistry*. **39**, 10812–10822

295. Heuberger, D. M., and Schuepbach, R. A. (2019) Protease-activated receptors (PARs): mechanisms of action and potential therapeutic modulators in PAR-driven inflammatory diseases. *Thromb J*. 10.1186/s12959-019-0194-8

296. Zhao, P., Metcalf, M., and Bunnett, N. W. (2014) Biased Signaling of Protease-Activated Receptors. *Front Endocrinol (Lausanne)*. 10.3389/fendo.2014.00067

297. Kawabata, A., Kuroda, R., Nishikawa, H., and Kawai, K. (1999) Modulation by protease-activated receptors of the rat duodenal motility in vitro: possible mechanisms underlying the evoked contraction and relaxation. *Br. J. Pharmacol.* **128**, 865–872

298. Kaufmann, R., Schulze, B., Krause, G., Mayr, L. M., Settmacher, U., and Henklein, P. (2005) Proteinase-activated receptors (PARs)–the PAR3 Neo-N-terminal peptide TFRGAP interacts with PAR1. *Regul Pept*. **125**, 61–66

299. Nakanishi-Matsui, M., Zheng, Y. W., Sulciner, D. J., Weiss, E. J., Ludeman, M. J., and Coughlin, S. R. (2000) PAR3 is a cofactor for PAR4 activation by thrombin. *Nature*. **404**, 609–613

300. Michelson, A. D. (2010) Antiplatelet therapies for the treatment of cardiovascular disease. *Nature reviews. Drug discovery*. **9**, 154–169

301. Altman, R., Luciardi, H. L., Muntaner, J., and Herrera, R. N. (2004) The antithrombotic profile of aspirin. Aspirin resistance, or simply failure? *Thrombosis Journal*. **2**, 1

302. Brown, S.-A., and Pereira, N. (2018) Pharmacogenomic Impact of CYP2C19 Variation on Clopidogrel Therapy in Precision Cardiovascular Medicine. *J Pers Med*. 10.3390/jpm8010008

303. Cryer, B., and Mahaffey, K. W. (2014) Gastrointestinal ulcers, role of aspirin, and clinical outcomes: pathobiology, diagnosis, and treatment. *J Multidiscip Healthc*. **7**, 137–146

304. Galandrin, S., Oligny-Longpre, G., and Bouvier, M. (2007) The evasive nature of drug efficacy: implications for drug discovery. *Trends in Pharmacological Sciences*. **28**, 423–430

305. Kenakin, T. (2011) Functional selectivity and biased receptor signaling. *The Journal of pharmacology and experimental therapeutics*. **336**, 296–302

306. Wootten, D., Christopoulos, A., Marti-Solano, M., Babu, M. M., and Sexton, P. M. (2018) Mechanisms of signalling and biased agonism in G protein-coupled receptors. *Nature Reviews Molecular Cell Biology*. **19**, 638–653

307. Manglik, A., Kim, T. H., Masureel, M., Altenbach, C., Yang, Z., Hilger, D., Lerch, M. T., Kobilka, T. S., Thian, F. S., Hubbell, W. L., Prosser, R. S., and Kobilka, B. K. (2015) Structural Insights into the Dynamic Process of β2-Adrenergic Receptor Signaling. *Cell*. **161**, 1101–1111

308. Wingler, L. M., Skiba, M. A., McMahon, C., Staus, D. P., Kleinhenz, A. L. W., Suomivuori, C.-M., Latorraca, N. R., Dror, R. O., Lefkowitz, R. J., and Kruse, A. C. (2020) Angiotensin and biased analogs induce structurally distinct active conformations within a GPCR. *Science*. **367**, 888–892

309. Wacker, D., Stevens, R. C., and Roth, B. L. (2017) How Ligands Illuminate GPCR Molecular Pharmacology. *Cell*. **170**, 414–427

310. Klages, B., Brandt, U., Simon, M. I., Schultz, G., and Offermanns, S. (1999) Activation of G12/G13 Results in Shape Change and Rho/Rho-Kinase–mediated Myosin Light Chain Phosphorylation in Mouse Platelets. *J Cell Biol*. **144**, 745–754

311. Carbajal, J. M., Gratrix, M. L., Yu, C. H., and Schaeffer, R. C. J. (2000) ROCK mediates thrombin's endothelial barrier dysfunction. *Am J Physiol Cell Physiol*. **279**, C195–204

312. Vouret-Craviari, V., Boquet, P., Pouyssegur, J., and Van Obberghen-Schilling, E. (1998) Regulation of the actin cytoskeleton by thrombin in human endothelial cells: role of Rho proteins in endothelial barrier function. *Mol Biol Cell*. **9**, 2639–2653

313. Bae, J. S., Yang, L., Manithody, C., and Rezaie, A. R. (2007) The ligand occupancy of endothelial protein C receptor switches the protease-activated receptor 1-dependent signaling specificity of thrombin from a permeability-enhancing to a barrier-protective response in endothelial cells. *Blood*. **110**, 3909–3916

314. Ramachandran, R. (2012) Developing PAR1 antagonists: minding the endothelial gap. *Discovery medicine*. **13**, 425–431

315. Ballesteros, J. A., and Weinstein, H. (1995) Integrated methods for the construction of three-dimensional models and computational probing of structure-function relations in G protein-coupled receptors. in *Methods in Neurosciences* (Sealfon, S. C. ed), pp. 366–428, Receptor Molecular Biology, Academic Press, **25**, 366–428

316. Aratake, Y., Okuno, T., Matsunobu, T., Saeki, K., Takayanagi, R., Furuya, S., and Yokomizo, T. (2012) Helix 8 of leukotriene B $_4$ receptor 1 inhibits ligand-induced internalization. *FASEB j.* **26**, 4068–4078

317. Ernst, O. P., Meyer, C. K., Marin, E. P., Henklein, P., Fu, W.-Y., Sakmar, T. P., and Hofmann, K. P. (2000) Mutation of the Fourth Cytoplasmic Loop of Rhodopsin Affects Binding of Transducin and Peptides Derived from the Carboxyl-terminal Sequences of Transducin α and γ Subunits. *J. Biol. Chem.* **275**, 1937–1943

318. Santos, N. M. D., Gardner, L. A., White, S. W., and Bahouth, S. W. (2006) Characterization of the Residues in Helix 8 of the Human β_1 -Adrenergic Receptor That Are Involved in Coupling the Receptor to G Proteins. *J. Biol. Chem.* **281**, 12896–12907

319. Tetsuka, M., Saito, Y., Imai, K., Doi, H., and Maruyama, K. (2004) The Basic Residues in the Membrane-Proximal C-Terminal Tail of the Rat Melanin-Concentrating Hormone Receptor 1 Are Required for Receptor Function. *Endocrinology*. **145**, 3712–3723

320. Charest, P. G., and Bouvier, M. (2003) Palmitoylation of the V2 Vasopressin Receptor Carboxyl Tail Enhances β-Arrestin Recruitment Leading to Efficient Receptor Endocytosis and ERK1/2 Activation. *J. Biol. Chem.* **278**, 41541–41551

321. Du, D., Raaka, B. M., Grimberg, H., Lupu-Meiri, M., Oron, Y., and Gershengorn, M. C. (2005) Carboxyl Tail Cysteine Mutants of the Thyrotropin-Releasing Hormone Receptor Type 1 Exhibit Constitutive Signaling: Role of Palmitoylation. *Mol Pharmacol*. **68**, 204–209

322. Gao, Z., Ni, Y., Szabo, G., and Linden, J. (1999) Palmitoylation of the recombinant human A1 adenosine receptor: enhanced proteolysis of palmitoylation-deficient mutant receptors. *The Biochemical journal*. **342 (Pt 2)**, 387–395

323. Hawtin, S. R., Tobin, A. B., Patel, S., and Wheatley, M. (2001) Palmitoylation of the vasopressin V1a receptor reveals different conformational requirements for signaling, agonist-induced receptor phosphorylation, and sequestration. *The Journal of biological chemistry*. **276**, 38139–38146

324. Hayashi, M. K., and Haga, T. (1997) Palmitoylation of muscarinic acetylcholine receptor m2 subtypes: reduction in their ability to activate G proteins by mutation of a putative palmitoylation site, cysteine 457, in the carboxyl-terminal tail. *Arch Biochem Biophys*. **340**, 376–382

325. Kennedy, M. E., and Limbird, L. E. (1994) Palmitoylation of the alpha 2A-adrenergic receptor. Analysis of the sequence requirements for and the dynamic properties of alpha 2A-adrenergic receptor palmitoylation. *The Journal of biological chemistry*. **269**, 31915–31922

326. Adams, M. N., Christensen, M. E., He, Y., Waterhouse, N. J., and Hooper, J. D. (2011) The role of palmitoylation in signalling, cellular trafficking and plasma membrane localization of protease-activated receptor-2. *PLoS ONE*. **6**, e28018

327. Alaluf, S., Mulvihill, E. R., and McIlhinney, R. A. (1995) Palmitoylation of metabotropic glutamate receptor subtype 4 but not 1 alpha expressed in permanently transfected BHK cells. *Biochemical Society transactions*. **23**, 87S

328. Botham, A., Guo, X., Xiao, Y. P., Morice, A. H., Compton, S. J., and Sadofsky, L. R. (2011) Palmitoylation of human proteinase-activated receptor-2 differentially regulates receptor-triggered ERK1/2 activation, calcium signalling and endocytosis. *Biochem. J.* **438**, 359–367

329. Canto, I., and Trejo, J. (2013) Palmitoylation of protease-activated receptor-1 regulates adaptor protein complex-2 and -3 interaction with tyrosine-based motifs and endocytic sorting. *Journal of Biological Chemistry*. **288**, 15900–15912

330. Altenbach, C., Kusnetzow, A. K., Ernst, O. P., Hofmann, K. P., and Hubbell, W. L. (2008) High-resolution distance mapping in rhodopsin reveals the pattern of helix movement due to activation. *Proceedings of the National Academy of Sciences*. **105**, 7439–7444

331. Ballesteros, J. A., Jensen, A. D., Liapakis, G., Rasmussen, S. G. F., Shi, L., Gether, U., and Javitch, J. A. (2001) Activation of the β_2-Adrenergic Receptor Involves Disruption of an Ionic Lock between the Cytoplasmic Ends of Transmembrane Segments 3 and 6. *J. Biol. Chem.* **276**, 29171–29177

332. Gether, U., Asmar, F., Meinild, A. K., and Rasmussen, S. G. F. (2002) Structural Basis for Activation of G-Protein-Coupled Receptors. *Pharmacology & Toxicology*. **91**, 304–312

333. Palczewski, K. (2000) Crystal Structure of Rhodopsin: A G Protein-Coupled Receptor. *Science*. **289**, 739–745

334. Rovati, G. E., Capra, V., and Neubig, R. R. (2007) The Highly Conserved DRY Motif of Class A G Protein-Coupled Receptors: Beyond the Ground State. *Molecular pharmacology*. **71**, 959–964

335. Scheerer, P., Park, J. H., Hildebrand, P. W., Kim, Y. J., Krauß, N., Choe, H.-W., Hofmann, K. P., and Ernst, O. P. (2008) Crystal structure of opsin in its G-protein-interacting conformation. *Nature*. **455**, 497–502

336. Sun, X., Ågren, H., and Tu, Y. (2014) Functional water molecules in rhodopsin activation. *J Phys Chem B*. **118**, 10863–10873

337. Tomobe, K., Yamamoto, E., Kholmurodov, K., and Yasuoka, K. (2017) Water permeation through the internal water pathway in activated GPCR rhodopsin. *PLoS One*. 10.1371/journal.pone.0176876

338. Yuan, S., Filipek, S., Palczewski, K., and Vogel, H. (2014) Activation of G-protein-coupled receptors correlates with the formation of a continuous internal water pathway. *Nature Communications*. **5**, 1–10

339. Cai, K., Klein-Seetharaman, J., Farrens, D., Zhang, C., Altenbach, C., Hubbell, W. L., and Khorana, H. G. (1999) Single-cysteine substitution mutants at amino acid positions 306-321 in rhodopsin, the sequence between the cytoplasmic end of helix VII and the palmitoylation sites: sulfhydryl reactivity and transducin activation reveal a tertiary structure. *Biochemistry*. **38**, 7925–7930

340. Marin, E. P., Krishna, A. G., Zvyaga, T. A., Isele, J., Siebert, F., and Sakmar, T. P. (2000) The Amino Terminus of the Fourth Cytoplasmic Loop of Rhodopsin Modulates Rhodopsin-Transducin Interaction. *J. Biol. Chem.* **275**, 1930–1936

341. Swift, S., Sheridan, P. J., Covic, L., and Kuliopulos, A. (2000) PAR1 thrombin receptor-G protein interactions. Separation of binding and coupling determinants in the galpha subunit. *The Journal of biological chemistry*. **275**, 2627–2635

342. The UniProt Consortium (2019) UniProt: a worldwide hub of protein knowledge. *Nucleic Acids Research*. **47**, D506–D515

343. Trzaskowski, B., Latek, D., Yuan, S., Ghoshdastider, U., Debinski, A., and Filipek, S. (2012) Action of Molecular Switches in GPCRs - Theoretical and Experimental Studies. *Curr Med Chem*. **19**, 1090–1109

344. Bahouth, S. W., and Nooh, M. M. (2017) Barcoding of GPCR trafficking and signaling through the various trafficking roadmaps by compartmentalized signaling networks. *Cellular Signalling*. **36**, 42–55

345. Yang, Z., Yang, F., Zhang, D., Liu, Z., Lin, A., Liu, C., Xiao, P., Yu, X., and Sun, J.-P. (2017) Phosphorylation of G Protein-Coupled Receptors: From the Barcode Hypothesis to the Flute Model. *Molecular pharmacology*. **92**, 201–210

346. Zhou, X. E., He, Y., Waal, P. W. de, Gao, X., Kang, Y., Eps, N. V., Yin, Y., Pal, K., Goswami, D., White, T. A., Barty, A., Latorraca, N. R., Chapman, H. N., Hubbell, W. L., Dror, R. O., Stevens, R. C., Cherezov, V., Gurevich, V. V., Griffin, P. R., Ernst, O. P., Melcher, K., and Xu, H. E. (2017) Identification of Phosphorylation Codes for Arrestin Recruitment by G Protein-Coupled Receptors. *Cell*. **170**, 457-469.e13

347. Ricks, T. K., and Trejo, J. (2009) Phosphorylation of protease-activated receptor-2 differentially regulates desensitization and internalization. *The Journal of biological chemistry*. **284**, 34444–34457

348. Seatter, M. J., Drummond, R., Kanke, T., Macfarlane, S. R., Hollenberg, M. D., and Plevin, R. (2004) The role of the C-terminal tail in protease-activated receptor-2-mediated Ca2+ signalling, proline-rich tyrosine kinase-2 activation, and mitogen-activated protein kinase activity. *Cell Signal*. **16**, 21–29

349. Ferguson, S. S. (2001) Evolving concepts in G protein-coupled receptor endocytosis: the role in receptor desensitization and signaling. *Pharmacol Rev*. **53**, 1–24

350. Soh, U. J., Dores, M. R., Chen, B., and Trejo, J. (2010) Signal transduction by protease-activated receptors. *British journal of pharmacology*. **160**, 191–203

351. Cunningham, M. R., McIntosh, K. A., Pediani, J. D., Robben, J., Cooke, A. E., Nilsson, M., Gould, G. W., Mundell, S., Milligan, G., and Plevin, R. (2012) Novel Role for Proteinase-activated Receptor 2 (PAR2) in Membrane Trafficking of Proteinase-activated Receptor 4 (PAR4). *Journal of Biological Chemistry*. **287**, 16656–16669

352. Smith, T. H., Coronel, L. J., Li, J. G., Dores, M. R., Nieman, M. T., and Trejo, J. (2016) Protease-activated Receptor-4 Signaling and Trafficking Is Regulated by the Clathrin Adaptor Protein Complex-2 Independent of β-Arrestins. *J. Biol. Chem.* **291**, 18453–18464

Chapter 2

2 Molecular basis for activation and biased signalling at the thrombin-activated GPCR Proteinase Activated Receptor-4 (PAR4)[iv]

[iv]A version of this chapter has been published: Thibeault, P. E., LeSarge, J. C., Arends, D., Fernandes, M., Chidiac, P., Stathopulos, P. B., Luyt, L. G., and Ramachandran, R. (2019) Molecular basis for activation and biased signaling at the thrombin-activated GPCR Proteinase Activated Receptor-4 (PAR4). *J. Biol. Chem.* 10.1074/jbc.RA119.011461

2.1 Introduction

G-Protein-coupled receptors (GPCRs) are the largest family of cell surface receptors and regulate a host of important physiological responses (1, 2). GPCRs respond to a variety of extracellular signals and regulate cellular behaviour through engaging intracellular effector molecules to activate various cell-signalling pathways (3, 4). In drug discovery, GPCRs are a valuable and highly tractable class of drug targets with over 30% of all currently approved drugs acting on GPCRs (5). GPCR activation occurs typically through binding of a soluble ligand and conformational changes that enable engagement of G-protein-dependent or β-arrestin-mediated signal transduction. The Proteinase Activated Receptors (PARs) are a four-member family of GPCRs with a distinct mechanism of activation that involves limited proteolysis and unmasking of a receptor activating motif called the tethered-ligand. PARs were first discovered in an effort to identify the cellular receptors responsible for actions of thrombin that were independent from its role in the coagulation cascade (6). Various proteinases have now been described as activators of the different members of the PAR family, but canonically PAR1 and PAR4 are described as thrombin-activated receptors, while PAR2 is activated by trypsin and other trypsin-like serine proteinases. PAR4 can also be activated by trypsin. Whether PAR3 signals independently is unclear, though thrombin can cleave the PAR3 N-terminus to reveal a tethered-ligand (7, 8). Following the discovery of PARs it was quickly realized that two receptors, PAR1 and PAR4, serve as the thrombin receptors on human platelets (9, 10). PAR1 and PAR4 both trigger platelet activation and aggregation. Given that anti-platelet agents are an important class of drugs for the treatment of various cardiovascular diseases, there has been a concerted effort aimed at understanding the role of these receptors in platelet activation and in identifying molecules that can act as PAR1 and PAR4 antagonists. A PAR1 antagonist was recently identified and approved for clinical use, however significant bleeding side effects were noted in patients administered this drug (11–13). While bleeding is a frequently encountered side effect of therapeutically targeting pathways involved in blood coagulation, it was hoped that targeting PAR1 would not present such liability. Much attention has now shifted to understanding and targeting the other thrombin receptor PAR4. Though both PAR1 and PAR4 are activated by thrombin, there are some key differences reported in the activation of these two

receptors on platelets that argue for PAR4 being a better anti-platelet drug target than PAR1. PAR1 possesses a hirudin-like binding site that enables it to bind thrombin with relatively high affinity (14, 15). In lacking this thrombin-binding site, PAR4 can only be activated at much higher concentrations of thrombin, such as may be encountered on a growing platelet thrombus. There are also reported differences in the kinetics of PAR1 and PAR4-dependent calcium signalling, with PAR4 causing a delayed but more sustained signal compared to PAR1 (16). This is thought to be due to dual proline residues in the PAR4 exodomain that provide low-affinity interactions with the thrombin active site and an anionic cluster that slows dissociation from thrombin (17). Overall, PAR1 is thought to initiate platelet activation in response to low concentrations of thrombin while PAR4 is engaged at higher concentrations to further consolidate and stabilize the clot.

Given the liabilities seen with targeting PAR1 as a platelet thrombin receptor there has been renewed interest in developing small molecule PAR4 antagonists (18–20). Recently small molecule antagonists of PAR4 have been described with efficacy in inhibiting injury induced thrombosis in both non-human primates and humans (21–23). Despite these promising advances there remains the question of whether a complete inhibition of PAR4 might also lead to bleeding liability. Our efforts have therefore focused on examining biased signalling through PAR4 in order to identify pathways that are responsible for platelet aggregation and that could be selectively manipulated for therapeutic efficacy. PAR4 can activate multiple signalling pathways through coupling to $G\alpha_{q/11}$, $G\alpha_{12/13}$ and β-arrestin (24–26). In previous work, we and others showed that pepducins targeting different intracellular motifs in PAR4 could be employed to differentially inhibit platelet activation by blocking G-protein-coupled or β-arrestin-dependent signalling (26, 27). The ability to selectively activate or inhibit GPCR signalling in a biased manner is of great interest and has been proposed as a strategy for obtaining therapeutically superior drugs for a number of conditions (28–30). In the case of the finely balanced signalling systems involved in coagulation and platelet activation, such subtle perturbations may be key to obtaining drugs which do not result in bleeding liability.

Here we seek to gain an understanding of the molecular interactions responsible for agonist docking to PAR4 and to identify interactions that can be manipulated to obtain biased ligands for PAR4. By screening a peptide library derived from the most widely used PAR4 agonist peptide, AYPGKF-NH_2, we have identified key residues that confer selective activation of $G\alpha_{q/11}$ coupled calcium signalling and/or β-arrestin recruitment. Through *in silico* docking and confirmatory mutagenesis experiments we further identify an extracellular loop 2 residue (Asp^{230}) that is critical for receptor activation and signalling. We also examine platelet activation by peptides that show differential activation of PAR4 signalling. Overall, these studies advance our understanding of PAR4 activation and signalling and will help guide future drug discovery efforts targeting this receptor.

2.2 Methods

2.2.1 Chemicals and reagents

All chemicals were purchased from Millipore-Sigma (Burlington, Massachusetts, United States), Thermo Fisher Scientific (Hampton, New Hampshire, United States), or BioShop Canada Inc. (Burlington, Ontario, Canada) unless otherwise stated. AYPGKF-NH_2 was purchased from and synthesized by Genscript (Piscataway, New Jersey, United States). Thrombin from human plasma was obtained from Millipore-Sigma (Cat. # 605195, 5000 units; Burlington, Massachusetts, United States).

2.2.2 Molecular cloning and constructs

The plasmid encoding PAR4-YFP was cloned and validated as described previously (26). The use of an in frame, C-terminal eYFP fusion with PAR4 has been utilized in several published studies and such modification does not significantly alter signalling downstream of PAR4 (26, 31–33). Plasmid DNA mutations in the predicted orthosteric binding site of PAR4 were generated using the QuikChange XL Multi Site-Directed Mutagenesis Kit (Agilent Technologies, Mississauga, ON, Canada) to generate all mutants described in this study. All constructs were verified by sanger sequencing (Robarts DNA sequencing facility, University of Western Ontario). Confocal microscopy of HEK-293 cells transfected with PAR4-YFP and PAR4-YFP mutants generated by site-

directed mutagenesis was employed to ensure proper localization of receptors to the plasma membrane (Supplementary Figure 2.5). Confocal microscopy was conducted on an Olympus FV1000 (60x magnification) following fixation of samples with 4% methanol-free formaldehyde and nuclear staining with DAPI (4′,6-Diamidino-2-phenylindole dihydrochloride; 1:1000). Renilla luciferase-tagged β-arrestin-1/-2 constructs were a kind gift from Michel Bouvier (Université de Montréal). PX458 vector for CRISPR/Cas9 targeting was a kind gift from Feng Zhang (Massachusetts Institute of Technology; Addgene # 48138)

2.2.3 Site-directed mutagenesis of predicted PAR4 receptor-peptide interaction sites.

Site-directed mutagenesis using Agilent QuikChange-XL was undertaken to generate mutations in highly predicted receptor residues to validate GalaxyPepDock modelling and determine key binding-site residues for the native PAR4 tethered ligand and PAR4 agonist peptide AYPGKF-NH_2. Residues were mutated by single-nucleotide substitutions replacing native residues with alanine. Successful mutations were confirmed by DNA sequencing (London Regional Genomics Centre, London, ON).

2.2.4 Cell lines and culture conditions

All media and cell culture reagents were purchased from Thermo Fisher Scientific (Hampton, New Hampshire, United States). HEK-293 cells (ATCC; Manassas, Virginia, United States) and CRISPR/Cas9 HEK-293 β-arrestin-1/-2-knockout HEK-293 cell lines were maintained in Dulbecco's modified Eagle's medium supplemented with 10% fetal bovine serum, 1% sodium pyruvate, and 1% streptomycin penicillin. Cells stably transfected with PAR4-YFP vector was routinely cultured in the above media supplemented with 600 µg/mL G418 sulfate (Geneticin; ThermoFisher Scientific Waltham, Massachusetts, United States). Since trypsin activates PAR4, cells were routinely sub-cultured using enzyme-free isotonic phosphate-buffered saline (PBS), pH 7.4, containing 1 mM EDTA followed by centrifugation to remove PBS-EDTA and plated in appropriate culture plates for further experimentation. Cells were transiently transfected with appropriate vectors using a modified calcium phosphate transfection

(Nuclease free water, 2.5M $CaCl_2$, and 2x HEPES Buffered Saline). Transient transfections were rinsed with phosphate buffered saline (PBS) 24 hours post-transfection and replaced with growth media. Transiently transfected cells were assayed or imaged at 48 hours post-transfection.

2.2.5 Generation of β-arrestin-1/-2 double knockout HEK-293 cells using CRISPR/Cas9.

A β-arrestin-1/-2-knockout HEK-293 cell line (β-arr. knockout) was generated using CRISPR/Cas9 mediated gene targeting. Guides sequences targeted to β-arrestin-1 or β-arrestin-2 were designed using the design tool at http://crispr.mit.edu. Gene targeting guides (β-arrestin 1; TGTGGACCACATCGACCTCG, β-arrestin 2; GCGGGACTTCGTAGATCACC, were ligated into the PX458 vector (Kind gift from Dr. Feng Zhang, MIT, Addgene plasmid #48138), verified by direct sequencing and transfected in HEK-293 cells via calcium phosphate transfection (34, 35). GFP expressing cells were single-cell selected by flow cytometry (FACSAria III; London Regional Flow Cytometry Facility) into wells of a 96-well plate. Clonal cell populations were expanded and screened by western blot to identify successful knockout (anti-β-arrestin-1/-2 antibody, rabbit mAb D24H9; Cell Signalling Technologies, Danvers, Massachusetts, United States; anti-β-actin antibody, mouse mAb 8H10D10; Cell Signalling Technologies; Supplementary Figure 2.4).

2.2.6 General methods for peptide synthesis

All synthesis reagents were purchased from Sigma-Aldrich, ChemImpex, or Thermo Fisher Scientific and used without further purification. Peptides were synthesized using standard Fmoc-solid phase peptide synthesis (SPPS) on Rink amide MBHA resin (256 mg, 0.1 mmol, 0.39 mmol/g) with a Biotage® Syrowave^{TM} automated peptide synthesizer (0.4 mmol of HCTU, 0.4 mmol of Fmoc-amino acids, 0.6 mmol of DIPEA, 1 h coupling). Some peptides also involved additional manual synthesis (see procedures below). Following automated and manual synthesis, peptides were cleaved off the resin by being shaken in a cleavage cocktail solution of 95% TFA, 2.5% TIPS, and 2.5% H_2O (4 mL, 5 h), precipitated in ice cold *tert*-butyl methyl ether, lyophilized, purified by

preparative RP-HPLC, and further lyophilized to obtain a dry powder. Purity was assessed by analytical RP-HPLC and characterized by mass spectrometry (MS). The analytical RP-HPLC was performed on a system consisting of an analytical Agilent Zorbax SB-C8 column (4.6 x 150 mm, 5 µm), Waters 600 controller, Waters in-line degasser, and Waters Masslynx software (version 4.1). Two mobile phases were used; eluent A (0.1% TFA in acetonitrile) and eluent B (0.1% TFA in MilliQ water). The flow rate was set at 1.5 $mLmin^{-1}$ over 10 minutes with an additional 5-minute wash (95% solvent A in solvent B). A Waters 2998 Photodiode array detector (200-800 nm) and an ESI-MS (Waters Quattro Micro API mass spectrometer) were used to monitor the column eluate. The preparative RP-HPLC used the same system, eluents, and detection method as mentioned above for the analytical RP-HPLC, except that a preparative Agilent Zorbax SB-C8 column (21.2 x 150 mm, 5 µm) at a flow rate of 20 $mLmin^{-1}$ was used. The mass spectra for all peptides were determined in positive mode using an ESI ion source on either a Bruker micrOToF II mass spectrometer or a Xevo QToF mass spectrometer (Supplementary Table 2.1). All peptides had purity >95% as determined by analytical HPLC (Supplementary Table 2.1, Appendix 1).

2.2.7 Synthesis of Ac-AYPGKF-NH_2

The hexapeptide (AYPGKF) was synthesized using the standard automated Fmoc-SPPS discussed in the general methods for peptide synthesis. While still on resin, with all of the side chains protected, and with the N-terminal Fmoc-deprotection completed, the N-terminus of this peptide was acetylated by being shaken in a solution of acetic anhydride and DMF (v/v 1:4, 5 mL, 30 min). Following this, the peptide was cleaved, purified, and analyzed as mentioned in the general methods for peptide synthesis.

2.2.8 Synthesis of peptides involving *N*-methylation of the peptide backbone

Peptides [(*N*-Me-A)-YPGKF-NH_2, (*N*-Me-S)-YPGKF-NH_2, A-(*N*-Me-Y)-PGKF-NH_2, AYPG-(N_α-Me-K)-F-NH_2, and AYPGK-(*N*-Me-F)-NH_2] were synthesized using abovementioned automated Fmoc-SPPS up to the desired amino acid that was *N*-methylated (e.g. KF-resin for AYPG-(N_α-Me-K)-F-NH_2). Following Fmoc-deprotection

of the resin-bound N-terminal amino acid (e.g. lysine for AYPG-(N_α-Me-K)-F-NH_2), site selective *N*-methylation of the N-terminal amino acid was completed as follows: First, protection of the primary amine was completed to favour monomethylation by adding 2-nitrobenzenesulfonyl chloride (110.8 mg, 0.5 mmol) and 2,4,6-trimethylpyridine (132 µL, 1.0 mmol) in NMP (4 mL) to the on-resin peptide (0.1 mmol) and shaken (15 min). Following completion of the protection reaction, the resin was washed thrice with NMP (3X 5 mL) and dry THF (3X 5 mL). Second, *N*-methylation was completed through Mitsunobu conditions by adding triphenylphosphine (131.2 mg, 0.5 mmol), diisopropyl azodicarboxylate (98 µL, 0.5 mmol), and methanol (41 µL, 1.0 mmol) in dry THF (4 mL) to the on-resin peptide and shaken under N_2 (10 min). Following completion of the *N*-methylation reaction, the resin was washed thrice with dry THF (3X 5mL) and NMP (3X 5 mL). Third, the methylated N-terminal amine was then deprotected by adding 2-mercaptoethanol (70 µL, 1.0 mmol) and 1,8-diazabicyclo(5.4.0)undec-7-ene (75 µL, 0.5 mmol) in NMP (4 mL) to the on-resin peptide and shaken (5 min). The solution turned bright yellow as expected. The solution was removed and then this third step was repeated, followed by being washed five times with NMP (5X 5 mL) and thrice with DMF (3X 5 mL). Addition of the next sequential amino acid (except for inapplicable peptides i.e. (*N*-Me-A)-YPGKF-NH_2 and (*N*-Me-S)-YPGKF-NH_2) was added manually [0.3 mmol of HATU, 0.3 mmol of Fmoc-amino acid (e.g. Fmoc-Gly-OH for AYPG-(N_α-Me-K)-F-NH_2), 0.6 mmol of DIPEA, 4 mL of DMF, 3 h coupling]. Following completion of the sequential amino acid reaction, the resin was washed 5 times with DMF (5X 5mL) and then the next sequential amino acid was added (on applicable peptides i.e AYPG-(N_α-Me-K)-F-NH_2 and AYPGK-(*N*-Me-F)-NH_2) using the automated procedure mentioned in the general methods for peptide synthesis. Following completion of the synthesis, the peptide was cleaved, purified, and analyzed as mentioned in the general methods for peptide synthesis. The amino acid *N*-methylglycine, commonly known as sarcosine, was obtained from a commercial source, and therefore, *N*-methylglycine containing peptides (i.e. Sar-YPGKF-NH_2 and AYP-Sar-KF-NH_2) were synthesized solely by the standard automated Fmoc-SPPS discussed in the general methods for peptide synthesis.

2.2.9 Synthesis of AYPG-(N_ε-Me-K)-F-NH_2

The hexapeptide (AYPGKF) was synthesized using the standard automated Fmoc-SPPS discussed in the general methods for peptide synthesis, except that Fmoc-Lys(Alloc)-OH was used in place of standard Fmoc-Lys(Boc)-OH. While still on resin, with all of the side chains protected, and with the N-terminal Fmoc-deprotection completed, the N-terminus of this peptide was Boc protected by adding Boc-ON (98.5 mg, 0.4 mmol) and DIPEA (70 µL, 0.4 mmol) in DMF (4 mL) and shaken (4 hours). The solution was removed and this Boc protection was repeated overnight (20 hours) to ensure reaction completion. The resin was washed thrice with DMF (3X 5 mL) and dry DCM (3X 5 mL) and was placed under N_2 for site selective Alloc deprotection of the on-resin lysine side chain. Phenylsilane (296 µL, 2.4 mmol) in dry DCM (2 mL) was added to the resin. Tetrakis(triphenylphosphine) palladium(0) (23.1 mg, 20 µmol) was dissolved in dry DCM (1 mL) and added to the resin. The peptide column was flushed with N_2 (2 min) followed by being shaken (5 min). The resin was washed thrice with dry DCM (3X 5 mL). The procedure was repeated and shaken again (30 min). The resin was washed four times with DCM (4X 5 mL) and DMF (4X 5 mL). Following this N-terminal Boc protection and subsequent side chain Alloc deprotection, *N*-methylation of the on-resin lysine side chain was completed through the site selective *N*-methylation procedure mentioned above. Following completion of the synthesis, the peptide was cleaved, purified, and analyzed as discussed in the general methods for peptide synthesis.

2.2.10 SPPS reaction monitoring

Three methods were used to monitor SPPS reactions. Two methods (the Kaiser Test and the small-scale resin cleavage) were used to monitor general peptide synthesis. Three methods (the Kaiser Test, the small-scale resin cleavage, and the Chloranil Test) were used to monitor synthesis of peptides involving *N*-methylation. For the Kaiser Test, several resin beads were placed in a test tube followed by the addition of 42.5 mM phenol in ethanol (50 µL), 20 µM potassium cyanide in pyridine (50 µL), and 280.7 mM ninhydrin in ethanol (50 µL). The mixture was then heated (100 °C, 5 min); where a positive test indicates the presence of a free primary amine. For the small-scale resin

cleavage method, several beads and cleavage cocktail (500 µL) are shaken, worked up as per the full cleavage of the resin procedure described above, and the desired peptide was confirmed through HPLC-MS. For the Chloranil Test, several resin beads were placed in a test tube followed by the addition of 357.8 mM acetaldehyde in DMF (50 µL) and 81.3 mM *p*-chloranil in DMF (50 µL) and allowed to stand at room temperature (5 min); where a positive test indicates the presence of a free secondary amine.

2.2.11 Calcium signalling assay

HEK-293 cells or HEK-293 cells stably expressing PAR4-YFP were loaded with calcium sensitive dye (Fluo-4 NW, F36206, Life Technologies, Thermo Fisher) and aliquoted into cuvettes with Hanks buffered salt solution (HBSS containing Ca^{2+} and Mg^{2+}). Samples were excited at 480 nm and emission recorded at 530 nm. Baseline fluorescence from PAR4-YFP excitation remains constant throughout experiment. Following baseline recording, agonist induced changes in fluorescence was recorded. Change in fluorescence from baseline to maximum response at a given agonist concentration (delta) were expressed as a percentage of maximum cellular response elicited by calcium ionophore (A23187, Sigma-Aldrich). For calcium signalling assay with PAR4 orthosteric site-directed mutants, HEK-293 cells were transiently transfected with 2 µg of wild-type YFP tagged PAR4 or PAR4 mutant receptors (described above) using the calcium phosphate transfection protocol as described above. Calcium signalling was investigated as described above for the wild type receptor.

2.2.12 Measurement of β-arrestin-1/-2 recruitment via bioluminescence resonance energy transfer

HEK-293 cells were co-transfected with either wild-type or mutant PAR4-YFP (2 µg) and β-arrestin-1- or -2-Renilla luciferase (rluc, 0.2 µg) using modified calcium phosphate transfection. Cells were re-plated (24 hours post-transfection) into white 96-well plates (Corning). At 48-hours post-transfection, agonist-stimulated β-arrestin recruitment to PAR4 was detected by measuring BRET following 20 minutes of agonist stimulation. h-coelenterazine (5 µM; Nanolight Technology, Pinetop, AZ) was added ten minutes prior to BRET collection using a Berthold Mithras LB 940 plate reader.

2.2.13 Testing peptide library specificity for PAR4

Previous studies have pointed to the possibility of PAR agonist peptides cross activating other members of this family. For example, the PAR1 tethered ligand peptide SFLLRN is able to activate PAR2 and substitution of a phenylalanine residue in certain PAR4 agonist peptides confers PAR1 activity (36–38). Activating peptides typically require an aromatic sidechain in position 2 (F in PAR1) and we wondered if substitution of tyrosine for phenylalanine may decrease selectivity at PAR4 and increase crosstalk with PAR1. We examined whether substitutions made to AYPGKF-NH_2 affected their selectivity using a calcium signalling assay in HEK-293 cells that endogenously express PAR1 and PAR2. None of the peptides tested elicited a signalling greater than 5% of the calcium ionophore A23187 showing that they retain selectivity towards PAR4 (Supplementary Figure 2.6). Additionally, we investigated specificity using BRET for β-arrestin-2 recruitment to cells expressing PAR4-YFP or PAR2-YFP. None of the peptides were able to induce β-arrestin recruitment in PAR2-YFP expressing HEK-293 cells (NET BRET of 0.05 and over) with the exception of AYPGK-1Nal-NH_2 (Supplementary Figure 2.7).

2.2.14 PAR4-stimulated mitogen-activated protein kinase (MAPK) signalling

2.2.14.1 MAPK signalling in PAR4-YFP stable cells with peptide library

Agonist-stimulated mitogen-activated protein kinase (MAPK) signalling in HEK-293 cells stably expressing PAR4-YFP were analyzed by western blot following stimulation with PAR4 peptide agonists. Cells were placed in serum free media (serum-free DMEM, Gibco) for 3 hours before beginning experiment. Cells were stimulated with either control (no agonist), AYPGKF-NH_2 or agonist peptides described at 100 μM concentration. Cells were stimulated for 10 minutes with agonist and lysed, quantified, and blot as previously described.

2.2.14.2 HEK-293 and CRISPR/Cas9 β-arrestin-1/-2 double knockout HEK-293

Agonist-stimulated mitogen-activated protein kinase (MAPK) signalling in CRISPR/Cas9 HEK-293 β-arrestin double knockout cells (β-arr. knockout) and wild-type HEK-293 cells transfected with PAR4-YFP were analyzed by western blot. Cells were placed in serum free media (serum-free DMEM, Gibco) for 3 hours before beginning experiment. Cells were then stimulated with 30 μM AYPGKF-NH_2 for varying time periods (0, 2, 5, 10, 20, 30, 60, 90 minutes) at 37 ˚C. Treated cells were placed on ice following stimulating period. Total protein was extracted adding kinase lysis buffer with phosphatase and protease inhibitors (20 mM Tris-HCl, pH 7.5, 100 mM NaCl, 10 mM $MgCl_2$, 1 mM EDTA, 1 mM EGTA, 0.5% NP-40, 2.5 mM sodium pyrophosphate, 1 mM b-glycerophosphate, 1 mM Na_3VO_4, 25 mM NaF, 1 mg/mL leupeptin, 1 mg/m aprotinin, 1 mM phenylmethylsulfonyl fluoride, and 1mM dithiothreitol) for 20 minutes and cell membranes were cleared by centrifugation (13,300g for 3 minutes). Protein concentrations were measured using the Pierce BCA Protein Assay (Thermo Fisher Scientific). Protein samples were heat-denatured at 98°C for 8 minutes in denaturing Laemmli buffer (containing 2-mercaptoethanol) and resolved on 4–12% gradient Invitrogen Bolt Bis-Tris Plus gels (Thermo Fisher Scientific). The resolved proteins were transferred via wet transfer in buffer (1X Tris-glycine, 20% methanol) to a polyvinylidene difluoride membrane and blocked in TBST buffer (TBS with 0.1% (v/v) Tween-20) supplemented with 1% ECL Advance Blocking Agent (GE Healthcare, Waukesha, WI) for 40 minutes at room temperature. p44/42 (Thr202/Tyr204) phosphorylation was detected with specific antibodies (Cell Signalling Technology, Danvers, MA; diluted 1:1000 in TBST) overnight at 4°C. phospho-p44/42 immunoreactivity was detected using the horseradish peroxidase-conjugated anti-rabbit secondary antibody (Cell Signalling Technology; 1:10,000 in TBST for 1 hour). After washing the membrane with TBST (3 x 10-minute washes), the peroxidase activity was detected with the chemiluminescence reagent ECL Advance (GE Healthcare) on iBright image Station (Invitrogen, Burlington, ON). Membranes were then stripped with blot stripping buffer (Thermo Fisher Scientific) at room temperature and blocked in TBST with 1% ECL Advance Blocking Agent before incubation with the p44/42 (1:1000 in

TBST with 1% ECL Advance Blocking Agent) overnight at 4°C. Following incubation with primary antibody, blots were rinsed in TBST and incubated with appropriate horseradish peroxidase -conjugated anti-rabbit or anti-mouse secondary antibody (1:10,000 in TBST for 1 hour). Membranes were washed and imaged as previously described. Band intensities representing activated MAPK were quantified using FIJI (39). Phospho-kinase levels were normalized for differences in protein loading by expressing the data as a ratio of the corresponding total-p44/42 signal. Data are expressed as a fold increase over unstimulated baseline control.

2.2.14.3 PAR4-stimulated MAPK signalling in HEK-293 +/- YM254890

Agonist-stimulated MAPK signalling in wild-type HEK-293 cells transfected with PAR4-YFP were analyzed by western blot. Cells were placed in serum free media (serum-free DMEM, Gibco) for 3 hours before beginning experiment. Prior to agonist stimulation cells were treated with either control (0.001% DMSO) or YM254890 (100 nM) for 20 minutes. Cells were then stimulated with 30μM AYPGKF-NH_2 for varying time periods (0, 2, 5, 10, 20, 30, 60, 90 minutes) at 37 degrees Celsius. Cells were lysed, protein quantified, and samples run and imaged as previously described.

2.2.15 Structural homology modelling of PAR4

Residues resolved in the PAR2 crystal (5NDD.pdb) were used to generate a homology model of wild-type human PAR2. Homology model of wild-type human PAR2 was then aligned with the wild-type human PAR4 amino acid sequence [National Center for Biotechnology Information (NCBI) accession number NM_003950) using Clustal Omega (40, 41). Only residues resolved in the crystal structure of PAR2 were used as template coordinates for PAR4 homology modelling. Twenty human PAR4 homology models were generated using the human PAR2 crystal structure coordinates (5NDD.pdb) (42) as a template in MODELLER (version 9.16) (43). The model with the lowest DOPE score was taken as the best structure and visualized using PyMOL (version 1.7.4, Schrödinger, LLC). Electrostatic surface potential was calculated after assignment of partial charges

using PDB2PQR and using the Adaptive Poisson-Boltzmann Solver plugin in PyMOL (44).

2.2.16 *in silico* docking of AYPGKF-NH_2 to the PAR4 homology model

in silico docking of PAR4 agonist peptide, AYPGKF-NH_2, to PAR4 homology model was undertaken using GalaxyPepDock (45). The lowest energy PAR4 homology model PDB file was loaded into GalaxyPepDock along with a text file of the PAR4 agonist peptide sequence which GalaxyPepDock uses to predict a peptide structure for docking analyses (Ala-Tyr-Pro-Gly-Lys-Phe; amidation is not included in the structure prediction). Ten models of PAR4-AP docking were generated. Frequency of receptor-peptide residue interactions, taken as atom-atom distances of less than 3 Angstroms, was quantified manually to determine highly recurrent interactions.

2.2.17 Determination of the AYPGKF-NH_2 structure by NMR

2.2.17.1 Collection of ^{1}H-NMR spectra

Peptide (AYPGKF-NH_2) solution was prepared to 10 mM with 10% D_2O. DSS (Sodium trimethylsilylpropanesulfonate, 30 µM) was used as an internal reference at 0.00 ppm. The ^{1}H NMR spectra were acquired on an Varian INOVA 600 MHz Spectrometer at 25 °C. Phase-sensitive, water-gated, two-dimensional correlated spectroscopy (COSY), total correlation spectroscopy (TOCSY), and nuclear Overhauser effect spectroscopy (NOESY) as previously described by our collaborators (46)**.** Data were collected using the VnmrJ 4.2 software. NMRPipe was used for spectral processing and visualization. Specifically, the two-dimensional data matrix was multiplied by a phase-shifted square-sine-bell window function and zero-filled prior to Fourier transformation. Phase correction was applied in both dimensions.

2.2.17.2 Structure calculations

^{1}H chemical shifts were manually assigned based on TOCSY (approximately 90% of peaks assigned) and COSY spectra using the NEASY plugin to CARA (47, 48). TOCSY peak assignments are reported for two apparent conformations of the peptide based on

peak doubling observed in the spectra and COSY connectivities (Supplementary table 2.2 and 2.3, respectively). Thus, two ^{1}H chemical shift lists were separately used to derive dihedral angle constraints in TALOS+ (49). NOESY peaks were manually picked, and peak intensities determined using the integration function of NEASY. The NOESY peaks were automatically assigned concomitant with structural derivation by CYANA (version 2.1), separately using the inputted chemical shift list and dihedral angle restraints for each conformation (Supplementary Tables 2.2 & 2.3) (50, 51). The unambiguous NMR distance and dihedral angle constraints for each AYPGKF-NH_2 structural ensemble are reported in Supplementary table 2.4. The NOESY spectra with assigned NOEs critical for defining each conformation are shown in Supplementary Figures 2.9 ("major") and 2.10 ("minor") (50, 51). The average backbone RMSD values are reported for the 10 lowest energy structures (Supplementary Table 2.4; Supplementary Figure 2.11).

2.2.18 Preparation of washed platelets and light-transmission aggregometry

Animal care and experimental procedures were carried out under a protocol (AUP# 2018-047) that was reviewed and approved by the University of Western Ontario Animal Care Committee in accordance with the Canadian Council on Animal Care (CCAC) standards and guidelines. Blood was drawn from the abdominal aorta or heart of Sprague-Dawley rats into trisodium citrate (3.4% w.v). The blood was centrifuged at 200g for 15 minutes at 22 degrees Celsius to isolate platelet-rich plasma (PRP). PRP was transferred to a 14 mL polypropylene round-bottom tube (Falcon) and centrifuged at 1800 rotations per minute (594g) for 10 minutes at 22˚C to pellet platelets and obtain platelet-poor plasma (PPP). PPP was decanted and used for 100% light transmission control. To obtain washed platelet sample, platelets were washed twice in Tyrode's buffer (12 mM $NaHCO_3$, 127 mM NaCl, 5 mM KCl, 0.5 mM NaH_2PO_4, 1 mM $MgCl_2$, 5 mM glucose, and 10 mM HEPES; Ramachandran et al., 2017) and resuspended to a volume equivalent to that of the initial blood draw. Washed platelet sample was equilibrated for one hour at ambient temperature following the addition of 1M $CaCl_2$ (1 µl/mL). 400 µl of this washed platelet suspension was used for light transmission aggregometry on a platelet aggregometer (Model 700; Chrono-Log Corp, Havertown, PA).

2.2.19 Data analysis and statistical testing

Data are shown as mean ± SEM. Calcium signalling and β-arrestin-1/-2 recruitment concentration effect curves were calculated using nonlinear regression curve fitting (three parameters; Prism7). EC_{50} values are reported (Table 2.1) where signal has saturated. Where signalling is not saturated EC_{50} is reported for calcium as not determined (*n.d.*). The F-statistic calculated to compare EC_{50} values was calculated using the extra sum-of-squares analysis (52). For table 2.1, values comparing percentage of signalling or recruitment at 100 µM to values obtained from the parental PAR4-AP, AYPGKF-NH_2, are shown. Significance was determined for comparisons with 100 µM AYPGKF-NH_2 and p44/42 phosphorylation by one-way analysis of variance (ANOVA). Western blot protein densitometry was quantified using FIJI. Transformation and analysis were conducted on raw data and significance is indicated by '*' ($p < 0.05$).

2.3 Results

In order to understand the rules governing agonist peptide activation of PAR4, we synthesized 37 hexapeptides through modification to the synthetic PAR4 agonist peptide AYPGKF-NH_2. A number of different modifications were examined at each of the six positions, including alanine, D-isomer, and *N*-methyl substitutions, as well as other modifications aimed at further probing each of the six agonist peptide positions. Henceforth, the parental PAR4 agonist peptide for this study, AYPGKF-NH_2 (Ala^1-Tyr^2-Pro^3-Gly^4-Lys^5-Phe^6-NH_2; superscript denotes position from N-terminus), will be referred to as PAR4-AP. $G\alpha_{q/11}$-coupled calcium signalling, β-arrestin-1/-2 recruitment (β-Arr-1-rluc, β-Arrestin-2-rluc respectively), and p44/42 mitogen-activated protein kinase (MAPK) signalling by each of these peptides was monitored and compared to responses triggered by PAR4-AP (Table 2.1). Whereas PAR4-AP triggered $G\alpha_{q/11}$ signalling reached a clear plateau over the range of concentrations tested (0.3 – 300 µM), β-arrestin recruitment did not and therefore the effective concentration required to achieve half-maximal response (EC_{50}) values could not be accurately assessed. In contrast, with the substituted peptides, $G\alpha_{q/11}$ signalling concentration-effect curves in some cases did not clearly plateau, whereas β-arrestin recruitment did. Where possible, EC_{50} values are

compared between PAR4-AP and substituted peptides. However, since clear maxima were not always obtained, comparisons of signal magnitude throughout the present study are presented as the response elicited by a given compound at 100 μM, shown as a percentage of responses elicited by PAR4-AP at the same concentration. Since the concentration-effect curve for PAR4-AP exhibits a saturating calcium signal, peptides that failed to saturate calcium signalling responses are depicted as having EC_{50} values that were 'not determined' (*n.d.*). Maximal calcium signal responses are shown as a percentage of the response obtained with the calcium ionophore A23187 (Table 2.1, Max; % of A23187 calcium ionophore) and are referred to throughout the results as a change in maximal calcium signalling as a measure of the efficacy of the peptides. Throughout the results, β-arrestin recruitment values are presented as a percentage (%) of the PAR4-AP-induced recruitment at 100 μM concentration. For ease of comparison, concentration-effect curves for PAR4-AP-mediated $G\alpha_{q/11}$ calcium signalling and β-arrestin recruitment are displayed as a repeated reference value in each of the Figures 2.1 through 2.7.

2.3.1 Effect of alanine substitutions on PAR4-AP-mediated signalling responses

Our first set of changes involved alanine substitutions at positions 2-6 of the PAR4-AP (calcium EC_{50} = 12.1 ± 3.1 μM; β-arrestin-1 recruitment at 100 μM for comparison is considered 100 ± 3.9%, and 100 ± 3.5% for β-arrestin-2) (Figure 2.1A-C, Table 2.1). Potency was decreased with respect to calcium signalling when tyrosine[2] was substituted with alanine and failed to reach a plateau over the concentration range tested (A**A**PGKF-NH_2; EC_{50} = *n.d.*). Correspondingly, β-arrestin recruitment was reduced compared to PAR4-AP at the same concentration (β-arr-1 47.3 ± 3.6%; β-arr-2 46.4 ± 3.2%). Substitution of proline[3] with alanine resulted in a significant decrease in potency for calcium signalling (AY**A**GKF-NH_2 EC_{50} = 63.7 ± 20.8 μM) and yielded reduced β-arrestin recruitment (β-arr-1 48.5 ± 7.9%; β-arr-2 43.4 ± 7.1%). Either glycine[4] or phenylalanine[6] substitution to alanine resulted in modest decreases in maximal calcium signalling compared to PAR4-AP at the same concentration, with no significant effect on potency (EC_{50} = 21.2 ± 6.6 μM; EC_{50} = 17.3 ± 5.0 μM, respectively). Additionally, alanine substitutions in these positions resulted in significantly reduced β-arrestin

recruitment, to levels approximately half of those observed with PAR4-AP (AYP**A**KF-NH_2 β-arr-1 56.4 ± 5.6%, β-arr-2 54.6 ± 5.1%; AYPGK**A**-NH_2 β-arr-1 47.9 ± 3.8%, β-arr-2 52.6 ± 3.5%). Interestingly, we observed that lysine^5 to alanine substitution had no appreciable impact on potency with respect to calcium signalling (AYPG**A**F-NH_2 EC_{50} = 9.8 ± 2.9 μM); and modestly reduced recruitment of β-arrestin-1 (59.3 ± 7.2%) and -2 (70.8 ± 6.5%). Collectively, alanine substitutions of positions 2-6 resulted in decreased β-arrestin recruitment compared to the parental peptide (Figure 2.1B-C, Table 2.1). Interestingly, we observe differential effects on calcium signalling with significant detriment to potency attributed to tyrosine substitution (Figure 2.1A). Additionally, substitution of glycine and phenylalanine moderately decreased maximal calcium signalling responses, perhaps indicating that these residues are important for full agonism of this pathway comparative to that achieved with the parental peptide. Notably, all single alanine substitutions of positions 2-6 of the PAR4-AP retained some agonist activity indicating that signalling is not wholly reliant on any single residue alone.

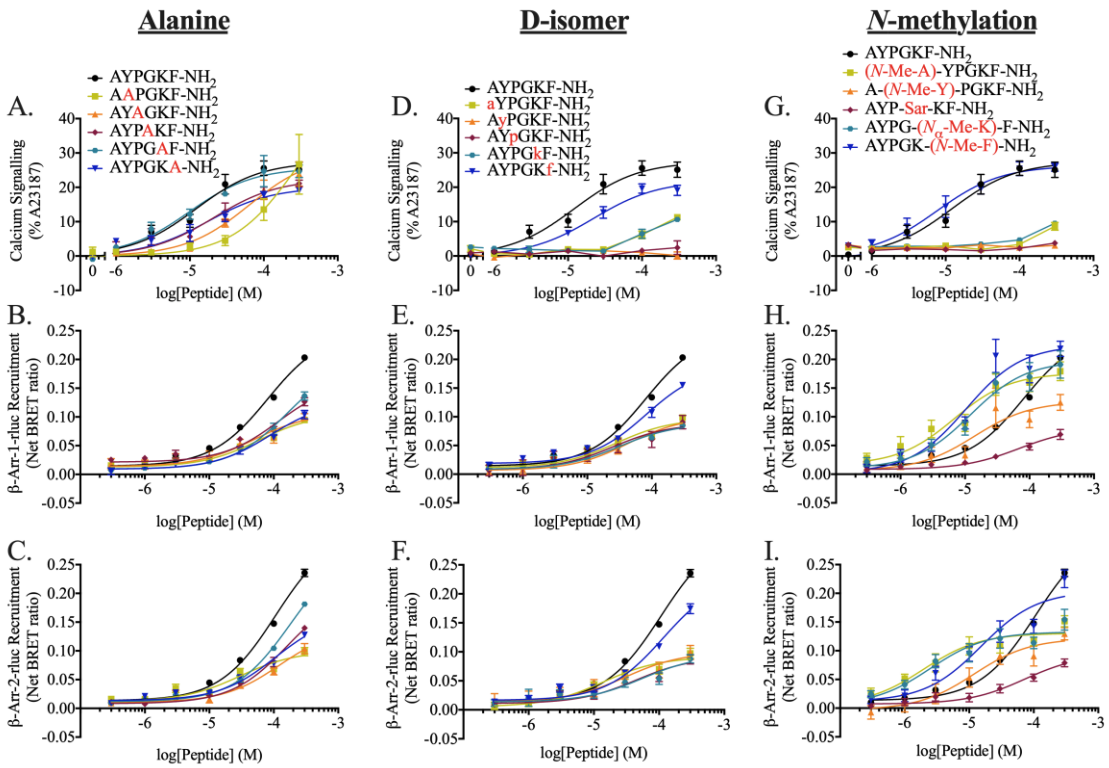

Figure 2.1 Calcium and β-arrestin recruitment in response to Alanine (A-C), D-isomer (D-F), or β-methylation (G-I) substitutions in the PAR4-AP. Calcium signalling (A, D, G) is shown as a percentage of the maximum calcium signalling obtained by application of calcium ionophore (A23187, 3 μM). (*n = 3-7*) Concentration effect curves of agonist-stimulated recruitment of β-arrestin-1 (B, E, H) or β-arrestin-2 (C, F, I) to PAR4. BRET values are presented as normalized net BRET ratio. (*n = 3*).

2.3.2 Effect of D-isomer amino acid substitutions on PAR4-AP-mediated signalling responses

To assess the impact of stereochemical inversion at each residue position, we generated five peptides with single amino acid substitutions from L- to their respective D-isomers (Figure 2.1D-F, Table 2.1). Glycine possesses only one isomeric form and thus is not substituted. Both L-alanine to D-alanine (**a**YPGKF-NH_2) and L-lysine to D-lysine (AYPG**k**F-NH_2) substitutions resulted in significant losses of potency in calcium signalling assays compared to PAR4-AP. Consistent with calcium data, we observed a significant decrease in β-arrestin recruitment compared to the parental PAR4-AP (**a**YPGKF-NH_2 β-arr-1 48.7 ± 2.6%, β-arr-2 47.5 ± 2.4%; AYPG**k**F-NH_2 β-arr-1 47.4 ± 1.0%, β-arr-2 36.5 ± 0.9%). Interestingly, both D-tyrosine (A**y**PGKF-NH_2) and D-proline (AY**p**GKF-NH_2) substitutions completely abolished calcium signalling. Comparably, β-arrestin recruitment was significantly reduced with stimulation by either peptide (A**y**PGKF-NH_2 β-arr-1 50.7 ± 4.6%, β-arr-2 46.4 ± 4.2%; AY**p**GKF-NH_2 β-arr-1 45.2 ± 10.5%, β-arr-2 38.1 ± 9.5%). In keeping with what we observed with phenylalanine to alanine substitution (Figure 2.1A-C), D-phenylalanine substitution in position 6 (AYPGK**f**-NH_2) resulted in less efficacious agonism of both calcium (EC_{50} = 22.2 ± 4.7 μM) and β-arrestin recruitment (β-arr-1 80.3 ± 6.6%, β-arr-2 74.1 ± 6.0%). Overall, D-isomers substitutions of amino acids alanine[1], tyrosine[2], proline[3], and lysine[5] resulted in significant reduction of (D-alanine, D-lysine) or abolition of (D-tyrosine, D-proline) calcium signalling while causing significant reductions in β-arrestin recruitment. Substitution of L-phenylalanine[6] for D-phenylalanine was the only D-isomer substitution that is somewhat tolerated, resulting in modest reductions in potency with respect to both calcium signalling and β-arrestin recruitment. These data reveal that the sidechain stereochemistry of residues within the AYPGKF-NH_2 peptide performs a role in agonism.

2.3.3 Effect of *N*-methylation substitutions on PAR4-AP-mediated signalling responses

We generated a series of peptides to investigate the pharmacological impact of *N*-methylation along the peptide backbone (Figure 2.1G-I, Table 2.1). In contrast to the

parental PAR4-AP, all but one of the N-methylated peptides evaluated yielded clear plateaus and discernible EC_{50} values in β-arrestin recruitment assays, and where applicable these are indicated below along with their relative responses compared to PAR4-AP at 100 μM. Substitution of alanine[1] with *N*-methyl-alanine [**(*N*-Me-A)**-YPGKF-NH_2] almost completely abolished calcium signalling (EC_{50} = *n.d.*). Interestingly, this peptide was able to initiate β-arrestin-1/-2 recruitment comparable to levels obtained with PAR4-AP (β-arr-1 119.2 ± 11.9%, EC_{50} = 6.8 ± 2.6 μM; β-arr-2 80.6 ± 10.8%; EC_{50} = 2.0 ± 0.7 μM). These results suggest that increasing steric bulk and hydrophobicity of the backbone at amide positions through the addition of an N-terminal methyl group drives PAR4 signalling towards β-arrestin pathways and causes only modest activation of calcium signalling. Substitution of tyrosine[2] for *N*-methyl-tyrosine [A-**(*N*-Me-Y)**-PGKF-NH_2] abolished calcium signalling up to 300 μM (EC_{50} = *n.d.*). Consistent with calcium signalling, we observed decreased signal magnitude in β-arrestin recruitment assays compared to PAR4-AP (β-arr-1 71.4 ± 10.8%, EC_{50} = 14.2 ± 8.6 μM; β-arr-2 61.5 ± 9.8%, EC_{50} = 11.8 ± 5.7 μM). Substitution of the PAR4-AP glycine[4] with sarcosine (Sar., a.k.a *N*-methyl-glycine; AYP-**Sar**-KF-NH_2) resulted in significantly reduced calcium potency (EC_{50} = *n.d.*) and significantly reduced β-arrestin-1/-2 recruitment (35.9 ± 4.3%, 36.1 ± 3.9% respectively). *N*-methylation of the alpha (α) amine of lysine[5] [AYPG-**(N_α-Me-K)**-F-NH_2] resulted in significantly reduced calcium signalling (EC_{50} = *n.d.*) with no significant effect on maximal β-arrestin recruitment (β-arr-1 126.7 ± 18.6%, EC_{50} = 12.2 ± 4.3 μM; β-arr-2 77.1 ± 16.9%, EC_{50} = 2.5 ± 1.0 μM). Substitution of phenylalanine[6] with *N*-methyl-phenylalanine [AYPGK-**(*N*-Me-F)**-NH_2] was equipotent for calcium signalling compared to PAR4-AP (EC_{50} = 7.6 ± 1.9 μM). Interestingly, this peptide showed increased recruitment of both β-arrestins (β-arr-1 136.9 ± 18.0%, EC_{50} = 10.4 ± 3.3 μM; β-arr-2 96.6 ± 16.4%, EC_{50} = 15.3 ± 4.6 μM). Together, these data reveal that *N*-methylation of positions 1, 2, 4, and 5 are deleterious to calcium signalling.

We were excited to observe evidence of β-arrestin-biased peptides within this group, all of which showed decreased calcium signalling and/or increased β-arrestin recruitment. Moreover, the leftward shifts in their associated β-arrestin concentration-effect profiles

imply that substitution of *N*-methylated alanine[1], tyrosine[2], lysine[5], or phenylalanine[6] residues increases peptide potency with respect to post-G-protein signalling. Only *N*-methylation of glycine[4] (sarcosine) resulted in a reduced overall ability to activate PAR4, with relative calcium and β-arrestin signals being reduced by approximately 90% and 60%, respectively.

2.3.4 Effect of N-terminal and position 1 modifications on PAR4-AP-mediated signalling responses

To further investigate the impact of *N*-terminal alterations to the PAR4-AP, we examined the impact of N-terminal acetylation and substitutions of position 1 (Figure 2.2A-C, Table 2.1). Previously it was demonstrated that protonation of the N-terminus of the PAR1 tethered-ligand (SFLLRN) is critical for agonist function (53). Additionally, substitution of glycine for mercaptoproprionic acid (Mpr), which lacks an amino-terminal protonated amine found in the native tethered-ligand-mimicking peptide GYPGQV, resulted in complete loss of agonist activity (37). Given the evidence for N-terminal protonation in PAR agonism, we sought to determine the impact of N-terminal acetylation on PAR4-AP activity. N-terminal acetylation of the PAR4-AP (**Ac**-AYPGKF-NH_2) negatively impacted both calcium signalling (EC_{50} = *n.d.*) as well as the magnitude of β-arrestin recruitment to PAR4 as expected (β-arr-1 47.3 ± 3.1%, EC_{50} = 15.0 ± 4.3 μM; β-arr-2 45.5 ± 2.8%, EC_{50} = 26.7 ± 5.6 μM). In contrast to the previously reported complete loss of activity with Mpr-YPGQV peptide (Mpr = mercaptopropionic acid), we observed partial agonism with the loss of protonation through acetylation of PAR4-AP. This could also be influenced by the additional methyl group of the Ala in Ac-AYPGKF-NH_2, which is not present in the Mpr-YPGQV peptide.

In both the native human PAR4 tethered-ligand sequence and the PAR4-AP, position 1 is occupied by small (tethered-ligand – glycine, PAR4-AP – alanine) and non-polar (PAR4-AP – alanine) residues. To investigate the role of position 1 in the PAR4-AP, we generated seven peptides with position 1 substitutions.

Introduction of steric bulk and increased hydrophobicity through substitution of alanine[1] for valine resulted in partial agonism of both calcium signalling and β-arrestin

recruitment (**V**YPGKF-NH_2 EC_{50} = 22.9 ± 8.3 μM; β-arr-1 73.6 ± 13.0%, EC_{50} = 33.8 ± 13.7 μM; β-arr-2 55.2 ± 11.8%, EC_{50} = 13.7 ± 8.2 μM). Additionally, increasing hydrophobic bulk at position 1, through substitution with norleucine, completely abolished calcium signalling (**Nle**-YPGKF-NH_2, EC_{50} = *n.d.*) and resulted in partial agonism of β-arrestin recruitment (β-arr-1 40.2 ± 9.7%; β-arr-2 36.5 ± 8.8%). Together, these data indicate that the precise steric bulk of the side chain in position 1 is important for PAR4 agonism.

Next, we evaluated the impact of steric bulk relocation in position 1. Relocation of the methyl group in alanine to the N-terminus and loss of side chain through substitution with sarcosine (**Sar**-YPGKF-NH_2) resulted in poor agonism at both calcium signalling (EC_{50} = *n.d.*) and β-arrestin recruitment (β-arr-1 35.6 ± 2.0%, β-arr-2 39.8 ± 1.8%). Further, the addition of an α-methyl group through substitution of alanine[1] with 2-aminoisobutyric acid (**Aib**-YPGKF-NH_2) resulted in a significantly less potent and partial agonist for calcium signalling (EC_{50} = 50.2 ± 15.3 μM); also resulting in a significant reduction in β-arrestin recruitment (β-arr-1 38.6 ± 3.9%; β-arr-2 37.3 ± 3.6%). Similarly, replacement with *N*-methyl-serine [**(N-Me-S)**-YPGKF-NH_2] also caused a significant attenuation of calcium signalling (EC_{50} = *n.d.*), while also revealing a decrease in β-arrestin recruitment compared to PAR4-AP (β-arr-1 78.1 ± 6.9%, β-arr-2 51.7 ± 6.3%). Thus, it is apparent that the precise position of the side chain in position 1 is important for agonism.

To further probe the importance of charge localization at the N-terminal region of the peptide, we made several additional substitutions to position 1. Substitution of alanine with either beta-alanine or isonipecotic acid significantly reduced the potency and activity of the PAR4-AP, similar to the results with PAR4-AP N-terminal acetylation (**betaAla**-YPGKF-NH_2 calcium EC_{50} = *n.d.*, β-arr-1 25.7 ± 4.8%, β-arr-2 31.8 ± 4.4%; **Inp**-YPGKF-NH_2 calcium EC_{50} = *n.d.*, β-arr-1 32.0 ± 3.3%, β-arr-2 26.9 ± 3.0%). Together, these data suggest a role for N-terminal charge localization in agonist activity.

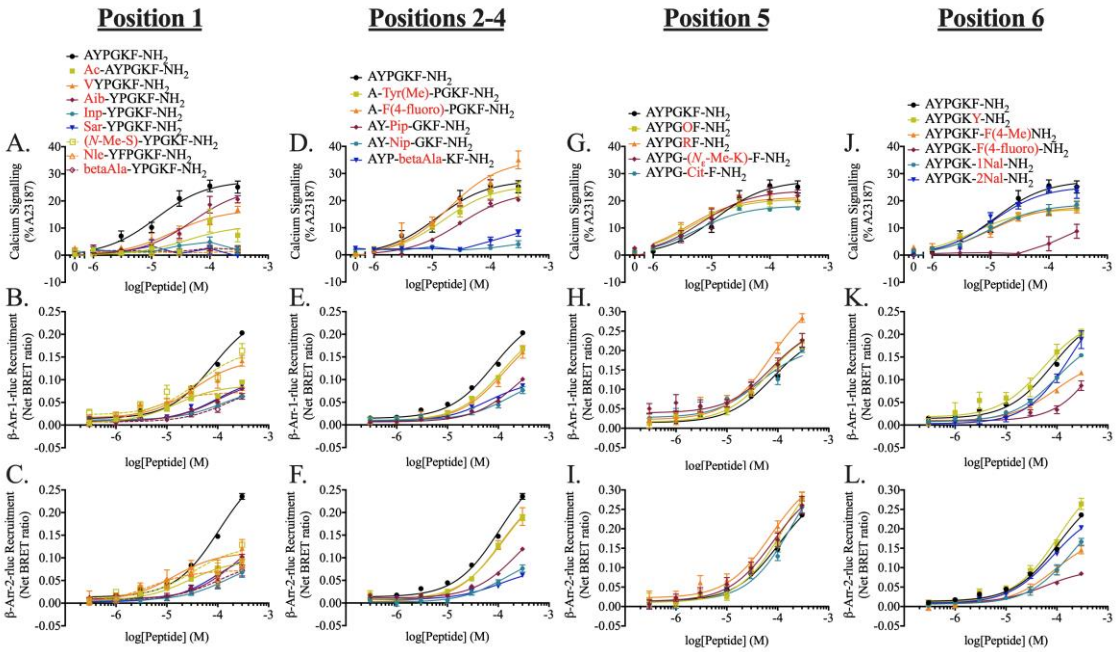

Figure 2.2 Calcium and β-arrestin recruitment in response to additional substitutions to the PAR4-AP by position. Calcium signalling (A, D, G, J) is shown as a percentage of the maximum calcium signalling obtained by application of calcium ionophore (A23187, 3 µM). (*n = 3-7)* Concentration effect curves of agonist-stimulated recruitment of β-arrestin-1 (B, E, H, K) and β-arrestin-2 (C, F, I, L) to PAR4. BRET values from cells treated increasing concentrations of peptide are presented as normalized net BRET ratio. (*n = 3*).

2.3.5 Effect of additional substitutions in positions 2-4 on PAR4-AP-mediated signalling

Previously, structure activity studies with PAR4 activating peptides revealed an apparent requirement for an aromatic residue in position 2 (tyrosine) and found that alterations to position 3 (proline) and position 4 (glycine) were not well tolerated (37). In the present study, we observed that substitution of either tyrosine, proline, or glycine with alanine reduced calcium signalling potency and β-arrestin recruitment, however none of these substitutions completely abolished the activity of the peptide (Figure 2.1A-C). Interestingly, substitution of either L-tyrosine or L-proline with the respective D-isomer significantly reduced the activity of the PAR4-AP (Figure 2.1D-F, Table 2.1). Together, these data suggested that while no individual residue is wholly required for agonist activity, the side chains of these residues and their positioning are important for agonist function. To further probe the contribution of these residues to PAR4-AP activity at PAR4, we generated peptides with alterations in the aromatic side chain of position 2, the backbone conformation of position 3, or position 4 (Figure 2.2D-F, Table 2.1).

Peptides with substitution of tyrosine[2] with either 4-fluoro-L-phenylalanine [A-**F(4-fluoro)**-PGKF-NH_2] or *O*-methyl-tyrosine [A-**Tyr(Me)**-PGKF-NH_2] retained calcium signalling and β-arrestin recruitment with no significant changes in potency compared to the PAR4-AP. These data may suggest that the side chain of tyrosine is a site in which further modifications can be made to the peptide without affecting agonism; however, by comparison to A**A**PGKF-NH_2, the presence of an aromatic ring in position 2 is of importance. Given the results obtained with alanine or D-proline substitution of proline[3] (Figure 2.1A-C & 2.1D-F, respectively), we furthered probed conformational contributions of this residue to the parental PAR4-AP. Proline was substituted with pipecolic acid (2-piperidinecarboxylic acid; Pip) which is structurally similar to proline but has an increased steric bulk and backbone elongation provided by a six-membered ring compared to the five-membered ring of proline. We observed partial agonism of calcium signalling in response to AY-**Pip**-GKF-NH_2 stimulation with no significant difference in agonist potency (EC_{50} = 30.7 ± 4.9 μM) with a correlating partial agonism of β-arrestin recruitment (β-arr-1 38.8 ± 3.0%; β-arr-2 44.0 ± 2.7%). Thus, it appears that

increasing steric bulk/backbone length may affect efficacy but still results in agonism. To further investigate the role of backbone conformation provided at position 3, proline was substituted with nipecotic acid (3-piperidinecarboxylic acid; Nip) which is similar to pipecolic acid, however, results in change of the peptide backbone direction (AY-**Nip**-GKF-NH_2). With this modification, both calcium signalling (EC_{50} = *n.d.*) and β-arrestin recruitment (β-arr-1 32.9 ± 4.9%; β-arr-2 30.9 ± 4.5%) were significantly decreased in response to PAR4 stimulation. Elongation of the backbone in position four (glycine) by substitution with beta-alanine (AYP-**betaAla**-KF-NH_2) was also significantly detrimental to both calcium signalling (EC_{50} = *n.d.*) and β-arrestin recruitment (β-arr-1 42.5 ± 1.8%, β-arr-2 24.9 ± 1.6%). Together these data suggest an important role for backbone conformation contributed by proline^3 and glycine^4 compactness in the PAR4-AP. As well, these data suggest peptide backbone length at proline^3 and glycine^4 has an important role; consistent with what we have observed with backbone elongation modifications at position 1 (**Inp**-YPGKF-NH_2 and **betaAla**-YPGKF-NH_2; Figure 2.2A-C, Table 2.1).

2.3.6 Effect of additional substitutions in position 5 on PAR4-AP-mediated signalling responses

Previously, investigations into glutamine substitutions in the native tethered-ligand mimicking peptide (GYPGQV) revealed that agonism is maintained when this position is substituted with a charged residue such as arginine or ornithine (37). In the present study, we have identified that substitution of position 5 (lysine) of the PAR4-AP (AYPGKF-NH_2) with alanine does not significantly affect the agonist capacity of the peptide (Figure 2.1A-C). Further, we identified that substitution of L-lysine with D-lysine significantly decreases agonist stimulation of calcium signalling and β-arrestin recruitment (Figure 2.1D-F). To further probe the effect of positively charged residues in position 5, we generated several PAR4-AP analogues with lysine^5 substitutions by either arginine or ornithine (Figure 2.2G-I, Table 2.1). Substitution of lysine^5 with arginine resulted in a partial agonist with respect to calcium signalling but increased β-arrestin recruitment compared to the parental peptide (AYPG**R**F-NH_2 calcium EC_{50} = 4.0 ± 1.1 μM, β-arr-1 154.2 ± 10.3%, β-arr-2 140.1 ± 9.4%). This substitution delocalizes the positive charge of the side chain compared to lysine and increases steric bulk. Interestingly, substitution

with ornithine, which is similarly charged but has a shortened distance between the charge and the peptide backbone compared to lysine, also resulted in partial agonism of PAR4-mediated calcium signalling accompanied by a modest increase in the recruitment of β-arrestins (AYPG**O**F-NH_2 calcium EC_{50} = 4.2 ± 1.1 μM, β-arr-1 121.7 ± 8.5%, β-arr-2 112.1 ± 7.7%). To further probe if steric bulk in the side chain of position 5 affects PAR4-AP potency, we increased steric bulk through methylation of the epsilon (ε) amine of lysine [AYPG-**(*N*$_ε$-Me-K)**-F-NH_2]. This substitution yielded a full agonist for calcium signalling (EC_{50} = 6.7 ± 1.9 μM) and a modestly more efficacious agonist for the recruitment of β-arrestins (β-arr-1 122.5 ± 12.4%; β-arr-2 116.7 ± 11.2%). All of these substitutions maintain a positive charge and are able to act as agonists for PAR4. To determine if charge in position 5 is required, we substituted lysine with citrulline, which maintains similar structure to arginine and lysine while removing a positive charge (AYPG-**Cit**-F-NH_2). Interestingly, we observed partial agonism with respect to calcium signalling (EC_{50} = 5.4 ± 0.8 μM) with equipotent β-arrestin recruitment compared to the PAR4-AP, consistent with the alanine scan data for this position. Thus, positively charged residues in position 5 seem to contribute to agonism. Interestingly, we observed similar increases in β-arrestin recruitment and equipotent calcium signalling when stericity was either increased (AYPG**R**F-NH_2) or decreased (AYPG**O**F-NH_2), suggesting that the positive charge in this position is more important than the size of the side chain. Finally, although both the charge and size of the size chain have an effect, all modifications to position 5, with the exception of D-lysine (Figure 2.1D-F, Table 2.1) and $N_α$-methyl-lysine (Figure 2.1G-I, Table 2.1) modifications, were generally well-tolerated and there appears to be modest freedom in the side-chain of this position. This makes the side chain a good candidate for further investigations of structure-activity relationships as well as a good region to label with an imagine modality.

2.3.7 Effect of additional substitutions in position 6 on PAR4-AP-mediated signalling responses.

Through our initial investigations into position 6 substitutions, we observed that replacement of phenylalanine[6] with either alanine, D-phenylalanine, or *N*-methyl-phenylalanine had varied effects on PAR4-AP potency and efficacy. Previous

investigations into position 6 substitutions in the native tethered-ligand (GYPGQV) revealed the requirement for an aromatic residue, as substitution with non-aromatic residues such as lysine or ornithine significantly decreased or abolished the activity of the peptide (37). In addition to being an aromatic residue, phenylalanine is a hydrophobic residue so we investigated the impact of altering the hydrophobicity/hydrophilicity and stericity while maintaining an aromatic residue (Figure 2.2J-L, Table 2.1).

We investigated the effect of polar changes that decrease hydrophobicity. Substitution of phenylalanine[6] with tyrosine results in the addition of a hydroxyl group to position 6 (AYPGK**Y**-NH_2). We observed partial agonism of calcium signalling with no significant change in potency compared to the PAR4-AP (AYPGK**Y**-NH_2, EC_{50} = 5.2 ± 1.0 μM). Interestingly, the peptide was able to recruit β-arrestins at least as well as the PAR4-AP (β-arr-1 120.5 ± 12.5%; β-arr-2 109.9 ± 11.4%). Further, replacing the tyrosine hydroxyl group with an electron withdrawing fluorine, by means of substitution with 4-fluoro-L-phenylalaine, caused significant impairment of agonist activity, both decreasing calcium signalling and significantly decreasing β-arrestin recruitment [AYPGK-**F(4-fluoro)**-NH_2, calcium EC_{50} = *n.d.*, β-arr-1 25.2 ± 6.5%; β-arr-2 41.3 ± 5.9%]. The results of these two substitutions suggest that altering the polarity, while maintaining aromaticity, in position 6 reduces efficacy (54). Since decreasing hydrophobicity did not increase PAR4-AP activity, we next investigated alterations that increase stericity and hydrophobicity. Substitution with 4-methyl-L-phenylalanine reduced the efficacy of the PAR4-AP to a partial agonist for both calcium signalling and β-arrestin recruitment [AYPGK-**F(4-Me)**-NH_2 calcium EC_{50} = 9.4 ±3.0 μM, β-arr-1 56.4 ± 1.2%; β-arr-2 63.2 ± 1.1%]. Given these results, we wanted to assess the pharmacological impact of substituting phenylalanine with (1-naphthyl)-L-alanine (1Nal) and (2-naphthyl)-L-alanine (2Nal) which not only increase hydrophobicity but also have a modest increase in steric bulk and π-stacking potential. Substitution of phenylalanine[6] with (1-naphthyl)-L-alanine (1Nal; AYPGK-**1Nal**-NH_2) generated a partial agonist for both calcium signalling (EC_{50} = 9.6 ±1.9 μM) and β-arrestin recruitment (β-arr-1 77.5 ± 2.3%; β-arr-2 64.1 ± 2.0%) compared to PAR4-AP. Notably, substitution to (2-naphthyl)-L-alanine (2Nal; AYPGK-**2Nal**-NH_2), which differs in orientation compared to (1-naphthyl)-L-alanine such that the alkyl chain is connected to position 2 of naphthyl group (instead of position one as in 1Nal), restored

potency of the peptide to the levels observed with PAR4-AP. AYPGK-**2Nal**-NH_2 was an equipotent agonist for calcium signalling (EC_{50} = 11.1 ± 2.3 μM) and β-arrestin recruitment (β-arr-1 77.0 ± 7.0%; β-arr-2 91.6 ± 6.4%). Together, these results indicate that hydrophobicity, stericity, and side chain positioning of the C-terminal residue all contributes to agonist peptide activity at PAR4.

2.3.8 Probing antagonism of PAR4-AP-stimulated calcium signalling by peptides unable to stimulate calcium signalling.

The failure of some substituted peptides to stimulate calcium signalling could reflect either a failure to bind or a loss of efficacy. To determine if such peptides can act as antagonists of PAR4-AP stimulated calcium signalling, we pre-incubated HEK-293 cells stably expressing PAR4-YFP prior to stimulation with PAR4-AP. Pre-treatment and competition with 100 μM of peptides unable to stimulate PAR4-dependent calcium signalling were largely unable to affect the calcium response elicited by 30 μM PAR4-AP (AYPGKF-NH_2) compared to vehicle treated controls. Interestingly, two peptides with substitution in position 3 or 4, that were unable to stimulate calcium signalling, were able to decrease calcium signals elicited by PAR4-AP. Calcium signalling in response to AYPGKF-NH_2 (30 μM) was significantly reduced following pre-treatment with AY-**Nip**-GKF-NH_2 (10.6 ± 0.9% of A23187; $p<0.05$) or AYP-**Sar**-KF-NH_2 (13.0 ± 1.5% of A23187; $p<0.05$) compared to non-pre-treated control (20.8 ± 1.3% of A23187; $p<0.05$) (Supplementary Figure 2.1).

2.3.9 PAR4-dependent calcium signalling is $G\alpha_{q/11}$-dependent.

In order to verify that PAR4-dependent calcium signalling was $G\alpha_{q/11}$-dependent, HEK-293 cells stably expressing PAR4-YFP were stimulated with 100 μM AYPGKF-NH_2 following pre-incubation with selective $G\alpha_{q/11}$-inhibitor YM254890 (55). YM254890 inhibited AYPGKF-NH_2-stimulated calcium signalling in a concentration-dependent manner, with an IC_{50} of 16.5 ± 6.1 nM and complete inhibition observed by 100 nM YM254890. The control vehicle (0.001% DMSO) had no effect on calcium signalling (Supplementary Figure 2.2).

2.3.10 Peptides unable to stimulate PAR4-dependent calcium signalling do not activate MAPK signalling.

Activation of G-protein and β-arrestin pathways downstream of GPCRs often converge on the activation of the p44/42 MAP kinase-signalling pathway (56). We therefore monitored phosphorylation of p44/42 MAPK in response to the 37 AYPGKF-NH_2 derivative peptides. HEK-293 cells, stably expressing PAR4-YFP, were incubated with control vehicle (0.001% DMSO), 100 μM of AYPGKF-NH_2, or derivative peptides (100 μM) for 10 minutes. Data were normalized as a ratio of phosphorylated-p44/42 (p-p44/42) to total-p44/42 (p44/42). Interestingly, we find that most peptides that were unable to stimulate calcium signalling were also unable to activate p44/42 MAPK signalling (*i.e.* A**y**PGKF-NH_2, AY**p**GKF-NH_2, **(*N*-Me-S)**-YPGKF-NH_2, **Inp**-YPGKF-NH_2, **Sar**-YPGKF-NH_2, AY-**Nip**-GKF-NH_2, AYP-**Sar**-KF-NH_2). Similarly, peptides that perform as partial agonists of $G\alpha_{q/11}$-mediated calcium signalling were also partial agonists for p44/42 phosphorylation. Several peptides were able to cause a significantly greater increase in phosphorylation compared to the parental peptide (*i.e.* **Nle**-YPGKF-NH_2, AYPG**O**F-NH_2, AYPG-**(*N*$_\varepsilon$-Me-K)**-F-NH_2, AYPG-**Cit**-F-NH_2, AYPGK**Y**-NH_2, AYPGK-**1Nal**-NH_2,) (Figure 2.3, Table 2.1; see Supplementary Figure 2.3 for representative blots).

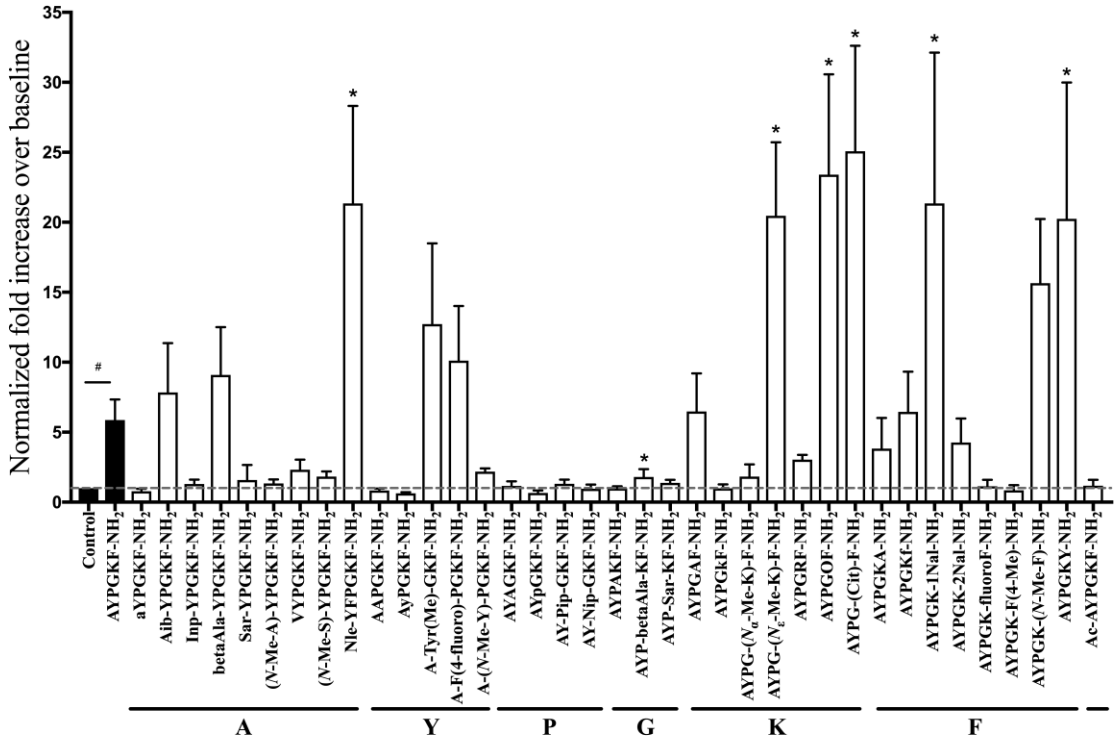

Figure 2.3 PAR4-mediated phosphorylation of p44/42(ERK) is attenuated upon stimulation of PAR4 with peptides unable to stimulate PAR4-dependent calcium signalling. HEK-293 cells stably expressing PAR4-YFP were stimulated with AYPGKF-NH_2 (30 µM) or peptide (30 µM) from library of compounds and Western blot for p44/42 phosphorylation (p-p44/42). Data are shown as normalized fold increase over unstimulated control cells. Dashed baseline shows mean of unstimulated baseline for comparison. Dotted baseline shows mean response achieved following AYPGKF-NH_2 stimulation. (# $p > 0.05$ AYPGKF-NH_2 compared to untreated control; *$p > 0.05$ peptide agonists compared to AYPGKF-NH_2; one-way ANOVA). Peptides that were unable to stimulate calcium signalling were also generally unable to stimulate phosphorylation of p44/42. Interestingly, several peptides were able to significantly increase phosphorylation of p44/42 compared to AYPGKF-NH_2. (Representative blots shown in Supplementary Figure 2.3; *n = 4-5*)

2.3.11 PAR4-mediated MAPK signalling is $G\alpha_{q/11}$-dependent and β-arrestin-independent.

To further probe the contribution of different pathways downstream of PAR4 to p44/42 phosphorylation, we examined the effective of blocking $G\alpha_{q/11}$-signalling with the specific antagonist YM254890 and examined the role of β-arrestins using a β-arrestin-1/-2 double knockout HEK-293 cell derived by CRISPR/Cas9-mediated targeting (Supplementary Figure 2.4). Pre-treatment of PAR4-YFP HEK-293 cells with 100 nM YM254890 for 20 minutes abolished PAR4-AP (30 μM) stimulated activation of MAP kinase signalling and subsequent phosphorylation of p-p44/42 at five minutes time (Figure 2.4A). In contrast, there was no significant difference in the phosphorylation of p44/42 MAPK between wild-type HEK-293 and β-arrestin-1/-2 knockout HEK-293 cells stimulated with 30 μM PAR4-AP for 0-90 minutes (Two-way ANOVA). p44/42 MAPK did remain sustained up to 90 minutes in the β-arrestin-1/-2 knockout HEK-293 cells while p44/42 MAPK phosphorylation in HEK-293 cells began to decrease towards baseline by 90 minutes (5-minute compared to 90-minute stimulation within cell line HEK-293 cells $p < 0.05$, β-arrestin-1/-2 knockout HEK-293 $p =$ *n.s.*, two-tailed t-test; Figure 2.4B).

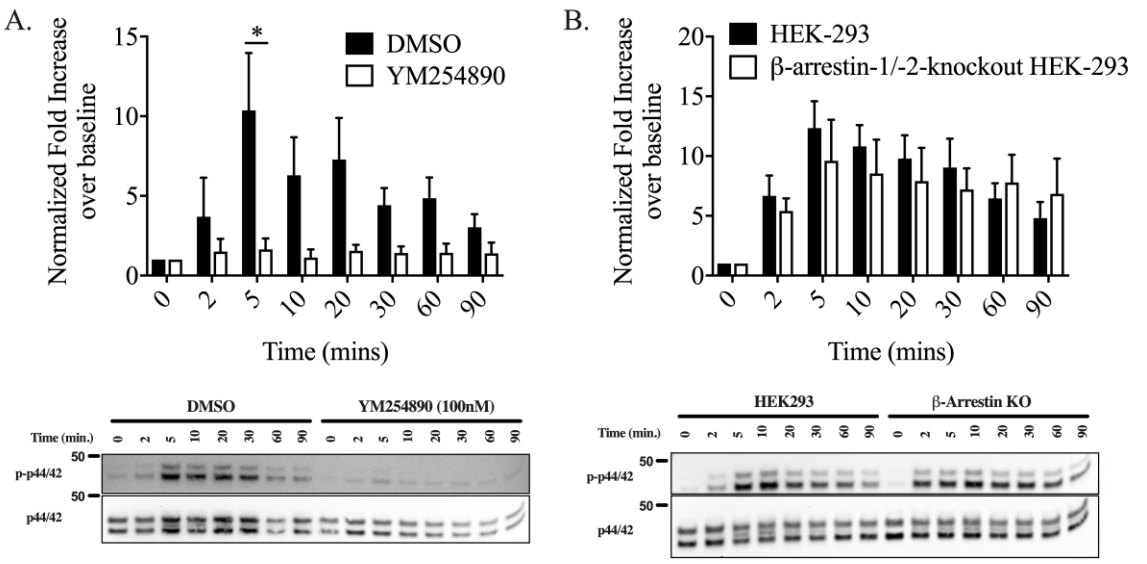

Figure 2.4 PAR4-mediated phosphorylation of p44/42 (ERK) is $G\alpha_{q/11}$-dependent and β-arrestin-independent. To evaluate contribution of $G\alpha_{q/11}$ and β-arrestin to p44/42 phosphorylation, p-p44/42 was monitored with western blot following stimulation with AYPGKF-NH_2 (30 μM) for various time points. (A) To evaluate contribution of $G\alpha_{q/11}$-signalling cells were incubated with vehicle control (0.001% DMSO) or Gαq/11-inhibitor, YM254890 (100 nM) prior to agonist stimulation. (B) To determine contribution of β-arrestin-signalling to p44/42 phosphorylation, MAPK activation in HEK-293 and β-arrestin-1/2-knockout HEK-293 cells was analyzed following agonist stimulation. Values are expressed as fold increase over unstimulated 0-minute time [(p-p44/22 / total p44/42) / (baseline p-p44/42 / total p44/42)]. We find that $G\alpha_{q/11}$ inhibition with YM254890 results in a significant reduction of p44/42 phosphorylation. We observe no statistical difference in ERK activation between HEK-293 and β-arrestin-1/-2-knockouts HEK-293 cells. Data were analyzed by two-way ANOVA (* indicates $p < 0.05$). p44/42 MAPK activation did remain sustained up to 90 minutes in the β-arrestin-1/-2 knockout HEK-293 cells while p44/42 MAPK phosphorylation in HEK-293 cells decrease towards the baseline by 90 minutes (5-minute compared to 90-minute time point is significantly different in HEK-293 cells $p < 0.05$ but not in β-arrestin-1/-2-knockout HEK-293 p = n.s., two-tailed t-test). (Representative blots shown; *n = 4*)

Table 2.1 Summary table of all calcium, β-arrestin, and p44/42 data. Calcium data is displayed as EC_{50} or not determined (n.d.) if EC_{50} could not be calculated. Maximum calcium response achieved with each peptide is shown as a percentage of the maximum calcium response achievable in a given experiment revealed by calcium ionophore (% of A23187 calcium ionophore). Statistically significant shifts in EC_{50} compared to PAR4-AP, AYPGKF-NH_2, were found using the F-statistic (*$p < 0.05$). Given that saturation did not always occur, all peptides are compared to the parental PAR4-AP, AYPGKF-NH_2, and shown as a percent of the response obtained with PAR4-AP at a given concentration (100 μM). Finally, fold increase over unstimulated baseline is shown for phosphorylation of p44/42 MAP kinase activation. Statistical significance for comparisons at 100 μM and p44/42 phosphorylation are calculated using one-way ANOVA of response compared to PAR4-AP (*$p < 0.05$).

				% of AYPGKF-NH_2 Response (100∝M)			
	Peptide (alterations shown in red)	**Ca^{2+} EC_{50} (∝M)**	**Ca^{2+} Max. (% of A23187)**	**Ca^{2+} signaling**	**b-Arr-1 recruitment**	**b-Arr-2 recruitment**	**p-p44/42 (fold over baseline; 100 µM)**
PAR4-AP	**AYPGKF-NH_2**	12.1 ± 3.1	27.4 ± 1.7	100.0 ± 8.2	100.0 ± 3.9	100 ± 3.5	5.9 ± 1.5
Alanine	AAPGKF-NH_2	*n.d.*	51.8 ± 25.4	52.9 ± 12.4*	47.3 ± 3.6*	46.4 ± 3.2*	0.8 ± 0.1
	AYAGKF-NH_2	63.7 ± 20.8*	29.7 ± 3.4	75.4 ± 11.1	48.5 ± 7.9*	43.4 ± 7.1*	1.2 ± 0.3
	AYPAKF-NH_2	21.2 ± 6.6	22.4 ± 1.9	72.2 ± 6.3	56.4 ± 5.6*	54.6 ± 5.1*	1.0 ± 0.2
	AYPGAF-NH_2	9.8 ± 2.9	25.7 ± 1.8	96.7 ± 17.8	59.3 ± 7.2*	70.8 ± 6.5	6.5 ± 2.7
	AYPGKA-NH_2	17.3 ± 5.0	20.0 ± 1.5	69.4 ± 4.1	47.9 ± 3.8*	52.6 ± 3.5*	3.8 ± 2.2
D-isomer	aYPGKF-NH_2	*n.d.*	19.2 ± 4.8	24.0 ± 4.4*	48.7 ± 2.6*	47.5 ± 2.4*	0.8 ± 0.2
	AyPGKF-NH_2	*n.d.*	1.1 ± 0.5	3.9 ± 2.8*	50.7 ± 4.6*	46.4 ± 4.2*	0.6 ± 0.1
	AYpGKF-NH_2	*n.d.*	1.2 ± 0.4	6.1 ± 3.4*	45.2 ± 10.5*	38.1 ± 9.5*	0.7 ± 0.2
	AYPGkF-NH_2	*n.d.*	16.9 ± 5.3	25.2 ± 5.2*	47.4 ± 1.0*	36.5 ± 0.9*	1.0 ± 0.3
	AYPGKf-NH_2	22.2 ± 4.7	21.9 ± 1.2	76.7 ± 5.2	80.3 ± 6.6	74.1 ± 6.0	6.5 ± 2.9
***N*-methyl.**	**(*N*-Me-A)**-YPGKF-NH_2	*n.d.*	15.0 ± 7.5	13.3 ± 1.3*	119.2 ± 11.9	80.6 ± 10.8	1.3 ± 0.3
	A-**(*N*-Me-Y)**-PGKF-NH_2	*n.d.*	2.7 ± 0.2	9.8 ± 2.9*	71.4 ± 10.8	61.5 ± 9.8*	2.2 ± 0.2
	AYP-**Sar**-KF- NH_2	*n.d.*	2.4 ± 0.3	8.8 ± 1.5*	35.9 ± 4.3*	36.1 ± 3.9*	1.4 ± 0.2
	AYPG-**(*N*$_a$-Me-K)**-F-NH_2	*n.d.*	9.6 ± 1.9	18.3 ± 1.5*	126.7 ± 18.6	77.1 ± 16.9	1.8 ± 0.9
	AYPGK-**(*N*-Me-F)**-NH_2	7.6 ± 1.9	26.3 ± 1.4	99.4 ± 7.8	136.9 ± 18.0*	96.6 ± 16.9	15.7 ± 4.6
***N*-terminal**	**Ac**-AYPGKF-NH_2	*n.d.*	11.0 ± 3.3	49.9 ± 16.5*	47.3 ± 3.1*	45.5 ± 2.8*	1.2 ± 0.4
Position 1	**V**YPGKF-NH_2	22.9 ± 8.3	16.8 ± 1.7	48.5 ± 4.6*	73.6 ± 13.0	55.2 ± 11.8*	2.3 ± 0.7
	Nle-YPGKF-NH_2	*n.d.*	1.1 ± 0.1	4.0 ± 1.1*	40.2 ± 9.7*	36.5 ± 8.8*	21.4 ± 7.0*
	Sar-YPGKF- NH_2	*n.d.*	1.6 ± 0.6	9.7 ± 8.5*	35.6 ± 2.0*	39.8 ± 1.8*	1.6 ± 1.1
	Aib-YPGKF-NH_2	50.2 ± 15.3*	25.1 ± 2.5	72.9 ± 12.0	38.6 ± 3.9*	37.3 ± 3.6*	7.8 ± 3.5
	(*N*-Me-S)-YPGKF-NH_2	*n.d.*	2.2 ± 0.5	8.8 ± 1.8*	78.1 ± 6.9	51.7 ± 6.3*	1.8 ± 0.4
	betaAla-YPGKF- NH_2	*n.d.*	1.9 ± 0.4	10.3 ± 3.9*	25.7 ± 4.8*	31.8 ± 4.4*	9.1 ± 3.4
	Inp-YPGKF-NH_2	*n.d.*	3.4 ± 0.8	18.9 ± 7.3*	32.0 ± 3.3*	26.9 ± 3.0*	1.3 ± 0.3
Position 2	A-**Tyr(Me)**-PGKF-NH_2	15.7 ± 4.0	25.7 ± 1.6	91.1 ± 10.1	77.9 ± 3.8	85.8 ± 3.4	12.7 ± 5.8
	A-**F-(4-fluoro)**-PGKF-NH_2	19.9 ± 5.4	35.1 ± 2.5	105.4 ± 9.0	72.1 ± 9.0	86.9 ± 8.1	10.1 ± 3.9
Position 3	AY-**Pip**-GKF- NH_2	30.7 ± 4.9	23.3 ± 1.1	74.2 ± 4.8	38.8 ± 3.0*	44.0 ± 2.7*	1.3 ± 0.3
	AY-**Nip**-GKF- NH_2	*n.d.*	2.5 ± 0.3	10.0 ± 1.8*	32.9 ± 4.9*	30.9 ± 4.5*	1.0 ± 0.3
Position 4	AYP-**betaAla**-KF- NH_2	*n.d.*	9.7 ± 2.4	19.8 ± 5.8*	42.5 ± 1.8*	24.9 ± 1.6*	1.8 ± 0.6
Position 5	AYPG**O**F- NH_2	4.2 ± 1.1	20.7 ± 1.1	77.3 ± 7.9	121.7 ± 8.5	112.1 ± 7.7	23.4 ± 7.2*
	AYPG**R**F-NH_2	4.0 ± 1.1	21.3 ± 1.2	82.0 ± 8.3	154.2 ± 10.3*	140.1 ± 9.4*	3.0 ± 0.3
	AYPG-**(*N*$_e$-Me-K)**-F-NH_2	6.7 ± 1.9	23.8 ± 1.5	88.9 ± 9.3	122.5 ± 12.4	116.7 ± 11.2	20.5 ± 5.3*
	AYPG-**Cit**-F-NH_2	5.4 ± 0.8	18.2 ± 0.6	65.5 ± 1.3	94.1 ± 10.1	87.7 ± 9.2	25.1 ± 7.5*
Position 6	AYPGK**Y**-NH_2	5.2 ± 1.0	16.9 ± 0.7	61.2 ± 4.3*	120.5 ± 12.5	109.9 ± 11.4	20.2 ± 9.7*
	AYPGK-**F(4-Me)**-NH_2	9.4 ± 3.0	17.8 ± 1.3	62.0 ± 5.5*	56.4 ± 1.2*	63.2 ± 1.1*	0.9 ± 0.4
	AYPGK-**F(4-fluoro)**-NH_2	*n.d.*	*n.d.*	16.5 ± 10.2*	25.2 ± 6.5*	41.3 ± 5.9*	1.1 ± 0.5
	AYPGK-**1Nal**-NH_2	9.6 ± 1.9	18.7 ± 0.9	65.4 ± 7.4	77.5 ± 2.3	64.1 ± 2.0*	21.3 ± 10.8*
	AYPGK-**2Nal**-NH_2	11.1 ± 2.3	25.3 ± 1.3	93.9 ± 4.2	77.0 ± 7.0	91.6 ± 6.4	4.3 ± 1.7

2.3.12 Homology modelling of PAR4 and in silico docking of AYPGKF-NH_2

In order to gain a better understanding of the ligand-binding pocket in PAR4 we turned to homology modelling and *in silico* docking experiments. A homology model of PAR4 was generated using known coordinates of the thermostabilized, antagonist-bound (AZ8838) human PAR2 crystal structure (2.8Å resolution, 5NDD.pdb) (42). Sequences of human PAR4 were aligned with the structure-resolved residues of PAR2 using Clustal Omega (40, 41). We generated a homology model of wild-type PAR2 on the PAR2 structure, which contained modifications necessary for crystallization. Twenty human PAR4 homology models, using the wild-type human PAR2 model as a template, were generated in MODELLER (43). The PAR4 model with the lowest discrete optimized protein energy (DOPE) score was utilized for *in silico* analyses.

Docking AYPGKF-NH_2 to the PAR4 homology model (GalaxyPepDock) (45) revealed a number of highly predicted peptide-receptor interaction sites (Figure 2.5A; Ser^{67}, Tyr^{157}, His^{229}, Asp^{230}, Leu^{232}, Leu^{234}, Asp^{235}, Ala^{238}, Gln^{242}, His^{306}, Tyr^{307}, Pro^{310}, Ser^{311}, Ala^{314}, Gly^{316}, Tyr^{319}, and Tyr^{322}). Of these, the most frequently predicted interactions were receptor residues His^{229}, Asp^{230}, and Gln^{242}. In peptide-docked models, Gln^{242} made contact with alanine, tyrosine, and lysine, with the most frequent prediction being with phenylalanine. His^{229} was predicted to interact with lysine and phenylalanine. Asp^{230} was frequently predicted to interact with lysine and phenylalanine and contacts with lysine appeared in 60% of predictions (Figure 2.5B). Interestingly, when visualizing receptor residues predicted to interact with the peptide, we found that a large number of these residues were localized on extracellular loop 2 (ECL2).

2.3.13 Calcium signalling and β-arrestin recruitment to predicted peptide binding-site mutant-PAR4

We experimentally examined *in silico* binding predictions through site-directed mutagenesis introducing alanine substitutions at the three most highly predicted interacting residues, His^{229}, Asp^{230}, and Gln^{242}. Additionally, we generated a double mutation, $PAR4^{H229A,\ D230A}$, to determine if combined loss of His^{229} and Asp^{230} would result in additive detriment to receptor activation. We evaluated the functional

consequences of these mutations by recording calcium signalling in response to AYPGKF-NH_2 with all mutants. We observed no calcium response in cells expressing $PAR4^{D230A}$-YFP or $PAR4^{H229A, D230A}$-YFP mutant receptors up to 300 μM AYPGKF-NH_2 (Figure 2.5C). Similarly, peptide-induced β-arrestin-1/-2 recruitment to $PAR4^{D230A}$-YFP and $PAR4^{H229A, D230A}$-YFP was significantly reduced compared to the wild-type PAR4. Both $PAR4^{H229A}$ and $PAR4^{Q242A}$ mutations were fully able to recruit β-arrestin-1/-2 to the same levels observed with wild-type PAR4-YFP (Figure 2.5D-E).

To investigate whether these sites are important for tethered-ligand activation of the receptor, we stimulated cells expressing wild-type and mutant constructs with thrombin. Thrombin cleavage of the receptor reveals the native tethered-ligand, GYPGQV (57). Comparable to activation with AYPGKF-NH_2, we observed significantly diminished calcium signalling in HEK-293 cells expressing $PAR4^{D230A}$-YFP and $PAR4^{H229A, D230A}$-YFP mutants, even up to 10 units/mL thrombin (Figure 2.5F). Additionally, β-arrestin-1/-2 recruitment was also impaired to $PAR4^{D230A}$ and $PAR4^{H229A, D230A}$ mutants (Figure 2.5G-H). We observed no appreciable difference in calcium signalling or β-arrestin recruitment when $PAR4^{H229A}$-YFP and $PAR4^{Q242A}$-YFP mutants were stimulated with thrombin, with the exception of a modest decrease in β-arrestin-1 recruitment to $PAR4^{Q242A}$-YFP mutant receptor. Thus, Asp^{230} interactions with either PAR4-AP or the tethered-ligand are critical for receptor activation.

To examine whether differences in cell surface localization of the mutant receptors could underlie the defect in signalling, we employed confocal microscopy to examine receptor localization. We found appropriate cell surface localization of the mutant receptors and qualitatively do not observe defects in expression level, although more quantitative investigation should be undertaken to determine expression levels (Supplementary Figure 2.5).

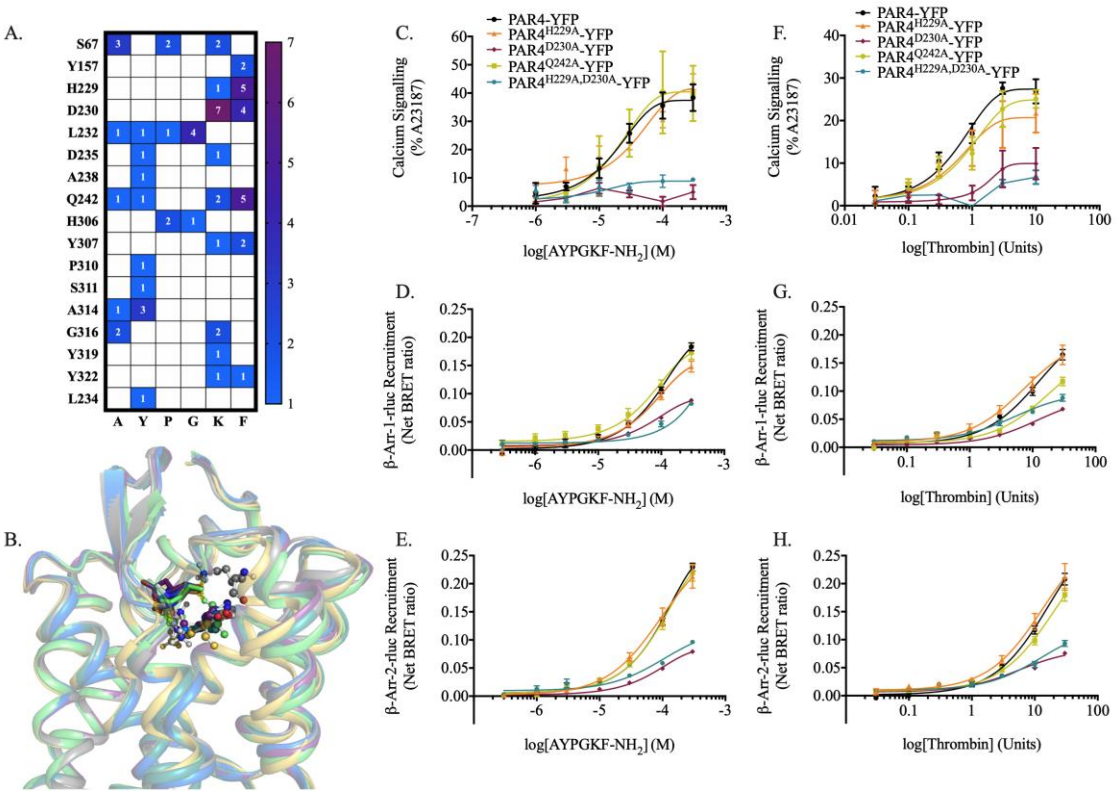

Figure 2.5 Asp^{230} is essential for PAR4 activation with both PAR4-AP and tethered-ligand (revealed by thrombin cleavage) activation. (A) Frequency table of PAR4/AYPGKF-NH_2 interactions as predicted by in silico peptide docking (GalaxyPepDock). Numbers represent the frequency with which an atom in a PAR4-AP residue was predicted to interact with an atom of a PAR4 residue. (B) Representation of the most highly predicted AYPGKF-NH_2 binding site (Asp230, shown as sticks) interacting (shown as yellow dashed lines) with position 5 (Lys^5; shown as ball and sticks) of AYPGKF-NH_2. Interaction of Lys^5 and Asp^{230} was highly predicted in 7/10 models (B). Alignment of the receptor backbone (shown as transparent cartoon) reveals similar binding poses adopted by the side chain position of Asp^{230} and the position of Lys^5 of AYPGKF-NH_2. AYPGKF-NH_2- and tethered-ligand-stimulated (thrombin revealed) calcium signalling and β-arrestin-1/-2 recruitment in PAR4 extracellular loop 2 mutants. Agonist-stimulated Calcium signalling Calcium signalling in response to AYPGKF-NH_2 (C) or thrombin (F) was recorded in HEK-293 cells transiently expressing PAR4-YFP, single site-directed mutant PAR4-YFP (PAR4^{H229A}-YFP, PAR4^{D230A}-YFP, PAR4^{Q242A}-YFP), or double site-directed mutant PAR4-YFP (PAR4$^{H229A,\ D230A}$-YFP).

Data are shown as a percentage of maximum response obtained in cells treated with the calcium ionophore A23187 (3 μM) for each transient cell line, per experimental day. AYPGKF-NH_2 concentration is in M and thrombin concentration is shown as units. (*n = 3-5*) Agonist-stimulated β-arrestin-1/-2 recruitment HEK-293 cells were transiently transfected with BRET pair of either β-arrestin-1-rluc or -2-rluc and PAR4-YFP or site-directed mutant PAR4-YFP (described above) and agonist-stimulated arrestin recruitment to PAR4 was monitored. Cells were incubated with increasing concentration of either AYPGKF-NH_2 (D, E) or thrombin (G, H) for 20 minutes and BRET values were recorded. BRET values from cells treated with HBSS were also collected to normalize the data. Renilla-luciferase substrate h-coelenterazine (5 μM) was added 10 minutes prior to data collection. Data are presented as the normalized net BRET ratio [eYFP/rluc - baseline (HBSS control)]. AYPGKF-NH_2 concentration is in M and thrombin concentration is shown as units. (*n = 4*)

2.3.14 ^{1}H NMR of AYPGKF-NH_2 reveals two distinct conformations in solution.

In our SAR studies of AYPGKF-NH_2 we observed that D-proline substitution of proline was significantly deleterious to both calcium signalling and β-arrestin recruitment (Figure 2.1D-F). Further, we identified that unnatural amino acid substitution of proline with pipecolic acid, which is similar to proline but has increased steric bulk and backbone elongation provided by a six-membered ring, maintained agonist properties at PAR4 (Figure 2.2D-F). Interestingly, substitution of proline with nipecotic acid, which changes the peptide backbone direction (relative to pipecolic acid and proline), significantly abolished agonist activity at PAR4 (Figure 2.2D-F). Similarly, elongation of the backbone in position 4 (glycine in the parental agonist peptide) reduced agonist activity at PAR4 (Figure 2.2D-F). Together, these data provided the impetus to assess the three-dimensional structure of AYPGKF-NH_2 by solution NMR.

Phase-sensitive, water-gated, two-dimensional correlated spectroscopy (COSY), total correlation spectroscopy (TOCSY), and nuclear Overhauser effect spectroscopy (NOESY) were recorded. Manual assignment of TOCSY chemical shifts revealed to distinct sets of chemical shifts for both Tyr^2 and Pro^3 of the peptide. These two distinct sets of chemical shifts indicated that AYPGKF-NH_2 may adopt two distinct structures – thus, assignments were made for both sets of chemical shifts for Tyr^2 and Pro^3, and these chemical shifts were associated with either a “major” or “minor” conformation of the peptide, based on peak intensity (Supplementary Figure 2.8). Chemical shift assignments for protons (^{1}H) identified in both the “major” (40 of 45 protons identified, 89%) and “minor” (39 of 45 protons identified, 87%) conformation of the peptide are reported in Supplementary Table 2.2 and 2.3, respectively. Using TALOS+, *phi* (Φ) and *psi* (ψ) backbone dihedral angles were calculated from both “major” and “minor” chemical shift lists. Chemical shift lists (Supplementary Table 2.2 & 2.4), calculated backbone torsion angles (Supplementary Table 2.4), and unassigned NOESY peak lists were used as inputs in the structural ensemble calculations using CYANA (version 2.1).

NOESY peaks for the “major” (84 of 149) and “minor” (65 of 149) were assigned by CYANA using the mentioned inputs (Supplementary Table 2.4). CYANA identified 12

inter-residue NOEs dictating the “major” conformation of AYPGKF-NH_2 and 6 inter-residue NOEs (Supplementary Table 2.4; Supplementary Figure 2.9 & 2.10, respectively). Remarkably, NOEs, distinct from those observed in the “major” conformation, were detected in the “minor” conformation and dependent on the alternate Pro^3 chemical shifts. The ten lowest energy ensembles for both “major” and “minor” conformations demonstrate low average backbone RMSD of 0.52Å and 0.66Å, respectively (Supplementary Table 2.4, Supplementary Figure 2.11). The lowest energy structures reveal that Tyr^2, Pro^3, and Phe^6 side chains are in distinct conformations between “major” and “minor) (Figure 2.6). Thus, the hexapeptide AYPGKF-NH_2 adopts two distinct structures in solution.

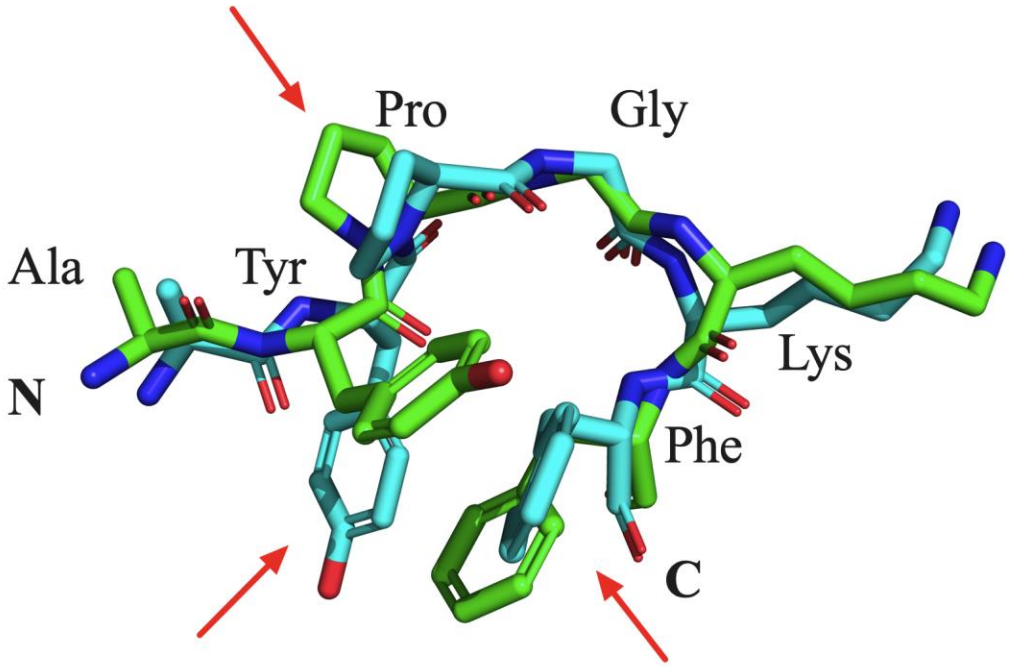

Figure 2.6 ^{1}H-NMR-solved structures of AYPGKF-NH_2 reveal two distinct conformations in solution. Aligned lowest energy structures from chemical shift assignments for two distinct conformations of AYPGKF-NH_2, so called "major" (green, peak assignments in Supplementary Table 2.2) and "minor" (cyan, peak assignments in Supplementary Table 2.3) determined by strength of chemical shift peak signal. Backbone alignment of lowest energy major and minor structures reveal tyrosine, proline, and phenylalanine side chains adopt distinct conformations (red arrows; calculated average RMSD of 2.9Å, based on 10 lowest energy structure ensembles between major and minor conformations, Supplementary Figure 2.11).

2.3.15 Platelet aggregation response to differential activation of PAR4 signalling

To determine the effects of targeted signalling observed with several peptides we investigated PAR4-mediated platelet aggregation in response to the β-arrestin biased, calcium signalling-null peptide, A**y**PGKF-NH_2, as well as a modestly more potent calcium agonist AYPG**R**F-NH_2 (compared to AYPGKF-NH_2). Thrombin (1 unit/mL) and 100 μM AYPGKF-NH_2 were used as controls to ensure successfully washed platelet preparations. In response to thrombin stimulation, we observed a characteristic aggregation trace resulting in 100% aggregation at 1 unit/mL. In agreement with previously published data, AYPGKF-NH_2 (100 μM) stimulation resulted in approximately 50% platelet aggregation (26). We observed that platelet aggregation was not stimulated by 100 μM A**y**PGKF-NH_2. Interestingly, when platelet preparations were stimulated with AYPG**R**F-NH_2, with which we observed a modest increase in potency in calcium signalling assays, enhanced β-arrestin recruitment, and an increased phosphorylation of p44/42, we observed platelet aggregation response comparable to levels observed with thrombin (1 unit/mL) (Figure 2.7).

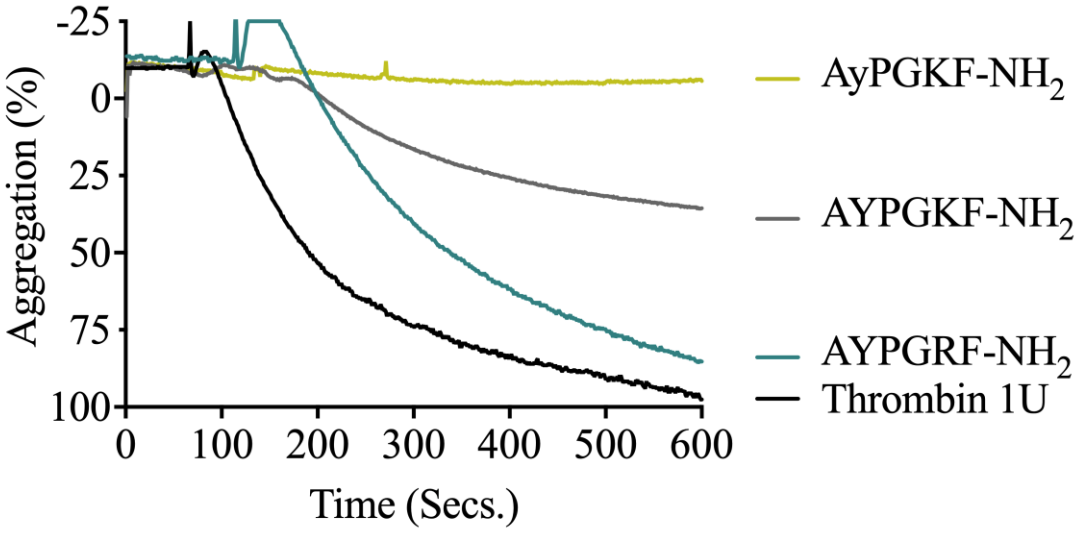

Figure 2.7 PAR4 agonist-mediated platelet aggregation. Both thrombin (1 unit/mL; shown in black) and AYPGKF-NH_2 (100 µM; shown in grey) initiated PAR4-dependent rat platelet aggregation. We observed that stimulation of washed platelet samples with a β-arrestin biased peptide that is unable to stimulate calcium signalling, AyPGKF-NH_2 (100 µM; shown in yellow), did not stimulate platelet aggregation. Further, stimulation of washed platelets with the peptide agonist AYPGRF-NH_2 (100 µM; shown in purple), caused a robust platelet aggregation comparable to the response with 1unit/mL thrombin response. (*n = 2-4*; representative trace shown)

2.4 Discussion

PAR4 is emerging as a novel anti-platelet drug target. Here we examine structure activity requirements for PAR4 activation of calcium signalling, β-arrestin recruitment and MAP kinase activation. PAR cleavage by a number of different enzymes has been reported (58). Canonically, thrombin has been described as a PAR1 and PAR4 activator while trypsin is described as a PAR2 and PAR4 activator. While PAR3 can be cleaved by thrombin, its ability to act as a signalling receptor remains ambiguous. In each case, cleavage by serine proteases occurs at an arginine-serine site which reveals a unique tethered-ligand specific to each PAR (59) - human PAR1- SFLLRNP… (6, 15), human PAR2- SLIGKV… (60, 61) and human PAR4- GYPGQV… (57, 62). While these tethered-ligand sequences are diverse, they retain some highly-conserved properties including a highly-conserved charged residue in position five of the revealed tethered-ligands (arginine in PAR1; lysine in PAR2). Additionally, PAR2 and PAR4 have a conserved glycine in position three and valine in position six of their tethered ligands. The similarities of the proteolytically-revealed tethered-ligands is also observed in the optimized tethered-ligand-mimicking synthetic agonist peptides. Hydrophobic residues leucine, isoleucine, and proline are preferred in position three of PAR1, PAR2, and PAR4 agonist peptides, respectively. Additionally, there is a basic residue in position five of the tethered-ligand peptide in all three receptors (arginine in PAR1 and PAR2 and lysine in PAR4 activating peptides). These conserved residue properties highlight some of the key requirements that a PAR4 agonist peptide must meet. Previous structure-activity work starting with the proteolytically-revealed sequences of human (GYPGQV) and murine (GYPGKF) PAR4 identified the hexapeptide AYPGKF-NH_2 or SYPGKF-NH_2 to be potent and selective agonists for PAR4 (37). In this study we started with the hexapeptide AYPGKF-NH_2, as our parental peptide agonist, and incorporated various modifications at each of the six positions in this peptide to investigate determinants of agonist-induced PAR4-coupling to $G\alpha_{q/11}$, MAP kinase and β-arrestin-1/-2 recruitment to guide development of biased agonists of PAR4.

Previously, it was demonstrated that substitution of alanine or serine in position 1 of the GYPGKF-NH_2 activating peptide retained the ability to trigger tritiated inositol 1,4,5-

triphosphate release to a level comparable to that observed with thrombin activation and much higher than release caused by the GYPGKF-NH_2 (37). Interestingly, substitution of position 1 with threonine was reported to significantly reduce the potency of the activating peptide (37). In keeping with results from previous studies, we find a requirement for small aliphatic side chains in position 1 of PAR4 activating peptides, with substitutions that increased bulk in this position consistently resulting in poor agonists for both calcium signalling and β-arrestin recruitment (*N*-Me-A Figure 2.1G-I; *N*-Me-S, Aib, Inp, V, Nle Fig 2.2A-C; Table 2.1). Additionally, we observed that both stereochemical inversion of L-alanine to D-alanine (D-alanine, Figure 2.1D-F) and backbone elongation (betaAla., Figure 2.2A-C) were detrimental to both calcium signalling and β-arrestin recruitment. Additionally, we observed that capping of the N-terminal charge via acetylation significantly decreases agonist potency. Together these results indicate that a positive charge and the localization of that charge in addition to precise side-chain positioning at position 1 are critical to effective PAR4-agonism.

The aromatic sidechain, and to a lesser extent the hydroxyl group, of the tyrosine^2 residue of the parental peptide also proved to be important for peptide activity with alanine or D-isomer substitutions resulting in decreased activity of all pathways tested. These results are consistent with previous reports that replacement of tyrosine with other aromatic residues, such as phenylalanine, significantly reduced both the selectivity and the potency of the activating peptide (37). Interestingly, substituting L-tyrosine^2 for either D-tyrosine (Figure 2.1D, Figure 2.3) or *N*-methyl-tyrosine (Figure 2.1G & 2.3) resulted in significant decreases in calcium and p44/42 signalling, while having relatively modest effects on β-arrestin recruitment (Fig, 2.1E-F & 2.1H-I, respectively; Table 2.1). Also, substitution of tyrosine with either 4-fluoro-phenylalanine or *O*-methyl-tyrosine did not significantly affect calcium transients, p44/42 phosphorylation or β-arrestin recruitment in comparison to AYPGKF-NH_2 (Figure 2.2D-F & 2.3; Table 2.1). Our findings, together with previously reported data (37), point to the necessity of an aromatic residue in position 2 to maintain agonist potency. Further, our data reveal that backbone orientation in position 2 is a key determinant of agonist potency. Future experiments fine-tuning the aromatic substituents may be beneficial for peptide analogue development.

Our data reveal that alterations affecting proline backbone conformation or glycine residue compactness are not well-tolerated, as these decreased calcium signalling, p44/42 MAP kinase signalling, and β-arrestin recruitment to PAR4. Calcium signalling has previously been reported to be negatively impacted by alterations to either of these two residues (37). Both proline and glycine residues are frequently found in β-turns, in which proline provides a characteristic kink, and the available data support the notion that the conformation(s) (proline^3 and glycine^4) and rigidity (proline^3) of PAR4 agonists permitted by these residues is/are important for receptor activation. To test this hypothesis further, we made several substitutions in position 3 (proline) aimed at evaluating favoured backbone conformations. We observed that a return to a predominantly trans-amide conformation by substitution of proline with alanine (Figure 2.1A-C), results in decreased potency in all pathways studied. Interestingly, this substitution did not abolish signalling but did significantly decrease agonist potency, which suggests that the backbone conformation of proline may be necessary for receptor binding but not receptor activation. Substitution of proline to pipecolic acid (Pip., Figure 2.2D-F), which has a similar peptide backbone orientation to proline with a six-membered aromatic ring, decreased β-arrestin recruitment with relatively modest effects for calcium signalling activation. Interestingly, substitution of proline with nipecotic acid (Nip., Figure 2.2D-F) abolished both calcium signalling and p44/42 phosphorylation while also significantly reducing β-arrestin recruitment. Nipecotic acid is similar to pipecolic acid with the exception that nipecotic acid changes the direction of the peptide backbone compared to that adopted by proline, while pipecolic acid favours a similar backbone directionality and conformation similar to proline. Interestingly, we observed a similar pharmacological profile observed with AY-**Nip**-GKF-NH_2 when we substituted D-proline in position 3, which also changes the backbone orientation from that of the of the parent peptide. These findings demonstrate that the backbone conformation provided by proline in position 3 of the parental peptide is necessary for agonism of PAR4 signalling pathways. Further, substitution of a proline^3 with alanine (AY**A**GKF-NH_2, Figure 2.1A-C) significantly and detrimentally altered the pharmacological profile compared to the parental peptide PAR4-AP, suggesting the possibility that agonist competency contributed by position 3 is largely conformational and not chemical.

Substitution of sarcosine or beta-alanine at position 4 also negatively affected all signalling pathways, while substitution of glycine^{4} with alanine resulted in a decrease in potency with calcium signalling as well as a reduction of β-arrestin recruitment. Together these substitutions reveal the requirement for a small flexible residue in position 4, consistent with previous reports (37).

It has been previously demonstrated that substitution of position 5 glutamine in the native tethered-ligand (GYPGQV) with arginine or ornithine results in decreased potency in the PAR4 agonist peptide for calcium signalling pathways (37). However, there is a basic residue found in position 5 of PAR1 (arginine, TFLL**R**), PAR2 (arginine, SLIG**R**L), and PAR4 (lysine, AYPG**K**F) tethered-ligand mimicking peptides. Given the conservation of charged residues in position 5 of PAR tethered-ligand mimicking peptides, we generated PAR4-AP derivative peptides with lysine^{5} substitutions that maintained or altered charge in this position to determine if this is a requirement for activity at PAR4. Substitution of lysine^{5} with alanine had no appreciable effect on calcium or MAP kinase signalling, while resulting in decreased β-arrestin recruitment (Figure 2.1A-C). Substitution of L-lysine^{5} with D-lysine, however, significantly reduced potency and efficacy in calcium signalling and β-arrestin recruitment assays and furthermore resulted in a loss of stimulation of MAP kinase signalling (Figs. 2.1D-F & 2.3). We continued our exploration of this position with an N_{α}-methyl-lysine substitution, which increases steric bulk through the addition of a methyl group to the backbone while also removing a hydrogen bond donor and increasing the amount of peptide in the cis-transformation of the amide bond between position 4 and 5. We found this substitution detrimental to calcium signalling but advantageous for β-arrestin recruitment, resulting in comparable maximal levels of recruitment to those observed with PAR4-AP but at lower concentrations (Figure 2.1G-I). Thus, backbone conformation and bulk at position 5 are important for agonism of calcium signalling and MAP kinase activation, while possibly being an important site for modification in the search for β-arrestin biased ligands.

We next turned our attention to analogues that resemble the side chain of lysine^{5}, with a specific interest on structure-activity in addition to ascertaining the importance of charge in this residue. In contrast to the observation with similar substitutions to the tethered-

ligand-mimicking peptide (GYPGQV) (37) wherein signalling was decreased compared to PAR4-AP, we found that both calcium signalling and β-arrestin recruitment are only modestly impacted by position 5 substitution to ornithine in the PAR4-AP, which decreases steric bulk and shortens the distance between the backbone and the positively charged amine compared to lysine (AYPG**O**F-NH_2; Figure 2.2G-I). Interestingly, however, we observed significantly increased p44/42 phosphorylation in response to AYPG**O**F-NH_2 stimulation (Figure 2.3). This is somewhat puzzling since we found p44/42 phosphorylation to be $G\alpha_{q/11}$-dependent (Figure 2.4A); however, it is important to note that MAP kinase and other cellular signalling pathways downstream of receptor activation are subject to amplification/deamplification processes within the cell (63) and these observations may point to additional differences in signalling stimulated by this peptide that needs to be examined. We further probed stericity in this position through increasing bulk with substitution of lysine[5] with arginine (AYPG**R**F-NH_2). Interestingly, this substitution also results in a delocalization of charge compared to the charge on the lysine[5] side chain. This modification provided a similar calcium signalling profile compared to that observed with ornithine substitution, however, it also resulted in a significant increase of β-arrestin recruitment compared to the parental PAR4-AP. Interestingly, there was no significant change in p44/42 phosphorylation unlike what was observed with ornithine substitution. Another peptide with increased steric bulk, N_ε-methyl-lysine substitution in position 5, improved calcium signalling potency, modestly improved β-arrestin recruitment, and significantly increased p44/42 phosphorylation [AYPG-**(*N*$_\varepsilon$-Me-K)**-F-NH_2, Figure 2.2G-I]. We further investigated whether charge was a significant determinant of agonism by substituting lysine[5] with citrulline (AYPG-**Cit**-F-NH_2), which lacks charge but retains a similar structure compared to arginine and, to a lesser extent, lysine. We observed decreased calcium, equivalent β-arrestin recruitment, and significantly increased p44/42 phosphorylation compared to the parental peptide (Figs. 2.2G-I & 3). Together these data reveal that changes to side chain charge, bond donors/acceptors, and steric bulk result in varied pharmacological responses that may be exploited to bias signalling responses in favour of β-arrestin recruitment (AYPG**R**F-NH_2) or p44/42 phosphorylation (AYPG**O**F-NH_2; AYPG-**(*N*$_\varepsilon$-Me-K)**-F-NH_2) with modest improvements to potency in calcium signalling. Interestingly, we observed that charge is

not wholly required for receptor activation as both alanine and citrulline substitutions resulted in agonism of PAR4.

Finally, our structure-activity investigation turned to position 6, phenylalanine, of the parental peptide. Given the significant impact that alterations to position 2 (tyrosine) had on agonist potency, we predicted that there may be a pi-pi (π-π) stacking interaction between tyrosine and phenylalanine which is supported by the backbone kink provided by proline in position 3. Substitution of position 6 with alanine or D-phenylalanine reduced calcium signalling potency while reducing β-arrestin recruitment and p44/42 phosphorylation. These alterations suggest that phenylalanine in position 6 is not essential for PAR4 activation by agonist peptide but is important for agonist potency and full activation of all signalling pathways. Methylation of the backbone nitrogen in phenylalanine (AYPGK-**(*N*-Me-F)**-NH_2) resulted in improved activation of calcium signalling, β-arrestin recruitment, and p44/42 phosphorylation compared to AYPGKF-NH_2 (Figure 2.3). Addition of either methyl (AYPGK-**F(4-Me)**-NH_2), fluorine (AYPGK-**F(4-fluoro)**-NH_2), or hydroxyl (AYPGK**Y**-NH_2) (Figure 2.2J-L) off of the *para*- position of the aromatic side chain of phenylalanine was deleterious to all signalling pathways studied. Substitution of unnatural residues that increase the size of steric bulk and π-stacking potential yielded mixed results based on the orientation of the naphthyl. Substitution of phenylalanine with (1-naphthyl)-L-alanine (1Nal) increased p44/42 phosphorylation but decreased both calcium signalling and β-arrestin recruitment (Figure 2.2J-L). Changing the alkyl chain connection from position 1 to position 2 of the naphthyl (AYPGK-**2Nal**-NH_2; Fig 2.2J-L) resulted in activity similar to AYPGKF-NH_2. With (2-naphthyl)-L-alanine showing some flexibility in the steric bulk of position 6, it would be interesting for future work to investigate increasing the π-stacking potential at position 2 while simultaneously increasing the π-stacking potential at position 6, since we hypothesize that these two residues' aromatic regions of the PAR4-AP may interact.

To determine if any of the peptides that failed to stimulate PAR4-dependent calcium signalling were able to act as antagonists, cells were pre-treated with these peptides and subsequently stimulated with AYPGKF-NH_2 to see if the parental peptide was able to still elicit a signal. We observed that both AY-**Nip**-GKF-NH_2 and AYP-**Sar**-KF-NH_2

were both able to significantly decrease the calcium signal elicited by PAR4-AP (Supplementary Figure 2.1). Interestingly, each of these substitutions resulted in ablation of both calcium and p44/42 signalling as well as significantly decreasing β-arrestin recruitment. These results may indicate that targeting PAR4 with small molecules mimicking position 3 and 4 dipeptides may provide a starting place for the design of novel PAR4 antagonists. Additionally, peptides that further explore modifications to position 3 and 4 could be investigated for potent PAR4 antagonists.

In platelets, it has previously been demonstrated that PAR4-mediated calcium mobilization induces activation and aggregation (24, 64). Both thrombin and AYPGKF-NH_2 initiated PAR4-dependent platelet aggregation to levels comparable to those previously reported in the literature in the same rat platelet system (26). As was hypothesized, we observed that stimulation of washed platelet samples with a β-arrestin biased peptide (A**y**PGKF-NH_2; 100 μM) that is unable to stimulate PAR4-dependent calcium signalling did not stimulate platelet aggregation (Figure 2.6). Further, stimulation of washed platelets with the agonist peptide, AYPG**R**F-NH_2 (Figure 2.2G-I), enhanced platelet aggregation to levels comparable to those observed with thrombin activation of PAR4 (Figure 2.6). AYPG**R**F-NH_2 stimulates calcium signalling to levels comparable to those seen with PAR4-AP but triggers more β-arrestin-1 recruitment than the parental peptide. These data suggest that calcium signalling is essential for triggering platelet activation, but β-arrestin recruitment may also play a role.

Having ascertained some of the governing agonist peptide residue characteristics enabling PAR4 activation and validated their signalling consequences in an *ex vivo* system, we turned our attention to investigating the ligand binding site of the receptor. The extracellular loops of many GPCRs have been demonstrated to be important facilitators of ligand entry into the orthosteric site, with ECL2 possessing the most diversity in sequence and structure (65, 66). Analysis of common mechanisms of GPCR ligand interaction derived from crystal structure and biochemical experiments reveal a possible role of ECL2 secondary loop in binding and facilitating entry, while the diversity of residue sequences across class A GPCRs is thought to confer their ligand specificity (65, 66). In many class A GPCRs, a disulfide bond between ECL2 and a transmembrane

3 cysteine ($Cys^{3.25}$, Ballesteros-Weinstein numbering) is thought to stabilize the extracellular topology such that ligand recognition at ECL2 and subsequent orthosteric binding can occur (67). All PAR receptors possess this canonical TM3 $Cys^{3.25}$ (PAR1 $Cys175^{3.25}$, PAR2 $Cys148^{3.25}$, PAR3 $Cys166^{3.25}$, PAR4 $Cys149^{3.25}$) and residues adjacent to this conserved cysteine are important for ligand binding and receptor activation. Investigations into the role of PAR ECL2 domains have previously demonstrated that all PAR receptors possess a homologous CHDxL motif (…CHDVL… - $PAR1^{C254\text{-}L258}$ and $PAR2^{C226\text{-}L230}$; …CHDVH… $PAR3^{C245\text{-}L249}$ …CHDAL; … $PAR4^{C226\text{-}L230}$) in their ECL2 (57, 68). Given that the activating peptides of PAR1 and PAR2 (38, 68) are similar (SFLLRN, PAR1; SLIGRL, PAR2), additional studies were conducted that revealed that ligand specificity is conferred by acidic residues distal to the CHDxL motif (PAR1, $N^{259}ETL^{261}$; PAR2 $P^{231}EQL^{234}$; (38, 69, 70). Interestingly, the equivalent human PAR4 ECL2 residues distal to the CHDAL domain, $P^{233}LDA^{236}$, share sequence homology with those distal to the human PAR2 CHDVL domain ($P^{231}EQL^{234}$), both of which contain an acidic residue. Al-Ani *et al.* (1999) demonstrated that glutamic acid residues in the rat PAR2 ECL2 (PEEVL) conferred specificity to PAR2 ligands. In previous studies, a series of aspartic acids in the PAR4 extracellular loop 2 (ECL2) and amino terminal (N)-tail were proposed to be key for thrombin binding to PAR4 (71–73). Mutations of ECL2 aspartic acid residues $D^{224}A$, $D^{230/235}A$ (double mutation), and $D^{224/230/235}A$ mutants were all found to decrease thrombin cleavage of PAR4 and activation in yeast models (73). Further, the activity of the PAR4 agonist peptide AYPGKF-NH_2 was also abolished in PAR4 mutants containing ECL2 single mutant D224A, double mutant $D^{230/235}A$, or triple mutant $D^{224/230/235}A$ aspartic acid mutations to alanine which the authors posit indicates that these aspartic acid residues may be important for both agonist peptide and tethered-ligand bindings and activation of PAR4. The $D^{230/235}A$ mutation to alanine removed two acidic residues in the highly conserved …$CHD^{230}AL$ domain (PAR1 Asp^{256}; PAR2 Asp^{228}) as well as the homologous $PLD^{235}A$… specificity conferring domain observed in PAR1 (Glu^{260}) and PAR2 (Glu^{232}) making it difficult to assess whether the loss of cleavage and activation is due to the $CHD^{230}AL$ or $PLD^{235}A$ aspartic acid.

In the present study, *in silico* docking to a homology model of PAR4 revealed 17 predicted sites of interaction with AYPGKF-NH_2 (Ser^{67}, Tyr^{157}, His^{229}, Asp^{230}, Leu^{232},

Leu^{234}, Asp^{235}, Ala^{238}, Gln^{242}, His^{306}, Tyr^{307}, Pro^{310}, Ser^{311}, Ala^{314}, Gly^{316}, Tyr^{319}, Tyr^{322}; Figure 2.5A). Interestingly, these predicted sites reveal residues that have been shown or predicted to have a role in PAR4 activation by thrombin or agonist peptide. These sites include aspartic acid residue Asp^{230} found in the highly conserved CHDxL domain in PARs as well as Asp^{235} in the downstream region that is homologous to the specificity conferring motif found in PAR1 and PAR2 (73). Additionally, previous *in silico* docking revealed a role for aspartic acid and histidine in this motif in binding of AYPGKF-NH_2 to PAR4 (74). We generated mutations of the most frequently predicted interaction sites (His^{229}, Asp^{230}, Gln^{242}, His^{229}/Asp^{230}) to alanine which revealed that Asp^{230} is essential for productive interaction of the peptide with the receptor, as mutation to alanine abolished calcium signal potentiation as well as β-arrestin recruitment. Interestingly, this loss of activity was observed with both peptide agonist AYPGKF-NH_2 as well as with thrombin stimulated activation of PAR4, which agrees with previous reports of the importance of these sites while also elucidating the importance of the conserved CHD^{230}AL motif in PAR4 activation, consistent with the role of this domain in PAR1 and PAR2 (38, 68–70, 73, 75). Another frequently predicted residue belonging to the CHDAL domain, His^{229}, when mutated to alanine did not alter the ability of either AYPGKF-NH_2 or the tethered-ligand as revealed by thrombin to activate calcium signalling or β-arrestin recruitment pathways. Further, we observed that a double mutation of both of these sites to alanine (His^{229}Ala, Asp^{230}Ala) did not result in any additive detriment to PAR4 activation; therefore, we conclude that Asp^{230} interaction with PAR4 peptide and tethered-ligand agonist performs an essential role in activation of PAR4.

Our SAR studies provided the impetus to explore solution NMR of AYPGKF-NH_2 to determine if the hexapeptide adopts a structure. Hexapeptides would be expected to be intrinsically disordered. In contrast, we found that AYPGKF-NH_2 adopts two stable and regular conformations. These structures are the first reported structures of a PAR agonist peptide and further, in concert with our SAR data, reveal that there may be a structural component to peptide activation of PAR4. It remains to be determined if the AYPGKF-NH_2 peptide conformation I determined in solution are necessary for binding and receptor

activation and whether the different conformations have differential effects on PAR4 activity. While these are not receptor-bound agonist structures, they are informative to help elucidate if the structure of PAR4-activating peptides is important for interaction with PAR4. NMR spectra for several additional peptides (AYpGKF-NH_2, AY-Pip-GKF-NH_2, AY-Nip-GKF-NH_2) have been collected to further determine if either of the two conformations adopted by AYPGKF-NH_2 is more analogous to peptides with agonist activity or those without. These additional analyses may provide further evidence for a structural component of agonism at PAR4.

Finally, in the context of platelet activation we find that our modified peptides that are able to cause a greater level of calcium signalling and β-arrestin recruitment than PAR4-AP could also trigger greater platelet aggregation. In our hands, PAR4-AP was unable to elicit greater than 50% of the aggregation observed in response to 1 unit/mL of thrombin, while the peptide AYPG**R**F-NH_2 was able to trigger aggregation comparable to that seen with thrombin. A role for PAR4-dependent calcium signalling is well established in platelet aggregation (64, 76, 77), and consistent with this, A**y**PGKF-NH_2, which is unable to stimulate calcium signalling, failed to induce aggregation. A role for β-arrestin mediated PAR4 signalling in platelets has also been demonstrated (26, 33). Together these data suggest that calcium signalling is critical for initiating PAR4-mediated platelet aggregation, but the precise role and hierarchy of the different PAR4 signalling pathways in platelet responses remains to be fully established.

In summary, the present studies identify key mechanisms involved in PAR4 activation and signalling. We also present and characterize a novel toolkit of PAR4 agonist peptides that could be used to study biased signalling through PAR4 in platelets as well as other physiological systems. We further show that platelet activation by PAR4 critically depends on the $G\alpha_{q/11}$ pathway, and selective targeting of this pathway might yield a useful anti-platelet agent. Overall, this study advances our understanding of agonist binding to PAR4 and will support future efforts aimed at defining signalling contribution in homeostatic signalling and the discovery of novel therapeutics targeting PAR4.

2.5 References

1. Fredriksson, R., and Schioth, H. B. (2005) The repertoire of G-protein-coupled receptors in fully sequenced genomes. *Molecular pharmacology*. **67**, 1414–1425

2. Pierce, K. L., Premont, R. T., and Lefkowitz, R. J. (2002) Seven-transmembrane receptors. *Nature Reviews Molecular Cell Biology*. **3**, 639–650

3. Erlandson, S. C., McMahon, C., and Kruse, A. C. (2018) Structural Basis for G Protein–Coupled Receptor Signaling. *doi.org*. **47**, annurev–biophys–070317–032931

4. Hilger, D., Masureel, M., and Kobilka, B. K. (2018) Structure and dynamics of GPCR signaling complexes. *Nature structural & molecular biology*. **25**, 4–12

5. Sriram, K., and Insel, P. A. (2018) G Protein-Coupled Receptors as Targets for Approved Drugs: How Many Targets and How Many Drugs? *Molecular pharmacology*. **93**, 251–258

6. Vu, T. K., Hung, D. T., Wheaton, V. I., and Coughlin, S. R. (1991) Molecular cloning of a functional thrombin receptor reveals a novel proteolytic mechanism of receptor activation. *Cell*. **64**, 1057–1068

7. Adams, M. N., Ramachandran, R., Yau, M.-K., Suen, J. Y., Fairlie, D. P., Hollenberg, M. D., and Hooper, J. D. (2011) Structure, function and pathophysiology of protease activated receptors. *Pharmacology & therapeutics*. **130**, 248–282

8. Ishihara, H., Connolly, A. J., Zeng, D., Kahn, M. L., Zheng, Y. W., Timmons, C., Tram, T., and Coughlin, S. R. (1997) Protease-activated receptor 3 is a second thrombin receptor in humans. *Nature*. **386**, 502–506

9. Coughlin, S. R. (2005) Protease-activated receptors in hemostasis, thrombosis and vascular biology. *J Thromb Haemost*. **3**, 1800–1814

10. Coughlin, S. R. (1999) How the protease thrombin talks to cells. *Proceedings of the National Academy of Sciences of the United States of America*. **96**, 11023–11027

11. Morrow, D. A., Braunwald, E., Bonaca, M. P., Ameriso, S. F., Dalby, A. J., Fish, M. P., Fox, K. A., Lipka, L. J., Liu, X., Nicolau, J. C., Ophuis, A. J., Paolasso, E., Scirica, B. M., Spinar, J., Theroux, P., Wiviott, S. D., Strony, J., and Murphy, S. A. (2012) Vorapaxar in the secondary prevention of atherothrombotic events. *The New England journal of medicine*. **366**, 1404–1413

12. Morrow, D. A., Scirica, B. M., Fox, K. A., Berman, G., Strony, J., Veltri, E., Bonaca, M. P., Fish, P., McCabe, C. H., and Braunwald, E. (2009) Evaluation of a novel antiplatelet agent for secondary prevention in patients with a history of

atherosclerotic disease: design and rationale for the Thrombin-Receptor Antagonist in Secondary Prevention of Atherothrombotic Ischemic Events (TRA 2 degrees P)-TIMI 50 trial. *Am Heart J*. **158**, 335–341 e3

13. Scirica, B. M., Bonaca, M. P., Braunwald, E., De Ferrari, G. M., Isaza, D., Lewis, B. S., Mehrhof, F., Merlini, P. A., Murphy, S. A., Sabatine, M. S., Tendera, M., Van de Werf, F., Wilcox, R., and Morrow, D. A. (2012) Vorapaxar for secondary prevention of thrombotic events for patients with previous myocardial infarction: a prespecified subgroup analysis of the TRA 2°P-TIMI 50 trial. *The Lancet*. **380**, 1317–1324

14. Jacques, S. L., LeMasurier, M., Sheridan, P. J., Seeley, S. K., and Kuliopulos, A. (2000) Substrate-assisted catalysis of the PAR1 thrombin receptor. Enhancement of macromolecular association and cleavage. *The Journal of biological chemistry*. **275**, 40671–40678

15. Liu, L. W., Vu, T. K., Esmon, C. T., and Coughlin, S. R. (1991) The region of the thrombin receptor resembling hirudin binds to thrombin and alters enzyme specificity. *The Journal of biological chemistry*. **266**, 16977–16980

16. Shapiro, M. J., Weiss, E. J., Faruqi, T. R., and Coughlin, S. R. (2000) Protease-activated receptors 1 and 4 are shut off with distinct kinetics after activation by thrombin. *The Journal of biological chemistry*. **275**, 25216–25221

17. Jacques, S. L., and Kuliopulos, A. (2003) Protease-activated receptor-4 uses dual prolines and an anionic retention motif for thrombin recognition and cleavage. *The Biochemical journal*. **376**, 733–740

18. Rwibasira Rudinga, G., Khan, G. J., and Kong, Y. (2018) Protease-Activated Receptor 4 (PAR4): A Promising Target for Antiplatelet Therapy. *Int J Mol Sci*. 10.3390/ijms19020573

19. Wu, C. C., Huang, S. W., Hwang, T. L., Kuo, S. C., Lee, F. Y., and Teng, C. M. (2000) YD-3, a novel inhibitor of protease-induced platelet activation. *Br J Pharmacol*. **130**, 1289–1296

20. Young, S. E., Duvernay, M. T., Schulte, M. L., Nance, K. D., Melancon, B. J., Engers, J., Wood, M. R., Hamm, H. E., and Lindsley, C. W. (2010) A Novel and Selective PAR4 Antagonist: ML354. in *Probe Reports from the NIH Molecular Libraries Program*, National Center for Biotechnology Information (US), Bethesda (MD), [online] http://www.ncbi.nlm.nih.gov/books/NBK280043/ (Accessed June 4, 2019)

21. Miller, M. M., Banville, J., Friends, T., Gagnon, M., Hangeland, J. J., Lavalee, J.-F., Martel, A., O'Grady, H., Remillard, R., Ruediger, E. H., Tremblay, F., Posy, S., Allegretto, N., Guarino, V. R., Harden, D., Harper, T. W., Hartl, K., Josephs, J., Malmstrom, S., Watson, C. A., Yang, Y., Zhang, G., Wong, P. C., Yang, J., Bouvier, M., Seiffert, D. A., Wexler, R. R., Lawrence, R. M., Priestley, E. S., and

Marinier, A. (2019) Discovery of Potent Protease-Activated Receptor 4 Antagonists with in vivo Antithrombotic Efficacy. *J. Med. Chem.* 10.1021/acs.jmedchem.9b00186

22. Wilson, S. J., Ismat, F. A., Wang, Z., Cerra, M., Narayan, H., Raftis, J., Gray, T. J., Connell, S., Garonzik, S., Ma, X., Yang, J., and Newby, D. E. (2017) PAR4 (Protease-Activated Receptor 4) Antagonism With BMS-986120 Inhibits Human Ex Vivo Thrombus Formation. *Arteriosclerosis, Thrombosis, and Vascular Biology*. 10.1161/ATVBAHA.117.310104

23. Wong, P. C., Seiffert, D., Bird, J. E., Watson, C. A., Bostwick, J. S., Giancarli, M., Allegretto, N., Hua, J., Harden, D., Guay, J., Callejo, M., Miller, M. M., Lawrence, R. M., Banville, J., Guy, J., Maxwell, B. D., Priestley, E. S., Marinier, A., Wexler, R. R., Bouvier, M., Gordon, D. A., Schumacher, W. A., and Yang, J. (2017) Blockade of protease-activated receptor-4 (PAR4) provides robust antithrombotic activity with low bleeding. *Science translational medicine*. **9**, eaaf5294

24. Holinstat, M., Voss, B., Bilodeau, M. L., McLaughlin, J. N., Cleator, J., and Hamm, H. E. (2006) PAR4, but not PAR1, signals human platelet aggregation via Ca2+ mobilization and synergistic P2Y12 receptor activation. *The Journal of biological chemistry*. **281**, 26665–26674

25. Li, D., D'Angelo, L., Chavez, M., and Woulfe, D. S. (2011) Arrestin-2 differentially regulates PAR4 and ADP receptor signaling in platelets. *The Journal of biological chemistry*. **286**, 3805–3814

26. Ramachandran, R., Mihara, K., Thibeault, P., Vanderboor, C. M., Petri, B., Saifeddine, M., Bouvier, M., and Hollenberg, M. D. (2017) Targeting a Proteinase-Activated Receptor 4 (PAR4) Carboxyl Terminal Motif to Regulate Platelet Function. *Molecular pharmacology*. **91**, 287–295

27. Covic, L., Misra, M., Badar, J., Singh, C., and Kuliopulos, A. (2002) Pepducin-based intervention of thrombin-receptor signaling and systemic platelet activation. *Nature Medicine*. **8**, 1161–1165

28. Bar-Shavit, R., Maoz, M., Kancharla, A., Jaber, M., Agranovich, D., Grisaru-Granovsky, S., and Uziely, B. (2016) Protease-activated receptors (PARs) in cancer: Novel biased signaling and targets for therapy. *Methods in cell biology*. **132**, 341–358

29. Hollenberg, M. D., Mihara, K., Polley, D., Suen, J. Y., Han, A., Fairlie, D. P., and Ramachandran, R. (2014) Biased signalling and proteinase-activated receptors (PARs): targeting inflammatory disease. *British journal of pharmacology*. **171**, 1180–1194

30. Seyedabadi, M., Ghahremani, M. H., and Albert, P. R. (2019) Biased signaling of G protein coupled receptors (GPCRs): Molecular determinants of

GPCR/transducer selectivity and therapeutic potential. *Pharmacol. Ther.* **200**, 148–178

31. Leger, A. J., Jacques, S. L., Badar, J., Kaneider, N. C., Derian, C. K., Andrade-Gordon, P., Covic, L., and Kuliopulos, A. (2006) Blocking the protease-activated receptor 1-4 heterodimer in platelet-mediated thrombosis. *Circulation*. **113**, 1244–1254

32. Vanderboor, C. M., Thibeault, P. E., Nixon, K. C., Gros, R., Kramer, J., and Ramachandran, R. (2019) *Proteinase-Activated Receptor 4 (PAR4) Activation Triggers Cell Membrane Blebbing through RhoA and β-arrestin*, Pharmacology and Toxicology, 10.1101/746677

33. Khan, A., Li, D., Ibrahim, S., Smyth, E., and Woulfe, D. S. (2014) The Physical Association of the P2Y12 Receptor with PAR4 Regulates Arrestin-Mediated Akt Activation. *Molecular pharmacology*. **86**, 1–11

34. Ferguson, S. S. G., and Caron, M. G. (2004) Green Fluorescent Protein-Tagged β-Arrestin Translocation as a Measure of G Protein-Coupled Receptor Activation. in *G Protein Signaling: Methods and Protocols* (Smrcka, A. V. ed), pp. 121–126, Methods in Molecular Biology™, Humana Press, Totowa, NJ, 10.1385/1-59259-430-1:121

35. Graham, F. L., and van der Eb, A. J. (1973) A new technique for the assay of infectivity of human adenovirus 5 DNA. *Virology*. **52**, 456–467

36. Boitano, S., Flynn, A. N., Schulz, S. M., Hoffman, J., Price, T. J., and Vagner, J. (2011) Potent Agonists of the Protease Activated Receptor 2 (PAR2). *J Med Chem*. **54**, 1308–1313

37. Faruqi, T. R., Weiss, E. J., Shapiro, M. J., Huang, W., and Coughlin, S. R. (2000) Structure-function analysis of protease-activated receptor 4 tethered ligand peptides. Determinants of specificity and utility in assays of receptor function. *The Journal of biological chemistry*. **275**, 19728–19734

38. Lerner, D. J., Chen, M., Tram, T., and Coughlin, S. R. (1996) Agonist recognition by proteinase-activated receptor 2 and thrombin receptor. Importance of extracellular loop interactions for receptor function. *The Journal of biological chemistry*. **271**, 13943–13947

39. Schindelin, J., Arganda-Carreras, I., Frise, E., Kaynig, V., Longair, M., Pietzsch, T., Preibisch, S., Rueden, C., Saalfeld, S., Schmid, B., Tinevez, J.-Y., White, D. J., Hartenstein, V., Eliceiri, K., Tomancak, P., and Cardona, A. (2012) Fiji: an open-source platform for biological-image analysis. *Nature Methods*. **9**, 676–682

40. Madeira, F., Park, Y. M., Lee, J., Buso, N., Gur, T., Madhusoodanan, N., Basutkar, P., Tivey, A. R. N., Potter, S. C., Finn, R. D., and Lopez, R. (2019) The EMBL-

EBI search and sequence analysis tools APIs in 2019. *Nucleic Acids Res*. **47**, W636–W641

41. Sievers, F., Wilm, A., Dineen, D., Gibson, T. J., Karplus, K., Li, W., Lopez, R., McWilliam, H., Remmert, M., Söding, J., Thompson, J. D., and Higgins, D. G. (2011) Fast, scalable generation of high-quality protein multiple sequence alignments using Clustal Omega. *Molecular Systems Biology*. **7**, 539

42. Cheng, R. K. Y., Fiez-Vandal, C., Schlenker, O., Edman, K., Aggeler, B., Brown, D. G., Brown, G. A., Cooke, R. M., Dumelin, C. E., Doré, A. S., Geschwindner, S., Grebner, C., Hermansson, N.-O., Jazayeri, A., Johansson, P., Leong, L., Prihandoko, R., Rappas, M., Soutter, H., Snijder, A., Sundström, L., Tehan, B., Thornton, P., Troast, D., Wiggin, G., Zhukov, A., Marshall, F. H., and Dekker, N. (2017) Structural insight into allosteric modulation of protease-activated receptor 2. *Nature*. **545**, 112–115

43. Webb, B., and Sali, A. (2017) Protein Structure Modeling with MODELLER. in *Functional Genomics*, pp. 39–54, Humana Press, New York, NY, New York, NY, 10.1007/978-1-4939-7231-9_4

44. Dolinsky, T. J., Nielsen, J. E., McCammon, J. A., and Baker, N. A. (2004) PDB2PQR: an automated pipeline for the setup of Poisson-Boltzmann electrostatics calculations. *Nucleic Acids Res.* **32**, W665-667

45. Lee, H., Heo, L., Lee, M. S., and Seok, C. (2015) GalaxyPepDock: a protein–peptide docking tool based on interaction similarity and energy optimization. *Nucleic Acids Res*. **43**, W431–W435

46. Lalonde, T. (2019) The Ghrelin Receptor and its Appetite for Highly Potent Ghrelin Analogues. *Electronic Thesis and Dissertation Repository*

47. Bartels, C., Xia, T. H., Billeter, M., Güntert, P., and Wüthrich, K. (1995) The program XEASY for computer-supported NMR spectral analysis of biological macromolecules. *J. Biomol. NMR*. **6**, 1–10

48. Keller, R. (2004) *The computer aided resonance assignment tutorial*, Cantina Verl., Goldau

49. Shen, Y., Delaglio, F., Cornilescu, G., and Bax, A. (2009) TALOS+: a hybrid method for predicting protein backbone torsion angles from NMR chemical shifts. *J. Biomol. NMR*. **44**, 213–223

50. Güntert, P. (2004) Automated NMR Structure Calculation With CYANA. in *Protein NMR Techniques* (Downing, A. K. ed), pp. 353–378, Methods in Molecular Biology™, Humana Press, Totowa, NJ, 10.1385/1-59259-809-9:353

51. Jee, J., and Güntert, P. (2003) Influence of the completeness of chemical shift assignments on NMR structures obtained with automated NOE assignment. *J Struct Func Genom*. **4**, 179–189

52. Kim, B. H., Wang, F. I., Pereverzev, A., Chidiac, P., and Dixon, S. J. (2019) Toward Defining the Pharmacophore for Positive Allosteric Modulation of PTH1 Receptor Signaling by Extracellular Nucleotides. *ACS Pharmacol. Transl. Sci.* **2**, 155–167

53. Scarborough, R. M., Naughton, M. A., Teng, W., Hung, D. T., Rose, J., Vu, T. K., Wheaton, V. I., Turck, C. W., and Coughlin, S. R. (1992) Tethered ligand agonist peptides. Structural requirements for thrombin receptor activation reveal mechanism of proteolytic unmasking of agonist function. *The Journal of biological chemistry*. **267**, 13146–13149

54. Hoffmann, W., Langenhan, J., Huhmann, S., Moschner, J., Chang, R., Accorsi, M., Seo, J., Rademann, J., Meijer, G., Koksch, B., Bowers, M. T., von Helden, G., and Pagel, K. (2019) An Intrinsic Hydrophobicity Scale for Amino Acids and Its Application to Fluorinated Compounds. *Angewandte Chemie International Edition*. **58**, 8216–8220

55. Takasaki, J., Saito, T., Taniguchi, M., Kawasaki, T., Moritani, Y., Hayashi, K., and Kobori, M. (2004) A novel Galphaq/11-selective inhibitor. *J. Biol. Chem.* **279**, 47438–47445

56. Jean-Charles, P.-Y., Kaur, S., and Shenoy, S. K. (2017) GPCR signaling via β-arrestin-dependent mechanisms. *J Cardiovasc Pharmacol*. **70**, 142–158

57. Xu, W. F., Andersen, H., Whitmore, T. E., Presnell, S. R., Yee, D. P., Ching, A., Gilbert, T., Davie, E. W., and Foster, D. C. (1998) Cloning and characterization of human protease-activated receptor 4. *Proceedings of the National Academy of Sciences of the United States of America*. **95**, 6642–6646

58. Soh, U. J., Dores, M. R., Chen, B., and Trejo, J. (2010) Signal transduction by protease-activated receptors. *British journal of pharmacology*. **160**, 191–203

59. Hollenberg, M. D. (2003) Proteinase-activated receptors: Tethered ligands and receptor-activating peptides. *Drug Dev. Res.* **59**, 336–343

60. Al-Ani, B., Wijesuriya, S. J., and Hollenberg, M. D. (2002) Proteinase-activated receptor 2: differential activation of the receptor by tethered ligand and soluble peptide analogs. *The Journal of pharmacology and experimental therapeutics*. **302**, 1046–1054

61. Nystedt, S., Emilsson, K., Wahlestedt, C., and Sundelin, J. (1994) Molecular cloning of a potential proteinase activated receptor. *Proceedings of the National Academy of Sciences of the United States of America*. **91**, 9208–9212

62. Kahn, M. L., Zheng, Y. W., Huang, W., Bigornia, V., Zeng, D., Moff, S., Farese, R. V. J., Tam, C., and Coughlin, S. R. (1998) A dual thrombin receptor system for platelet activation. *Nature*. **394**, 690–694

63. Chidiac, P. (2016) RGS proteins destroy spare receptors: Effects of GPCR-interacting proteins and signal deamplification on measurements of GPCR agonist potency. *Methods*. **92**, 87–93

64. Edelstein, L. C., Simon, L. M., Lindsay, C. R., Kong, X., Teruel-Montoya, R., Tourdot, B. E., Chen, E. S., Ma, L., Coughlin, S., Nieman, M., Holinstat, M., Shaw, C. A., and Bray, P. F. (2014) Common variants in the human platelet PAR4 thrombin receptor alter platelet function and differ by race. *Blood*. **124**, 3450–3458

65. Venkatakrishnan, A. J., Deupi, X., Lebon, G., Tate, C. G., Schertler, G. F., and Babu, M. M. (2014) Molecular signatures of G-protein-coupled receptors. *Nature*. **494**, 185–194

66. Woolley, M. J., and Conner, A. C. (2017) Understanding the common themes and diverse roles of the second extracellular loop (ECL2) of the GPCR super-family. *Molecular and Cellular Endocrinology*. **449**, 3–11

67. Wheatley, M., Wootten, D., Conner, M. T., Simms, J., Kendrick, R., Logan, R. T., Poyner, D. R., and Barwell, J. (2012) Lifting the lid on GPCRs: the role of extracellular loops. *Br. J. Pharmacol.* **165**, 1688–1703

68. Al-Ani, B., Saifeddine, M., Kawabata, A., and Hollenberg, M. D. (1999) Proteinase activated receptor 2: Role of extracellular loop 2 for ligand-mediated activation. *Br J Pharmacol*. **128**, 1105–1113

69. Gerszten, R. E., Chen, J., Ishii, M., Ishii, K., Wang, L., Nanevicz, T., Turck, C. W., Vu, T. K., and Coughlin, S. R. (1994) Specificity of the thrombin receptor for agonist peptide is defined by its extracellular surface. *Nature*. **368**, 648–651

70. Nanevicz, T., Ishii, M., Wang, L., Chen, M., Chen, J., Turck, C. W., Cohen, F. E., and Coughlin, S. R. (1995) Mechanisms of thrombin receptor agonist specificity. Chimeric receptors and complementary mutations identify an agonist recognition site. *The Journal of biological chemistry*. **270**, 21619–21625

71. Nieman, M. T. (2008) Protease-Activated Receptor 4 Uses Anionic Residues To Interact with α-Thrombin in the Absence or Presence of Protease-Activated Receptor 1. *Biochemistry*. **47**, 13279–13286

72. Nieman, M. T., and Schmaier, A. H. (2007) Interaction of Thrombin with PAR1 and PAR4 at the Thrombin Cleavage Site. *Biochemistry*. **46**, 8603–8610

73. Sánchez Centellas, D., Gudlur, S., Vicente-Carrillo, A., Ramström, S., and Lindahl, T. L. (2017) A cluster of aspartic residues in the extracellular loop II of

PAR 4 is important for thrombin interaction and activation of platelets. *Thrombosis Research*. **154**, 84–92

74. Moschonas, I. C., Kellici, T. F., Mavromoustakos, T., Stathopoulos, P., Tsikaris, V., Magafa, V., Tzakos, A. G., and Tselepis, A. D. (2017) Molecular requirements involving the human platelet protease-activated receptor-4 mechanism of activation by peptide analogues of its tethered-ligand. *Platelets*. **28**, 812–821

75. Blackhart, B. D., Emilsson, K., Nguyen, D., Teng, W., Martelli, A. J., Nystedt, S., Sundelin, J., and Scarborough, R. M. (1996) Ligand cross-reactivity within the protease-activated receptor family. *The Journal of biological chemistry*. **271**, 16466–16471

76. French, S. L., and Hamilton, J. R. (2016) Protease-activated receptor 4: from structure to function and back again. *Br J Pharmacol*. **173**, 2952–2965

77. Tourdot, B. E., Stoveken, H., Trumbo, D., Yeung, J., Kanthi, Y., Edelstein, L. C., Bray, P. F., Tall, G. G., and Holinstat, M. (2018) Genetic Variant in Human PAR (Protease-Activated Receptor) 4 Enhances Thrombus Formation Resulting in Resistance to Antiplatelet Therapeutics. *Arterioscler. Thromb. Vasc. Biol.* **38**, 1632–1643

2.6 Chapter 2 Supplementary Information

Supplementary Table 2.1 Mass spectrometry (MS) data of synthesized peptides

Compound	Molecular Formula (M)	Calc. $[M+H]^+$ (*m/z*)	Found $[M+H]^+$ (*m/z*)
Ac-AYPGKF-NH$_2$	$C_{36}H_{50}N_8O_8$	723.38	723.43
AAPGKF-NH$_2$	$C_{28}H_{44}N_8O_6$	589.35	589.30
AYAGKF-NH$_2$	$C_{32}H_{46}N_8O_7$	655.36	655.43
AYPAKF-NH$_2$	$C_{35}H_{50}N_8O_7$	695.39	695.46
AYPGAF-NH$_2$	$C_{31}H_{41}N_7O_7$	624.31	625.36
AYPGKA-NH$_2$	$C_{28}H_{44}N_8O_7$	605.34	606.42
aYPGKF-NH$_2$	$C_{34}H_{48}N_8O_7$	681.37	681.44
AyPGKF-NH$_2$	$C_{34}H_{48}N_8O_7$	681.37	681.44
AYPGkF-NH$_2$	$C_{34}H_{48}N_8O_7$	681.37	681.46
AYPGKf-NH$_2$	$C_{34}H_{48}N_8O_7$	681.37	681.48
Aib-YPGKF-NH$_2$	$C_{35}H_{50}N_8O_7$	695.39	695.49
Sar-YPGKF-NH$_2$	$C_{34}H_{48}N_8O_7$	681.37	681.38
Inp-YPGKF-NH$_2$	$C_{37}H_{52}N_8O_7$	721.40	721.50
betaAla-YPGKF-NH$_2$	$C_{34}H_{48}N_8O_7$	681.37	681.46
A-Tyr(Me)-PGKF-NH$_2$	$C_{35}H_{50}N_8O_7$	695.39	695.48
A-F(4-fluoro)-PGKF-NH$_2$	$C_{34}H_{47}N_8O_6F$	683.37	683.36
AY-Pip-GKF-NH$_2$	$C_{35}H_{50}N_8O_7$	695.39	695.39
AY-Nip-GKF-NH$_2$	$C_{35}H_{50}N_8O_7$	695.39	695.39
AYP-Sar-KF-NH$_2$	$C_{35}H_{50}N_8O_7$	695.39	695.39
AYP-betaAla-KF-NH$_2$	$C_{35}H_{50}N_8O_7$	695.39	695.48
AYPGK-1Nal-NH$_2$	$C_{38}H_{50}N_8O_7$	731.38	731.48
AYPGK-2Nal-NH$_2$	$C_{38}H_{50}N_8O_7$	731.38	731.50
AYPGK-F(4-fluoro)-NH$_2$	$C_{34}H_{47}N_8O_7F$	699.36	699.38
AYPGK-F(4-Me)-NH$_2$	$C_{35}H_{50}N_8O_7$	695.39	695.39
AYpGKF-NH$_2$	$C_{34}H_{48}N_8O_7$	681.37	681.37
AYPGK-(*N*-Me-F)-NH$_2$	$C_{35}H_{50}N_8O_7$	695.39	695.39
AYPG-(N_α-Me-K)-F-NH$_2$	$C_{35}H_{50}N_8O_7$	695.39	695.39
A-(*N*-Me-Y)-PGKF-NH$_2$	$C_{35}H_{50}N_8O_7$	695.39	695.39
(*N*-Me-A)-YPGKF-NH$_2$	$C_{35}H_{50}N_8O_7$	695.39	695.39
VYPGKF-NH$_2$	$C_{36}H_{52}N_8O_7$	709.40	709.40
(*N*-Me-S)-YPGKF-NH$_2$	$C_{35}H_{50}N_8O_8$	711.38	711.38
Nle-YPGKF-NH$_2$	$C_{37}H_{54}N_8O_7$	723.42	723.42
AYPGRF-NH$_2$	$C_{34}H_{48}N_{10}O_7$	709.38	709.38
AYPGOF-NH$_2$	$C_{33}H_{46}N_8O_7$	667.36	667.36
AYPG-Cit-F-NH$_2$	$C_{34}H_{47}N_9O_8$	710.36	710.36
AYPG-(N_ε-Me-K)-F-NH$_2$	$C_{35}H_{50}N_8O_7$	695.39	695.39
AYPGKY-NH$_2$	$C_{34}H_{48}N_8O_8$	697.37	697.37

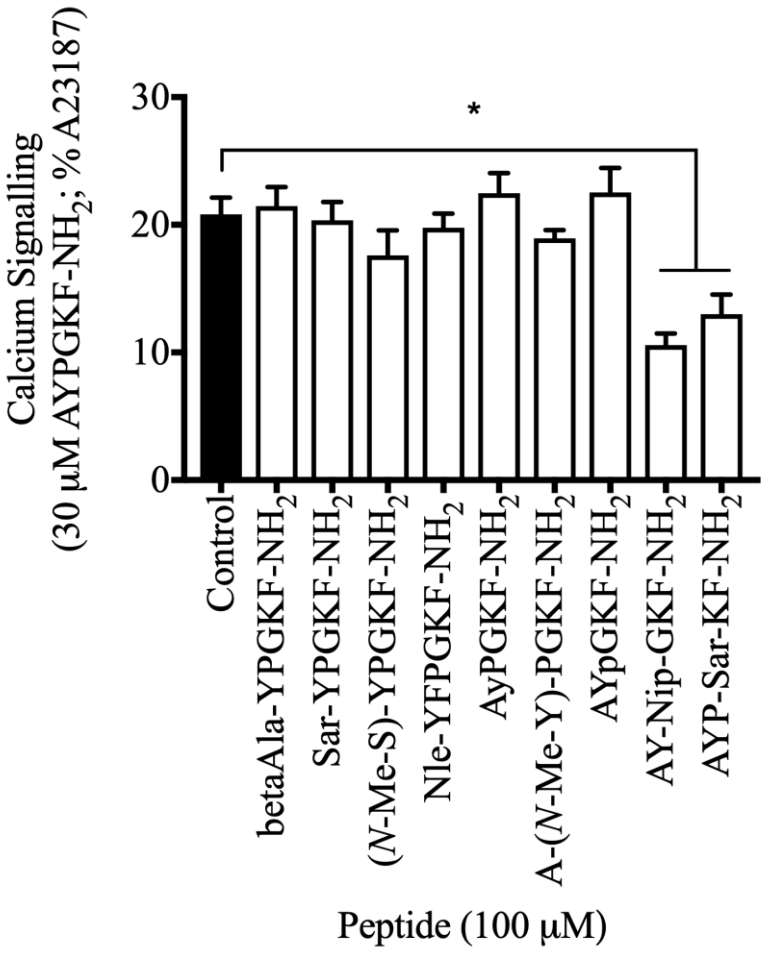

Supplementary Figure 2.1 PAR4-AP (AYPGKF-NH_2) stimulated calcium signalling responses following pre-treatment with PAR4 agonist peptides unable to stimulate calcium signalling. Calcium signalling (Fluorescence Em_{530}) in HEK-293 cells stably expressing PAR4-YFP were recorded following 30 μM AYPGKF-NH_2 addition after 30-minute pre-treatment incubation with 100 μM of calcium signalling-null peptides. Data are shown as a percentage of maximum response obtained in cells treated with the calcium ionophore A23187 (3 μM). Agonist peptide concentrations are in M. Pre-treatment with peptides unable to stimulate calcium signalling did not affect AYPGKF-NH_2-stimulated calcium signalling in most cases with the exceptions of AY-Nip-GKF-NH_2 and AYP-Sar-KF-NH_2, which significantly decreased AYPGKF-NH_2 stimulated calcium signalling compared to vehicle treated control. (*$p > 0.05$; $n = 3$)

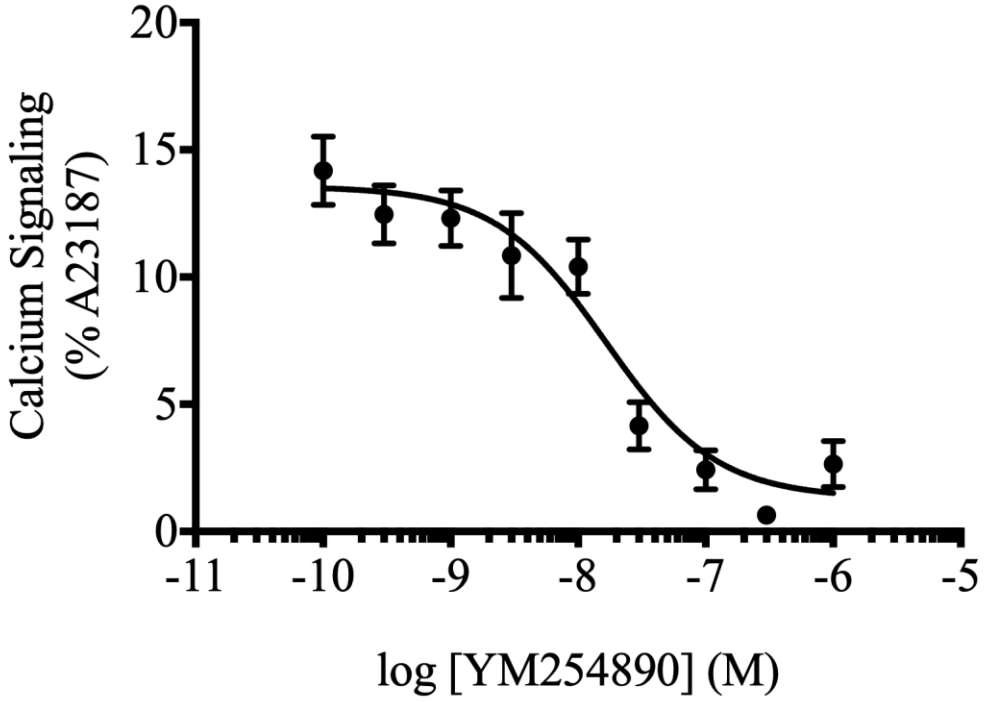

Supplementary Figure 2.2 PAR4-mediated calcium signalling is $G\alpha_{q/11}$-dependent. HEK-293 cells stably expressing PAR4 were pre-treated with either DMSO vehicle control (0.001%) or increasing concentration of the selective $G\alpha_{q/11}$ inhibitor YM254890. Calcium signalling following stimulation with AYPGKF-NH_2 (30μM) was recorded. PAR4-mediated calcium signalling was inhibited by YM254890, with an IC_{50} of 16.5 ± 6.1 nM. (*n = 4*)

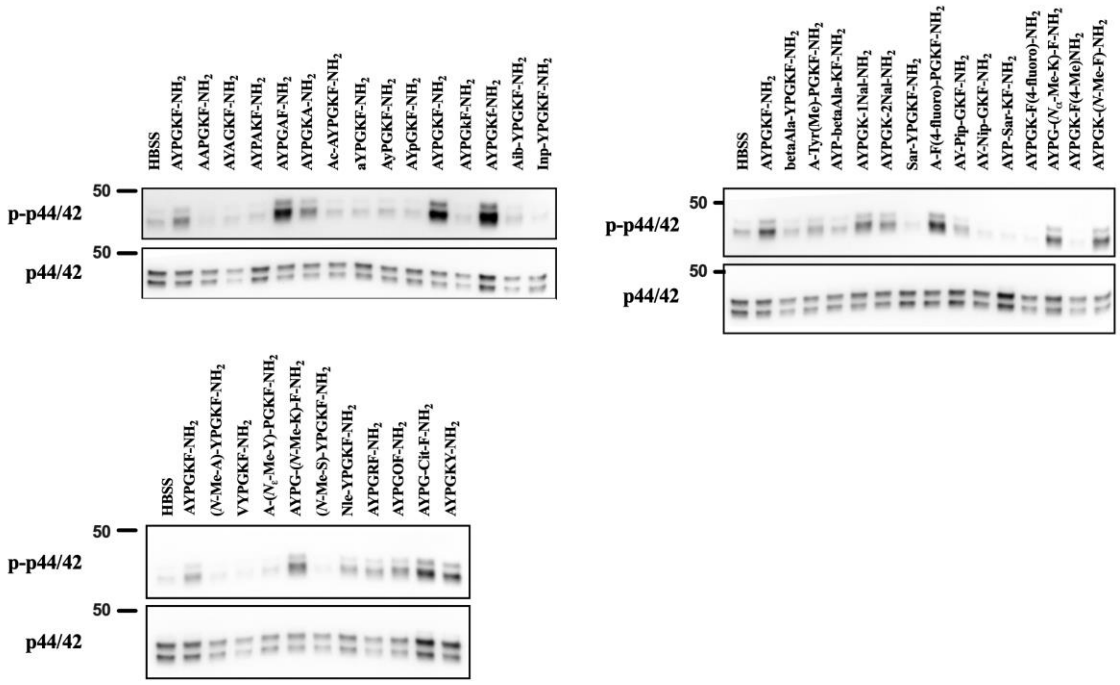

Supplementary Figure 2.3 Representative blots of ERK phosphorylation in response to 100 µM of AYPGKF-NH_2 and derivative peptides.

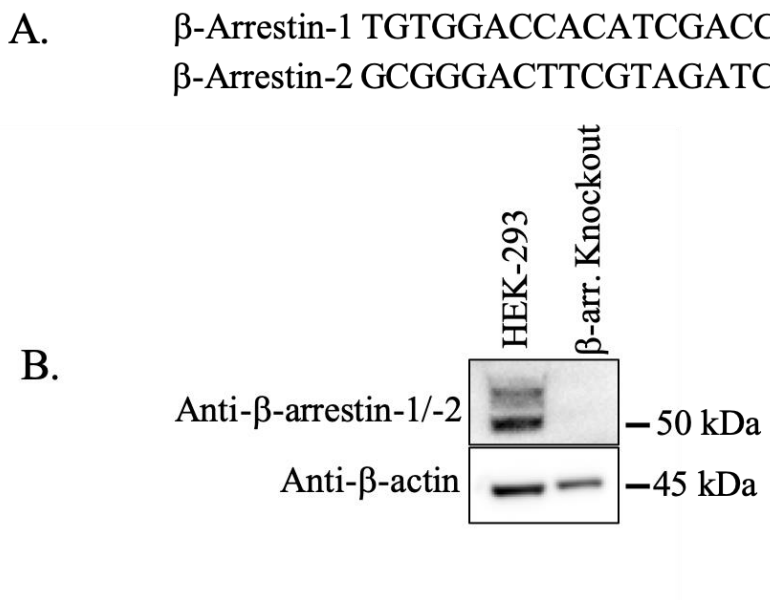

Supplementary Figure 2.4 Guide RNA sequences and representative blots validating β-arrestin-1/-2-knockout HEK-293 cells. (A) Guide RNA sequences designed to target either β-arrestin-1 or -2. (B) Representative blots of β-arrestin-1/-2 protein from HEK-293 and β-arrestin-1/-2 double knockout HEK-293 (β-arr. Knockout) cells. We observe no β-arrestin-1/-2 protein in the β-arr. knockout HEK-293 cell line.

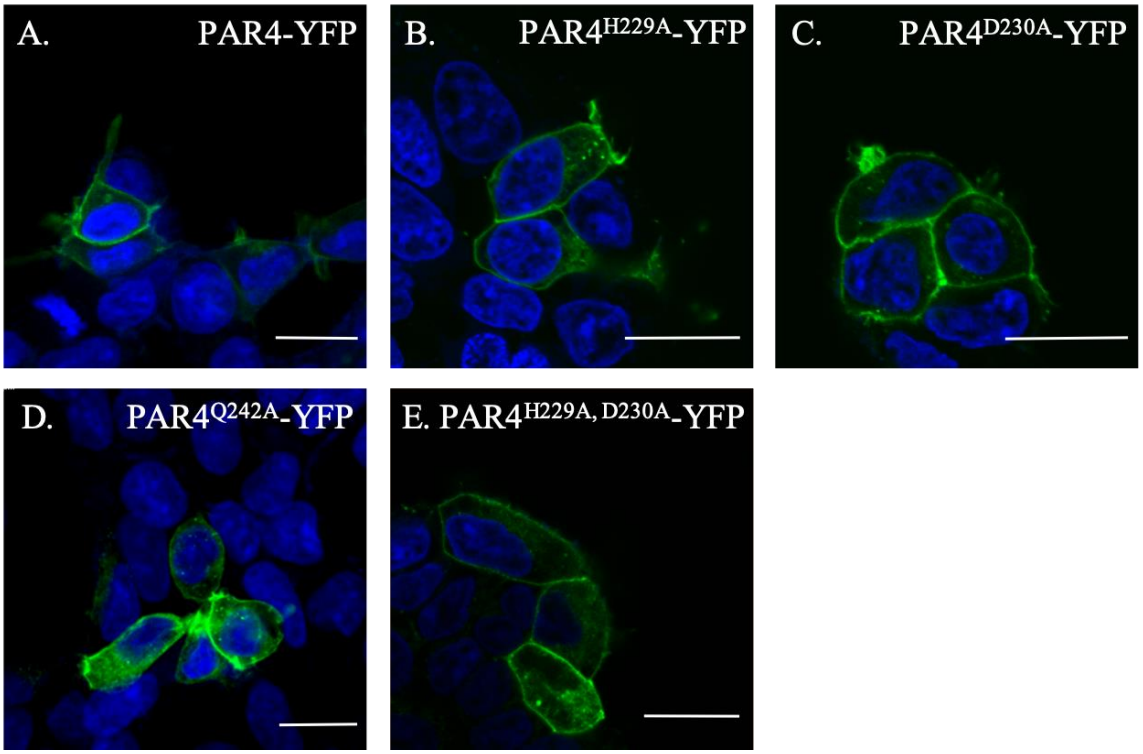

Supplementary Figure 2.5 Confocal microscopy of PAR4-YFP and mutant PAR4-YFP constructs. Confocal microscopy of PAR4-YFP (A) and mutant PAR4-YFP constructs PAR4^{H229A}-YFP (B), PAR4^{D230A}-YFP (C), PAR4^{Q242A}-YFP (D), and PAR4$^{H229A, D230A}$-YFP. Confocal microscopy was employed to assess the appropriate membrane localization of each PAR4 receptor construct. Receptor constructs are shown in green (eYFP) and DAPI (blue) shows the nucleus of the cell. We observe no defect in membrane localization between the wild-type and mutant PAR4 receptors. (*n = 3*)

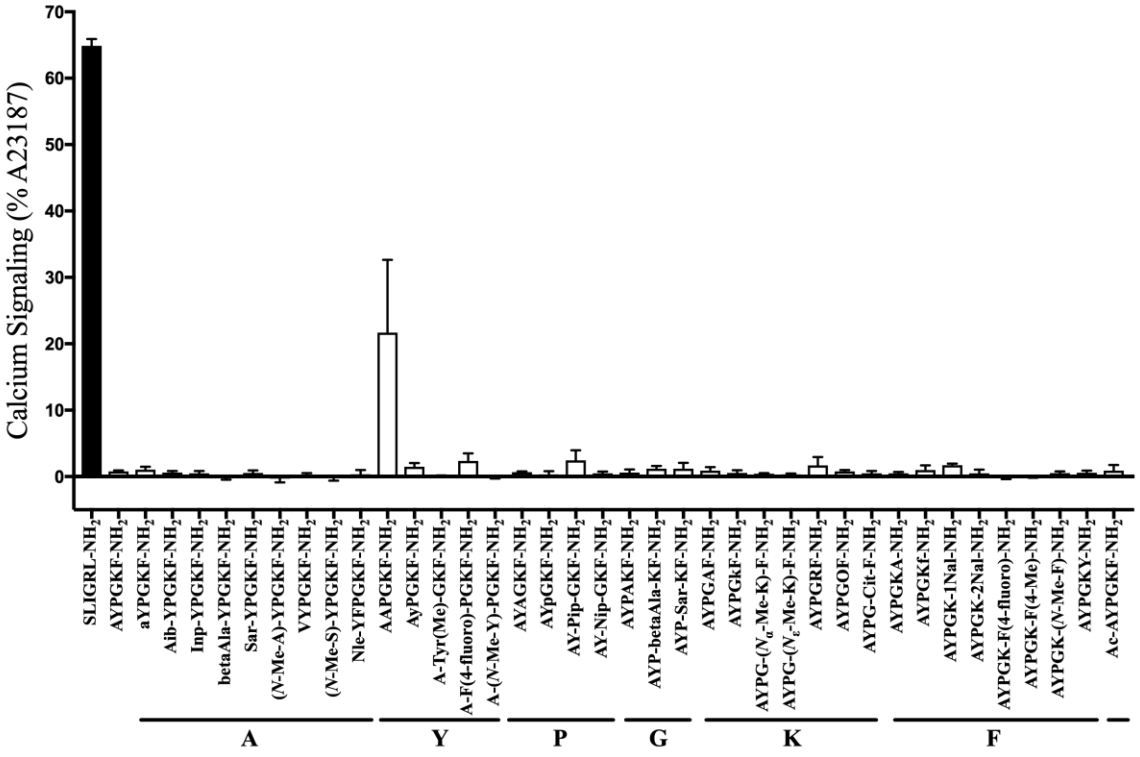

Supplementary Figure 2.6 Peptide PAR4-specificity evaluated by calcium signalling assay. PAR4 peptide library is specific for PAR4 as shown by lack of calcium signalling in HEK-293 cells which do not endogenously express PAR4. Peptide AAPGKF-NH_2 was found to have basal fluorescence even in the absence of cells. (*n = 3*)

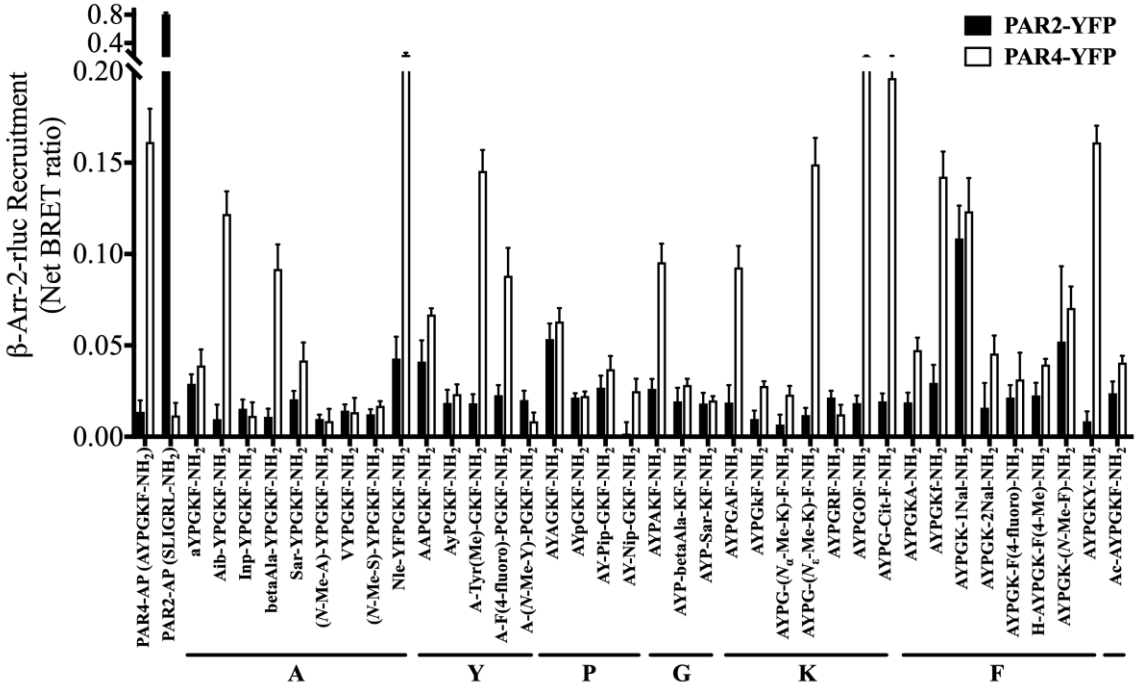

Supplementary Figure 2.7 Peptide PAR4-specificity evaluated by BRET. PAR4 peptide library is specific for PAR4 and does not cause recruitment of β-arrestin-2 to PAR2 (shown as black bars) at 100 μM, with the exception of AYPGK-1Nal-NH_2 which shows some β-arrestin recruitment to PAR2. BRET ratios obtained with the parental peptides for both PAR4 (AYPGKF-NH_2) and PAR2 (SLIGRL-NH_2) are shown. (*n = 3*)

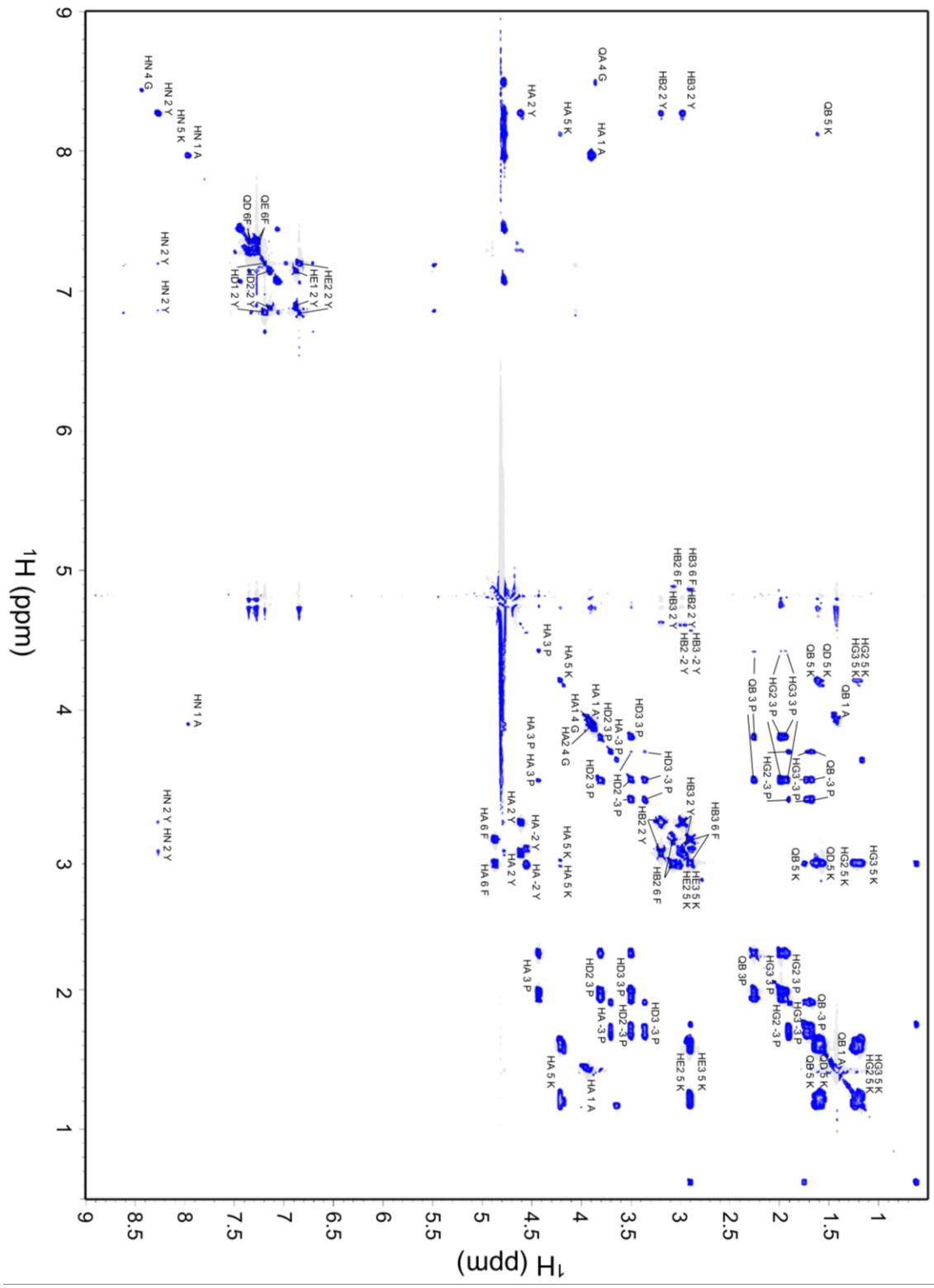
^{1}H (ppm)
^{1}H (ppm)

Supplementary Figure 2.8 Annotated TOCSY spectrum of AYPGKF-NH_2. We observed two distinct sets of chemical shifts for tyrosine (position 2) and proline (position 3). Stronger peaks correspond to higher abundance and thus associated with the "major" conformation of AYPGKF-NH_2; while, weaker peaks are associated with the "minor" conformation. Proton chemical shifts assigned in Ala (1 A), Tyr (2 Y, major; -2 Y, minor), Pro (3 P, major; -3 P, minor), Lys (5 K), Phe (6 F) are shown. Chemical shift values are reported for the major and minor conformations in Supplementary Tables 2.2 and 2.3, respectively.

Supplementary Table 2.2 Assigned ^{1}H chemical shifts* (ppm) from TOCSY and COSY of AYPGKF-NH_2 "major" confirmation at 25°C.

	NH	$C_\alpha H$	$C_\beta H$	Other
Ala[1]	7.97	3.91	1.41	
Tyr[2]	8.27	4.61	3.20, 2.98	$C_{\delta1}H$ 7.19, $C_{\varepsilon1}H$ 6.87, $C_{\delta2}H$ 7.14, $C_{\varepsilon2}H$ 6.85
Pro[3]		4.43	2.25	$C_\delta H_2$ 3.80, $C_\delta H_3$ 3.50, $C_\gamma H_2$ 1.99, $C_\gamma H_3$ 1.94
Gly[4]	8.48	3.86, 3.89		
Lys[5]	8.13	4.20	1.61	$C_\delta H$ 1.57, $C_\gamma H_2$ 1.24, $C_\gamma H_3$ 1.18, $C_\varepsilon H_2$ 2.92, $C_\varepsilon H_3$ 2.88
Phe[6]		4.87	3.07, 2.90	$C_\delta H$ 7.36, $C_\varepsilon H$ 7.29

*40 of 45 protons assigned (89%) assuming the same chemical shift for all protons attached to the carbon used by CYANA.

Supplementary Table 2.3 Assigned ^{1}H chemical shifts* (ppm) from TOCSY and COSY of AYPGKF-NH_2 "minor" confirmation at 25°C.

	NH	$C_\alpha H$	$C_\beta H$	Other
Ala[1]	7.97	3.91	1.41	
Tyr[2]		4.55	3.00, 2.89	$C_{\delta 1}H$ 7.19, $C_{\varepsilon 1}H$ 6.87, $C_{\delta 2}H$ 7.14, $C_{\varepsilon 2}H$ 6.85
Pro[3]		3.70	1.67	$C_\delta H_2$ 3.50, $C_\delta H_3$ 3.36, $C_\gamma H_2$ 1.90, $C_\gamma H_3$ 1.73
Gly[4]	8.48	3.86, 3.89		
Lys[5]	8.13	4.20	1.61	$C_\delta H$ 1.57, $C_\gamma H_2$ 1.24, $C_\gamma H_3$ 1.18, $C_\varepsilon H_2$ 2.92, $C_\varepsilon H_3$ 2.88
Phe[6]		4.87	3.07, 2.90	$C_\delta H$ 7.36, $C_\varepsilon H$ 7.29
*39 of 45 protons assigned (87%) assuming the same chemical shift for all protons attached to the carbon used by CYANA.				

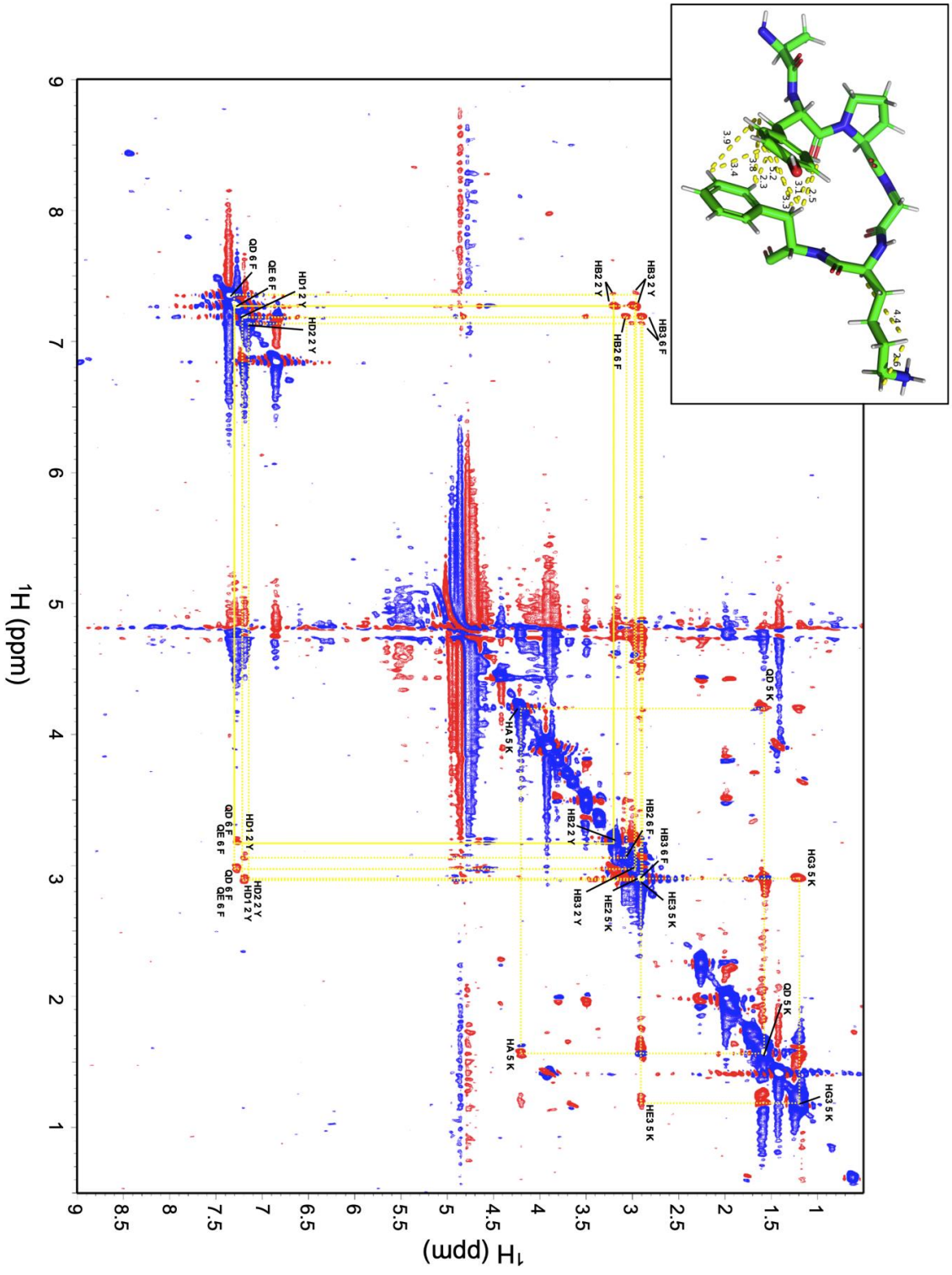

Supplementary Figure 2.9 NOESY spectra with NOEs restraining the "major" conformation of AYPGKF-NH_2 at 25°C. NOESY spectra of AYPGKF-NH_2 is shown (blue and red) with NOEs labelled (black). NOE cross-peaks are shown (yellow square)

which form the restraints for structural ensemble calculation in CYANA of the major conformation of AYPGKF-NH_2 (inset, upper left). Restraints used in ensemble calculation are shown on the structure (yellow dashed lines) with length (Å). (see Supplementary Table 2.4 for NOE statistics).

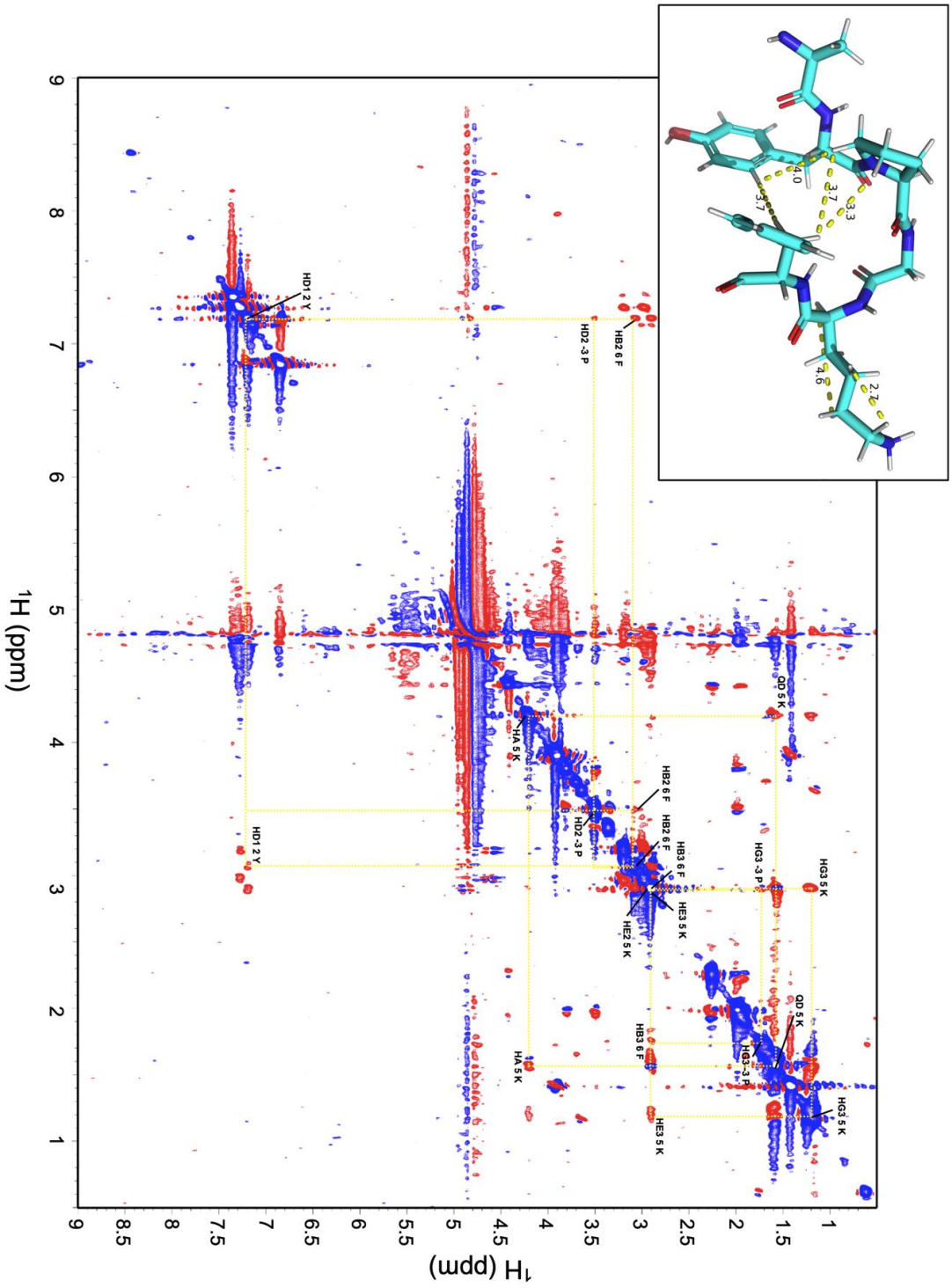

Supplementary Figure 2.10 NOESY spectra with NOEs restraining the "minor" conformation of AYPGKF-NH_2 at 25°C. NOESY spectra of AYPGKF-NH_2 is shown (blue and red) with NOEs labelled (black). NOE cross-peaks are shown (yellow square)

which form the restraints for structural ensemble calculation in CYANA of the minor conformation of AYPGKF-NH_2 (inset, upper left). Restraints used in ensemble calculation are shown on the structure (yellow dashed lines) with length (Å). (see Supplementary Table 2.4 for NOE statistics).

Supplementary Table 2.4 Solution NMR structure calculation statistics for AYPGKF-NH_2.

NOESY Peaks	**Major**	**Minor**
Selected	149	149
Assigned	84	65
Unassigned	65	84
With off diagonal	61	44
With short range assignments |i-j|<1	47	39
With medium range assignments 1<|i-j|<5	14	5
Unambiguous NMR distance and dihedral constraints	Major	Minor
Total	12	6
Sequential: |i-j|=1	2	3
Medium range: 1<|i-j|<5	10	3
Total dihedral angle restraints		
ϕ (phi)	1	1
ψ (psi)	1	1
RMSD (residues 1-6)*		
Average backbone RMSD to mean	0.52	0.66
Average heavy atom RMSD to mean	1.24	1.62

*Average RMSD values are reported for the top 10 lowest energy ensembles generated which demonstrate excellent backbone and heavy atom RMSD in calculated ensembles (See Supplementary Figure 2.11 for backbone alignment).

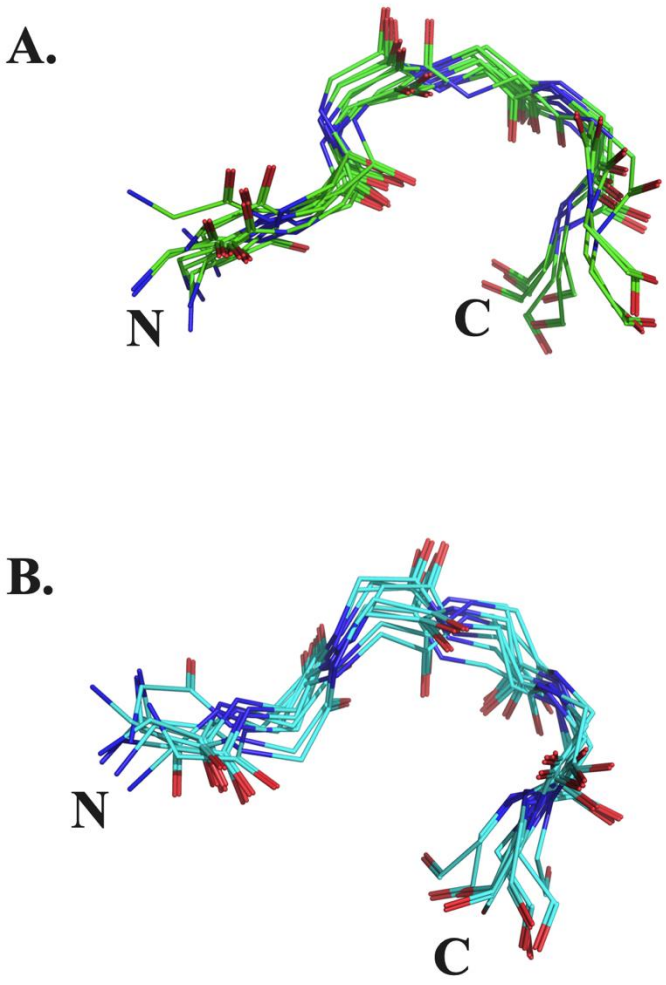

Supplementary Figure 2.11 Alignment of backbone atoms of "major" (A, green) and "minor" (B, cyan) conformations of AYPGKF-NH_2. The ten lowest energy structures are aligned for each conformation. Average backbone RMSD to mean of the "major" conformation (0.52Å) and "minor" conformation (0.66Å) as calculated in comparison to the mean structure. (See Supplementary Table 2.4 for additionally ensemble statistics)

Chapter 3

3 Role of the Helix-8 and C-terminal tail in regulating Proteinase Activated Receptor 2 (PAR2) signalling[v]

[v]A version of this chapter has been published: Thibeault, P. E., and Ramachandran, R. (2020) Role of the Helix-8 and C-Terminal Tail in Regulating Proteinase Activated Receptor 2 Signaling. *ACS Pharmacol. Transl. Sci.* 10.1021/acsptsci.0c00039

3.1 Introduction

G-protein-coupled receptors (GPCRs) are important cell surface receptors that regulate diverse physiological processes in response to a variety of extracellular stimuli (1). The proteinase activated receptors (PARs) are a four-member family of GPCRs that are activated by a wide range of proteolytic enzymes including coagulation cascade-, immune cell-, and pathogen-derived proteinases (2, 3). PAR activation occurs when proteolytic enzymes remove a portion of the receptor N-terminus to reveal a cryptic tethered-ligand which can bind intramolecularly to activate the receptor (3). Synthetic hexapeptide mimetics of the tethered ligand can also be used to selectively activate individual members of this family (4–7).

PAR2 is a trypsin-like serine proteinase-activated, member of this family and is well established as a major regulator of inflammatory responses (8, 9). PAR2-targeted compounds are highly sought after as novel anti-inflammatory agents. In recent studies, there is also an emerging realization that different proteolytic enzymes cleave and activate PAR2 in a manner that favours differential coupling to various intracellular effectors (10). This has given impetus to studies investigating molecular mechanisms underlying biased signalling through this receptor.

In keeping with observations in a variety of other GPCRs, PAR2 can signal through both G-protein coupling or via interactions with the multi-functional scaffold proteins, β-arrestin-1 and -2 (11). PAR2 activation by the enzymatically- (e.g. trypsin) revealed tethered-ligand or synthetic activating peptides (e.g. SLIGRL-NH_2) trigger robust $G\alpha_{q/11}$ coupling; and activation of $G\alpha_{12/13}$ by this receptor has also been reported (12). Some non-canonical enzymatic activators of PAR2 are also reported to cause receptor coupling to other G-proteins (13). Additionally, PAR2 is a strong recruiter of β-arrestin-1/-2 in response to both tethered-ligand and peptide activation (14, 15).

β-arrestin-1/-2 interaction with activated GPCRs has a role in desensitizing G-protein-mediated signalling events. Moreover, β-arrestins act as scaffolds for other intracellular signalling effectors that are activated by GPCRs including PAR2 (11, 16). β-arrestin

interaction with activated GPCRs is believed to occur in a two-step manner with the first contacts at GPCR kinase (GRKs) phosphorylated serine and threonine residues in the C-terminal tail of the receptors which is followed by additional stable interactions with the receptor transmembrane core (17–20).

Previous studies have examined the consequence of modifying the C-terminal tail of PAR2. Deletion of certain segments in the PAR2 C-tail (Ala^{355}-Ser^{363}) or truncation of the tail (His^{354}-Stop) resulted in a loss of agonist-mediated internalization and inositol 1,4,5-trisphosphate (IP_3) accumulation (21). In the same study, deletion of the PAR2 C-tail Ala^{355}-Ser^{363} segment did not affect p44/42 MAPK activation, while His^{354}-Stop mutation did have an effect on this signalling pathway (21). The truncation mutations described above encompass two key regulatory sites, clusters of serine/threonine residues that are sites of phosphorylation and a cysteine residue that is a site for palmitoylation. More recently mutational studies of PAR2 receptors with alanine substitutions to clusters of serine/threonine residues have been conducted in Rat1 fibroblasts and HeLa cells to establish that C-tail phosphorylation is important for receptor desensitization and trafficking (22).

The role of the C-terminal cysteine residue that is part of the truncations described above have also been probed and Cys^{361} was established as the primary site of palmitoylation in PAR2 (23, 24). In these studies, CHO cells expressing a Cys^{361} mutant showed decreased calcium signalling but enhanced p44/42 MAPK activation in response to both trypsin and the activating peptide SLIGRL-NH_2 (23). A reduction in agonist-induced β-arrestin recruitment, receptor endocytosis and degradation is also reported in these mutants (24).

Together, these studies have pointed to multiple mechanisms, that are dependent on the PAR2 C-tail, in regulating receptor-mediated signalling and desensitization. However, a clear understanding of C-terminal motifs as determinants of PAR2 signalling and desensitization has remained elusive. One of the challenges with synthesizing information from previous studies probing this question is that studies were conducted in a variety of different cell lines and in some cases have utilized cells that endogenously expressed low levels of wild-type (wt) PAR2. Here, we attempt to gain a more direct

comparison of the contribution of C-terminal tail sites in PAR2 signalling, following activation with both the trypsin revealed tethered ligand and a synthetic receptor activating peptide in a PAR2-deficient HEK-293 cell line generated by CRISPR/Cas9 targeting. We examined signalling responses in this cell line from reconstituted wt-PAR2 and four mutant PAR2 receptors with alanine substitutions of the C-terminal serine/threonine residues or the helix-8 cysteine residue. We find that several such modifications have a significant impact on β-arrestin recruitment to PAR2. Additionally, PAR2-mediated calcium signalling is desensitized less efficiently in cells that express mutants that are not able to recruit β-arrestin efficiently. In agreement with this finding, PAR2 desensitization is also delayed in β-arrestin-1/-2 knockout HEK-293 cell line. Interestingly we find that p44/42 MAPK activation by PAR2 is dependent on $G\alpha_{q/11}$-mediated signalling and was exaggerated in cells expressing mutated receptors that did not recruit β-arrestin-1/-2 comparably. These studies further clarify mechanisms underlying PAR2-dependent signalling via G-proteins and β-arrestins.

3.2 Methods

3.2.1 Chemicals and reagents

Porcine trypsin (catalogue no. T-7418; ∼14,900 units/mg) was purchased from Sigma-Aldrich (St. Louis, MI). A maximum specific activity of 20,000 units/mg was used to calculate the approximate molar concentration of porcine pancreatic trypsin in the incubation medium (1 unit/ml, ∼2 nM) as described previously (14). SLIGRL-NH_2 (> 95% purity by HPLC/MS) was purchased from Genscript (Piscataway, NJ) or EZBiolabs (Carmel, IN). Agonists were prepared in 4-(2-hydroxyethyl)-1-piperazineethanesulfonic acid (HEPES, 25 mM). All chemicals were purchased from Millipore-Sigma, Thermo Fisher Scientific (Hampton, NH), or BioShop Canada, Inc. (Burlington, Ontario, Canada), unless otherwise stated.

3.2.2 Molecular cloning and constructs

The plasmid encoding the human PAR2 receptor with an in frame enhanced yellow fluorescent protein fusion tag (PAR2-YFP) was constructed as previously described (25).

The use of an in-frame, PAR2 C-terminal fusion of enhanced yellow fluorescent protein has been utilized in several previous studies which demonstrated that PAR2-YFP couples to its known signalling pathways appropriately (26–28). Plasmid DNA mutations in the C-terminus of PAR2 were created using QuikChange XL Multi Site-Directed Mutagenesis kit (Agilent Technologies, Mississauga, ON, Canada) to generate all mutants described in this study. A summary figure of mutations made within each mutant construct (Figure 3.1B) and their position in the C-tail (Figure 3.1A) has been created for visualization purposes. All constructs were verified by sanger sequencing (London Regional Genomics Centre, University of Western Ontario).

3.2.3 Cell lines and culture conditions

All media and cell culture reagents were purchased from Thermo Fisher Scientific (Waltham, MA). Human embryonic kidney (HEK) cells (HEK-293; ATCC), PAR2-knockout HEK-293, and β-arrestin-1/-2-knockout HEK-293 (β-arrestin-knockout HEK-293) cell lines were maintained in Dulbecco's modified Eagle's medium supplemented with 10% fetal bovine serum, 1% sodium pyruvate, and penicillin streptomycin solution (50,000 units penicillin, 50,000 μg streptomycin) (29). Since trypsin activates the PARs, cells were routinely sub-cultured using enzyme-free isotonic phosphate-buffered saline (PBS) containing EDTA (1 mM). Cells were transfected with PAR2-YFP or mutated PAR2-YFP receptor vectors using calcium phosphate [Nuclease-free water, 2.5M $CaCl_2$, and 2x HEPES-buffered saline (HBS)] or Fugene6 transfection methods (Promega, Madison, WI). Transiently transfected cells were always assayed or imaged at 48 hours post-transfection (30).

3.2.4 Generation CRISPR/Cas9 PAR2-knockout HEK-293 cell line

HEK-293 cells endogenously express PAR2 (31). In order to study mutant receptors in a null-background, we generated PAR2-knockout HEK-293 cells using CRISPR/Cas9 targeting. The knockout design and procedures used to derive PAR2-knockout HEK-293 cells from the wild-type HEK-293 cells were as previously described (32, 33). A PAR2 specific guide (CCCCAGCAGCCACGCCGCGC) was cloned into the lentiCRISPR v2 plasmid (Addgene plasmid # 52961). 48 hours after transfection, cells were selected in

media containing puromycin (5 μg/mL). PAR2-deficient cells were identified by functional screening of responses to PAR2 specific agonists using a calcium signalling assay (Supplementary Figure 3.1).

3.2.5 Calcium signalling assay

Agonist-stimulated calcium signalling was recorded in PAR2-knockout HEK-293 cells as previously described (25, 29, 34). Cells were detached in enzyme-free cell dissociation buffer, centrifuged to pellet (1000 rpm, 5 minutes), and resuspended in Fluo-4 NW (no wash) calcium indicator dye (Thermo Fisher Scientific). Following a 30-minute incubation at ambient temperature, intracellular fluorescence (excitation 480 nm; emission recorded at 530 nm) was monitored before and after addition of agonists (trypsin or SLIGRL-NH_2) on a PTI spectrophotometer (Photon Technology International, Birmingham, NJ). Responses were normalized to the fluorescence obtained with calcium ionophore (A23187, 3 μM; Sigma-Aldrich).

3.2.6 Bioluminescence resonance energy transfer (BRET) detection of β-arrestin-1/-2 recruitment

Bioluminescence resonance energy transfer (BRET) based detection of β-arrestin-1/-2 interaction with PAR2-YFP and mutant PAR2-YFP constructs was monitored in HEK-293 cells as described (14, 25). PAR2-YFP or mutant PAR2-YFP constructs (2 μg) and Renilla luciferase-tagged β-arrestin-1 or -2 (β-arr-1 and -2-rluc; 0.2 μg) were transiently transfected for 48 hours. Cells were plated in white 96-well culture plates (Corning; Oneonta, NY) and interactions between receptor and β-arrestin-1/-2 were detected by measuring BRET following 20 minutes of agonist stimulation and the addition of 5 μM h-coelenterazine prior to BRET recording (NanoLight Technology, Pinetop, AZ) on a Mithras LB940 plate reader (Berthold Technologies, Bad Wildbad, Germany) (29).

3.2.7 Mitogen-activated protein kinase (MAPK) Western blot assay

Agonist-stimulated mitogen-activated protein kinase (MAPK) signalling in PAR2-knockout HEK-293 cells expressing PAR2-YFP or mutant PAR2-YFP was monitored by Western blot analysis as previously described (25, 29, 34). Cells expressing PAR2

receptor constructs were serum starved (2 hours) and stimulated with sub-maximal concentrations of SLIGRL-NH_2 (3 μM) or trypsin (0.3 nM) for 10 minutes at 37℃. Protein lysates were separated on 4-12% Bis-Tris gels (Invitrogen, Thermo Fisher Scientific). Phosphorylated p44/42 (p-p44/42; activated ERK) and total p44/42 (p44/42; total ERK) proteins were detected with antibodies (9101S and 9102S antibody clones, respectively, Cell Signalling Technology, Danvers, MA; 1:1000 concentration) and imaged by use of HRP-conjugated secondary antibodies (anti-rabbit IgG HRP-linked 7074S clone; Cell Signalling Technology, Danvers, MA; 1:10,000 concentration). Chemiluminescence was recorded on an iBright CL1000 gel doc (Invitrogen, Thermo Fisher Scientific) following application of ECL Prime detection reagent (GE Healthcare). Band intensities representing activated and inactive MAPK ERK proteins were quantified using the FIJI is just ImageJ (FIJI) quantification software (35). Phospho-kinase levels were normalized by expressing the data as a percentage of the corresponding total-kinase signal. Fold increase above baseline was calculated by normalizing data to baseline p44/42 phosphorylation in unstimulated samples.

3.2.8 Assessing the contribution of $G\alpha_{q/11}$ and β-arrestin-1/-2 in MAPK activation downstream of PAR2 activation

To examine the contribution of $G\alpha_{q/11}$ signalling on PAR2-dependent MAPK activation, HEK-293, endogenously expressing PAR2 were pretreated with either vehicle control (DMSO, 0.01%) or YM254890 (100 nM) for 20 minutes prior to agonist stimulation with SLIGRL-NH_2 (30 μM) (36). To assess the contribution of β-arrestin-1/-2 signalling in PAR2-dependent MAPK activation, HEK-293 and β-arrestin-knockout HEK-293 cells endogenously expressing PAR2 were assayed for p44/42 phosphorylation following stimulation with SLIGRL-NH_2 (30 μM) (29).

3.2.9 Confocal Microscopy

HEK-293 cells transiently transfected with PAR2-YFP or mutant PAR2-YFP (Fugene 6, Promega) were sub-cultured onto 35-mm glass-bottom culture dishes (MatTek Corporation, Ashland, MA) to be analyzed by confocal microscopy. Cells were fixed with 4% w/v paraformaldehyde solution, stained with 4′,6-diamidino-2-phenylindole

(DAPI), to identify the nucleus, and receptor localization to the plasma membrane was assessed by imaging eYFP expression with an Olympus FV1000 (Centre Valley, PA) or Leica SP8 confocal microscope system (Buffalo Grove, IL) (Supplementary Figure 3.2).

3.2.10 Statistical analysis

Statistical analysis of data, curve fitting (three-parameter nonlinear regression), and area under the curve analyses were done with Prism 7 software (GraphPad Software, La Jolla, CA). Statistical significance of EC_{50} shifts and concentration-effect curve top (indicated as "Max.") were calculated using the extra sum of squares analysis and indicated in table 1 (*$p < 0.05$; Table 1) (29, 37). Statistical significance for western blots was assessed using two-way analysis of variance (*$p < 0.05$). Data are expressed as mean ± S.E. throughout the text, table, and figure legends. Where appropriate p-values are reported in the text and determined by the statistical methods described.

3.3 Results

The C-terminal tail of G-protein-coupled receptors contain important regulatory sites that enable interaction with intracellular signalling effectors. Here we examine the relative contribution of the C-tail serine/threonine phosphorylation sites ($Ser^{383\text{-}385}$, Ser^{387}-Thr^{392}) and the helix-8 palmitoylation site (C^{361}) in signalling regulation downstream of the proteolytically-activated GPCR, PAR2 (Figure 3.1).

A.

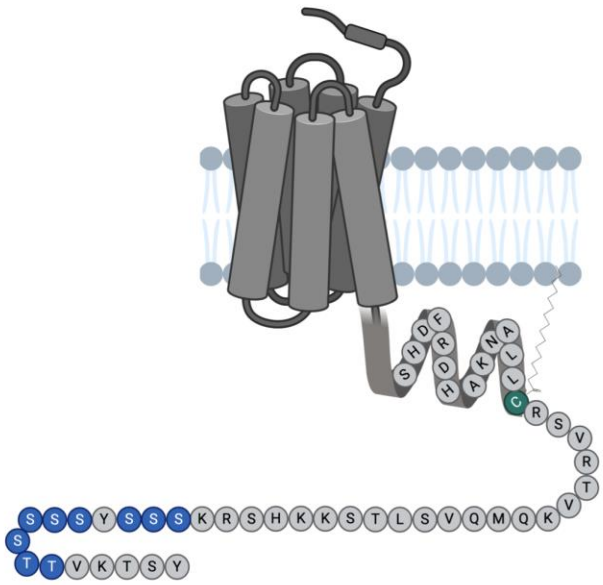

B.

PAR2	SHDFRDHAKNALLCRSVRTVKQMQVSLTSKKHSRKSSSYSSSSTTVKTSY
PAR2^{C361A}	SHDFRDHAKNALL**A**RSVRTVKQMQVSLTSKKHSRKSSSYSSSSTTVKTSY
PAR2$^{S383-385A}$	SHDFRDHAKNALLCRSVRTVKQMQVSLTSKKHSRK**AAA**YSSSSTTVKTSY
PAR2$^{S387-392A}$	SHDFRDHAKNALLCRSVRTVKQMQVSLTSKKHSRKSSSY**AAAAAA**VKTSY
PAR2$^{S383-385A,S387-T392A}$	SHDFRDHAKNALLCRSVRTVKQMQVSLTSKKHSRK**AAA**Y**AAAAAA**VKTSY

Figure 3.1 Summary of PAR2 C-tail residue mutations (A) Cartoon depicting the PAR2 Helix-8 and C-tail with palmitoylation site (green) and phosphorylation sites studied (blue) shown (made in BioRender - biorender.com). (B) Mutant receptor clones generated using Agilent QuikChange XL site-directed mutagenesis. Sequences of the wild-type PAR2 and mutant PAR2 receptor C-tail constructs (underlined) generated by site-directed mutagenesis.

3.3.1 SLIGRL-NH_2-stimulated β-arrestin recruitment to PAR2 C-tail mutants.

To investigate the role of C-tail mutations (Figure 3.1) on the recruitment of β-arrestins, we employed bioluminescence resonance energy transfer (BRET) using C-terminal enhanced yellow fluorescent protein (YFP) tagged receptor constructs as our photon acceptor and Renilla luciferase (rluc) tagged β-arresin-1-rluc or β-arresin-2-rluc as the photon donor. As expected, in the PAR2-YFP expressing cells, SLIGRL-NH_2 stimulated receptor recruitment of β-arrestin-1 and -2 in a concentration-dependent manner. The potency (EC_{50}) of SLIGRL-NH_2-stimulated β-arrestin recruitment to PAR2-YFP was observed to be consistent between β-arrestin-1 and β-arrestin-2 (EC_{50} 12.1 ± 1.6 μM and 11.1 ± 1.2 μM, respectively) (Figure 3.2). Next, to determine the impact of mutations in the PAR2 C-tail helix-8 palmitoylation site, we assessed recruitment of β-arrestins to PAR2 with a Cys^{361}Ala mutation ($PAR2^{C361A}$-YFP). We observed that SLIGRL-NH_2-stimulated recruitment of both β-arrestin-1 and -2 recruitment by $PAR2^{C361A}$-YFP was significantly decreased compared to PAR2-YFP with a pronounced rightward shift in the concentration effect curve (EC_{50} = 28.8 ± 4.0 μM and 27.4 ± 2.5 μM, respectively). Additionally, we observed a significant decrease in maximal net BRET (Max.; top of the curve utilized for nonlinear regression curve fitting) in $PAR2^{C361A}$-YFP (β-arrestin-1 Max. = 0.28 ± 0.01; β-arrestin-2 Max. = 0.32 ± 0.01) compared to PAR2-YFP (β-arrestin-1 Max. = 0.39 ± 0.01; β-arrestin-2 Max. = 0.53 ± 0.01) (Figure 3.2; Table 3.1). Thus, loss of the palmitoylation site in the PAR2 C-tail helix-8 is deleterious for SLIGRL-NH_2-stimulated β-arrestin recruitment.

Next, we evaluated mutations to serine and threonine residues which are sites of GRK-mediated phosphorylation in the PAR2 C-tail. Mutation of the membrane proximal $Ser^{383-385}$ to alanine ($PAR2^{S383-385A}$-YFP) did not significantly affect recruitment of β-arrestin-1 or -2 (EC_{50} = 12.5 ± 2.8 μM and 15.1 ± 2.7 μM, respectively) (Figure 3.2; Table 3.1). Mutation of Ser^{387}-Thr^{392} to alanine ($PAR2^{S387-T392A}$-YFP) however, significantly reduced both EC_{50} and maximal net BRET for both β-arrestin-1 (EC_{50} = 52.4 ± 12.1 μM; Max. = 0.27 ± 0.02) and β-arrestin-2 (EC_{50} = 41.7 ± 6.3 μM; Max. = 0.40 ± 0.02) compared to the wild-type receptor. Interestingly, combined mutation of both $Ser^{383-385}$ and Ser^{387}-

Thr^{392} to alanine ($PAR2^{S383\text{-}385A,\ S387\text{-}T392A}$-YFP) resulted in a further apparent decrease in β-arrestin-2 ($p < 0.05$) recruitment compared to the Ser^{387}-Thr^{392} to Ala-alone substituted mutant. When compared to PAR2-YFP, maximal recruitment of both β-arrestin-1 (EC_{50} = 56.2 ± 18.0 μM; Max. = 0.16 ± 0.01) and β-arrestin-2 (EC_{50} = 29.9 ± 8.6; Max. = 0.23 ± 0.02) was significantly decreased in the $PAR2^{S383\text{-}385A,\ S387\text{-}T392A}$-YFP mutant (Figure 3.2; Table 3.1).

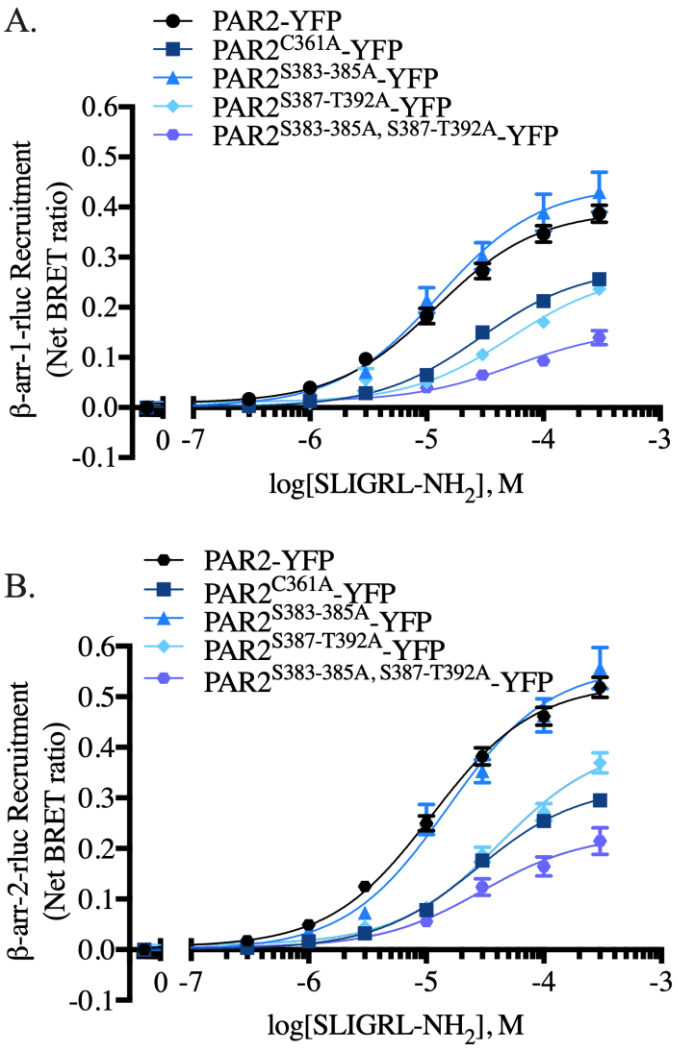

Figure 3.2 β-arrestin-1/-2 recruitment in PAR2 cysteine and phosphorylation mutants in response to SLIGRL-NH_2 stimulation. β-arrestin recruitment concentration-effect curves for HEK-293 cells transiently expressing PAR2 or C-tail mutant PAR2 constructs ($PAR2^{C361A}$-YFP, square; $PAR2^{S383\text{-}385A}$-YFP, triangle; $PAR2^{S387\text{-}T392A}$-YFP, diamond; $PAR2^{S383\text{-}385A,\ S387\text{-}T392A}$-YFP, hexagon) with β-arrestin-1-rluc (A) or -2-rluc (B) were stimulated with PAR2 peptide agonist, SLIGRL-NH_2. Nonlinear regression curve fits are shown (mean ± S.E.) for three to four independent experiments with triplicate data points for each concentration and receptor collected within each experiment. We find that Cys^{361}Ala mutation significantly increased the concentration of SLIGRL-NH_2 required to achieve half-maximal β-arrestin recruitment

while concurrently demonstrating decreased maximal recruitment. Interestingly, $Ser^{383-385}$Ala mutation did not significantly alter β-arrestin recruitment. Recruitment of β-arrestins was significantly decreased to both PAR2 Ser^{387}-Thr^{392}Ala and PAR2 $Ser^{383-385}$Ala/Ser^{387}-Thr^{392}Ala receptors. *(n = 3-4)*

3.3.2 Trypsin-stimulated β-arrestin recruitment to PAR2 C-tail mutants.

To investigate the effect of C-tail mutations on the recruitment of β-arrestins in response to tethered-ligand activation of PAR2, we employed BRET assays with PAR2 and PAR2 C-tail mutants, stimulating with increasing concentrations of trypsin. In PAR2-YFP expressing cells trypsin-stimulated a concentration-dependent recruitment of β-arrestin-1 (EC_{50} = 9.4 ± 1.6 nM; Max. = 0.17 ± 0.01) and -2 (EC_{50} = 6.1 ± 1.2 nM; Max. = 0.14 ± 0.01) (Figure 3.3). Trypsin treatment of $PAR2^{C361A}$ expressing cells also triggered β-arrestin recruitment with comparable EC_{50} (EC_{50} = 5.7 ± 1.1 nM; Max. = 0.12 ± 0.01) and -2 (EC_{50} = 4.9 ± 0.7 nM; Max. = 0.12 ± 0.00) in this mutant. However, we observed that the maximal recruitment of β-arrestin-1, but not β-arrestin-2, to $PAR2^{C361A}$-YFP was significantly decreased in response to trypsin activation of this mutant (Figure 3.3A).

We then turned our investigation to the effect of mutations in C-tail phosphorylation sites and their impact on trypsin-mediated β-arrestin recruitment. The potency of trypsin-stimulated β-arrestin recruitment was equivalent between PAR2-YFP and all PAR2 C-tail phosphorylation mutant receptors tested here (Table 3.1). Interestingly, we did observe that while maximal β-arrestin-2 recruitment was also equivalent with each mutant when compared to the wild-type receptor, the maximal recruitment of β-arrestin-1 to all of the C-tail mutants was decreased compared to the wild-type receptor (Figure 3.3; Table 3.1) pointing to a possible difference in mechanisms underlying different β-arrestin isoform recruitment to peptide- or trypsin-stimulated PAR2.

In summary, mutations of the C-terminal Cys^{361} residue resulted in a decrease in β-arrestin recruitment to PAR2. Mutations to clusters of serine and threonine residues show a clear role for the Ser^{387}-Thr^{392} cluster, but not for the $Ser^{383-385}$ cluster in recruiting β-arrestin to the agonist-peptide-activated receptor. However, none of the phosphorylation site mutations appear to have a role in β-arrestin-2 recruitment following trypsin activation. (Figure 3.3; Table 3.1)

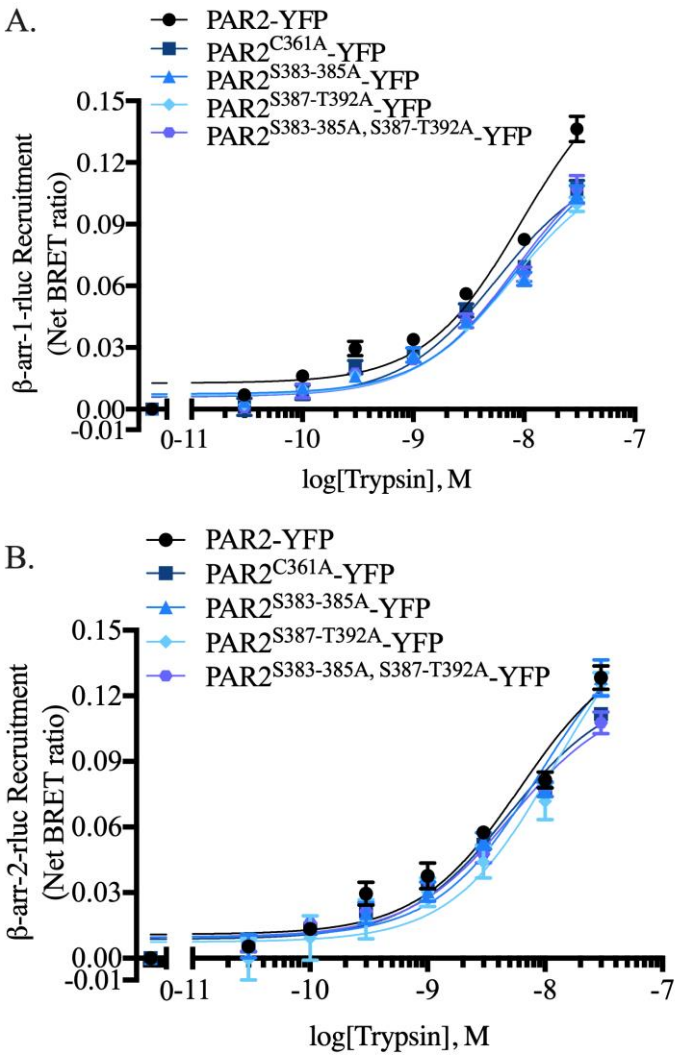

Figure 3.3 β-arrestin-1/-2 recruitment in PAR2 cysteine and phosphorylation mutants in response to tethered ligand agonism by trypsin stimulation. β-arrestin recruitment concentration-effect curves for HEK-293 cells transiently expressing PAR2 or C-tail mutant PAR2 constructs ($PAR2^{C361A}$-YFP, square; $PAR2^{S383-385A}$-YFP, triangle; $PAR2^{S387-T392A}$-YFP, diamond; $PAR2^{S383-385A, S387-T392A}$-YFP, hexagon) with β-arrestin-1-rluc (A) or -2-rluc (B) stimulated with trypsin. Nonlinear regression curve fits are shown (mean ± S.E.) for three to four independent experiments with triplicate data points for each concentration and receptor collected within each experiment. We find that no mutations resulted in significant shifts to EC_{50} of trypsin-stimulated β-arrestin-1 or -2

recruitment; however, significant decreases in maximal β-arrestin-1-rluc recruitment were observed with all mutants. *(n = 3-4)*

3.3.3 β-arrestin recruitment to PAR2 in the absence of $G\alpha_{q/11}$ signalling.

To determine whether $G\alpha_{q/11}$ activation is necessary to stimulate recruitment of β-arrestins to PAR2, we monitored β-arrestin recruitment following inhibition of $G\alpha_{q/11}$ with the specific inhibitor YM254890 (Wako Chemicals). We observed a significant decrease in the maximal β-arrestin recruitment in cells pretreated with $G\alpha_{q/11}$ inhibitor (YM254890, 100 nM) compared to vehicle treated control (0.1% DMSO) following activation of PAR2 with SLIGRL-NH_2 (Figure 3.4A, B, & E). No significant changes in EC_{50} was noted (Figure 3.4E). SLIGRL-NH_2-stimulated β-arrestin-1 recruitment was determined to have an EC_{50} of 15.7 ± 3.6 μM in vehicle-treated controls and 20.9 ± 2.4 μM in YM254890 treated cells. β-arrestin-2 recruitment was determined to have an EC_{50} of 19.0 ± 2.8 μM in cells pre-incubated with vehicle control and 26.5 ± 3.2 μM in cells pretreated with YM254890.

In the case of trypsin activation of PAR2, no differences were observed in β-arrestin-1 or -2 recruitment (Figure 3.4C & D). We determined EC_{50} of trypsin-stimulated β-arrestin-1 recruitment to be 8.7 ± 2.3 nM in cells pretreated with vehicle control compared with 10.4 ± 1.9 nM in cells pretreated with YM254890. Trypsin-stimulated recruitment of β-arrestin-2 was determined to be 14.9 ± 4.4 nM in control cells compared to 16.1 ± 5.1 nM in inhibitor-treated cells (Figure 3.4E). Overall, these data indicate that β-arrestin recruitment to PAR2 can occur independently of $G\alpha_{q/11}$ activation, with β-arrestin recruitment showing modest to no differences when this pathway is blocked.

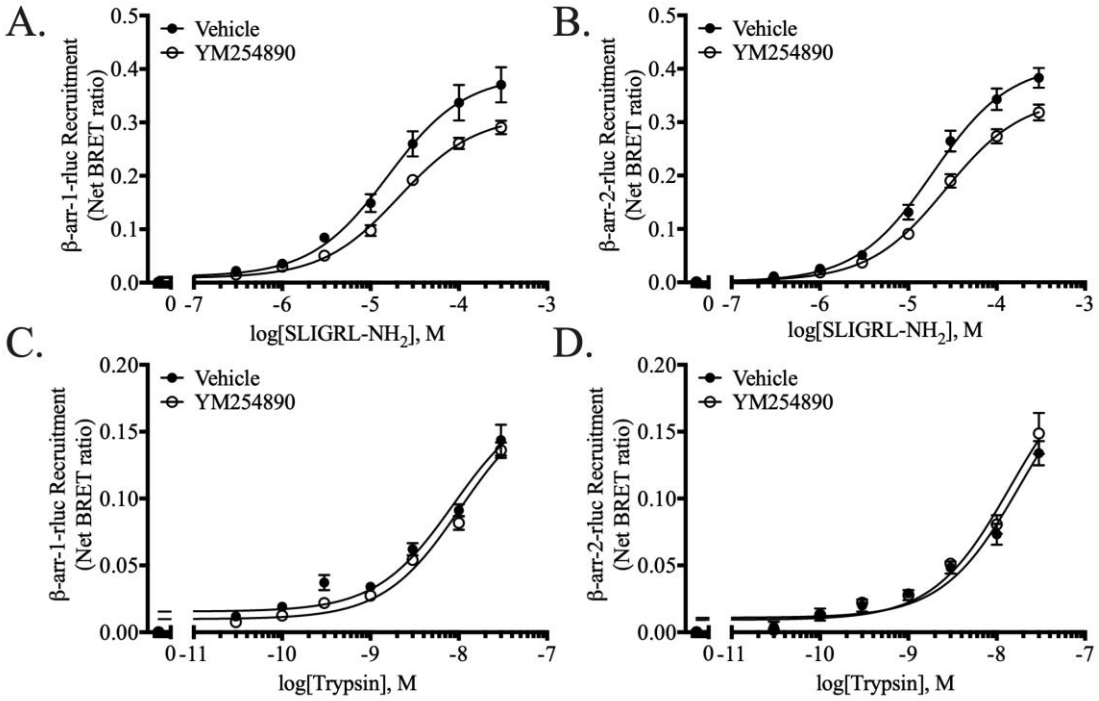

E.

	β-arrestin-1 Recruitment		β-arrestin-2 Recruitment	
SLIGRL-NH_2	***EC_{50} (μM)***	***Max. (net BRET)***	***EC_{50} (μM)***	***Max. (net BRET)***
Vehicle	15.7 ± 3.6	0.38 ± 0.02	19.0 ± 2.8	0.41 ± 0.01
YM254890	20.9 ± 2.4	0.31 ± 0.01*	26.5 ± 3.2	0.35 ± 0.01*
Trypsin	***EC_{50} (nM)***	***Max. (net BRET)***	***EC_{50} (nM)***	***Max. (net BRET)***
Vehicle	8.7 ± 2.3	0.18 ± 0.01	14.9 ± 4.4	0.19 ± 0.02
YM254890	10.4 ± 1.9	0.18 ± 0.01	16.1 ± 5.1	0.22 ± 0.03

Figure 3.4 PAR2 agonist-dependent β-arrestin recruitment occurs independent of $G\alpha_{q/11}$ activation. HEK-293 cells transiently expressing PAR2-YFP and either β-arrestin-1-rluc or -2-rluc were stimulated with increasing concentrations of either SLIGRL-NH_2 [β-arr-1- (A), β-arr-2-rluc (B)] or trypsin (β-arr-1- (C), β-arr-2-rluc (D)) following preincubation with either vehicle control (DMSO, 0.01%; solid circles) or $G\alpha_{q/11}$ selective inhibitor, YM254890 (100 nM; open circles). There were no significant shifts in EC_{50} between vehicle- or YM254890-treated following stimulation with either SLIGRL-NH_2 or trypsin. Maximal recruitment of β-arrestin (Max.) was significantly decreased in response to SLIGRL-NH_2, but not trypsin stimulation. Nonlinear regression curve fits are shown for data collected in triplicates for each of at least three independent experiments (mean ± S.E.) for three to five independent experiments with triplicate data

points collected in each experiment. A summary table of EC_{50} and maximal net BRET values obtained are shown with S.E. (E). Significance indicated by '*' $p < 0.05$ by extra sum of squares analysis compared to wild-type values. (*n = 3-5*)

3.3.4 PAR2-mediated calcium signalling in β-arrestin-1/-2-knockout HEK-293

In order to probe an effect of β-arrestins on $G\alpha_{q/11}$-mediated calcium signalling, we compared SLIGRL-NH_2- and trypsin-stimulated PAR2 signalling in HEK-293 cells and CRISPR/Cas9 β-arrestin-knockout HEK-293 cells endogenously expressing PAR2. We observed a significant increase in SLIGRL-NH_2-stimulated calcium signalling in β-arrestin-knockout HEK-293 cells (Figure 3.5B) compared to HEK-293 cells (Figure 3.5A) (EC_{50} = 14.1 ± 3.3 μM and EC_{50} = 55.0 ± 13.8 μM, respectively; $p < 0.05$). In addition to an evident leftward shift in the concentration effect curve for calcium signalling (Figure 3.5D), we analyzed the area under the curve for the response over 80 seconds post-agonist addition to determine if there was a prolongation in the calcium signal in the absence of β-arrestin desensitization of PAR2. Area under the curve analysis revealed a concomitant prolongation of calcium signalling duration in β-arrestin-knockout HEK-293 cells (Max. = 4718 ± 4, arbitrary units) compared to HEK-293 cells (Max. = 2870 ± 7, arbitrary units) (Figure 3.5C). A similar trend was observed in response to PAR2 activation with trypsin with the area under the curve increased in β-arrestin-knockout HEK-293 cells (Max. = 4677 ± 2) compared to wild-type HEK-293 cells (Max. = 2287 ± 3, arbitrary units) (Figure 3.5G). Unlike signalling stimulated by SLIGRL-NH_2, potency of trypsin-stimulated calcium signalling (as a % of response from 3 μM A23187) was not significantly different from response in HEK-293 cells (Figure 3.5H) (β-arrestin-knockout HEK-293 EC_{50} = 4.7 ± 0.5 nM; HEK-293 EC_{50} = 6.6 ± 1.4 nM; Figure 3.5F & 3.5E, respectively; $p = 0.12$). Although no shift in potency was observed, it is notable that there was a statistically significant increase in the maximal calcium signal achieved with trypsin in β-arrestin-knockout HEK-293 compared to wild-type HEK-293 (β-arrestin-knockout HEK-293 Max. = 84.1 ± 1.7 % of A23187; HEK-293 Max. = 67.8 ± 2.9 % of A23187; $p < 0.05$, Figure 3.5G). Thus, in response to either peptide or tethered ligand activation of PAR2, calcium signalling is prolonged and receptor desensitization is impaired in the absence of β-arrestins.

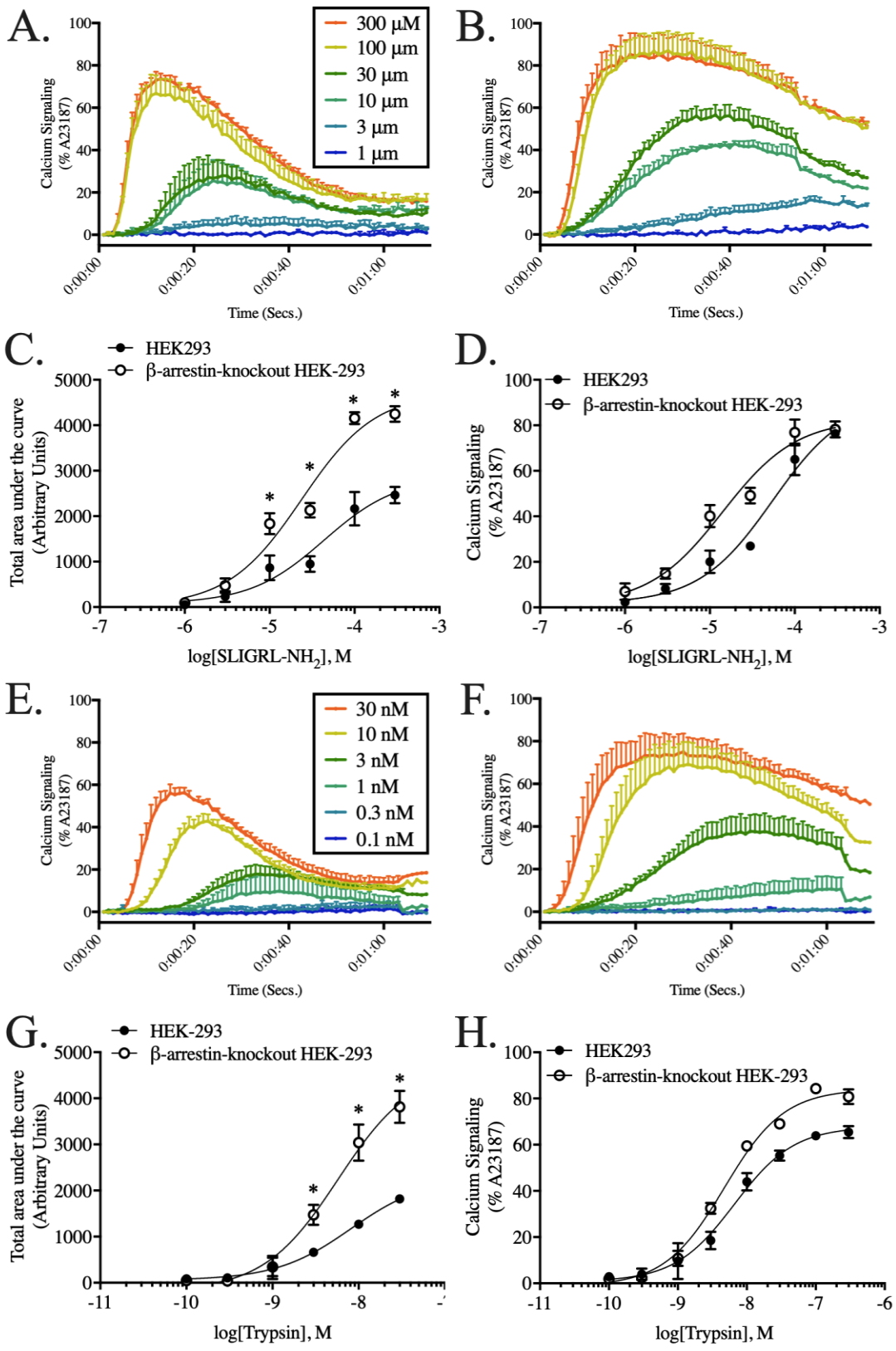
A.
300 µM
100 µm
30 µm
10 µm
3 µm
1 µm
Calcium Signaling (% A23187)
Time (Secs.)
B.
C.
HEK293
β-arrestin-knockout HEK-293
Total area under the curve (Arbitrary Units)
log[SLIGRL-NH2], M
D.
E.
30 nM
10 nM
3 nM
1 nM
0.3 nM
0.1 nM
F.
G.
HEK-293
β-arrestin-knockout HEK-293
log[Trypsin], M
H.

Figure 3.5 PAR2 agonist-dependent $G\alpha_{q/11}$-mediated calcium signalling is prolonged and sensitized in β-arrestin-knockout HEK-293 cells compared to wild-type HEK-293 cells. SLIGRL-NH_2-stimulated calcium signalling traces in HEK-293 (A) and β-arrestin-knockout HEK-293 (B) show prolonged signalling in β-arrestin-knockout HEK-293 cells. Both area under the curve analysis (C) and peak response concentration-effect curve (D) of SLIGRL-NH_2-stimulated calcium signalling reveal that signalling is prolonged and sensitized (SLIGRL-NH_2 EC_{50} - HEK-293 55.0 ± 13.8, β-arrestin-knockout HEK-293 14.1 ± 3.3 μM, $p < 0.05$) in β-arrestin-knockout HEK-293 cells compared to wild-type HEK-293 cells. Trypsin-stimulated calcium signalling traces in HEK-293 (E) and β-arrestin-knockout HEK-293 (F) show prolonged signalling in β-arrestin-knockout HEK-293 cells. Both area under the curve analysis (G) and peak response recorded concentration-effect curve (H) of trypsin-stimulated calcium signalling reveal that signalling is prolonged and sensitized in β-arrestin-knockout HEK-293 cells compared to wild-type HEK-293 cells. Calcium signalling is shown as a function of time, area under the curve, and maximal calcium signalling at given concentrations for three independent experiments. Statistical significance of maximal signal achieved at a given concentration is indicated by '*' ($p < 0.05$). (*n = 3*)

3.3.5 SLIGRL-NH_2-stimulated calcium signalling in PAR2 C-tail mutants.

To determine the importance of PAR2 C-tail palmitoylation and phosphorylation sites in calcium signal regulation, PAR2 C-tail mutants were expressed in PAR2-knockout HEK-293 cells (38) and calcium signalling was recorded in response to increasing concentrations of SLIGRL-NH_2. No response to SLIGRL-NH_2 was evident in non-transfected cells (Supplementary Figure 3.1) but reconstituting wild-type PAR2-YFP resulted in a concentration-dependent response to SLIGRL-NH_2 (0.3-300 µM) (EC_{50} = 1.1 ± 0.1 µM and Max. = 1433 ± 21) (Figure 3.6A & F). Interestingly, a significant decrease in potency of SLIGRL-NH_2-stimulated signalling was seen (rightward of shift in concentration effect curve; $p < 0.05$) in $PAR2^{C361A}$-YFP expressing cells (EC_{50} = 7.1 ± 0.9 µM) accompanied by a significant increase in maximal calcium response (Max. = 1711 ± 37, $p < 0.05$) (Figure 3.6B & F).

The potency of SLIGRL-NH_2-stimulated calcium signalling in the C-tail phosphorylation site mutant, $PAR2^{S383\text{-}385A}$-YFP, was no different than the wild-type receptor expressing cells (EC_{50} = 0.8 ± 0.1 µM), however, we observed a significant decrease in the maximal calcium signalling (Max. = 1165 ± 28, $p < 0.05$) compared to PAR2-YFP (Figure 3.6C & F). The other phosphorylation site mutant $PAR2^{S387\text{-}T392A}$-YFP, showed a significant increase in calcium signalling (EC_{50} = 0.3 ± 0.1 µM, $p < 0.05$) accompanied by decreased maximal calcium signal compared to the wild-type receptor (Max. = 1242 ± 23, $p < 0.05$) (Figure 3.6D & F). Combination of both $Ser^{383\text{-}385}$Ala and $Ser^{387\text{-}T392}$Ala mutations ($PAR2^{S383\text{-}385A,\ S387\text{-}T392A}$-YFP) resulted in a statistically significant increase in SLIGRL-NH_2-stimulated calcium signalling compared to wild-type receptor expressing cells (EC_{50} = 0.2 ± 0.1 µM, $p < 0.05$). This combined mutation, however, also resulted in a dramatic decrease in the total maximal signal elicited (Max. = 652 ± 44, $p < 0.05$) (Figure 3.6E & F).

Overall, these data indicate that loss of phosphorylatable residues ($PAR2^{S387\text{-}T392A}$-YFP and $PAR2^{S383\text{-}385A,\ S387\text{-}T392}$-YFP) sensitizes the calcium signal response to SLIGRL-NH_2, however, these serine/threonine residues also appear to be important for calcium signalling since a decrease in the maximal calcium response following PAR2 activation is

evident. Conversely, the loss of the helix-8 cysteine residue resulted in a rightward shift in the concentration effect curve accompanied by an increase in the maximal calcium signalling response.

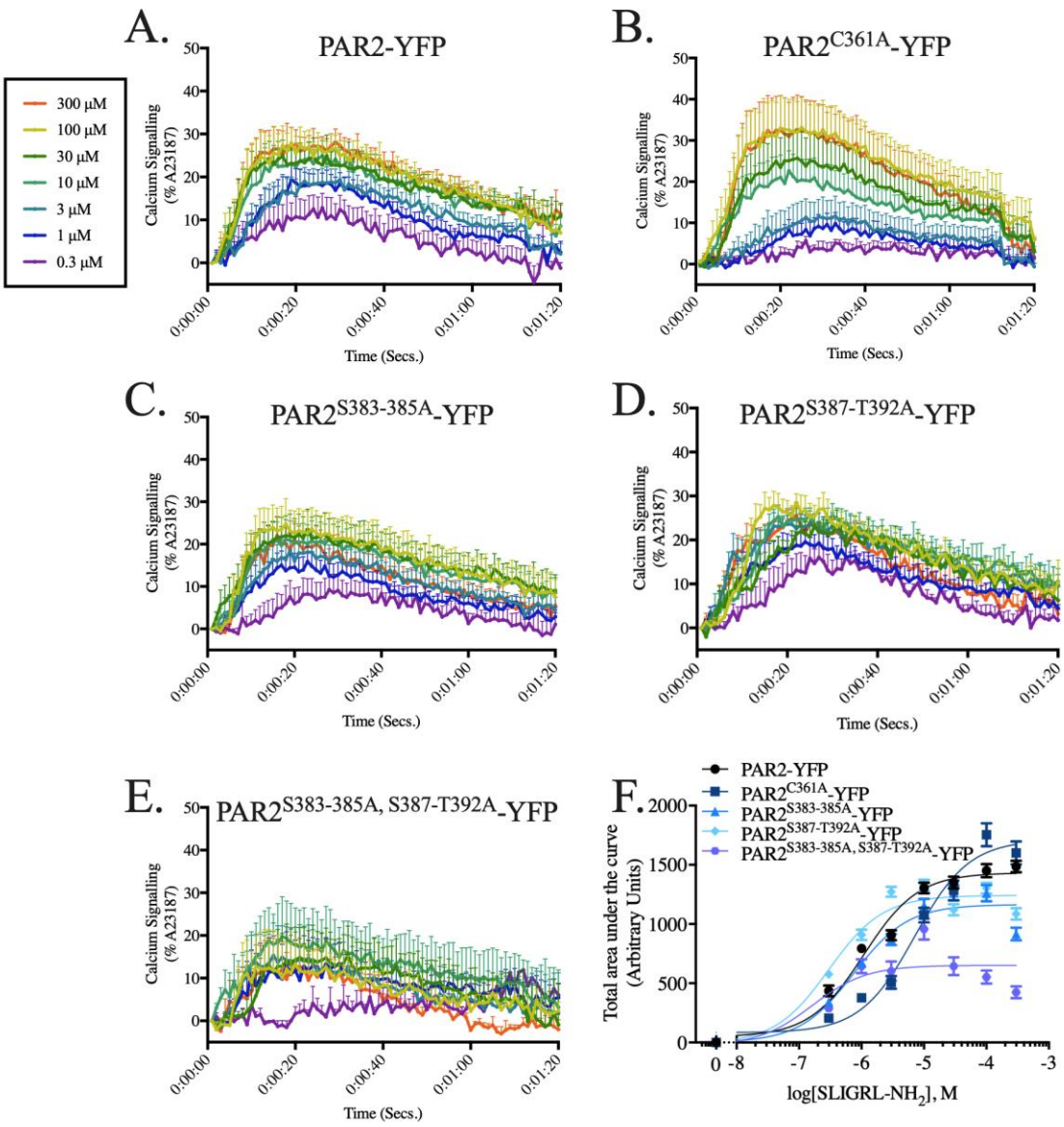

Figure 3.6 Differential calcium signalling in PAR2 mutant receptors compared to PAR2-YFP in response to stimulation with SLIGRL-NH_2. Representative kinetic traces are shown for SLIGRL-NH_2-stimulated intracellular calcium signalling (mean ± S.E.) for four to six independent experiments with PAR2-YFP (A), $PAR2^{C361A}$-YFP (B), $PAR2^{S383\text{-}385A}$-YFP (C), $PAR2^{S387\text{-}T392A}$-YFP (D), and $PAR2^{S383\text{-}385A,\ S387\text{-}T392A}$-YFP (E) receptors. Analysis of $PAR2^{C361A}$-YFP mutant reveals significant dysregulation of calcium signalling compared to wild-type PAR2-YFP signalling. Serine mutations (Ser^{387}-Thr^{392}Ala and $Ser^{383\text{-}385}$Ala/Ser^{387}-Thr^{392}Ala) enhanced potency of SLIGRL-NH_2 compared to PAR2-YFP (EC_{50}, $p < 0.05$ compared to wild-type PAR2-YFP).

Interestingly, all serine/threonine mutants exhibited decreased maximal signalling elicited by SLIGRL-NH_2 stimulation, with the most substantial decrease observed with the combined Ser./Thr. mutant ($Ser^{383-385}$Ala/Ser^{387}-Thr^{392}Ala). Nonlinear regression curve fit of area under the curve shown for area under the curve (calculated with Prism 7) (F). (*n = 4-6*)

3.3.6 Trypsin-stimulated calcium signalling in PAR2 C-tail mutants

To investigate the importance of PAR2 C-tail palmitoylation site and phosphorylation sites in calcium signalling responses to receptor activation with the PAR2 tethered ligand, we monitored calcium signalling following activation with trypsin. Trypsin (0.03-30 nM) elicited a concentration dependent calcium signalling response in PAR2-YFP expressing cells and (EC_{50} of 0.6 ± 0.2 nM and Max. 1729 ± 125) (Figure 3.7A & F). As with SLIGRL-NH_2 activation, mutation of Cys^{361} to alanine resulted in a rightward shift in the concentration effect curve for the calcium signalling response (EC_{50} = 2.3 ± 0.9 nM, $p < 0.05$), with equivalent maximum total area under the curve compared to PAR2-YFP (Max. = 2081 ± 193, p = 0.12) (Figure 3.7B & F).

To investigate the effect of phosphorylation site mutations on calcium signalling in response to trypsin revealed tethered-ligand activation of the receptor, we compared wild-type receptor and our three phosphorylation mutant receptors. In response to trypsin stimulation, we observe that $PAR^{S383\text{-}385A}$-YFP signals similarly to PAR2-YFP with equivalence in both potency (EC_{50} = 2.6 ± 0.1 nM, p = 0.28) and maximum total area (Max. = 1442 ± 112, p = 0.10) (Figure 3.7C & F). Both $PAR2^{S387\text{-}T392A}$-YFP (Figure 3.7D) and combination mutant, $PAR2^{S383\text{-}385A,\ S387\text{-}T392A}$-YFP (Figure 3.7E), elicited calcium signalling comparably to PAR2-YFP in response to trypsin (EC_{50} = 0.2 ± 0.1 nM, p = 0.07; EC_{50} = 0.2 ± 0.1 nM, p = 0.08, respectively) but showed a significant decreased in the maximal total area under the curve relative to PAR2-YFP (Max. = 1241 ± 67 and Max. = 1236 ± 57, respectively; $p < 0.05$) (Figure 3.7F).

These data mirror those recorded for peptide-stimulated calcium signalling through PAR2, with the maximal calcium signal achieved with the phosphorylation mutants decreased compared to wild-type PAR2-YFP. Loss of the helix-8 cysteine palmitoylation site similarly resulted in less potent activation of the $G\alpha_{q/11}$ pathway but a more prolonged signalling response also suggested less efficient desensitization of calcium signalling in this mutant.

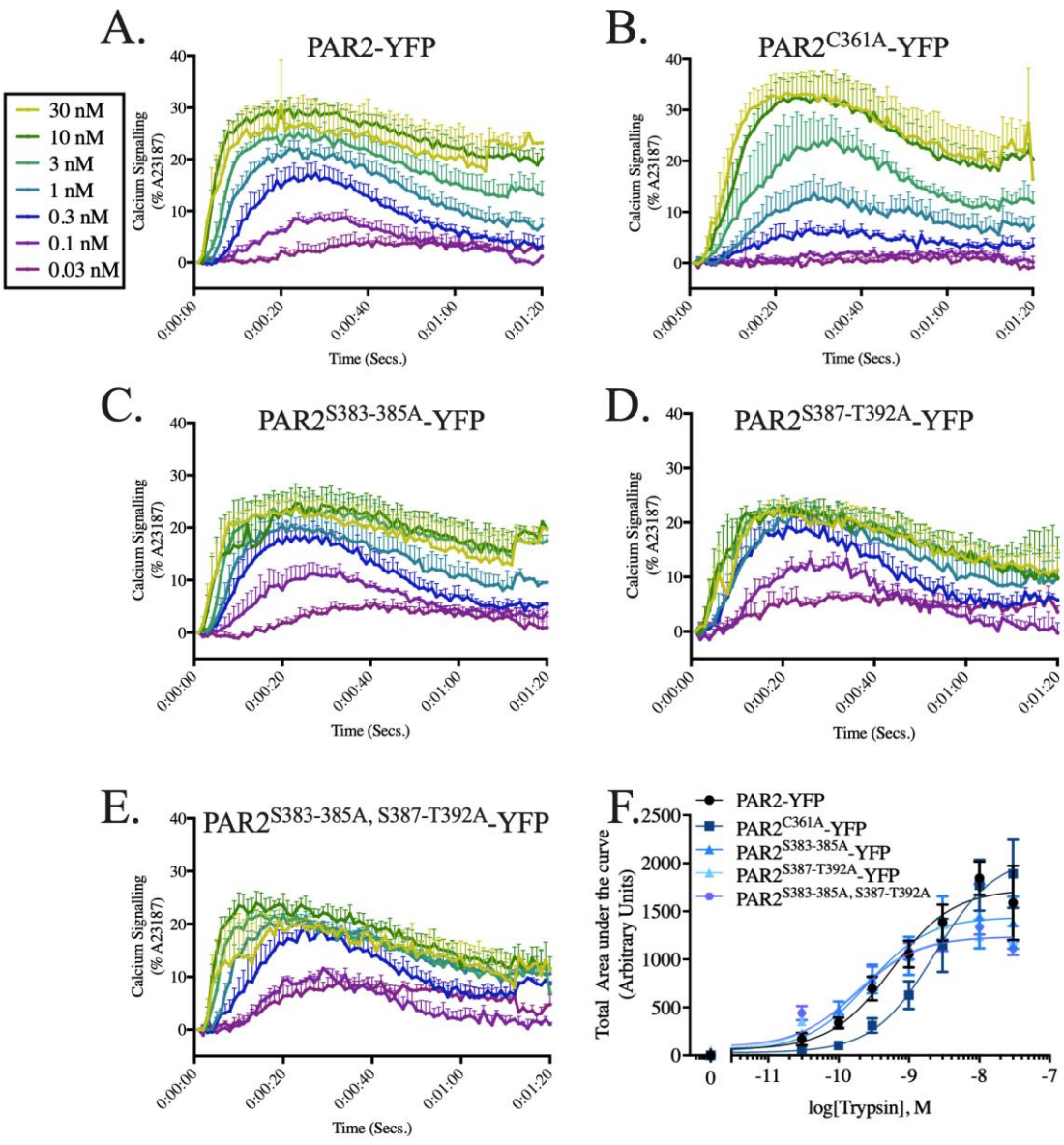

Figure 3.7 Differential calcium signalling in PAR2 mutant receptors compared to PAR2-YFP in response to stimulation with trypsin. Representative kinetic traces are shown for trypsin-stimulated intracellular calcium signalling (mean ± S.E.) for three independent experiments with PAR2-YFP (A), PAR2^{C361A}-YFP (B), PAR2$^{S383-385A}$-YFP (C), PAR2$^{S387-T392A}$-YFP (D), and PAR2$^{S383-385A, S387-T392A}$-YFP (E) receptors. Analysis of PAR2^{C361A}-YFP mutant shows rightward shift in potency compared to wild-type PAR2-YFP signalling ($p < 0.05$). As observed with calcium signalling in response to SLIGRL-NH_2 stimulation, all PAR2 C-tail phosphorylation site mutant receptors were observed to

have decreased maximal calcium signalling compared to PAR2-YFP. Nonlinear regression curve fit of area under the curve shown for area under the curve (calculated with Prism 7) (F). (*n = 3*)

3.3.7 Role of $G\alpha_{q/11}$ and β-arrestin in PAR2-stimulated ERK activation

Since GPCR-mediated ERK activation can occur downstream of $G\alpha_{q/11}$-dependent and/or β-arrestin-dependent/post-G-protein signalling pathways, we employed pharmacological inhibition of $G\alpha_{q/11}$ with the compound YM254890 and CRISPR/Cas9 β-arrestin-knockout HEK-293 cells (29) to probe these pathways downstream of PAR2. Cells were stimulated with SLIGRL-NH_2 (30 μM) for various time points to record ERK phosphorylation (p-p44/42). We observe that SLIGRL-NH_2-mediated ERK phosphorylation was significantly inhibited in cells treated with 100 nM YM254890 prior to agonist stimulation (Vehicle AUC = 841 ± 183; YM254890 AUC = 206 ± 69) (Figure 3.8A & C). Interestingly, we find that ERK signalling was not statistically different in β-arrestin double knockouts cells compared to HEK-293 cells (HEK-293 AUC = 812 ± 249; β-arrestin-knockout HEK-293 AUC = 2652 ± 855) (Figure 3.8B & D). These data suggest that phosphorylation of ERK downstream of PAR2 stimulation of SLIGRL-NH_2 is mediated by $G\alpha_{q/11}$-dependent signalling and is independent of β-arrestin-1/-2.

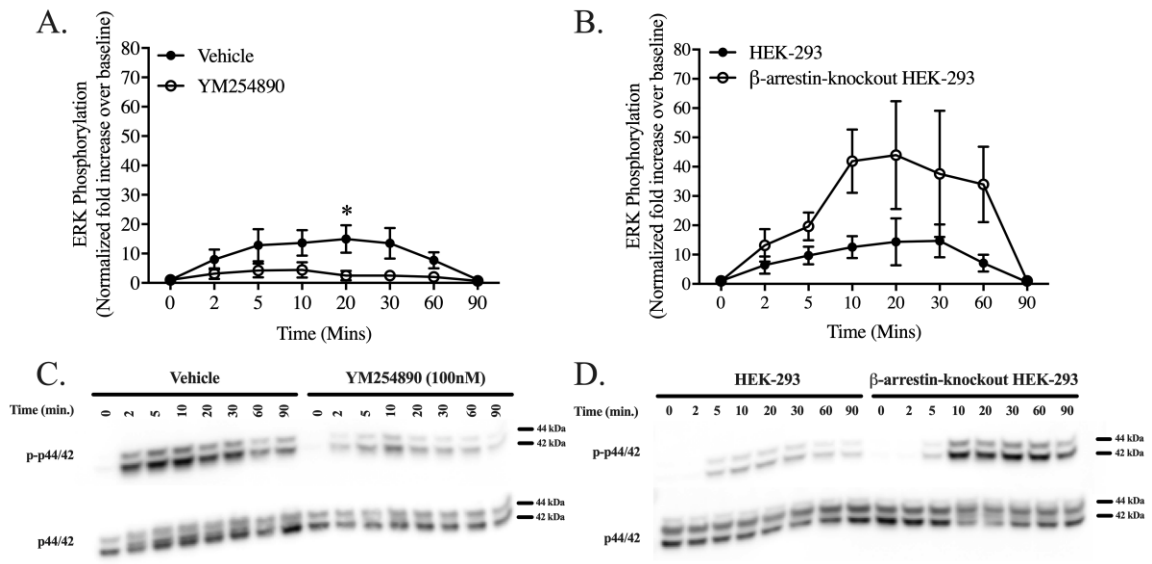

Figure 3.8 SLIGRL-NH$_2$-stimulated, PAR2-mediated MAPK activation is G$\alpha_{q/11}$-dependent and negatively regulated by β-arrestins. PAR2-mediated p44/42 phosphorylation is G$\alpha_{q/11}$ dependent. (A) SLIGRL-NH$_2$-stimulated (30 μM) p44/42 phosphorylation over time in HEK-293 cells pre-treated with vehicle control (DMSO, 0.01%) or G$\alpha_{q/11}$ inhibitor YM254890 (100 nM) for 20 minutes. (B) PAR2-mediated p44/42 phosphorylation in HEK-293 compared to β-arrestin-knockout HEK-293 cells following stimulation with SLIGRL-NH$_2$ (30 μM). Analysis of p44/42 phosphorylation reveal that PAR2-stimulated MAPK activation is largely G$\alpha_{q/11}$-dependent. Interestingly, normalized fold increase in p44/42 phosphorylation in HEK-293 and β-arrestin-knockout HEK-293 cells reveal that β-arrestin may be responsible for negative regulation/desensitization of PAR2-stimulated ERK phosphorylation. Data shown are representative of at least three independent experiments (phosphorylated to total p44/42, normalized to baseline phosphorylation at 0 minutes; mean ± S.E.; *$p < 0.05$) Representative blots of phosphorylated p44/42 (p-p44/42) and total p44/42 (p44/42) for vehicle/YM254890 (C) and HEK-293/β-arrestin-knockout HEK-293 (D) experiments are shown. *(n = 3-4)*

3.3.8 Mutations of PAR2 C-tail stimulate increased levels of ERK phosphorylation

To investigate the effect of PAR2 C-tail mutations on phosphorylation of ERK we stimulated PAR2-knockout HEK-293, transiently expressing PAR2 C-tail mutants, for 10 minutes with a low receptor-activating concentration (based on calcium signalling data) of SLIGRL-NH_2 (3 μM) or trypsin (0.3nM). These concentrations were selected as they do not activate significant levels of calcium signalling (Figure 3.5D & H) and ERK phosphorylation in the wild-type PAR2 receptor. We reasoned that increases in ERK activation in the mutant receptor would be more readily detected under these conditions since ERK signalling downstream of receptor activation may be subject to amplification/deamplification processes that could mask significant increases in ERK phosphorylation downstream of mutant PAR2 receptor constructs at the highest concentrations of agonists used in this study. Interestingly, we observed similar ERK signalling [fold increase over baseline = (p-p44/42)/(p-44/42) normalized to untreated] with $PAR2^{C361A}$-YFP (SLIGRL-NH_2, 1.6 ± 0.3; trypsin, 1.2 ± 0.2), $PAR2^{S383\text{-}385A}$-YFP (SLIGRL-NH_2, 1.8 ± 0.4; trypsin, 1.3 ± 0.3), and $PAR2^{S387\text{-}T392A}$-YFP (SLIGRL-NH_2, 1.3 ± 0.2; trypsin, 1.3 ± 0.3), compared to wild-type PAR2-YFP in response to SLIGRL-NH_2 (3 μM; PAR2-YFP = 0.9 ± 0.2) and trypsin (0.3 nM; PAR2-YFP = 0.7 ± 0.1). However, we find that there is a significant increase in $PAR2^{S383\text{-}385A,\ S387\text{-}T392A}$-YFP in response to both SLIGRL-NH_2 (2.0 ± 0.3-fold increase over baseline) and trypsin (1.9 ± 0.6-fold increase over baseline) (Figure 3.9A). Thus, ERK signalling is primarily $G\alpha_{q/11}$-dependent and β-arrestin-independent (Figure 3.8A & B), but receptor mutants that had decreased activation of the $G\alpha_{q/11}$ pathway remain competent in activating ERK. This suggests that sufficient second messenger amplification may be occurring in the $G\alpha_{q/11}$ pathway to indistinguishable levels of ERK activation or that activation of additional G-protein pathways leading to ERK activation may remain functional in these PAR2 mutants.

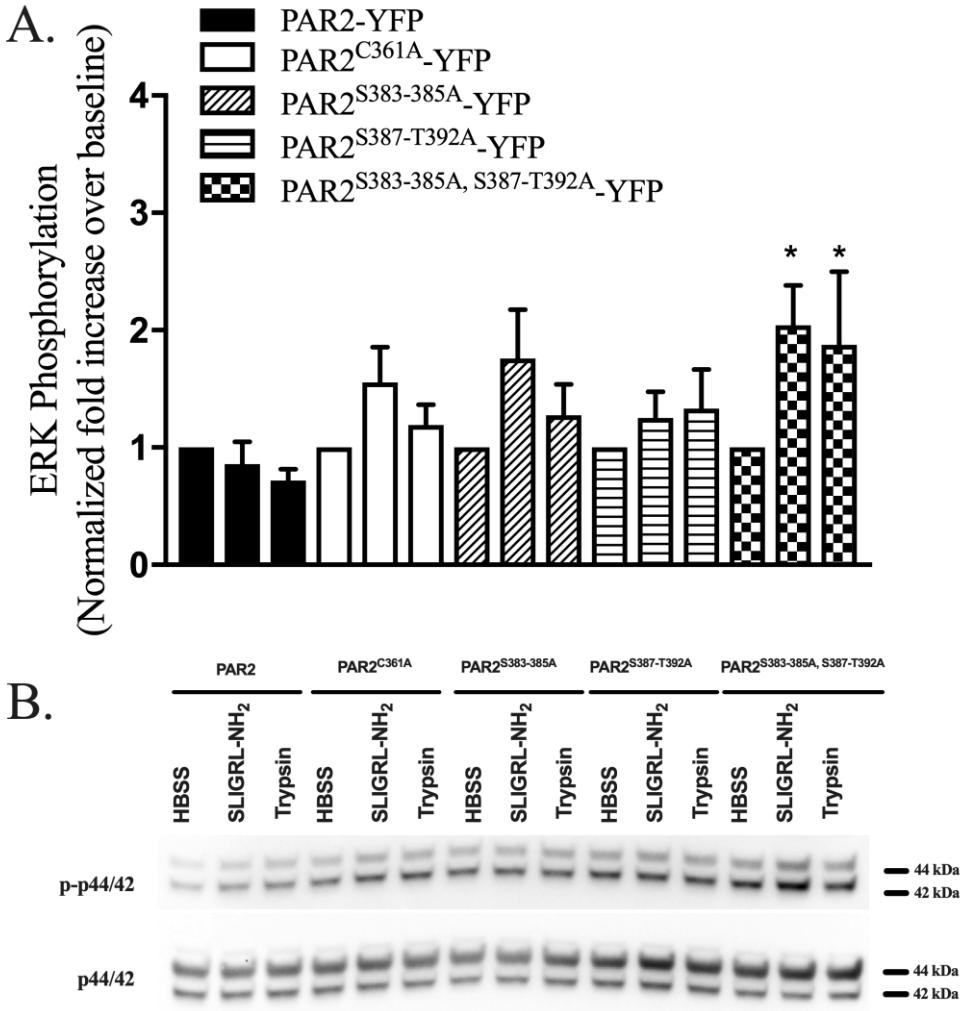

Figure 3.9 PAR2 C-tail phosphorylation mutation, Ser$^{383\text{-}385}$Ala/Ser^{385}-Thr^{392}Ala, increases ERK phosphorylation in response to SLIGRL-NH_2 and trypsin stimulation. (A) Summary data of p44/42 phosphorylation in PAR2-knockout HEK-293 cells expressing PAR2-YFP or PAR2 C-tail mutant receptors stimulated for 10 minutes with SLIGRL-NH_2 (3 μM) or trypsin (0.3 nM). Sub-maximal concentrations of SLIGRL-NH_2 and trypsin were chosen to avoid ERK activation with wild-type receptor to visual receptor mutations enhancing phosphorylation. Statistical analysis (two-way ANOVA) reveals that C-tail cysteine and phosphorylation mutants increase ERK phosphorylation compared to wild-type PAR2-YFP. Data shown are representative of four independent experiments (mean ± S.E.). (B) Representative blot of phosphorylated p44/42 (p-p44/42) and total p44/42 (p44/42) are shown. (*n = 4*)

Table 3.1 Summary of data β-arrestin-recruitment, calcium signalling, and MAPK activation with PAR2-YFP and PAR2-YFP mutants with SLIGRL-NH_2 (top) and trypsin (bottom) stimulation.

	β-arrestin-1 Recruitment		*β-arrestin-2 Recruitment*		*Calcium*		*ERK Phosphorylation*
SLIGRL-NH_2	***EC_{50} (μM)***	***Max. (net BRET)***	***EC_{50} (μM)***	***Max. (net BRET)***	***EC_{50} (μM)***	***Max. (A.U.C.)***	***Normalized fold increase over baseline***
PAR2-YFP	12.1 ± 1.6	0.39 ± 0.01	11.1 ± 1.2	0.53 ± 0.01	1.1 ± 0.1	1433 ± 21	0.9 ± 0.2
$PAR2^{C361A}$-YFP	28.8 ± 4.0*	0.28 ± 0.01*	27.4 ± 2.5*	0.32 ± 0.01*	7.1 ± 0.9*	1711 ± 37*	1.6 ± 0.3
$PAR2^{S383\text{-}385A}$-YFP	12.5 ± 2.8	0.44 ± 0.02*	15.1 ± 2.7	0.56 ± 0.02	0.8 ± 0.1	1165 ± 28*	1.8 ± 0.4
$PAR2^{S387\text{-}T392A}$-YFP	52.4 ± 12.1*	0.27 ± 0.02*	41.7 ± 6.3*	0.40 ± 0.02*	0.3 ± 0.1*	1242 ± 23*	1.3 ± 0.2
$PAR2^{S383\text{-}385A,\ S387\text{-}T392A}$-YFP	56.2 ± 18.0	0.16 ± 0.01*	29.9 ± 8.6	0.23 ± 0.02*	0.2 ± 0.1*	652 ± 44*	2.0 ± 0.3*
Trypsin	***EC_{50} (nM)***	***Max. (net BRET)***	***EC_{50} (nM)***	***Max. (net BRET)***	***EC_{50} (nM)***	***Max. (A.U.C)***	***Normalized fold increase over baseline***
PAR2-YFP	9.4 ± 1.6	0.17 ± 0.01	6.1 ± 1.2	0.14 ± 0.01	0.6 ± 0.2	1729 ± 125	0.7 ± 0.1
$PAR2^{C361A}$-YFP	5.7 ± 1.1	0.12 ± 0.01*	4.9 ± 0.7	0.12 ± 0.00	2.3 ± 0.9*	2081 ± 192	1.2 ± 0.2
$PAR2^{S383\text{-}385A}$-YFP	8.7 ± 1.6	0.13 ± 0.01*	8.8 ± 2.1	0.16 ± 0.01	2.6 ± 0.1	1442 ± 112	1.3 ± 0.3
$PAR2^{S387\text{-}T392A}$-YFP	7.8 ± 1.2	0.12 ± 0.01*	11.9 ± 4.6	0.17 ± 0.02	0.2 ± 0.1	1241 ± 67*	1.3 ± 0.3
$PAR2^{S383\text{-}385A,\ S387\text{-}T392A}$-YFP	8.4 ± 1.8	0.13 ± 0.01*	5.1 ± 1.0	0.12 ± 0.01	0.2 ± 0.1	1236 ± 57*	1.9 ± 0.6*

β-arrestin recruitment (EC_{50}; "Max." denotes maximum BRET signal obtained with a mutant up 300 μM SLIGRL-NH_2 or 300 nM trypsin), calcium signalling [EC_{50}; "Max." denotes maximum calcium signal at 300 μM SLIGRL-NH_2 or 300 nM trypsin (area under the curve; arbitrary units)], and phosphorylation of ERK (phosphorylated p44/42 / total p44/42; expressed as fold increase over unstimulated baseline) for PAR2-YFP and C-tail mutant PAR2-YFP receptors in response to SLIGRL-NH_2 and trypsin. Statistical significance (* $p < 0.05$) was determined by extra sum of squares analysis (EC_{50} and Max.) or two-way ANOVA (ERK phosphorylation).

3.4 Discussion

PAR2 is a proteolytically-activated GPCR and a key regulator of inflammatory responses (39). The mechanisms that underlie biased signalling through PAR2 are of interest both for understanding receptor regulation of cellular behaviour and for developing therapeutic strategies that selectively target certain pathways. Here we examined receptor C-tail motifs as determinants of PAR2 coupling to two key effectors, $G\alpha_{q/11}$ and β-arrestins. Building on previous work, we find that a helix-8 cysteine residue (Cys^{361}) is involved in PAR2 interaction with both $G\alpha_{q/11}$ signalling and the recruitment of β-arrestins (21–23). Clusters of serine and threonine residues, that are sites of phosphorylation by GPCR kinases (GRKs), in contrast, regulated β-arrestin interaction with PAR2 and resulted in a prolongation of the calcium signalling consistent with a deficit in receptor desensitization. A modest decrease in maximal calcium signalling was seen with some of the phosphorylation site mutants, perhaps reflecting differences in receptor expression that warrant further study with more quantitative methods.

The ability of some GPCRs to signal independently of G-proteins via β-arrestins has emerged in recent years as a paradigm that has expanded the scope of GPCR signalling (16). Previous studies have provided compelling evidence that β-arrestin recruitment to GPCRs, such as the histamine H_4 receptor, D prostanoid receptor-2, GPR17, and free fatty acid receptor-2, can occur without G-protein activation (40, 41). In the case of PAR2, such signalling has been implicated in scaffolding the p44/42 MAPK pathway (11). However, recent studies using CRISPR/Cas9 knockout of G-proteins and β-arrestins have questioned whether G-protein activation is necessary for the β-arrestin scaffolded signalling (41). Here we took advantage of a specific $G\alpha_{q/11}$ inhibitor and our newly developed β-arrestin double-knockout cell line to re-examine this question for PAR2. We found that β-arrestin recruitment to PAR2 was reduced but not completely abolished by pre-treatment with a $G\alpha_{q/11}$-specific inhibitor in response to SLIGRL-NH_2 stimulation. When PAR2 is activated with trypsin there was no difference in β-arrestin recruitment to cells pretreated with vehicle or the $G\alpha_{q/11}$ inhibitor. This was surprising and suggests that PAR2 can indeed recruit β-arrestins independent of $G\alpha_{q/11}$ activation. We must note that

PAR2 can couple to multiple G-proteins and this lack of reduction in β-arrestin recruitment likely reflect coupling to other Gα proteins preceding β-arrestin interactions with PAR2. β-arrestin-1/-2 however clearly have a role in regulating $G\alpha_{q/11}$-dependent signalling through PAR2. We observed a significant increase in the $G\alpha_{q/11}$-dependent calcium signal, with increases in both magnitude and duration of signal observed with both trypsin and SLIGRL-NH_2 in β-arrestin deficient cells which is entirely in keeping with the well-established role of β-arrestins as regulators of desensitization in a variety of GPCRs including PAR2 (22, 42–45). PAR2-mediated calcium mobilization can also involve additional effectors such as TRP family ion channels (13, 46, 47). Therefore, it is possible that the prolongation and sensitization of calcium signalling noted here may also reflect changes in ion channel sensitization by PAR2. Further studies are required to examine this.

More surprisingly, when we examined PAR2-dependent p44/42 MAPK activation, we found that the $G\alpha_{q/11}$-inhibitor, YM254890, significantly attenuated phosphorylation of PAR2-dependent p44/42 MAPK activation. Since YM254890 did not abolish β-arrestin recruitment to PAR2, this decrease in ERK activation appears to stem entirely from an inhibition of the $G\alpha_{q/11}$ signalling pathway. Further, in keeping with our observation of enhanced $G\alpha_{q/11}$ signalling in β-arrestin-knockout HEK-293 cells, we find that phosphorylation of p44/42 in β-arrestin-knockout HEK-293 cells was increased, though not significantly, compared to wild-type HEK-293 cells. These data support the interpretation that $G\alpha_{q/11}$ signalling through PAR2 leads to p44/42 MAPK activation, which is negatively regulated by β-arrestins. PAR2 can also trigger p44/42 MAPK signalling following activation by enzymes such as Neutrophil Elastase and Cathepsin-S that cleave the receptor at sites downstream from the trypsin cleavage site (25). These non-canonical cleavage events reveal tethered-ligands that are unable to engage either $G\alpha_{q/11}$ or β-arrestin but instead appear to switch receptor coupling to $G\alpha_{12/13}$ or $G\alpha_s$ dependent pathway. Further work is warranted to fully understand multiple mechanisms that facilitate MAPK activation by PAR2.

Phosphorylation of the C-tail is known to increase β-arrestin affinity for GPCRs (20, 48, 49). Additionally, molecular and structural studies have established a role for the 8th helix in enabling both visual arrestin and β-arrestin interactions with GPCRs (17, 50–52). In probing the relative contributions of these two mechanisms, we examined G-protein and β-arrestin engagement to PAR2 mutants with serine/threonine to alanine substitution and a construct where the 8th helix cysteine residue was mutated to alanine. Mutation of Cys^{361} to alanine significantly decreased recruitment of β-arrestin-1/-2 following agonist stimulation with SLIGRL-NH_2. The decrease in β-arrestin recruitment in the helix-8 cysteine mutant is in keeping with other GPCRs where this has been observed including the vasopressin receptor and the thyrotropin receptor (53, 54). Intriguingly, β-arrestin recruitment to this mutant was largely unaffected when the receptor was activated with trypsin and may be reflective of differences in peptide versus tethered agonist driven active receptor conformations. Previously, it was demonstrated that there is an evident reversal in rank order potency between thrombin- and peptide-activated PAR1, dependent on which signalling effector is studied (55). Such differences in effector coupling to helix-8 mutants of PAR1 activated by peptide versus tethered ligand agonists have also been reported (56). Thus, it is possible that a similar mechanism may underscore the differential effect we observed in this mutant between peptide and trypsin activated PAR2.

Since helix-8 is also reported to be a site for G-protein interactions in GPCRs, we examined $G\alpha_{q/11}$-mediated calcium signalling to PAR2 in the helix-8 cysteine mutant. We observe that the Cys^{361}Ala mutation in PAR2 results in significant dysregulation of calcium signalling. This is demonstrated by both a higher concentration of agonist required to elicit a half-maximal response and also by prolonged signalling following activation by either SLIGRL-NH_2 or trypsin. The decrease in potency of PAR2 activators may be indicative of decreased $G\alpha_{q/11}$ affinity with this mutant, while the slow desensitization and elevated maxima may reflect the deficiency in β-arrestin recruitment as noted with wild-type receptor in β-arrestin-knockout HEK-293. Such defects in G-protein-coupling to helix-8 mutants have been noted for PAR1, β2-adrenergic receptor, M1 muscarinic acetylcholine receptor, M2 muscarinic acetylcholine receptor, glucagon

like peptide-1 receptor, 5-Hydroxytryptamine(1A) receptor, CCR2 receptors, and some odorant receptors - to highlight a few examples (56–63). In the case of the M3 muscarinic acetylcholine receptor, chemical cross-linking studies have implicated helix-8 residues 8.49 and 8.52 (Ballesteros-Weinstein GPCR numbering system) in making agonist-promoted contacts with the α4-β6 loop of $G\alpha_q$ (64). In contrast, G-protein-mediated signalling through other GPCRs such as the α_{2A}-adrenergic receptor and the vasopressin V_{1A} receptor are not affected by mutations to the C-terminal cysteine residues (65, 66). In the case of the vasopressin receptor, receptor phosphorylation under both basal and agonist-stimulated conditions was abolished when the helix-8 cysteine residue was mutated, suggesting a role in recruitment of GPCR kinases (GRKs) (66). Whether Cys^{361}Ala in PAR2 similarly affects GRK-mediated phosphorylation to affect β-arrestin recruitment, is not yet known. Thus, it is possible that the decrease in β-arrestin-recruitment to PAR2 in the helix-8 cysteine mutant could be occurring through a direct disruption of a β-arrestin contact site or through a deficit in GRK interaction and consequent defect in phosphorylation of the activated receptor. Our data suggest that a more direct role for helix-8 as a site for interaction between $G\alpha_{q/11}$ and PAR2 is likely.

GRK-mediated phosphorylation of GPCRs is well established as a critical modification required for β-arrestin interactions (45, 67). Further, the pattern of phosphorylation at different serine and threonine residues is GRK specific and can stabilize different β-arrestin conformations at activated receptors (68). The C-tail in PAR2 contains multiple clusters of serine and threonine residues that are established as sites of phosphorylation (22). We focused on two of these clusters encompassing residues $Ser^{383\text{-}385}$ and Ser^{387}-Thr^{392}. We also generated a construct with combined alanine substitution of both these clusters. We find that the membrane proximal cluster of serine residues, $Ser^{383\text{-}385}$, does not play a role in agonist-dependent recruitment of β-arrestin-1/-2. In contrast, mutation of the second cluster of six serine and threonine residues (Ser^{387}-Thr^{392}) to alanine significantly decreased SLIGRL-NH_2-stimulated β-arrestin recruitment. Thus, this site is a key regulator of β-arrestin recruitment following peptide activation of PAR2. Interestingly, we once again noted only a modest deficit in trypsin-stimulated β-arrestin recruitment to this mutant indicating that there are differences in peptide versus tethered-

ligand stabilized active structures and their interaction with β-arrestin. The reasons for β-arrestin recruitment to trypsin activated PAR2 remaining resistant to C-tail mutations are unclear. We speculate that multiple GRKs might phosphorylate activated PAR2 with different GRKs engaged when receptors are activated by trypsin vs agonist peptide. In this scenario mutations we studied here might not eliminate all of the trypsin recruited GRK interactions, enabling β-arrestin recruitment, while effectively disrupting the GRK mediated phosphorylation that occurs following peptide activation. These mechanisms require further study. Much of the published research comparing the effects of peptide- versus proteolytically-stimulated signalling has also centered around $G\alpha_{q/11}$ dependent pathways. Our results here highlight the importance of comparing multiple signalling effector interactions when studying different PAR agonists.

Combined deletion of both clusters of phosphorylation sites phenocopied β-arrestin recruitment and calcium signalling patterns seen with mutations to Ser^{387}-Thr^{392} implicating these residues as a key motif in PAR2 β-arrestin interaction though other phosphorylatable residues are also likely to provide additional sites for β-arrestin contacts (22). The combined mutations to the two phosphorylation clusters was, however, required to cause an increase in ERK activation. However, in all other C-tail mutants, ERK activation was not significantly different than wild-type receptor, despite having decreased β-arrestin recruitment and decreased $G\alpha_{q/11}$ calcium signalling. These data may indicate that despite the apparent decrease in β-arrestin recruitment to these mutants, the quanta of β-arrestin recruited may be sufficient to inhibit $G\alpha_{q/11}$-stimulated MAPK signalling, or that the level of $G\alpha_{q/11}$-activation downstream of mutant receptor activation is insufficient to lead to MAPK signalling at the concentrations evaluated. Further, the data may highlight a role for other G-protein pathways in regulating ERK activation downstream of these PAR2 mutants. In keeping with our findings in PAR2, studies in the β2-adrenergic receptor have demonstrated both G-protein-dependent and G-protein-independent/β-arrestin-dependent ERK activation (69, 70). Therefore, mechanisms of GPCR-mediated ERK activation are likely agonist and context specific, as reported for other GPCRs, and warrant further study.

Previously studies have noted that a phosphorylation null PAR2 mutant shows evident defects in trafficking (22). While appropriate membrane localization was observed for all mutants studied here (Supplementary Figure 3.2), a more thorough investigation of the impacts of PAR2 C-tail mutations on trafficking should be undertaken to further probe the role of G-proteins and β-arrestin in this process. This study also highlights the importance of considering differences between peptide- and trypsin-stimulated activation of PAR2, as has been previously reported for PAR1 (55, 71). Overall, our results highlight an important role for the helix-8 and clusters of phosphorylated serine and threonine residues as essential interaction sites for β-arrestin recruitment to PAR2. Loss of β-arrestin recruitment resulted in exaggerated G-protein-mediated signalling from this receptor. The modest effect of mutations studied here on trypsin-stimulated recruitment of β-arrestins is intriguing and warrants further study to understand agonist specific differences in PAR2 effector interactions.

3.5 References

1. Fredriksson, R., Lagerström, M. C., Lundin, L.-G., and Schiöth, H. B. (2003) The G-Protein-Coupled Receptors in the Human Genome Form Five Main Families. Phylogenetic Analysis, Paralogon Groups, and Fingerprints. *Mol Pharmacol*. **63**, 1256–1272

2. Macfarlane, S. R., Seatter, M. J., Kanke, T., Hunter, G. D., and Plevin, R. (2001) Proteinase-activated receptors. *Pharmacol Rev*. **53**, 245–282

3. Adams, M. N., Ramachandran, R., Yau, M.-K., Suen, J. Y., Fairlie, D. P., Hollenberg, M. D., and Hooper, J. D. (2011) Structure, function and pathophysiology of protease activated receptors. *Pharmacology & therapeutics*. **130**, 248–282

4. Chen, J., Bernstein, H. S., Chen, M., Wang, L., Ishii, M., Turck, C. W., and Coughlin, S. R. (1995) Tethered ligand library for discovery of peptide agonists. *The Journal of biological chemistry*. **270**, 23398–23401

5. Faruqi, T. R., Weiss, E. J., Shapiro, M. J., Huang, W., and Coughlin, S. R. (2000) Structure-function analysis of protease-activated receptor 4 tethered ligand peptides. Determinants of specificity and utility in assays of receptor function. *The Journal of biological chemistry*. **275**, 19728–19734

6. Kawabata, A., Kanke, T., Yonezawa, D., Ishiki, T., Saka, M., Kabeya, M., Sekiguchi, F., Kubo, S., Kuroda, R., Iwaki, M., Katsura, K., and Plevin, R. (2004) Potent and metabolically stable agonists for protease-activated receptor-2: evaluation of activity in multiple assay systems in vitro and in vivo. *The Journal of pharmacology and experimental therapeutics*. **309**, 1098–1107

7. Hollenberg, M. D., Saifeddine, M., Al-Ani, B., and Kawabata, A. (1997) Proteinase-activated receptors: structural requirements for activity, receptor cross-reactivity, and receptor selectivity of receptor-activating peptides. *Can J Physiol Pharmacol*. **75**, 832–841

8. Miike, S., McWilliam, A. S., and Kita, H. (2001) Trypsin induces activation and inflammatory mediator release from human eosinophils through protease-activated receptor-2. *Journal of immunology (Baltimore, Md. : 1950)*. **167**, 6615–6622

9. Heuberger, D. M., and Schuepbach, R. A. (2019) Protease-activated receptors (PARs): mechanisms of action and potential therapeutic modulators in PAR-driven inflammatory diseases. *Thromb J*. 10.1186/s12959-019-0194-8

10. Zhao, P., Metcalf, M., and Bunnett, N. W. (2014) Biased Signaling of Protease-Activated Receptors. *Front Endocrinol (Lausanne)*. 10.3389/fendo.2014.00067

11. DeFea, K. A., Zalevsky, J., Thoma, M. S., Dery, O., Mullins, R. D., and Bunnett, N. W. (2000) beta-arrestin-dependent endocytosis of proteinase-activated receptor

2 is required for intracellular targeting of activated ERK1/2. *J Cell Biol*. **148**, 1267–1281

12. McCoy, K. L., Traynelis, S. F., and Hepler, J. R. (2010) PAR1 and PAR2 couple to overlapping and distinct sets of G proteins and linked signaling pathways to differentially regulate cell physiology. *Molecular pharmacology*. **77**, 1005–1015

13. Zhao, P., Lieu, T., Barlow, N., Metcalf, M., Veldhuis, N. A., Jensen, D. D., Kocan, M., Sostegni, S., Haerteis, S., Baraznenok, V., Henderson, I., Lindström, E., Guerrero-Alba, R., Valdez-Morales, E. E., Liedtke, W., McIntyre, P., Vanner, S. J., Korbmacher, C., and Bunnett, N. W. (2014) Cathepsin S causes inflammatory pain via biased agonism of PAR2 and TRPV4. *J. Biol. Chem.* **289**, 27215–27234

14. Ramachandran, R., Mihara, K., Mathur, M., Rochdi, M. D., Bouvier, M., DeFea, K., and Hollenberg, M. D. (2009) Agonist-biased signaling via proteinase activated receptor-2: differential activation of calcium and mitogen-activated protein kinase pathways. *Molecular pharmacology*. **76**, 791–801

15. Dery, O., Thoma, M. S., Wong, H., Grady, E. F., and Bunnett, N. W. (1999) Trafficking of proteinase-activated receptor-2 and beta-arrestin-1 tagged with green fluorescent protein. beta-Arrestin-dependent endocytosis of a proteinase receptor. *The Journal of biological chemistry*. **274**, 18524–18535

16. Lefkowitz, R. J., and Shenoy, S. K. (2005) Transduction of receptor signals by beta-arrestins. *Science*. **308**, 512–517

17. Kang, Y., Zhou, X. E., Gao, X., He, Y., Liu, W., Ishchenko, A., Barty, A., White, T. A., Yefanov, O., Han, G. W., Xu, Q., de Waal, P. W., Ke, J., Tan, M. H. E., Zhang, C., Moeller, A., West, G. M., Pascal, B. D., Van Eps, N., Caro, L. N., Vishnivetskiy, S. A., Lee, R. J., Suino-Powell, K. M., Gu, X., Pal, K., Ma, J., Zhi, X., Boutet, S., Williams, G. J., Messerschmidt, M., Gati, C., Zatsepin, N. A., Wang, D., James, D., Basu, S., Roy-Chowdhury, S., Conrad, C. E., Coe, J., Liu, H., Lisova, S., Kupitz, C., Grotjohann, I., Fromme, R., Jiang, Y., Tan, M., Yang, H., Li, J., Wang, M., Zheng, Z., Li, D., Howe, N., Zhao, Y., Standfuss, J., Diederichs, K., Dong, Y., Potter, C. S., Carragher, B., Caffrey, M., Jiang, H., Chapman, H. N., Spence, J. C. H., Fromme, P., Weierstall, U., Ernst, O. P., Katritch, V., Gurevich, V. V., Griffin, P. R., Hubbell, W. L., Stevens, R. C., Cherezov, V., Melcher, K., and Xu, H. E. (2015) Crystal structure of rhodopsin bound to arrestin by femtosecond X-ray laser. *Nature*. **523**, 561–567

18. Cahill, T. J., Thomsen, A. R. B., Tarrasch, J. T., Plouffe, B., Nguyen, A. H., Yang, F., Huang, L.-Y., Kahsai, A. W., Bassoni, D. L., Gavino, B. J., Lamerdin, J. E., Triest, S., Shukla, A. K., Berger, B., Little, J., Antar, A., Blanc, A., Qu, C.-X., Chen, X., Kawakami, K., Inoue, A., Aoki, J., Steyaert, J., Sun, J.-P., Bouvier, M., Skiniotis, G., and Lefkowitz, R. J. (2017) Distinct conformations of GPCR–β-arrestin complexes mediate desensitization, signaling, and endocytosis. *Proceedings of the National Academy of Sciences*. **114**, 2562–2567

19. Komolov, K. E., and Benovic, J. L. (2017) G protein-coupled receptor kinases_ Past, present and future. *Cell Signal*. 10.1016/j.cellsig.2017.07.004

20. Shukla, A. K., Manglik, A., Kruse, A. C., Xiao, K., Reis, R. I., Tseng, W.-C., Staus, D. P., Hilger, D., Uysal, S., Huang, L.-Y., Paduch, M., Tripathi-Shukla, P., Koide, A., Koide, S., Weis, W. I., Kossiakoff, A. A., Kobilka, B. K., and Lefkowitz, R. J. (2013) Structure of active β-arrestin-1 bound to a G-protein-coupled receptor phosphopeptide. *Nature*. **497**, 137–141

21. Seatter, M. J., Drummond, R., Kanke, T., Macfarlane, S. R., Hollenberg, M. D., and Plevin, R. (2004) The role of the C-terminal tail in protease-activated receptor-2-mediated Ca2+ signalling, proline-rich tyrosine kinase-2 activation, and mitogen-activated protein kinase activity. *Cell Signal*. **16**, 21–29

22. Ricks, T. K., and Trejo, J. (2009) Phosphorylation of protease-activated receptor-2 differentially regulates desensitization and internalization. *The Journal of biological chemistry*. **284**, 34444–34457

23. Botham, A., Guo, X., Xiao, Y. P., Morice, A. H., Compton, S. J., and Sadofsky, L. R. (2011) Palmitoylation of human proteinase-activated receptor-2 differentially regulates receptor-triggered ERK1/2 activation, calcium signalling and endocytosis. *Biochem. J.* **438**, 359–367

24. Adams, M. N., Christensen, M. E., He, Y., Waterhouse, N. J., and Hooper, J. D. (2011) The role of palmitoylation in signalling, cellular trafficking and plasma membrane localization of protease-activated receptor-2. *PLoS ONE*. **6**, e28018

25. Ramachandran, R., Mihara, K., Chung, H., Renaux, B., Lau, C. S., Muruve, D. A., DeFea, K. A., Bouvier, M., and Hollenberg, M. D. (2011) Neutrophil elastase acts as a biased agonist for proteinase-activated receptor-2 (PAR2). *The Journal of biological chemistry*. **286**, 24638–24648

26. Mihara, K., Ramachandran, R., Saifeddine, M., Hansen, K. K., Renaux, B., Polley, D., Gibson, S., Vanderboor, C., and Hollenberg, M. D. (2016) Thrombin-Mediated Direct Activation of Proteinase-Activated Receptor-2: Another Target for Thrombin Signaling. *Molecular pharmacology*. **89**, 606–614

27. Yee, M. C., Nichols, H. L., Polley, D., Saifeddine, M., Pal, K., Lee, K., Wilson, E. H., Daines, M. O., Hollenberg, M. D., Boitano, S., and DeFea, K. A. Protease-activated receptor-2 signaling through ᵑ-arrestin-2 mediates Alternaria alkaline serine protease-induced airway inflammation

28. Ayoub, M. A., and Pin, J.-P. R. (2013) Interaction of Protease-Activated Receptor 2 with G Proteins and β-Arrestin 1 Studied by Bioluminescence Resonance Energy Transfer. *Front. Endocrinol.* 10.3389/fendo.2013.00196

29. Thibeault, P. E., LeSarge, J. C., Arends, D., Fernandes, M., Chidiac, P., Stathopulos, P. B., Luyt, L. G., and Ramachandran, R. (2019) Molecular basis for

activation and biased signalling at the thrombin-activated GPCR Proteinase Activated Receptor-4 (PAR4). *J. Biol. Chem.* 10.1074/jbc.RA119.011461

30. Ferguson, S. S. G., and Caron, M. G. (2004) Green Fluorescent Protein-Tagged β-Arrestin Translocation as a Measure of G Protein-Coupled Receptor Activation. in *G Protein Signaling: Methods and Protocols* (Smrcka, A. V. ed), pp. 121–126, Methods in Molecular Biology™, Humana Press, Totowa, NJ, 10.1385/1-59259-430-1:121

31. Kawabata, A., Saifeddine, M., Al-Ani, B., Leblond, L., and Hollenberg, M. D. (1999) Evaluation of proteinase-activated receptor-1 (PAR1) agonists and antagonists using a cultured cell receptor desensitization assay: activation of PAR2 by PAR1-targeted ligands. *The Journal of pharmacology and experimental therapeutics*. **288**, 358–370

32. Sanjana, N. E., Shalem, O., and Zhang, F. (2014) Improved vectors and genome-wide libraries for CRISPR screening. *Nature Methods*. **11**, 783–784

33. Shalem, O., Sanjana, N. E., Hartenian, E., Shi, X., Scott, D. A., Mikkelsen, T. S., Heckl, D., Ebert, B. L., Root, D. E., Doench, J. G., and Zhang, F. (2014) Genome-Scale CRISPR-Cas9 Knockout Screening in Human Cells. *Science*. **343**, 84–87

34. Mihara, K., Ramachandran, R., Renaux, B., Saifeddine, M., and Hollenberg, M. D. (2013) Neutrophil elastase and proteinase-3 trigger G protein-biased signaling through proteinase-activated receptor-1 (PAR1). *The Journal of biological chemistry*. **288**, 32979–32990

35. Schindelin, J., Arganda-Carreras, I., Frise, E., Kaynig, V., Longair, M., Pietzsch, T., Preibisch, S., Rueden, C., Saalfeld, S., Schmid, B., Tinevez, J.-Y., White, D. J., Hartenstein, V., Eliceiri, K., Tomancak, P., and Cardona, A. (2012) Fiji: an open-source platform for biological-image analysis. *Nature Methods*. **9**, 676–682

36. Takasaki, J., Saito, T., Taniguchi, M., Kawasaki, T., Moritani, Y., Hayashi, K., and Kobori, M. (2004) A novel Galphaq/11-selective inhibitor. *J. Biol. Chem.* **279**, 47438–47445

37. Kim, B. H., Wang, F. I., Pereverzev, A., Chidiac, P., and Dixon, S. J. (2019) Toward Defining the Pharmacophore for Positive Allosteric Modulation of PTH1 Receptor Signaling by Extracellular Nucleotides. *ACS Pharmacol. Transl. Sci.* **2**, 155–167

38. LeSarge, J. C., Thibeault, P., Milne, M., Ramachandran, R., and Luyt, L. G. (2019) High Affinity Fluorescent Probe for Proteinase-Activated Receptor 2 (PAR2). *ACS Med. Chem. Lett.* **10**, 1045–1050

39. Ramachandran, R., Noorbakhsh, F., Defea, K., and Hollenberg, M. D. (2012) Targeting proteinase-activated receptors: therapeutic potential and challenges. *Nature Reviews Drug Discovery*. **11**, 69–86

40. Rosethorne, E. M., and Charlton, S. J. (2011) Agonist-Biased Signaling at the Histamine H4 Receptor: JNJ7777120 Recruits β-Arrestin without Activating G Proteins. *Mol Pharmacol*. **79**, 749–757

41. Grundmann, M., Merten, N., Malfacini, D., Inoue, A., Preis, P., Simon, K., Rüttiger, N., Ziegler, N., Benkel, T., Schmitt, N. K., Ishida, S., Müller, I., Reher, R., Kawakami, K., Inoue, A., Rick, U., Kühl, T., Imhof, D., Aoki, J., König, G. M., Hoffmann, C., Gomeza, J., Wess, J., and Kostenis, E. (2018) Lack of beta-arrestin signaling in the absence of active G proteins. *Nat Commun*. **9**, 341

42. Stalheim, L., Ding, Y., Gullapalli, A., Paing, M. M., Wolfe, B. L., Morris, D. R., and Trejo, J. (2005) Multiple independent functions of arrestins in the regulation of protease-activated receptor-2 signaling and trafficking. *Molecular pharmacology*. **67**, 78–87

43. DeFea, K., Schmidlin, F., Dery, O., Grady, E. F., and Bunnett, N. W. (2000) Mechanisms of initiation and termination of signalling by neuropeptide receptors: a comparison with the proteinase-activated receptors. *Biochemical Society transactions*. **28**, 419–426

44. Ferguson, S. S. (2001) Evolving concepts in G protein-coupled receptor endocytosis: the role in receptor desensitization and signaling. *Pharmacol Rev*. **53**, 1–24

45. Peterson, Y. K., and Luttrell, L. M. (2017) The Diverse Roles of Arrestin Scaffolds in G Protein-Coupled Receptor Signaling. *Pharmacol Rev*. **69**, 256–297

46. Poole, D. P., Amadesi, S., Veldhuis, N. A., Abogadie, F. C., Lieu, T., Darby, W., Liedtke, W., Lew, M. J., McIntyre, P., and Bunnett, N. W. (2013) Protease-activated receptor 2 (PAR2) protein and transient receptor potential vanilloid 4 (TRPV4) protein coupling is required for sustained inflammatory signaling. *The Journal of biological chemistry*. **288**, 5790–5802

47. Rayees, S., Joshi, J. C., Tauseef, M., Anwar, M., Baweja, S., Rochford, I., Joshi, B., Hollenberg, M. D., Reddy, S. P., and Mehta, D. (2019) PAR2-Mediated cAMP Generation Suppresses TRPV4-Dependent Ca2+ Signaling in Alveolar Macrophages to Resolve TLR4-Induced Inflammation. *Cell Reports*. **27**, 793-805.e4

48. Sente, A., Peer, R., Srivastava, A., Baidya, M., Lesk, A. M., Balaji, S., Shukla, A. K., Babu, M. M., and Flock, T. (2018) Molecular mechanism of modulating arrestin conformation by GPCR phosphorylation. *Nature Structural & Molecular Biology*. **25**, 538–545

49. Mayer, D., Damberger, F. F., Samarasimhareddy, M., Feldmueller, M., Vuckovic, Z., Flock, T., Bauer, B., Mutt, E., Zosel, F., Allain, F. H. T., Standfuss, J., Schertler, G. F. X., Deupi, X., Sommer, M. E., Hurevich, M., Friedler, A., and Veprintsev, D. B. (2019) Distinct G protein-coupled receptor phosphorylation

motifs modulate arrestin affinity and activation and global conformation. *Nat Commun*. **10**, 1261

50. Gagnon, L., Cao, Y., Cho, A., Sedki, D., Huber, T., Sakmar, T. P., and Laporte, S. A. (2019) Genetic code expansion and photocross-linking identify different β-arrestin binding modes to the angiotensin II type 1 receptor. *J. Biol. Chem.* **294**, 17409–17420

51. Kirchberg, K., Kim, T.-Y., Möller, M., Skegro, D., Raju, G. D., Granzin, J., Büldt, G., Schlesinger, R., and Alexiev, U. (2011) Conformational dynamics of helix 8 in the GPCR rhodopsin controls arrestin activation in the desensitization process. *PNAS*. **108**, 18690–18695

52. Feierler, J., Wirth, M., Welte, B., Schüssler, S., Jochum, M., and Faussner, A. (2011) Helix 8 Plays a Crucial Role in Bradykinin B2 Receptor Trafficking and Signaling. *J. Biol. Chem.* **286**, 43282–43293

53. Gehret, A. U., Jones, B. W., Tran, P. N., Cook, L. B., Greuber, E. K., and Hinkle, P. M. (2009) Role of Helix 8 of the Thyrotropin-Releasing Hormone Receptor in Phosphorylation by G Protein-Coupled Receptor Kinase. *Mol Pharmacol*. 10.1124/mol.109.059733

54. Charest, P. G., and Bouvier, M. (2003) Palmitoylation of the V2 Vasopressin Receptor Carboxyl Tail Enhances β-Arrestin Recruitment Leading to Efficient Receptor Endocytosis and ERK1/2 Activation. *J. Biol. Chem.* **278**, 41541–41551

55. McLaughlin, J. N., Shen, L., Holinstat, M., Brooks, J. D., Dibenedetto, E., and Hamm, H. E. (2005) Functional selectivity of G protein signaling by agonist peptides and thrombin for the protease-activated receptor-1. *The Journal of biological chemistry*. **280**, 25048–25059

56. Swift, S., Leger, A. J., Talavera, J., Zhang, L., Bohm, A., and Kuliopulos, A. (2006) Role of the PAR1 Receptor 8th Helix in Signaling THE 7-8-1 RECEPTOR ACTIVATION MECHANISM. *J. Biol. Chem.* **281**, 4109–4116

57. O'Dowd, B. F., Hnatowich, M., Caron, M. G., Lefkowitz, R. J., and Bouvier, M. (1989) Palmitoylation of the human beta 2-adrenergic receptor. Mutation of Cys341 in the carboxyl tail leads to an uncoupled nonpalmitoylated form of the receptor. *J. Biol. Chem.* **264**, 7564–7569

58. Mouillac, B., Caron, M., Bonin, H., Dennis, M., and Bouvier, M. (1992) Agonist-modulated palmitoylation of beta 2-adrenergic receptor in Sf9 cells. *J. Biol. Chem.* **267**, 21733–21737

59. Hayashi, M. K., and Haga, T. (1997) Palmitoylation of muscarinic acetylcholine receptor m2 subtypes: reduction in their ability to activate G proteins by mutation of a putative palmitoylation site, cysteine 457, in the carboxyl-terminal tail. *Arch Biochem Biophys*. **340**, 376–382

60. Vázquez, P., Roncero, I., Blázquez, E., and Alvarez, E. (2020) Substitution of the cysteine 438 residue in the cytoplasmic tail of the glucagon-like peptide-1 receptor alters signal transduction activity. *Journal of Endocrinology*. **185**, 35–44

61. Papoucheva, E., Dumuis, A., Sebben, M., Richter, D. W., and Ponimaskin, E. G. (2004) The 5-Hydroxytryptamine(1A) Receptor Is Stably Palmitoylated, and Acylation Is Critical for Communication of Receptor with Gi Protein. *J. Biol. Chem.* **279**, 3280–3291

62. Markx, D., Schuhholz, J., Abadier, M., Beier, S., Lang, M., and Moepps, B. (2019) Arginine 313 of the putative 8th helix mediates Gαq/14 coupling of human CC chemokine receptors CCR2a and CCR2b. *Cell. Signal.* **53**, 170–183

63. Kawasaki, T., Saka, T., Mine, S., Mizohata, E., Inoue, T., Matsumura, H., and Sato, T. (2015) The N-terminal acidic residue of the cytosolic helix 8 of an odorant receptor is responsible for different response dynamics via G-protein. *FEBS Lett.* **589**, 1136–1142

64. Hu, J., Wang, Y., Zhang, X., Lloyd, J. R., Li, J. H., Karpiak, J., Costanzi, S., and Wess, J. (2010) Structural basis of G protein–coupled receptor–G protein interactions. *Nature Chemical Biology*. **6**, 541–548

65. Kennedy, M. E., and Limbird, L. E. (1993) Mutations of the alpha 2A-adrenergic receptor that eliminate detectable palmitoylation do not perturb receptor-G-protein coupling. *The Journal of biological chemistry*. **268**, 8003–8011

66. Hawtin, S. R., Tobin, A. B., Patel, S., and Wheatley, M. (2001) Palmitoylation of the vasopressin V1a receptor reveals different conformational requirements for signaling, agonist-induced receptor phosphorylation, and sequestration. *The Journal of biological chemistry*. **276**, 38139–38146

67. Luttrell, L. M., and Lefkowitz, R. J. (2002) The role of beta-arrestins in the termination and transduction of G-protein-coupled receptor signals. *J Cell Sci*. **115**, 455–465

68. Nobles, K. N., Xiao, K., Ahn, S., Shukla, A. K., Lam, C. M., Rajagopal, S., Strachan, R. T., Huang, T.-Y., Bressler, E. A., Hara, M. R., Shenoy, S. K., Gygi, S. P., and Lefkowitz, R. J. (2011) Distinct phosphorylation sites on the β(2)-adrenergic receptor establish a barcode that encodes differential functions of β-arrestin. *Science Signaling*. **4**, ra51–ra51

69. Luttrell, L. M., Wang, J., Plouffe, B., Smith, J. S., Yamani, L., Kaur, S., Jean-Charles, P.-Y., Gauthier, C., Lee, M.-H., Pani, B., Kim, J., Ahn, S., Rajagopal, S., Reiter, E., Bouvier, M., Shenoy, S. K., Laporte, S. A., Rockman, H. A., and Lefkowitz, R. J. (2018) Manifold roles of β-arrestins in GPCR signaling elucidated with siRNA and CRISPR/Cas9. *Sci. Signal.* 10.1126/scisignal.aat7650

70. O'Hayre, M., Eichel, K., Avino, S., Zhao, X., Steffen, D. J., Feng, X., Kawakami, K., Aoki, J., Messer, K., Sunahara, R., Inoue, A., Zastrow, M. von, and Gutkind, J. S. (2017) Genetic evidence that β-arrestins are dispensable for the initiation of β2-adrenergic receptor signaling to ERK. *Sci. Signal.* 10.1126/scisignal.aal3395

71. Blackhart, B. D., Ruslim-Litrus, L., Lu, C. C., Alves, V. L., Teng, W., Scarborough, R. M., Reynolds, E. E., and Oksenberg, D. (2000) Extracellular mutations of protease-activated receptor-1 result in differential activation by thrombin and thrombin receptor agonist peptide. *Molecular pharmacology*. **58**, 1178–1187

3.6 Chapter 3 Supplementary Information

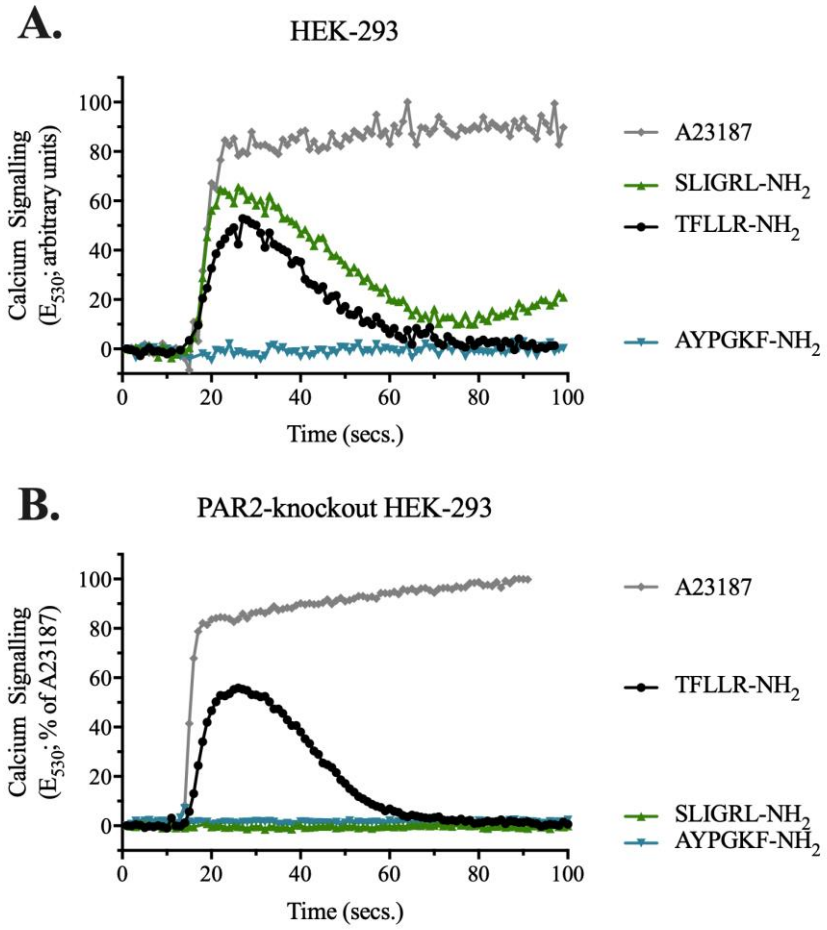

Supplementary Figure 3.1 Functional validation of PAR2-knockout HEK-293 cells
To evaluate functional knockout of PAR2 we recorded calcium signalling in PAR2-knocout HEK-293 cells and compared them to signalling in wild-type HEK-293 cells. Signalling in HEK-293 cells, which endogenously express both PAR1 and PAR2 but not PAR4, was recorded and demonstrates response to peptide agonists (100 µM) for PAR1 (TFLLR-NH_2) and PAR2 (SLIGRL-NH_2) but no response to PAR4 (AYPGKF-NH_2), as expected (A). PAR2-knockout HEK-293 cells signal peptide agonist-stimulated calcium for PAR1 but not PAR2, confirming a functional knockout of PAR2 (B). Calcium signalling in response peptide agonists is shown as a percentage of the maximum calcium signal obtained in response to calcium ionophore stimulation (A23187, 3 µM) is shown (grey).

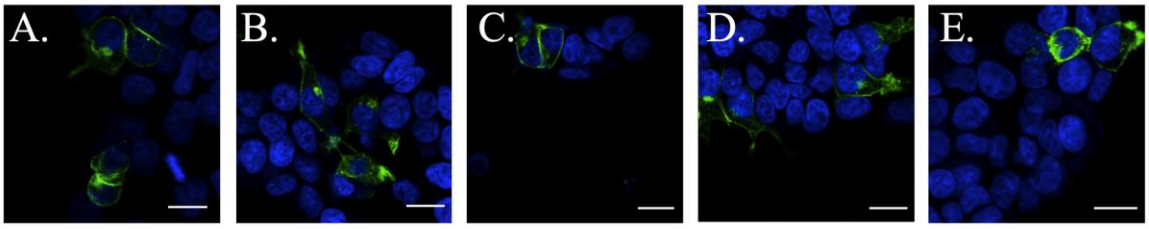

Supplementary Figure 3.2 Representative confocal micrographs of PAR2-YFP and PAR2-YFP mutant receptor expression and localization Expression of PAR2-YFP (A), PAR2^{C361A}-YFP (B), PAR2$^{S383\text{-}385A}$-YFP (C), PAR2$^{S387\text{-}T392A}$-YFP (D), and PAR2$^{S383\text{-}385A,\ S387\text{-}T392A}$-YFP (E). All receptor mutants are expressed on the cellular surface as expected and observed with PAR2-YFP (YFP shown in green, nuclear DAPI stain shown in blue).

Chapter 4

4 Differential Role of Helix-8 and C-terminal Tail Residues in Signalling and Regulation of Peptide- and Thrombin-activated Proteinase Activated Receptor 4 (PAR4)

4.1 Introduction

G-protein-coupled receptors (GPCRs) are the largest family of cell membrane signalling proteins expressed in eukaryotic cells (1, 2). These receptors convert extracellular ligand binding into intracellular signalling to mediate cellular affects. Ligand binding activates the GPCR through a series of structural reorganizations that allow for effectors, such as G-proteins, to bind and become activated. In addition to the intracellular loops of GPCRs, the Helix-8 and C-terminal tail also play important roles in effector interaction. Proteinase activated receptors (PARs), are a family of four rhodopsin-like (Class A) GPCRs, which are activated by a host of proteolytic enzymes from coagulation cascade-, immune cell-, and pathogen-derived sources (3–5). PARs are unique, compared to other Class A GPCR counterparts, in their mechanism of activation. PAR activation occurs following proteolysis of the receptor N-terminus which reveals a novel N-terminal sequence which is often termed the tethered ligand that is capable of activating the receptor through intramolecular binding (3). Alternatively, subtype-selective PAR activation can occur in the absence of proteolytic cleavage, through application of synthetic hexapeptide tethered ligand-mimetics (6–9).

PAR4 is a proteolytically-activated GPCR with an important role in thrombosis and haemostasis platelet activation/aggregation (3, 10–12). PAR4 is activated by a host of enzymes, such as thrombin, which mediate its physiological functions in platelet haemostasis (5). Proteolytic cleavage unmasks a tethered ligand sequence, GYPGQV, which binds intramolecularly to the receptor leading to its activation. Alternatively, PAR4 can be activated by the tethered ligand-mimicking peptide, AYPGKF-NH_2, which can activate the receptor in the absence of proteolytic cleavage (7, 13). PAR-mediated platelet activation downstream of thrombin release at the site of vessel injury is well-described, and as such, these receptors have been the target for anti-platelet therapeutic approaches (10, 11, 14, 15).

When activated with either the thrombin cleavage-revealed tethered ligand, $G^{48}YPGQV^{53}$, or tethered ligand-mimicking peptide, AYPGKF-NH_2, PAR4 engages $G\alpha_{q/11}$, $G\alpha_{12/13}$, and $G\alpha_i$ G-protein subtypes, although it is unclear if PAR4 can couple to

$G\alpha_i$ independent of crosstalk with purinergic receptors in certain tissue contexts (7, 16–19). Previously, we demonstrated key differences in C-tail regulation of β-arrestin-1/-2 recruitment and G-protein signal regulation with peptide- (SLIGRL-NH_2) versus proteolytically-activated (trypsin) PAR2 receptor (20). When activated, PAR4 signals primarily through $G\alpha_{q/11}$ and $G\alpha_{12/13}$, as well as through β-arrestins (7, 13, 16, 21). In contrast to many other Class A GPCRs, PAR4 lacks certain conserved residues and motifs implicated in effector interaction and signalling, such as a Helix-8 cysteine residue and C-tail clusters of serine/threonine residues. Thus, the molecular mechanisms that underlie PAR4 signalling and signal regulation are of interest – both for understanding the mechanisms of effector interactions with PAR4 as well as for the development of targeted therapeutic strategies. Further, probing differential contributions of residues to signalling and regulation downstream of either peptide activation or proteolytic cleavage provides insight into how these two different modes of activation may differentially regulate these interactions.

4.2 Methods

4.2.1 Chemicals and Other Reagents

Thrombin from human plasma (catalogue no. 605195) was purchased from Millipore-Sigma (St. Louis, MI). AYPGKF-NH_2 (> 95% purity by HPLC/MS) was purchased from Genscript (Piscataway, NJ). Agonists were prepared in 4-(2-hydroxyethyl)-1-piperazineethanesulfonic acid (HEPES, 25 mM). All other chemicals or reagents were purchased from Millipore-Sigma, Thermo Fisher Scientific, or BioShop Canada, Inc. (Burlington, Ontario, Canada), unless otherwise stated.

4.2.2 Molecular Cloning and Constructs

The plasmid encoding the human PAR4 receptor with an in frame enhanced yellow fluorescent protein fusion tag (PAR4-YFP) has been previously described (22). The use of an in-frame, C-terminal fusion of enhanced yellow fluorescent protein (eYFP) has been employed to study many GPCRs. eYFP fused PAR4 has been utilized in several previous studies where we have demonstrated that PAR4-YFP couples to the known PAR4 signalling pathways appropriately (13, 22–24). QuikChange XL Multi Site-

Directed Mutagenesis kit (Agilent Technologies, Mississauga, ON, Canada) was used to generate all Helix-8 and the C-terminal tail PAR4 mutants described in this study. All constructs were verified by sanger sequencing (London Regional Genomics Centre, University of Western Ontario).

4.2.3 Cell Lines and Culture Conditions

All media and cell culture reagents were purchased from Thermo Fisher Scientific (Waltham, MA). Human embryonic kidney (HEK) cells (HEK-293; ATCC), PAR1-knockout HEK-293 (23), and β-arrestin-1/-2-knockout HEK-293 (β-arrestin-knockout HEK-293) (13, 24) cell lines were maintained in Dulbecco's modified Eagle's medium supplemented with 10% fetal bovine serum, 1% sodium pyruvate, and penicillin streptomycin solution (50,000 units penicillin, 50,000 μg streptomycin). Since trypsin activates PAR4, cells were routinely sub-cultured using enzyme-free isotonic phosphate-buffered saline (PBS) containing EDTA (1 mM). Cells were transfected with PAR4-YFP or mutated PAR4-YFP receptor vectors using X-tremeGENE 9 (Millipore-Sigma). Transiently transfected cells were always assayed or imaged at 48 hours post-transfection to ensure consistent levels of protein expression.

4.2.4 Calcium Signalling

Agonist-stimulated calcium signalling was recorded in HEK-293 and PAR1-knockout HEK-293 cells, as previously described (13, 25, 26). Cells were detached in enzyme-free cell dissociation buffer, pelleted, and resuspended in Fluo-4 NW (no wash) calcium indicator dye (Thermo Fisher Scientific). Following a 30-minute incubation at ambient temperature, intracellular fluorescence (excitation 480 nm; emission recorded at 530 nm) was monitored before and after addition of agonists (thrombin, PAR1-knockout HEK-293; or AYPGKF-NH_2, HEK-293) on a PTI spectrophotometer (Photon Technology International, Birmingham, NJ). Responses were normalized to the fluorescence obtained with calcium ionophore (A23187, 3 μM; Sigma-Aldrich).

4.2.5 Bioluminescence Resonance Energy Transfer Detection of β-arrestin-1/-2 Recruitment

Bioluminescence resonance energy transfer (BRET) assays were employed to detect agonist-stimulated β-arrestin-1/-2 recruitment to PAR4-YFP and mutant PAR4-YFP constructs in HEK-293 cells as described (13, 22, 24). PAR4-YFP or mutant PAR4-YFP constructs (1 μg) and Renilla luciferase-tagged β-arrestin-1 or -2 (β-arr-1 and -2-rluc; 0.1 μg) were transiently transfected for 48 hours. Cells were plated in white 96-well culture plates (Corning; Oneonta, NY) and recruitment of β-arresitin-1/-2 to PAR4 were detected by measuring the BRET signal 20 minutes after agonist stimulation and the addition of 5 μM h-coelenterazine prior to BRET recording (NanoLight Technology, Pinetop, AZ) on a Mithras LB940 plate reader (Berthold Technologies, Bad Wildbad, Germany), as previously described (13, 22).

4.2.6 Confocal Microscopy

HEK-293 cells transiently transfected with PAR4-YFP or mutant PAR4-YFP were sub-cultured onto glass coverslips (Thermo Fisher Scientific) and analyzed by confocal microscopy to ensure appropriate cell surface expression. Cells were fixed with 4% w/v paraformaldehyde solution (methanol-free; Fisher Scientific), stained with DAPI for nuclear staining, and the cellular localization of receptor assessed by imaging eYFP expression with an Olympus FV1000 (Centre Valley, PA). (Supplementary Figure 4.1)

4.2.7 Statistical Analysis

Curve fitting (three-parameter, nonlinear regression) and statistical analysis was completed with Prism 7 software (GraphPad Software, La Jolla, CA). Statistical significance of EC_{50} shifts was calculated using the extra sum of squares analysis ($^*p < 0.05$; Table 1) (13, 20, 27). Net BRET and calcium signalling obtained with AYPGKF-NH_2 (300 μM) or thrombin (10 units/mL) was used to calculated maximal signal achieved in our study for comparison of mutant PAR4 constructs to wild-type PAR4. Previously we have demonstrated that β-arrestin recruitment to PAR4 does not saturate upon stimulation with AYPGKF-NH_2 and thrombin (13, 22, 24). Thus, statistical significance of maximal net BRET (300 μM AYPGKF-NH_2, 10 units/mL thrombin) was

determined using t-test (*$p < 0.05$). Data are expressed as mean ± S.E. throughout the text, table, and figure legends.

4.3 Results

4.3.1 AYPGKF-NH_2- and thrombin-stimulated calcium signalling is dependent on Leu^{355}-Gln^{357} residues in Helix-8

Previously, we reported that the deletion of PAR4 Helix-8 residues R^{352}AGLFQRS^{359} (construct designated dRS-PAR), exhibited defects in agonist-stimulated calcium signalling in addition to abrogation of β-arrestin-1/-2 recruitment (22). This study employed deletion of these residues, which may have contributed to some the deficits observed, therefore, in our current investigation we sought to determine a role for these residues in PAR4-mediated calcium signalling through alanine scanning mutations. First, we wanted to determine if we could recapitulate the findings of our previous study in a mutational model (rather than residue deletion), and further determine which residues, if not all, are involved in the loss of calcium signalling previously observed. Calcium signalling was recorded in response to stimulation of receptor with either AYPGKF-NH_2 or thrombin and reported as a percentage of the maximum calcium signal obtained in the sample using the calcium ionophore, A23187 (3 µM). Similar to our previous study with "R^{352}AGLFQRS^{359}" deletion, we observe that mutation of the entire motif to alanine ($PAR4^{R352\text{-}S359A}$-YFP) significantly decreased both AYPGKF-NH_2- (EC_{50} = *n.d.*, Max. = 2.5 ± 2.5%, Figure 4.2A; where "Max." represents mean ± SEM of percent of A23187 calcium signal at 300 µM AYPGKF-NH_2 or 10 units/mL thrombin) and thrombin-stimulated (EC_{50} = *n.d.*, Max. = 6.1 ± 1.0%, Figure 4.1B) calcium signalling compared to wild-type PAR4-YFP (AYPGKF-NH_2 EC_{50} = 26.7 ± 9.6 µM, Max. = 26.3 ± 2.5%, Figure 4.1A; thrombin EC_{50} = 0.3 ± 0.1 units/mL, Max. = 14.8 ± 1.4%, Figure 4.1B) (Table 4.1). Therefore, we conclude that residues with the Helix-8 "R^{352}AGLFQRS^{359}" motif is involved in agonist-stimulated calcium signalling from PAR4.

To determine which of these Helix-8 residues, if not all, are involved in PAR4-mediated calcium signalling we recorded agonist-stimulated calcium signalling from PAR4 receptor mutants with sequential Helix-8 mutations. We observed no significant

difference in calcium signalling from Arg^{352}-Gly^{354}Ala mutation (AYPGKF-NH_2 EC_{50} = 15.6 ± 5.0 μM, Max. = 19.7 ± 1.5%, Figure 4.1A; thrombin EC_{50} = 0.4 ± 0.2 units/mL Max. = 14.5 ± 2.2%, Figure 4.1B; Table 4.1) compared to wild-type PAR4-YFP. Similarly, we observed no defect in calcium signalling in PAR4 receptor with Arg^{358}-Ser^{359}Ala mutation in response to either AYPGKF-NH_2 (EC_{50} = *n.d.*, Max. = 25.8 ± 0.6%, Figure 4.1A) or thrombin (EC_{50} = *n.d.*, Max. = 13.9 ± 0.5%, Figure 4.1B) (Table 4.1). Interestingly, mutation of Leu^{355}-Gln^{357} to alanine significantly decreased calcium signalling in response to both AYPGKF-NH_2 (EC_{50} = *n.d.*, Max. = 7.4 ± 1.9%, Figure 4.1A) thrombin (EC_{50} = *n.d.*, Max. = 2.9 ± 2.8%, Figure 4.1B) (Table 4.1). Therefore, we conclude that the loss of calcium signalling, previously reported with the Helix-8 "R^{352}AGLFQRS^{359}" motif deletion (22) and full motif mutation to alanine in the current study, is not due to truncation or shortening of the C-tail; rather, the deficits in calcium signalling appear to be mediated through loss of effector interactions with this site. Thus, Helix-8 Leu^{355}-Gln^{357} residues are involved in agonist-stimulated calcium signalling downstream of activated PAR4. Further, since these findings were consistent with both peptide and thrombin activation of PAR4, we propose that these residues are important for appropriate activation of the $G\alpha_{q/11}$-mediated calcium signalling pathway downstream of PAR4 activation, independent of which agonist is applied.

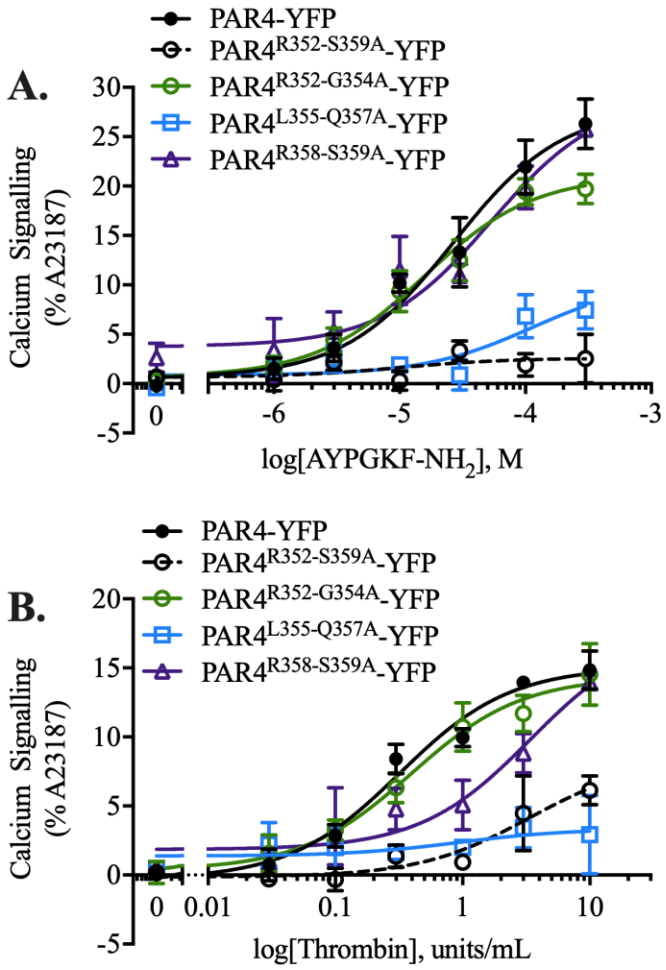

Figure 4.1 Helix-8 Leu^{355}-Gln^{357} are necessary for appropriate AYPGKF-NH$_2$- or thrombin-stimulated PAR4-mediated calcium signalling. Calcium signalling from wild-type PAR4-YFP and R^{352}AGLFQRS^{359} mutant PAR4 receptors in response to AYPGKF-NH$_2$ (A) or thrombin (B) stimulation. Signalling downstream of both peptide (A) and thrombin (B) activation of the PAR4$^{L355\text{-}Q357A}$-YFP receptor mutant was significantly decreased compared to wild-type receptor, comparable to the deficit observed with the PAR4$^{R352\text{-}S359A}$-YFP complete Helix-8 Arg^{352}-Ser^{359}Ala sequence mutation. Nonlinear regression curve fits are shown (mean ± S.E.) for three independent experiments. (*n = 3*)

Table 4.1 Summary table of calcium signalling in HEK-293 cells expressing wild-type or Helix-8 "R^{352}AGLFQRS^{359}" sequence mutants in response to receptor activation with either peptide (AYPGKF-NH_2) or thrombin-revealed tethered ligand.

	AYPGKF-NH_2		Thrombin	
	Ca^{2+} EC_{50} (μM)	**Ca^{2+} Max. (% A23187)**	**Ca^{2+} EC_{50} (μM)**	**Ca^{2+} Max. (% A23187)**
PAR4-YFP	26.7 ± 9.6	26.3 ± 2.5	0.3 ± 0.1	14.8 ± 1.4
$PAR4^{R352\text{-}S359A}$-YFP	*n.d.*	2.5 ± 2.5*	*n.d.*	6.1 ± 1.0*
$PAR4^{R352\text{-}G354A}$-YFP	15.6 ± 5.0	19.7 ± 1.5	0.4 ± 0.2	14.5 ± 2.2
$PAR4^{L355\text{-}Q357A}$-YFP	*n.d.*	7.4 ± 1.9*	*n.d.*	2.9 ± 2.8*
$PAR4^{R358\text{-}S359A}$-YFP	*n.d.*	25.8 ± 0.6	*n.d.*	13.9 ± 0.5

EC_{50} not determined (*n.d.*). Statistical analysis for EC_{50} was conducted by sum of least squares analysis (Prism 7). Statistical analysis for maximal calcium signal obtained was conducted by two-tailed t-test on calcium signalling data (% A23187, 3 μM) collected for the highest concentration tested in the study (AYPGKF-NH_2 300 μM, thrombin 10 units/mL; mean ± S.E. shown). Statistical significance is shown (*$p < 0.05$ compared to wild-type). (*n = 3*)

4.3.2 β-arrestin-1 and -2 recruitment to PAR4 involves Helix-8 Leu^{355}-Gln^{357} downstream of bothAYPGKF-NH_2 and thrombin stimulation.

Previously, we reported that in addition to defects in agonist-stimulated calcium signalling, deletion of the Helix-8 "R^{352}AGLFQRS^{359}" motif (dRS-PAR4) decreased β-arrestin recruitment to PAR4 (22). As with calcium signalling, we sought to determine the role of Helix-8 mutations on β-arrestin-1/-2 recruitment in response to either peptide- or enzyme-mediated activation of PAR4. As previously demonstrated, β-arrestin-1/-2 recruitment to PAR4 does not saturate in response to either peptide or thrombin activation, therefore the data presented throughout for β-arrestin recruitment are presented as the net BRET ratio at the highest concentration tested for each agonist for comparison between receptors (AYPGKF-NH_2 300 μM, thrombin 10 units/mL). In response to AYPGKF-NH_2-stimulation, we observed β-arrestin-1 (Max. = 0.22 ± 0.01; where "Max." represents mean ± SEM of net BRET at 300 μM AYPGKF-NH_2) and β-arrestin-2 (Max. = 0.29 ± 0.01), again consistent with values previously reported (13, 22). Thrombin-stimulated recruitment of β-arrestin-1 (Max. = 0.18 ± 0.01; where "Max." represents mean ± SEM of net BRET at 10 units/mL thrombin) and β-arrestin-2 (Max. = 0.21 ± 0.01) was also recorded. As previously observed, recruitment of β-arrestin-1/-2 in response to thrombin exhibits decreased maximal recruitment compared to peptide agonism of the receptor (21, 22).

Mutation of the entire Helix-8 "R^{352}AGLFQRS^{359}" sequence to alanine, $PAR4^{R352\text{-}S359A}$-YFP, mirror the findings of our previous study using deletion of these residues – providing confidence that the residues, and not their deletion, were responsible for the effects previously observed. β-arrestin-1/-2 recruitment to $PAR4^{R352\text{-}S359A}$-YFP was significantly decreased in response to both AYPGKF-NH_2 (β-Arr-1 Max. 0.10 ± 0.01, β-Arr-2 Max. 0.11 ± 0.00; Figure 4.2A) and thrombin (β-Arr-1 Max. 0.08 ± 0.01, β-Arr-2 Max. 0.08 ± 0.00; Figure 4.2D) stimulation (Table 4.2). Therefore, we conclude that these residues are indeed involved in β-arrestin-1/-2 recruitment to PAR4.

To determine whether the whole Helix-8 "R^{352}AGLFQRS^{359}" sequence, or a specific subset of these residues, are participating in agonist-stimulated recruitment of β-arrestins, we utilized the sequential Helix-8 mutant receptors and recorded recruitment. The first of these mutations, Arg^{352}-Gly^{354}Ala, significantly increased recruitment of β-arrestin-1 (Max. = 0.24 ± 0.01) and -2 (Max. = 0.29 ± 0.00) compared to wild-type PAR4-YFP in response to AYPGKF-NH_2 stimulation (Figure 4.2B & C; Table 4.2). Interestingly, we observed differential agonist-dependent recruitment of β-arrestins to receptor with Arg^{352}-Gly^{354}Ala mutation ($PAR4^{R352\text{-}G354A}$-YFP) when the receptor was stimulated with thrombin (Table 4.2). Thrombin-stimulated recruitment of β-arrestin-1 to $PAR4^{R352\text{-}G354A}$-YFP (Max. = 0.15 ± 0.01; Figure 4.2E) was not significantly different than wild-type receptor, however, the recruitment of β-arrestin-2 was significantly reduced (Max. = 0.16 ± 0.00; Figure 4.2F). Therefore, these data may represent a varied role for these residues in β-arrestin recruitment that is agonist-dependent.

Leu^{355}-Gln^{357} to alanine mutation ($PAR4^{L355\text{-}Q357A}$-YFP) resulted in decreased β-arrestin-1/-2 recruitment to PAR4 in response to both agonists studied. AYPGKF-NH_2-stimulated recruitment of β-arrestin-1 (Max. = 0.10 ± 0.00; Figure 4.2B) and -2 (Max. = 0.10 ± 0.00; Figure 4.2C) to $PAR4^{L355\text{-}Q357A}$-YFP was significantly reduced compared to wild-type receptor. Further, thrombin-stimulated recruitment of β-arrestin-1 (Max. = 0.10 ± 0.01; Figure 4.2E) and -2 (Max. = 0.08 ± 0.00; Figure 4.2F) was also significantly reduced compared to thrombin-activated PAR4. Given that both peptide- and thrombin-stimulated recruitment of β-arrestins was affected by Leu^{355}-Gln^{357}Ala mutation, we determine a role for these residues in β-arrestin recruitment to PAR4, independent of agonist.

Finally, we evaluated the effect of alanine mutation Arg^{358} and Ser^{359} ($PAR4^{R358\text{-}S359A}$-YFP). We observed that AYPGKF-NH_2-stimulated recruitment of both β-arrestin-1 (Max. = 0.17 ± 0.00; Figure 4.2B) and -2 (Max. = 0.23 ± 0.01; Figure 4.2C) was significantly reduced compared to wild-type receptor (Table 4.2). Interestingly, as observed with Arg^{352}-Gly^{354}Ala mutation, thrombin-stimulated β-arrestin-1 recruitment was unaffected with Arg^{358}-Ser^{359}Ala mutation (Max. = 0.13 ± 0.01; Figure 4.2E);

however, β-arrestin-2 recruitment was significantly reduced Max. = 0.15 ± 0.00; Figure 4.2F) (Table 4.2).

These data highlight an important role for Helix-8 "R^{352}AGLFQRS^{359}" residues in the recruitment of β-arrestins to PAR4. Sequential mutation revealed a role for Leu^{355}-Gln^{357} residues in agonist-stimulated β-arrestin recruitment, regardless of which PAR4-agonist was applied. Thus, these residues may be a key regulatory site for this interaction as the phenotype is observed in response to either agonist tested. Interestingly, the data also reveal key agonist-dependent differences in which residues are important for arrestin recruitment. Peptide-stimulated β-arrestin-1/-2 recruitment to PAR4 was altered by all of the Helix-8 mutations studied, with Leu^{355}-Gln^{357}Ala mutation more deleterious than the other mutations studied ($^{‡}p < 0.05$; Table 4.2). Interestingly, thrombin-stimulated recruitment of β-arrestin-1/-2 was also significantly decreased compared to wild-type receptor, similar to the effect observed with peptide stimulation of this mutant. All mutations studied were significantly deleterious to β-arrestin-2 recruitment downstream of thrombin-activation of the receptor; however, only Leu^{355}-Gln^{357}Ala mutation altered thrombin-stimulated recruitment of β-arrestin-1 in comparison to wild-type receptor (Table 4.2). Thus, these data implicate both an agonist-dependent, and β-arrestin-subtype dependent role for Helix-8 residues in recruitment to activated PAR4.

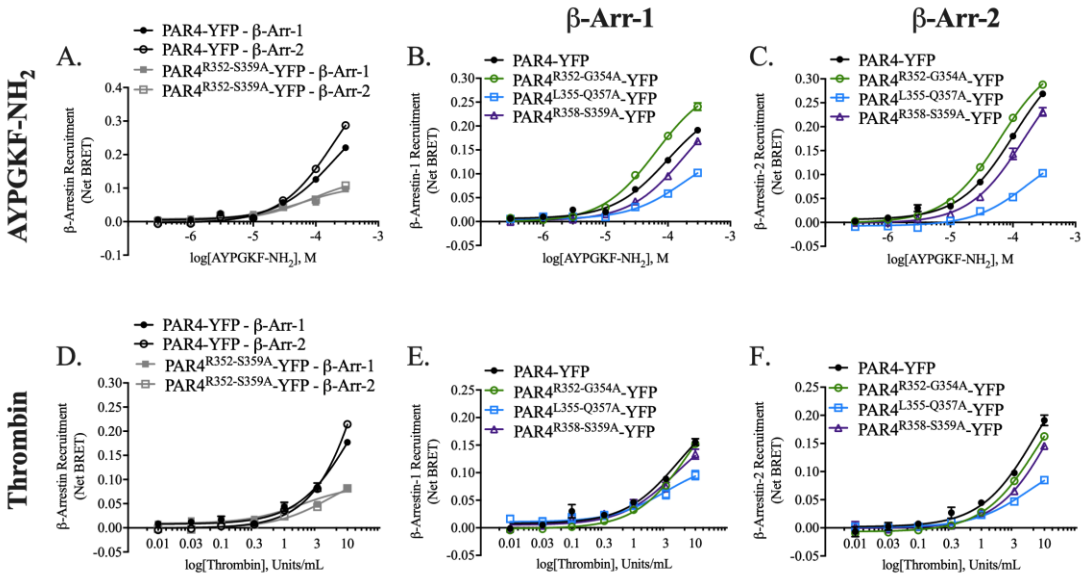

Figure 4.2 β-arrestin-1/-2 recruitment to PAR4 and PAR4 with Helix-8, R^{352}AGLFQRS^{359}, mutations in response to stimulation with AYPGKF-NH_2 (A-C) or tethered ligand revealed by thrombin (D-F) reveals Leu^{355}-Gln^{357} plays a role in β-arrestin recruitment to PAR4. Recruitment of β-arrestin-1/-2 to PAR4 with mutation of the full R^{352}AGLFQRS^{359} sequence to alanine was significantly decreased in comparison to wild-type PAR4 following stimulation with AYPGKF-NH_2 (A) or thrombin (D). Recruitment of β-arrestin-1 (B) or -2 (C) to PAR4 and sectional R^{352}AGLFQRS^{359} mutations in response to AYPGKF-NH_2. Recruitment of β-arrestin proteins to $PAR4^{L355\text{-}Q357A}$-YFP was significantly decreased, while, recruitment to $PAR4^{R352\text{-}G354A}$-YFP was increased in response to peptide stimulation. Recruitment of β-arrestin-1 (E) or -2 (F) was significantly decreased to PAR4 with Leu^{355}-Gln^{357}Ala mutation compared to wild-type receptor in response to thrombin stimulation. Nonlinear regression curve fits are shown (mean ± S.E.) for three to four independent experiments with triplicate data points for each concentration and receptor collected within each experiment. (*n = 3-4)*

Table 4.2 Summary table of β-arrestin-1 and -2 recruitment with wild-type or Helix-8 "R^{352}AGLFQRS^{359}" sequence mutants in response to receptor activation with either peptide (AYPGKF-NH$_2$) or thrombin-revealed tethered ligand.

	AYPGKF-NH$_2$		Thrombin	
	β-Arr-1 Recruitment	β-Arr-2 Recruitment	β-Arr-1 Recruitment	β-Arr-2 Recruitment
PAR4-YFP	0.22 ± 0.01	0.29 ± 0.01	0.18 ± 0.01	0.21 ± 0.01
PAR4$^{R352\text{-}S359A}$-YFP	0.10 ± 0.01*	0.11 ± 0.00*	0.08 ± 0.01*	0.08 ± 0.00*
PAR4-YFP	0.19 ± 0.01	0.27 ± 0.00	0.16 ± 0.01	0.19 ± 0.01
PAR4$^{R352\text{-}G354A}$-YFP	0.24 ± 0.01*	0.29 ± 0.00*	0.15 ± 0.01	0.16 ± 0.00*
PAR4$^{L355\text{-}Q357A}$-YFP	0.10 ± 0.00*‡	0.10 ± 0.00*‡	0.10 ± 0.01*	0.08 ± 0.00*‡
PAR4$^{R358\text{-}S359A}$-YFP	0.17 ± 0.00*	0.23 ± 0.01*	0.13 ± 0.01	0.15 ± 0.00*

Statistical analysis was conducted by two-tailed t-test on net BRET ratios on data for the highest concentration tested in the study (AYPGKF-NH$_2$ 300 μM, thrombin 10 units/mL; mean ± S.E. shown). Statistical significance is shown (*$p < 0.05$ compared to wild-type; $^{‡}p < 0.05$ compared to PAR4$^{R352\text{-}G354}$-YFP or PAR4$^{R358\text{-}S359A}$-YFP). (*n = 3-4*)

4.3.3 PAR4 stimulated calcium signalling involves Helix-8 Lys^{350} following receptor activation with either AYPGKF-NH_2 or thrombin

Helix-8 and C-terminal tail lysine residues have been shown for many Class A GPCRs to be involved in interactions with both G-proteins and β-arrestins, as well as changes in the activation state of GPCRs (28–30). Specifically, lysine residues located in the Helix-8, which are adjacent to the canonical NPxxY$X_{5,6}$F motif, have been implicated to be a binding site for various G-protein subtypes including G_t, G_i, and G_s (30–33). The PAR4 Helix-8 and C-terminal contains two lysine residues, Lys^{350} (8.53, Ballesteros-Weinstein numbering) and Lys^{367}, which are distal to the PAR4 DPxxY$X_{5,6}$F motif. Given the emerging role for Helix-8 lysine residues in GPCR-G-protein interaction, we investigated $G\alpha_{q/11}$-mediated calcium signalling using our PAR4 receptors with C-terminal tail lysine mutations. Calcium signalling in HEK-293 cells expressing PAR4-YFP was recorded in response to AYPGKF-NH_2- (EC_{50} = 35.9 ± 12.8 μM, Max. = 26.1 ± 2.6%; Figure 4.3A, Table 4.3) or thrombin-stimulation (EC_{50} = 1.3 ± 0.5 units/mL, Max. = 16.2 ± 1.7%; Figure 4.3B, Table 4.3). Cells expressing PAR4 with Helix-8 lysine, Lys^{350}Ala mutation (PAR4^{K350A}-YFP) had significantly decreased calcium signalling in response to both AYPGKF-NH_2 (EC_{50} = *n.d.*, Max. = 8.5 ± 1.8%; Figure 4.3A, Table 4.3) and thrombin (EC_{50} = *n.d.*, Max. = 4.3 ± 0.7%; Figure 4.3B, Table 4.3). Thus, PAR4 Helix-8 Lys^{350} may be a site for effector interaction or receptor activation states, as is observed for some class A GPCRs.

Interestingly, calcium signalling in cells expressing the distal C-terminal lysine PAR4-mutant (PAR4^{K367A}-YFP) was unexpectedly decreased following receptor stimulation with AYPGKF-NH_2 (EC_{50} = *n.d.*, Max. = 10.6 ± 4.4%; Figure 4.3A, Table 4.3); however, was not significantly altered in response to thrombin-stimulation (EC_{50} = 0.5 ± 0.3, Max. = 10.8 ± 1.9%; Figure 4.3B, Table 4.3). Combination of these lysine mutations (PAR4$^{K350A,\ K367A}$-YFP) also significantly reduced agonist-stimulated calcium signalling in response to AYPGKF-NH_2 activation of the receptor (Max. 4.0 ± 1.7%; Figure 4.3A, Table 4.3) compared to wild-type receptor, however, the decrease was not more deleterious than mutation of Lys^{350}Ala ($p = 0.12$) or Lys^{367}Ala ($p = 0.21$), alone. Interestingly, we did not detect any statistically significant differences with mutation of

either Lys^{367}Ala or combined mutation (EC_{50} = 1.8 ± 2.0 units/mL, Max. = 8.2 ± 3.0%) in response to thrombin stimulation of these receptors compared to wild-type (Figure 4.3B, Table 4.3).

These data implicate a previously unreported role of Helix-8 Lys^{350} in PAR4 $G\alpha_{q/11}$-mediated calcium signalling downstream of PAR4 activation with either agonist peptide-mediated or thrombin cleavage-mediated activation of calcium signalling. Whether the residue is involved in direct effector binding or a structural interaction with other active state receptor motifs, such as the $NPxxYx_{4,5}F$ motif or through receptor post-translational modifications (e.g. ubiquitination), remains to be explored. Additionally, the role of the more distal Lys^{367} in peptide-activated PAR4 could provide some insight into key differences in effector signalling between peptide-activated and thrombin-activated PAR4.

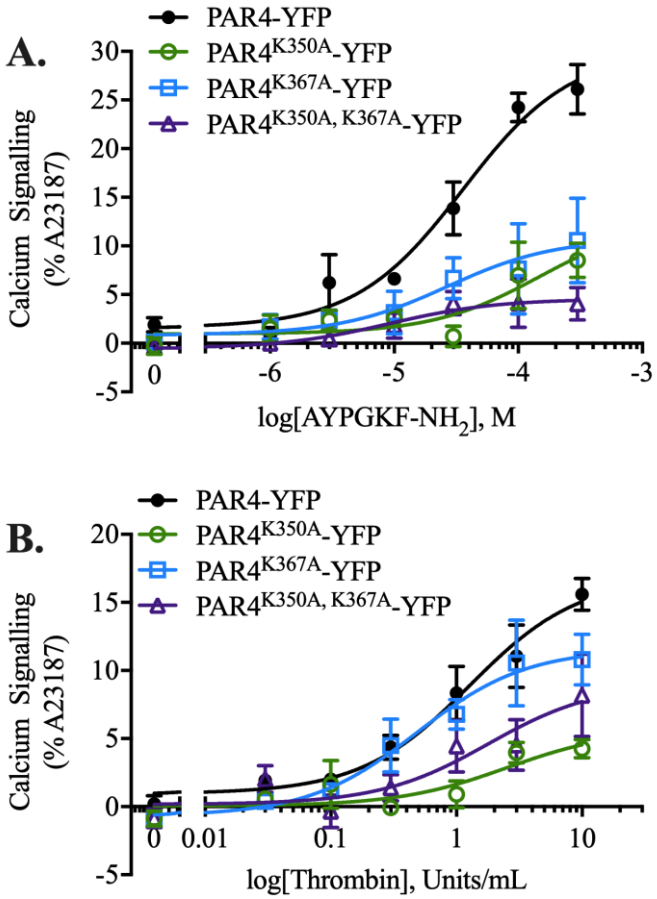

Figure 4.3 C-terminal tail lysine residues, Lys^{350} (Helix-8), is necessary for appropriate AYPGKF-NH$_2$- or thrombin-stimulated, PAR4-mediated, calcium signalling. AYPGKF-NH$_2$-stimulated calcium signalling from wild-type PAR4-YFP and C-terminal tail lysine mutant PAR4 receptors are significantly decreased compared to wild-type receptor (A). Thrombin-stimulated calcium signalling was significantly decreased to PAR4 receptor with Lys^{350}Ala mutation, but not Lys^{367}Ala mutation, with no additive detriment to combined mutation of both residues (B). Nonlinear regression curve fits are shown (mean ± S.E.) for three to four independent experiments. (*n = 3-4*)

Table 4.3 Summary table of calcium signalling in HEK-293 cells expressing wild-type or C-terminal tail lysine residue mutations in response to receptor activation with either peptide (AYPGKF-NH_2) or thrombin-revealed tethered ligand.

	AYPGKF-NH_2		Thrombin	
	Ca^{2+} EC_{50} (μM)	**Ca^{2+} Max. (% A23187)**	**Ca^{2+} EC_{50} (μM)**	**Ca^{2+} Max. (% A23187)**
PAR4-YFP	35.9 ± 12.8	26.1 ± 2.6	1.3 ± 0.5	16.2 ± 1.7
$PAR4^{K350A}$-YFP	*n.d.*	8.5 ± 1.8*	*n.d.*	4.3 ± 0.7*‡
$PAR4^{K367A}$-YFP	*n.d.*	10.6 ± 4.4*	0.5 ± 0.3	10.8 ± 1.9
$PAR4^{K350A, K367A}$-YFP	9.1 ± 10.2	4.0 ± 1.7*	1.8 ± 2.0	8.2 ± 3.0

EC_{50} not determined (*n.d.*). Statistical analysis for EC_{50} was conducted by sum of least squares analysis (Prism 7). Statistical analysis for maximal calcium signal obtained was conducted by two-tailed t-test on calcium signalling data (% A23187, 3 μM) collected for the highest concentration tested in the study (AYPGKF-NH_2 300 μM, thrombin 10 units/mL; mean ± S.E. shown). Statistical significance is shown (*$p < 0.05$ compared to wild-type; ‡$p < 0.05$ compared to $PAR4^{K367A}$-YFP). (*n = 3-4*)

4.3.4 Importance of Lys^{350} in AYPGKF-NH_2- and thrombin-stimulated β-arrestin-1 and -2 recruitment revealed by PAR4 C-tail lysine mutants

Lysine residues located in the Helix-8, adjacent to the canonical $NPxxYX_{5,6}F$ motif, have also been implicated to have a role in interactions with the β-arrestin finger-loop, assisting the β-arrestin proteins in recognizing an active conformation of the receptor. To determine if these C-terminal tail lysine residues play a role in β-arrestin recruitment to activated PAR4, we recorded β-arrestin recruitment to $PAR4^{K350A}$-YFP and $PAR4^{K367A-YFP}$. Lys^{350}Ala significantly reduced agonist-stimulated β-arrestin recruitment to PAR4 in response to AYPGKF-NH_2 stimulation ($PAR4^{K350A}$-YFP, β-Arr-1 Max. = 0.13 ± 0.00, β-Arr-2 Max. = 0.16 ± 0.01) compared to wild-type PAR4-YFP (β-Arr-1 Max. = 0.24 ± 0.00, β-Arr-2 Max. = 0.29 ± 0.01) (Figure 4.4A, Table 4.4). Additionally, thrombin-stimulated β-arrestin recruitment was also significantly decreased to $PAR4^{K350A}$-YFP (β-Arr-1 Max. = 0.12 ± 0.00, β-Arr-2 Max. = 0.12 ± 0.00) compared to wild-type receptor (β-Arr-1 Max. = 0.18 ± 0.01, β-Arr-2 Max. = 0.20 ± 0.00) (Figure 4.4D, Table 4.4).

As mentioned, the C-tail of PAR4 contains one additional, non-helix-8 lysine residue, Lys^{367}. Lys^{367}Ala mutation had no effect on agonist-stimulated β-arrestin recruitment to the receptor compared to wild-type receptor in response to either AYPGKF-NH_2 (β-Arr-1 Max. = 0.22 ± 0.01, β-Arr-2 Max. = 0.32 ± 0.01; Figure 4.4B) or thrombin (β-Arr-1 Max. = 0.19 ± 0.01, β-Arr-2 Max. = 0.26 ± 0.02; Figure 4.4E) compared to wild-type receptor (AYPGKF-NH_2 β-Arr-1 Max. = 0.22 ± 0.01, β-Arr-2 Max. = 0.29 ± 0.01, Figure 4.4B; thrombin β-Arr-1 Max. = 0.19 ± 0.01, β-Arr-2 Max. = 0.23 ± 0.01, Figure 4.4E) (Table 4.4).

Interestingly, combined mutation of both lysine residues ($PAR4^{K350A, K367A}$-YFP), reveals some agonist specific differences for β-arrestin recruitment to the receptor. In response to peptide agonism of the double mutant receptor, β-arrestin-1 recruitment was significantly decreased when compared to Lys^{350}Ala mutation alone (Max. = 0.12 ± 0.00, Table 4.4); however, β-arrestin-2 recruitment was not significantly more decreased than single mutation of the Helix-8 lysine (Max. = 0.17 ± 0.01, p = 0.07). Oppositely, thrombin-

stimulated β-arrestin-1 recruitment was not significantly more reduced that with the single Lys^{350}Ala mutation alone (Max. = 0.12 ± 0.01, p = 0.95; Figure 4.4C, Table 4.4), however, β-arrestin-2 recruitment was not as reduced as with the Lys^{350}Ala mutation alone (Max. = 0.16 ± 0.01; Figure 4.4F, Table 4.4). Thus, the Helix-8 Lys^{350} residue appears to have a role in agonist-stimulated β-arrestin recruitment. Additionally, there may be a role for the distal Lys^{367} in agonist-dependent or subtype specific differential recruitment of β-arrestins.

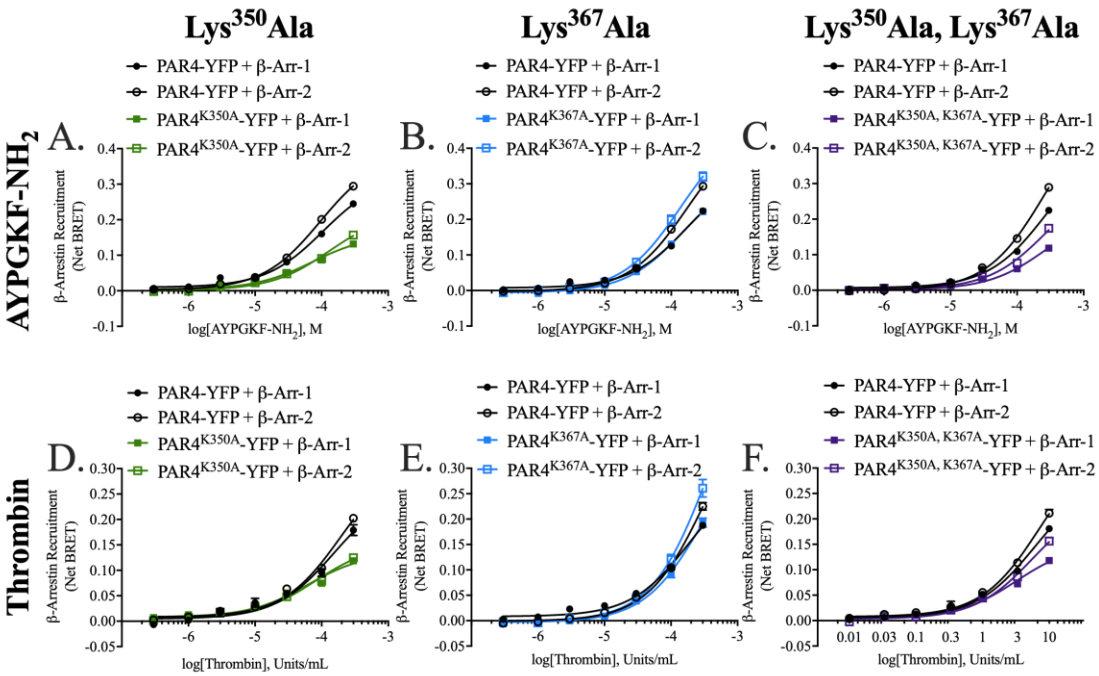

Figure 4.4 Lys^{350} is involved in β-arrestin-1 and -2 recruitment to PAR4 in response to AYPGKF-NH$_2$ or thrombin activation. β-arrestin-1/-2 recruitment to PAR4 and PAR4 with C-terminal tail lysine residue mutations in response to peptide (A-C) or thrombin (D-F) stimulation. Recruitment of β-arrestin-1/-2 recruitment to PAR4 with mutation of Helix-8 Lys^{350} to alanine was significantly decreased compared to wild-type PAR4-YFP in response to receptor activation with either AYPGKF-NH$_2$ (A) or thrombin (D). C-terminal tail mutation Lys^{367}Ala reveals no role for Lys^{367} in β-arrestin-1/-2 recruitment following receptor stimulation with either AYPGKF-NH$_2$ (B) or thrombin (E). As expected, given the decreased recruitment observed with Lys^{350}Ala, combined mutation of both Lys^{350}/Lys^{367} to alanine was significantly reduced β-arrestin-1/-2 recruitment compared to PAR4-YFP in response to AYPGKF-NH$_2$ (C) or thrombin (F). Nonlinear regression curve fits are shown (mean ± S.E.) for three to four independent experiments with triplicate data points for each concentration and receptor collected within each experiment. (*n = 3)*

Table 4.4 Summary table of β-arrestin-1 and -2 recruitment, with wild-type or C-terminal tail lysine residue (Lys^{350}, Lys^{367}) mutations, in response to receptor activation with either peptide (AYPGKF-NH_2) or thrombin-revealed tethered ligand.

	AYPGKF-NH_2		Thrombin	
	β-Arr-1 Recruitment	β-Arr-2 Recruitment	β-Arr-1 Recruitment	β-Arr-2 Recruitment
PAR4-YFP	0.24 ± 0.00	0.29 ± 0.01	0.18 ± 0.01	0.20 ± 0.00
PAR4^{K350A}-YFP	0.13 ± 0.00*	0.16 ± 0.01*	0.12 ± 0.00*	0.12 ± 0.00*
PAR4-YFP	0.22 ± 0.01	0.29 ± 0.01	0.19 ± 0.01	0.23 ± 0.01
PAR4^{K367A}-YFP	0.22 ± 0.01	0.32 ± 0.01	0.19 ± 0.01	0.26 ± 0.02
PAR4-YFP	0.22 ± 0.01	0.29 ± 0.01	0.18 ± 0.00	0.21 ± 0.01
PAR4$^{K350A, K367A}$-YFP	0.12 ± 0.00*‡	0.17 ± 0.01*	0.12 ± 0.01*	0.16 ± 0.01*‡

Statistical analysis was conducted by two-tailed t-test on net BRET ratios on data for the highest concentration tested in the study (AYPGKF-NH_2 300 μM, thrombin 10 units/mL; mean ± S.E. shown). Statistical significance is shown (*$p < 0.05$ compared to wild-type). (*n = 3*)

4.3.5 DPxxYx$_6$F motif residues, Tyr^{340} and Phe^{347}, are necessary for G$\alpha_{q/11}$-mediated calcium signalling from activated PAR4.

Helix-8 and C-terminal tail residues have been shown for many Class A GPCRs to be involved in both interactions with β-arrestins and G-proteins and changes in the activation state of the GPCR (28–30). Many Class A GPCRs possess a canonical NPxxYX$_{5,6}$F motif/domain, spanning TM7 and Helix-8, including Asn$^{7.49}$, Pro$^{7.50}$, Tyr$^{7.53}$, and Helix-8 Phe$^{8.50}$. This motif is thought to be involved in stabilizing the inactive state of Class A GPCRs. Additionally, mutational studies have demonstrated deficits in G-protein activation and signalling when Tyr$^{7.53}$ and Phe$^{8.50}$ are mutated to alanine (34, 35). In PAR4, the NPxxYx$_{5,6}$F motif is D$^{7.49}$PFIY$^{7.53}$YYVSAEF$^{8.50}$. To determine if there is similar role for Tyr$^{7.53}$ and Phe$^{8.50}$ in PAR4-mediated activation of G$\alpha_{q/11}$, single amino acid mutations of Tyr^{340} (PAR4^{Y340A}-YFP) and Phe^{347} (PAR4^{F347A}-YFP) to alanine were generated.

Calcium signalling in HEK-293 cells expressing PAR4-YFP was recorded in response to AYPGKF-NH$_2$- (EC$_{50}$ = 19.4 ± 8.4 μM, Max. = 20.6 ± 1.8%; Figure 4.5A, Table 4.5) or thrombin-stimulation (EC$_{50}$ = 0.4 ± 0.2 units/mL, Max. = 19.4 ± 2.6%; Figure 4.5B, Table 4.5). Cells expressing PAR4 with mutation of TM7, Tyr^{340}Ala (PAR4^{Y340A}-YFP) had significantly decreased calcium signalling in response to both AYPGKF-NH$_2$ (EC$_{50}$ = *n.d.*, Max. = 0.9 ± 2.4%; Figure 4.5A, Table 4.5) and thrombin (EC$_{50}$ = *n.d.*, Max. = 2.8 ± 0.5%; Figure 4.5B, Table 4.5). To determine whether the loss of function observed with PAR4^{Y340A}-YFP is due to the loss of interaction with the Helix-8 Phe^{347} residue, as would be expected as part of a traditional NPxxY$_6$F motif, we generated a concomitant Phe^{347}Ala mutant receptor and recorded calcium signalling. Similar to the deficits observed with Tyr^{340}Ala mutation, PAR4^{F347A}-YFP mutation significantly abrogated calcium signalling downstream of PAR4 activation with both AYPGKF-NH$_2$ (EC$_{50}$ = *n.d.*, Max. = 5.1 ± 2.4%; Figure 4.5A, Table 4.5) and thrombin (EC$_{50}$ = *n.d.*, Max. = 4.1 ± 0.3%; Figure 4.5B, Table 4.5) stimulation. Thus, TM7 Tyr^{340} appears to perform an integral role in the DPxxYx$_6$F motif in PAR4 through association with Helix-8 Phe^{347}.

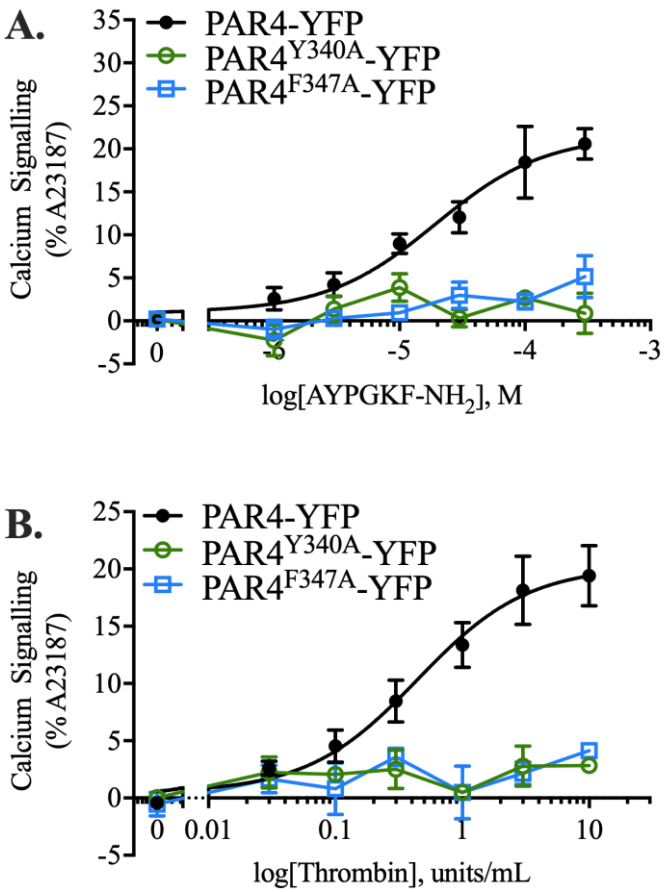

Figure 4.5 Mutation of PAR4 DPxxYx$_6$F motif residues, Tyr^{340} and Phe^{347}, abrogates both peptide- (AYPGKF-NH$_2$) and enzyme-stimulated (thrombin) G$\alpha_{q/11}$ calcium signalling. Calcium signalling from DPxxYx$_6$F motif mutant PAR4 receptors, PAR4^{Y340A}-YFP and PAR4^{F347A}-YFP, are significantly decreased compared to wild-type receptor in response to both peptide-stimulation (AYPGKF-NH$_2$) (A) and enzyme-cleavage (thrombin) (B). Nonlinear regression curve fits are shown (mean ± S.E.) for three independent experiments. (*n = 3*)

Table 4.5 Summary table of calcium signalling in HEK-293 cells expressing wild-type or DPxxYx$_6$F motif residue mutations, Tyr^{340}Ala and Phe^{347}Ala, in response to receptor activation with either peptide (AYPGKF-NH$_2$) or thrombin-revealed tethered ligand.

	AYPGKF-NH$_2$		Thrombin	
	Ca^{2+} EC_{50} (μM)	**Ca^{2+} Max. (% A23187)**	**Ca^{2+} EC_{50} (units/mL)**	**Ca^{2+} Max. (% A23187)**
PAR4-YFP	19.4 ± 8.4	20.6 ± 1.8	0.4 ± 0.2	19.4 ± 2.6
PAR4^{Y340A}-YFP	*n.d.*	0.9 ± 2.4*	*n.d.*	2.8 ± 0.5*
PAR4^{F347A}-YFP	*n.d.*	5.1 ± 2.4*	*n.d.*	4.1 ± 0.3*

EC_{50} not determined (*n.d.*). Statistical analysis for EC_{50} was conducted by sum of least squares analysis (Prism 7). Statistical analysis for maximal calcium signal obtained was conducted by two-tailed t-test on calcium signalling data (% A23187, 3 μM) collected for the highest concentration tested in the study (AYPGKF-NH$_2$ 300 μM, thrombin 10 units/mL; mean ± S.E. shown). Statistical significance is shown (*$p < 0.05$ compared to wild-type). ($n = 3$)

4.3.6 The role of DPxxYx$_6$F motif residues, Tyr^{340} and Phe^{347}, in β-arrestin-1/-2 recruitment to activated PAR4.

To determine whether there are any alterations in the recruitment of β-arrestin-1/-2 to PAR4 NPxxYx$_6$F mutants of Tyr$^{7.53}$ (Tyr^{340}Ala) and Phe$^{8.50}$ (Phe^{347}Ala), β-arrestin recruitment was measured. Tyr^{340}Ala mutation significantly reduced agonist-stimulated β-arrestin recruitment to PAR4 in response to AYPGKF-NH_2 stimulation (β-Arr-1 Max. = 0.09 ± 0.00, β-Arr-2 Max. = 0.10 ± 0.00) compared to wild-type PAR4-YFP (β-Arr-1 Max. = 0.19 ± 0.01, β-Arr-2 Max. = 0.25 ± 0.01) (Figure 4.6A & B, Table 4.6). Interestingly, Phe^{347}Ala mutation yielded almost superimposable deficits in peptide-stimulated β-arrestin recruitment, when compared to Tyr^{340}Ala mutation (Phe^{347}Ala, β-Arr-1 Max. = 0.09 ± 0.00, β-Arr-2 Max. = 0.09 ± 0.01) (Figure 4.6A & B, Table 4.6).

Given the reduced recruitment observed with these mutations in response to peptide stimulation of the receptor, we next determined if there were any impacts on β-arrestin recruitment to tethered ligand activation of PAR4 via thrombin cleavage. Similar to the decreases observed with peptide stimulation, β-arrestin-1/-2 recruitment was significantly reduced in both PAR4^{Y340A}-YFP (β-Arr-1 Max. = 0.09 ± 0.00, β-Arr-2 Max. = 0.09 ± 0.00) and PAR4^{F347A}-YFP (β-Arr-1 Max. = 0.08 ± 0.00, β-Arr-2 Max. = 0.09 ± 0.00) mutants compared to wild-type receptor (β-Arr-1 Max. = 0.19 ± 0.01, β-Arr-2 Max. = 0.24 ± 0.01) when stimulated with thrombin (Figure 4.6C & D, Table 4.6).

Given the significant reduction in β-arrestin recruitment observed with both thrombin- and peptide-stimulated PAR4 containing these mutations, these data suggest that Tyr^{340} and Phe^{347} are key residues in the TM7/Helix-8 interactions governing β-arrestin recruitment. Further, given the almost superimposable reductions of both Tyr^{340}Ala and Phe^{347}Ala, these data implicate an interaction between these two residues as a part of the DPxxYx$_6$F motif in PAR4 which is important for both G-protein activation and β-arrestin recruitment.

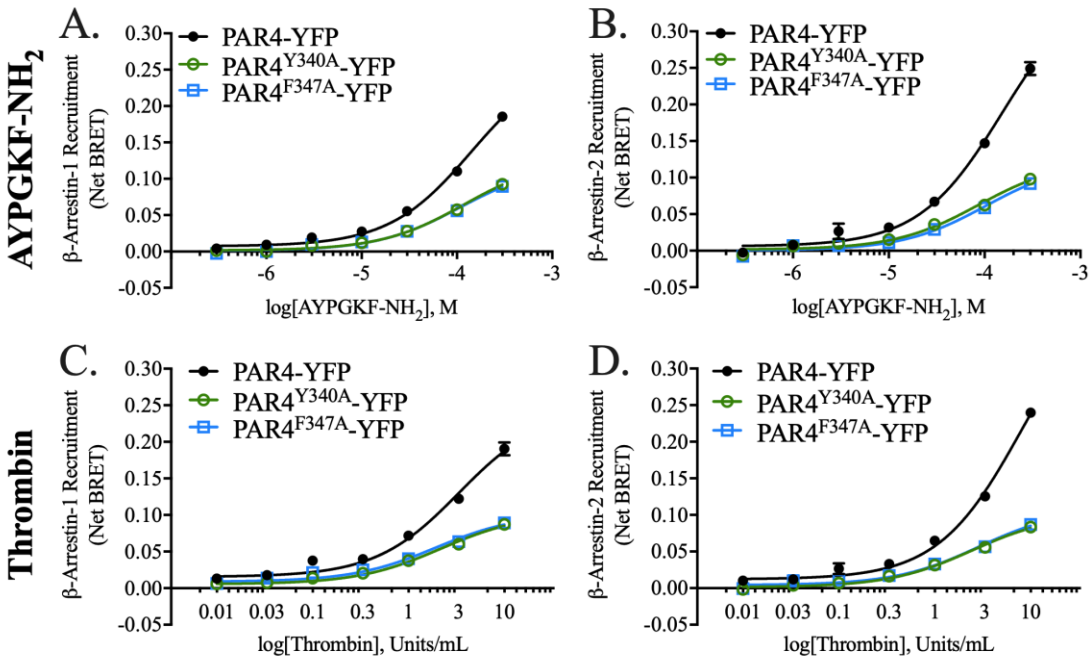

Figure 4.6 PAR4 DPxxYx$_6$F mutations, Tyr^{340}Ala and Phe^{347}Ala, are detrimental to β-arrestin-1/-2 recruitment with either peptide- or enzyme-mediated activation of PAR4. β-arrestin-1/-2 recruitment to PAR4 and PAR4 with DPxxYx$_6$F residue mutations, Tyr^{340}Ala or Phe^{347}Ala, in response to peptide (A-B) or thrombin (C-D) stimulation. Recruitment of β-arrestin-1 recruitment to wild-type and mutant PAR4 receptors with either AYPGKF-NH$_2$ (A) or thrombin (C) reveal that both Tyr^{340} and Phe^{347} are important residues for β-arrestin recruitment. Further, β-arrestin-2 recruitment was similarly reduced in response to peptide (B) or thrombin (D) stimulation. Nonlinear regression curve fits are shown (mean ± S.E.) for three independent experiments with triplicate data points for each concentration and receptor collected within each experiment. (*n = 3)*

Table 4.6 Summary table of β-arrestin-1 and -2 recruitment, with wild-type or DPxxYx$_6$F mutants (Tyr^{340}Ala, Phe^{347}Ala) mutations, in response to receptor activation with either peptide (AYPGKF-NH$_2$) or thrombin-revealed tethered ligand.

	AYPGKF-NH$_2$		Thrombin	
	β-Arr-1 Recruitment	β-Arr-2 Recruitment	β-Arr-1 Recruitment	β-Arr-2 Recruitment
PAR4-YFP	0.19 ± 0.01	0.25 ± 0.01	0.19 ± 0.01	0.24 ± 0.01
PAR4^{Y340A}-YFP	0.09 ± 0.00*	0.10 ± 0.00*	0.09 ± 0.00*	0.08 ± 0.00*
PAR4^{F347A}-YFP	0.09 ± 0.00*	0.09 ± 0.01*	0.09 ± 0.00*	0.09 ± 0.00*

Statistical analysis was conducted by two-tailed t-test on net BRET ratios on data for the highest concentration tested in the study (AYPGKF-NH$_2$ 300 μM, thrombin 10 units/mL; mean ± S.E. shown). Statistical significance is shown (*$p < 0.05$ compared to wild-type). (*n = 3*)

4.3.7 Role for “complete” phosphorylation barcode motif and C-tail phosphorylation sites in differential recruitment of β-arrestins to PAR4 dependent on either AYPGKF-NH_2 or thrombin-revealed tethered ligand.

4.3.7.1 Phosphorylation Barcode

A role for phosphorylation-dependent GPCR-mediated recruitment of β-arrestins is well established (36, 37). The importance of phosphorylation codes/motifs in β-arrestin binding and signalling has also been demonstrated for many GPCRs including the β2-adrenergic receptor, rhodopsin receptor and vasopressin receptors (Table 4.7) (38–41). A so-called “complete” barcode motif, involves three phosphorylatable residues interspaced by two residues [Px(x)PxxP, wherein “P” denotes a phosphorylatable serine or threonine residue, and “x” denotes any other residue], which have been shown to be a key component of receptor C-tail/arrestin interaction (42). Additionally, partial barcode motifs have been identified wherein a phosphorylatable residue spot within the motif is occupied by another residue, frequently an acidic residue (42). Phosphorylation motifs in the PAR4 C-terminal tail were identified using the PhosCoFinder tool (42) which identified one complete motif and several partial motifs. We focused our study of barcode motifs in the PAR4 C-tail on the complete motif (Thr^{363}/Ser^{366}/Ser^{369}, Table 4.7). β-arrestin recruitment was significantly reduced to $PAR4^{T363A,\ S366A,\ S369A}$-YFP in response to AYPGKF-NH_2 stimulation of the receptor (β-Arr-1 Max. = 0.10 ± 0.01, β-Arr-2 Max. = 0.18 ± 0.02; Figure 4.7A, Table 4.8) compared to wild-type receptor (β-Arr-1 Max. = 0.15 ± 0.01, β-Arr-2 Max. = 0.26 ± 0.02; Figure 4.7A, Table 4.8). Interestingly, in response to thrombin stimulation only β-arrestin-1 recruitment was decreased (Max. = 0.07 ± 0.01) compared to wild-type receptor (Max. = 0.14 ± 0.01) (Figure 4.7B, Table 4.8); while β-arrestin-2 recruitment (Max. = 0.12 ± 0.02) was not statistically different than thrombin-stimulated recruitment to wild-type receptor (Max. = 0.17 ± 0.02) (Figure 4.7B, Table 4.8).

Further studies are needed to fully identify the role of phosphorylation barcodes in the C-terminal tail of PAR4. However, our data reveal that the complete C-tail barcode motif Thr^{363}/Ser^{366}/Ser^{369} is involved in peptide-stimulated recruitment of β-arrestin-1 and -2 to

PAR4 and thrombin-stimulated β-arrestin-1 recruitment. Given that β-arrestin-2 recruitment following thrombin-activation of PAR4 was unaltered in the complete motif mutation, it does not appear that this motif is involved in thrombin-stimulated recruitment of β-arrestin-2. Therefore, this could signal the presence of agonist-dependent differential regulation of β-arrestin subtype recruitment to PAR4; however, a comprehensive mutational study of these motifs would need to be undertaken to determine agonist-dependent interactions between arrestin subtypes and this motif to verify this interaction.

4.3.7.2 Phosphorylation-site-null PAR4 C-tail

Given that we do not observe a complete loss of β-arrestin-1/-2 recruitment with the "complete" barcode motif mutation ($Thr^{363}Ala/Ser^{366}Ala/Ser^{369}Ala$), we generated a mutant PAR4 receptor wherein all of the C-tail serine/threonine residues are mutated to alanine ($PAR4^{0P}$-YFP) to determine if there was any further loss of recruitment (Figure 4.8). Recruitment of β-arrestin-1 to $PAR4^{0P}$-YFP was significantly reduced compared to wild-type receptor, however, was not significantly more detrimental than the barcode motif mutation alone [AYPGKF-NH_2 (β-Arr-1 Max. = 0.11 ± 0.00; p = 0.70 compared to $PAR4^{T363A/S366A/S369A}$-YFP); thrombin (β-Arr-1 Max. = 0.08 ± 0.01; p = 0.35 compared to $PAR4^{T363A/S366A/S369A}$-YFP] (Figure 4.9A-B, Table 4.8). Additionally, β-arrestin-2 recruitment in response to thrombin stimulation of PAR4 was significantly decreased compared to wild-type receptor, however, not more so than the barcode mutation alone (β-Arr-2 Max. = 0.10 ± 0.00; p = 0.23 compared to $PAR4^{T363A/S366A/S369A}$-YFP) (Figure 4.9B, Table 4.8). Interestingly, we observed a further reduction of β-arrestin-2 recruitment to PAR4 in response to peptide stimulation in $PAR4^{0P}$-YFP compared to barcode motif mutation alone (β-Arr-2 Max. = 0.10 ± 0.01; p = 0.01 compared to $PAR4^{T363A/S366A/S369A}$-YFP). These data may therefore highlight a role for agonist-dependent subtype selectivity, as was observed with the mutation of the complete phosphorylation barcode, as well as reveal residues involved in arrestin-subtype selectivity in the C-tail of PAR4. These data, however, should be carefully followed up with a further investigation of which residues may enable this effect.

Table 4.7 Phosphorylation barcodes of PAR4 and other common Class A GPCRs.[†]

Receptor	**Rho**		**V2R**		**β_2AR**		**PAR4**	
Res. ID	**334**	**336**	**355**	**355**	**354**	**391**	**361**	**353**
	S	T	D	D	Y	Q	G	A
	A	V	E	E	S	G	D	G
	T	**S**	**S**	**S**	**S**	**T**	**T**	F
	V	K	C	C	N	V	V	Q
	--	--	T	**T**	G	P	A	R
	S	**T**	**T**	T	N	**S**	**S**	**S**
	K	E	A	A	T	D	K	P
	T	T	S	**S**	G	N	A	G
	E	**S**	**S**	**S**	**E**	I	**S**	**D**
	T	Q	S	S	Q	D	A	T
	S	V	L	L	S	S	E	V
Res. ID	**343**	**345**	**365**	**365**	**364**	**401**	**371**	**364**

[†]Phosphorylation barcodes determined by the PhosCoFinder tool for rhodopsin (Rho), vasopressin (V2R), β_2-adrenergic (β_2AR), and PAR4 receptors. Phosphorylation barcode residues are shown for "complete" (green) and "partial" (orange) motifs.

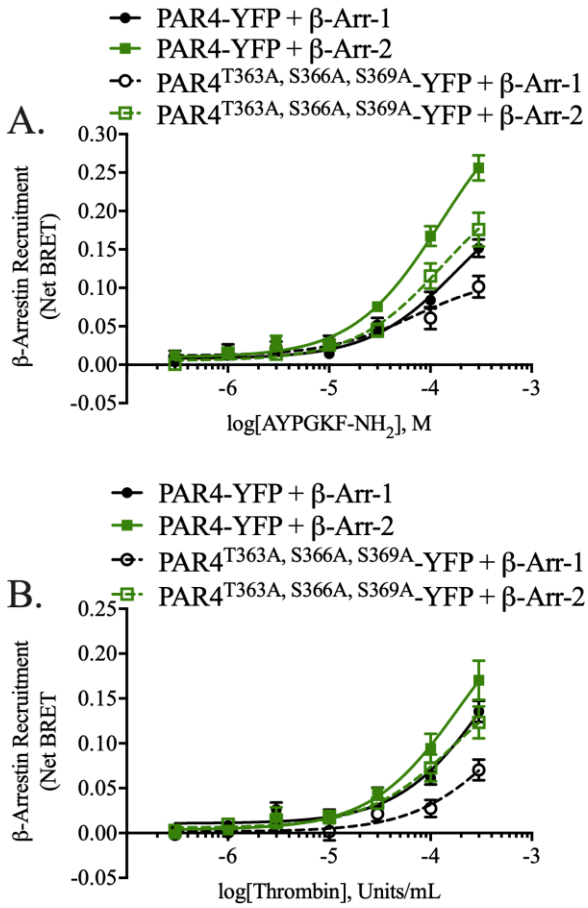

Figure 4.7 Mutation of PAR4 phosphorylation barcode significantly reduces β-arrestin-1/-2 recruitment to peptide-stimulated PAR4. β-arrestin-1/-2 recruitment to PAR4 and PAR4 with complete phosphorylation barcode mutation, $Thr^{363}Ala/Ser^{366}Ala/Ser^{369}Ala$, in response to peptide (A) or thrombin (B) stimulation. Recruitment of β-arrestin-1/-2 recruitment to wild-type and mutant PAR4 receptor with AYPGKF-NH_2 (A) reveals that the complete phosphorylation barcode is important for β-arrestin recruitment. Thrombin recruitment of β-arrestin-1, but not β-arrestin-2, recruitment to $PAR4^{T363A/S366A/S369A}$-YFP receptor is significantly reduced (B). Nonlinear regression curve fits are shown (mean ± S.E.) for three independent experiments with triplicate data points for each concentration and receptor collected within each experiment. (*n = 3-4)*

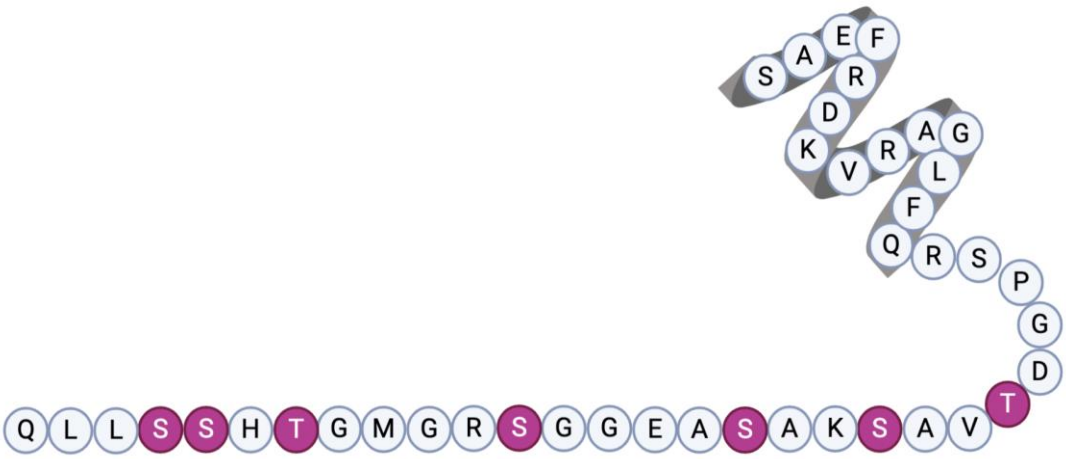

Figure 4.8 Schematic of Helix-8 and C-tail of PAR4, with all modified residues of the PAR4^{0P} mutant receptor. Schematic of the C-tail of PAR4 with all mutated Ser/Thr residues (magenta) in the phosphorylation-site-null mutant PAR4 (PAR4^{0P}-YFP). Created with BioRender.com

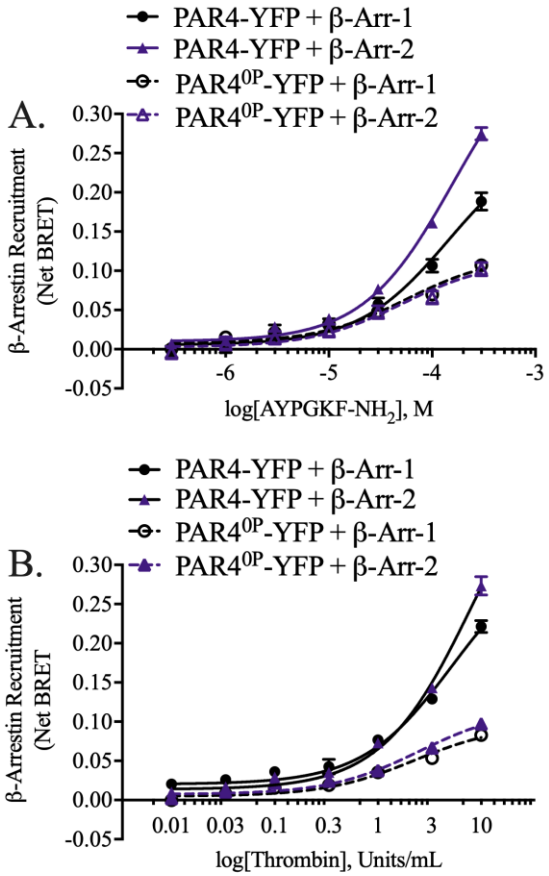

Figure 4.9 Phosphorylation-site-null PAR4 C-tail significantly decreased β-arrestin-1/-2 recruitment to both peptide- and enzyme-activated PAR4. β-arrestin-1/-2 recruitment to PAR4 and PAR4 with all C-tail phosphorylation sites mutated to alanine (PAR4^{0P}-YFP) in response to peptide (A) or thrombin (B) stimulation. Recruitment of β-arrestin-1/-2 recruitment to wild-type and mutant PAR4 receptor with either AYPGKF-NH_2 (A) or thrombin (B) reveals that phosphorylation sites are important regulators of β-arrestin-1/-2 recruitment to activated PAR4. Nonlinear regression curve fits are shown (mean ± S.E.) for three independent experiments with triplicate data points for each concentration and receptor collected within each experiment. (*n = 3)*

Table 4.8 Summary table of β-arrestin-1 and -2 recruitment, with wild-type or C-tail phosphorylation residue mutations (PAR4$^{T363A/S366A/S369A}$-YFP, PAR4^{0P}-YFP), in response to receptor activation with either peptide (AYPGKF-NH_2) or thrombin-revealed tethered ligand.

	AYPGKF-NH_2		Thrombin	
	β-Arr-1 Recruitment	β-Arr-2 Recruitment	β-Arr-1 Recruitment	β-Arr-2 Recruitment
PAR4-YFP	0.15 ± 0.01	0.26 ± 0.02	0.14 ± 0.01	0.17 ± 0.02
PAR4$^{T363A/S366A/S369A}$-YFP	0.10 ± 0.01*	0.18 ± 0.02*	0.07 ± 0.01*	0.12 ± 0.02
PAR4-YFP	0.19 ± 0.01	0.27 ± 0.01	0.22 ± 0.01	0.27 ± 0.01*
PAR4^{0P}-YFP	0.11 ± 0.00*	0.10 ± 0.01*‡	0.08 ± 0.01*	0.10 ± 0.00*

Statistical analysis was conducted by two-tailed t-test on net BRET ratios on data for the highest concentration tested in the study (AYPGKF-NH_2 300 μM, thrombin 10 units/mL; mean ± S.E. shown). Statistical significance is shown (*$p < 0.05$ compared to wild-type, $^{‡}p < 0.05$ compared to PAR4$^{T363A/S366A/S369A}$-YFP). (*n = 3-4*)

4.3.8 Impact of phosphorylation mutations on PAR4-stimulated, $G\alpha_{q/11}$-stimulated calcium signalling.

β-arrestin-mediated desensitization of GPCR G-protein signalling is well-established (43–46). Within the PAR family of receptors, it has been demonstrated that PAR2 phosphorylation is a requirement for β-arrestin recruitment, ultimately leading to desensitization of the receptor (47, 48). In keeping with the well-established role of β-arrestins in GPCR desensitization, we previously demonstrated that of β-arrestin-1/-2 CRISPR/Cas9 knockout HEK-293 cells had both increased and prolonged calcium signalling following PAR2 stimulation (20). Previously, it was reported that serine/threonine C-tail mutations in PAR1 increased G-protein signalling, while analogous mutations to PAR4 had no impact on signalling (49). To determine if a similar mechanism of β-arrestin-mediated receptor desensitization is acting on PAR4, we recorded calcium signalling in our two phosphorylation-site mutant receptors. We observed significant decreases in β-arrestin-1/-2 recruitment to PAR4 phosphorylation site mutations, thus, we expected that if a similar mode of desensitization, as observed with PAR2, is present we should observe increased calcium signalling. $PAR4^{T363A/S366A/S369A}$-YFP-mediated calcium signalling (EC_{50} = 14.0 ± 4.1 μM, Max. = 23.7 ± 3.3%, Figure 4.10A) was not significantly different than wild-type PAR4-YFP receptor (EC_{50} = 21.1 ± 3.5 μM, Max. = 29.6 ± 1.0%; Figure 4.10A, Table 4.9) in response to AYPGKF-NH_2 stimulation (EC_{50} p = 0.22; Max. p = 0.18). Similarly, the EC_{50} of thrombin-stimulated calcium signalling from $PAR4^{T363A/S366A/S369A}$-YFP (EC_{50} = 0.8 ± 0.2 units/mL) was also not significantly different than PAR4-YFP (EC_{50} = 0.5 ± 0.2 units/mL, p = 0.53); however, maximal calcium signal was significantly reduced (Max. = 14.8 ± 0.4%) compared to wild-type receptor (Max. = 17.8 ± 0.8%) (Figure 4.10C, Table 4.9).

When calcium signalling was recorded in the phosphorylation-site-null $PAR4^{0P}$-YFP receptor, neither peptide- (EC_{50} = 20.9 ± 15.3 μM, Max. = 10.9 ± 1.9%; Figure 4.10B, Table 4.9) nor thrombin-stimulated (EC_{50} = 1.4 ± 1.3 units/mL, Max. = 6.9 ± 1.6%; Figure 4.10D, Table 4.9) calcium signalling was different than PAR4-YFP (AYPGKF-NH_2 EC_{50} = 22.6 ± 15.5 μM, Max. = 0.4 ± 0.2%; thrombin EC_{50} = 0.4 ± 0.2 units/mL,

Max. = 10.2 ± 3.0%; Figure 4.10B & D, respectively; Table 4.9). Therefore, unlike PAR2 which had significantly increased and prolonged calcium signalling in the absence of β-arrestins, removal of PAR4-phosphorylation sites, which reduced β-arrestin recruitment, did not significantly increase calcium signalling.

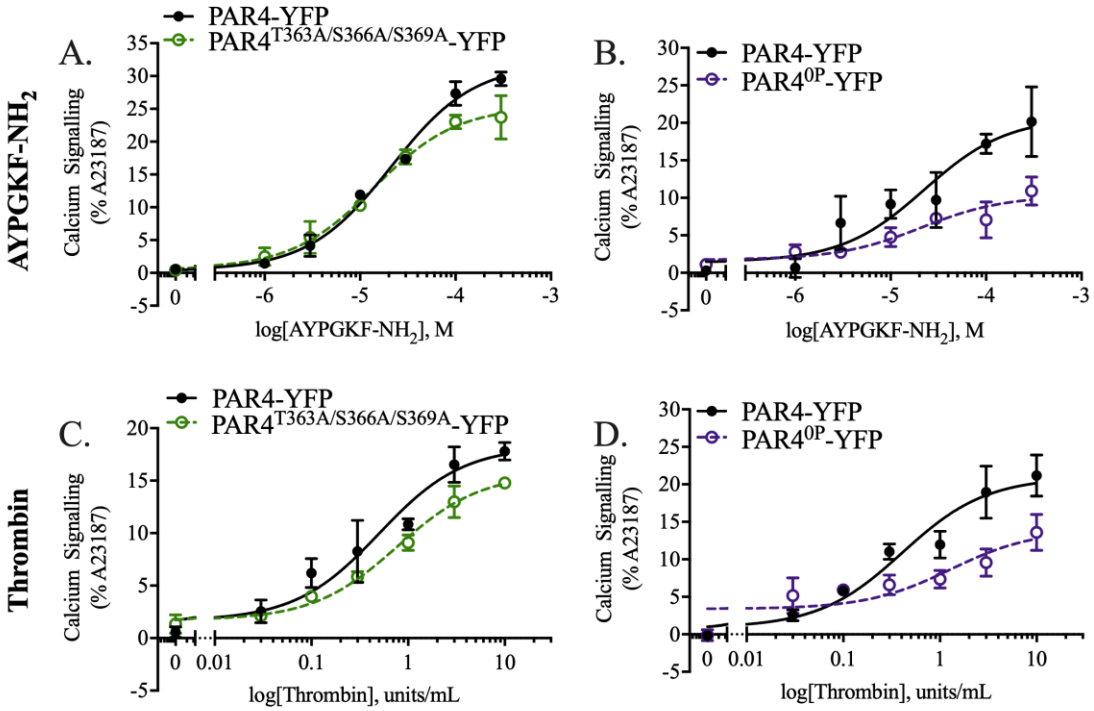

Figure 4.10 Mutation of all possible phosphorylatable residues in the C-tail of PAR4 is deleterious for $G\alpha_{q/11}$-stimulated calcium signalling. Calcium signalling from complete phosphorylation barcode mutant, $PAR4^{T363A/S366A/S369A}$-YFP, is comparable to wild-type receptor response to both peptide-stimulation (AYPGKF-NH_2) (A) and enzyme-cleavage (thrombin) (C). Phosphorylation-site-null PAR4 mutant, PAR^{0P}-YFP, has decreased calcium signalling compared to wild-type receptor in response to stimulation with either AYPGKF-NH_2 (B) or thrombin (D). Nonlinear regression curve fits are shown (mean ± S.E.) for three independent experiments. (*n = 3-4*)

Table 4.9 Summary table of calcium signalling in HEK-293 cells expressing wild-type or phosphorylatable residue mutations in response to receptor activation with either peptide (AYPGKF-NH_2) or thrombin-revealed tethered ligand.

	AYPGKF-NH_2		Thrombin	
	Ca^{2+} EC_{50} (μM)	**Ca^{2+} Max. (% A23187)**	**Ca^{2+} EC_{50} (units/mL)**	**Ca^{2+} Max. (% A23187)**
PAR4-YFP	21.1 ± 3.5	29.6 ± 1.0	0.5 ± 0.2	17.8 ± 0.8
$PAR4^{T363A/S366A/S369A}$-YFP	14.0 ± 4.1	23.7 ± 3.3	0.8 ± 0.2	14.8 ± 0.4*
PAR4-YFP	22.6 ± 15.5	20.1 ± 4.6	0.4 ± 0.2	10.2 ± 3.0
$PAR4^{0P}$-YFP	20.9 ± 15.3	10.9 ± 1.9	1.4 ± 1.3	6.9 ± 1.6

Statistical analysis for EC_{50} was conducted by sum of least squares analysis (Prism 7). Statistical analysis for maximal calcium signal obtained was conducted by two-tailed t-test on calcium signalling data (% A23187, 3 μM) collected for the highest concentration tested in the study (AYPGKF-NH_2 300 μM, thrombin 10 units/mL; mean ± S.E. shown). Statistical significance is shown (*$p < 0.05$ compared to wild-type). (*n = 3-4*)

4.4 Discussion

Here, we examined residues found within the C-terminal tail, including Helix-8, as determinants of PAR4 coupling to two major signalling pathways – $G\alpha_{q/11}$ and β-arrestin. We find that residues in the PAR4 Helix-8 (Lys^{350}, Leu^{355}, Phe^{356}, Gln^{357}) are necessary for appropriate calcium signalling and β-arrestin-1/-2 recruitment. Additionally, we find that a TM7/Helix-8 interaction (Tyr^{340}/Phe^{347}) is important in receptor signalling activity. Additionally, we demonstrate that a phosphorylation barcode (Thr^{363}/Ser^{366}/Ser^{369}) is crucial for β-arrestin-1/-2 recruitment. Interestingly, we also observed key differences in the relative importance of these sites, dependent on whether PAR4 was activated by the proteolytically-revealed tethered ligand or through peptide stimulation. Thus, this study highlights the importance of Helix-8 and C-tail residues in PAR4 signalling as well as underscores the necessity to evaluate how the contributions of these residues differs dependent on the mode of receptor activation.

Helix-8 $R^{352}AGLFQRS^{359}$ Motif

The Helix-8 and C-terminal tail of GPCRs are key sites of recruitment, interaction, and activation of intracellular effectors, such as G-proteins and β-arrestins. Structures of $G\alpha_s$-, $G\alpha_i$-, $G\alpha_o$-, and $G\alpha_q$-bound GPCRs have shown that residues within the Helix-8 of adenosine 2A ($A_{2A}R$), β_2AR, μ-opioid (MOR), adenosine A1 (A_1R), serotonin 1B ($5HT_{1B}R$), rhodopsin, and 5-HT_{2A} receptors make contacts with the α and β (β1 or β2) subunits of their respective G-proteins (50, 51). Additionally, studies of dopamine D1 and D2 receptor Helix-8 chimeras have further shown that the Helix-8 is not involved in dopamine receptor G-protein selectivity; however, significantly reduce β-arrestin-mediated receptor desensitization (52). Previously, we demonstrated that deletion of similar eight amino acid sequence in the Helix-8 of PAR4 ($R^{352}AGLFQRS^{359}$) abrogates $G\alpha_{q/11}$-mediated calcium signalling and significantly decreased β-arrestin-1/-2 recruitment (22). In the current study observed that mutation of this entire sequence to alanine ($PAR4^{R352\text{-}S359A}$-YFP) mimicked the abrogation of calcium signalling and reduced β-arrestin recruitment previously reported.

Previously, residues within the PAR1 Helix-8 (S^{375}SECQRYVYSILCC^{388}) were shown to be necessary for $G\alpha_q$ signalling. Specifically, mutation of hydrophilic residues (Gln^{379}Ala/Arg^{380}Ala) significantly reduced $G\alpha_q$-PLC-β-dependent inositol phosphate production by approximately 25% in response to both thrombin and peptide activation of PAR1 (53). When this mutation was combined with intracellular loop 1 mutant, Lys^{135}Ala, a 40-50% reduction was observed in $G\alpha_q$-PLC-β activity, highlighting the importance of an ICL1/Helix-8 activation motif in PAR1-mediated $G\alpha_q$ activation (53). Mutational studies of the rhodopsin receptor revealed a different mechanism wherein Arg^{314}/Asn^{315} mutation, located at analogous sites to PAR1 Gln^{379}/Arg^{380} (8.51/8.52), had no impact on $G\alpha_t$ activation; however, mutation of hydrophobic residues (Phe^{313}, $Met^{8.54}$) significantly reduced $G\alpha_t$ activation (34, 54). Further, mutation of the analogous PAR1 residues (Cys^{378}, Val^{382}) did not impact $G\alpha_q$-coupling which may suggest a role for Helix-8 in G-protein subtype selectivity (53). Similar to findings with rhodopsin, mutation of hydrophobic residues (Leu^{404}, Phe^{408}, and Phe^{412}) in the Helix-8 of cannabinoid 1 receptor (CB_1) is reported to decreased G-protein activation, while basic residue mutation had no effect (55). In the current study, we identified that the deleterious effects observed in our previous study are mediated by mutation of Leu^{355}-Gln^{357}, as both calcium signalling and β-arrestin-1/-2 recruitment are significantly diminished from activated PAR4. Interestingly, we observed the effect of this mutation on both peptide- and enzyme-activated PAR4, revealing that these residues are key residues for G-protein activation and β-arrestin recruitment, irrespective of the activating ligand. Therefore PAR4, like PAR1, may have a similar requirement of Helix-8 glutamine for efficacious and potent $G\alpha_q$ activation. Like in CB_1, mutation of leucine may remove a necessary hydrophobic residue for G-protein binding and activation (55).

Following a similar strategy, we investigated β-arrestin recruitment to the segmental mutations of the R^{352}AGLFQRS^{359} motif. As we observed with calcium signalling, β-arrestin-1/-2 recruitment was significantly reduced with PAR4 Leu^{355}-Gln^{357}Ala mutation in response to both thrombin and peptide stimulation. Both peptide- and thrombin-stimulated β-arrestin-1 recruitment was decreased to PAR4 with Arg^{358}-Ser^{359}Ala mutation; however, only peptide-stimulated β-arrestin-2 recruitment was diminished in

this mutant. Further, we observed a reduction in thrombin-stimulated β-arrestin-2 recruitment to PAR4 mutant with Arg^{352}-Gly^{354}Ala mutation. Interestingly, Arg^{352}-Gly^{354}Ala mutation enhanced both β-arrestin-1 and -2 recruitment following peptide stimulation. Thus, while the overall decrease observed with Leu^{355}-Gln^{357}Ala mutation may represent a more global phenotype, when considering this mutant also had decreased calcium signalling, there may be a role for other components of the R^{352}AGLFQRS^{359} motif in arrestin-subtype selectivity and agonist-dependent differences in modulation of β-arrestin-1/-2 recruitment. Chimeric studies wherein the Helix-8 of dopamine D1 (D1R) and D2 (D2R) receptors revealed a role for Helix-8 in β-arrestin-1/-2-mediated desensitization in D1R, but not D2R (52). When the D1R Helix-8 is replaced with the D2R Helix-8, β-arrestin-1/2-mediated receptor desensitization was abolished. However, when the D2R Helix-8 is replaced with the D1R Helix-8 there was no significant β-arrestin-mediated desensitization, thus the D1R Helix-8 alone was not sufficient to trigger receptor desensitization (52). Therefore, the authors concluded that β-arrestin-mediated desensitization involves the D1R Helix-8 in coordination with other D1R regions (phosphorylated C-tail), but not D2R which has other regions (large ICL3) that aid in β-arrestin desensitization (52, 56, 57). Additionally, the data suggest a role for Helix-8 conformational dynamics in having a role in this interaction (52). Further, the Helix-8 of rhodopsin has been shown to mediate phosphate sensing through changes in conformational dynamics during the "pre-binding" state, where C-tail phosphorylated residues are not yet interacting with the polar core of visual arrestin (58). Therefore, our findings should be followed up with studies evaluating whether mutations perturb interactions of the PAR4 Helix-8 with β-arrestins directly or whether mutations in Helix-8 impact conformational dynamics of Helix-8 resulting in the diminished β-arrestin recruitment observed.

The Helix-8 of many GPCRs are known to interact with other regions of the GPCR to stabilize receptor conformations which are crucial to maintain both inactive and active conformations as well as mediate effector interaction (31, 53, 58). In our current investigation of the Helix-8 R^{352}AGLFQRS^{359} sequence we have not evaluated the

potential loss of intramolecular contacts within the GPCR and thus more detailed investigations of the inter-domain interactions should be undertaken.

Lysine

The PAR4 C-tail contains two lysine residues – Lys^{350} in the Helix-8 and Lys^{367} distal to Helix-8. Mutation of Lys^{350} to alanine significantly decreased both peptide- and thrombin-stimulated calcium signalling and β-arrestin-1/-2 recruitment. Interestingly, Lys^{367}Ala mutation also significantly reduced peptide-stimulated calcium signalling from PAR4, however, not as significantly as Helix-8 Lys^{350}Ala mutation and with no detrimental impact on peptide- or thrombin-stimulated β-arrestin recruitment. While the mechanism underlying the contribution of Lys^{350} to $G\alpha_{q/11}$ binding were not investigated in this study, there is a clear and supported role for charged Helix-8 lysine residue in direct $G\alpha_{q/11}$ interaction demonstrated in other class A GPCRs. Mutational studies with the muscarinic 3 receptor (M3R) revealed lysine within the N-terminal domain of Helix-8 made contacts with the α4/β6 loop of $G\alpha_{q/11}$ (30). Further, studies with μ-opioid receptor (μOR) implicate Helix-8 lysine as having decreased solvent accessibility upon G-protein binding following activation (28). Similar to our observations with PAR4 Lys^{350}Ala mutation (8.53), Lys^{320}Gln (8.52) mutation in MCH_1R decreased MCH-stimulated, $G\alpha_q$-mediated calcium mobilization (32). It is important to note that Helix-8 lysine mutations in several GPCRs, including the melanin-concentrating hormone (MCH) receptor 1 (MCH_1R) and bradykinin B_2 receptor (B_2R), result in reduced plasma membrane expression (32, 33). To ensure that reduction in calcium signalling is not due to poor membrane localization of lysine mutant PAR4 receptor, we confirmed by confocal microscopy that PAR4 Lys^{350}Ala, Lys^{367}Ala, and Lys^{350}Ala/Lys^{367}Ala double mutant all expressed appropriately on the cell membrane.

As previously stated, mutation of Lys^{350} decreased both peptide- and thrombin-stimulated β-arrestin-1/-2 recruitment, while Lys^{367}Ala had no effect on agonist-stimulated recruitment. Additionally, combined mutation was no more detrimental than Lys^{350}Ala mutation alone. Previous studies of the thyrotropin-releasing hormone (TRH) receptor (TRH_1R) and B_2R revealed that Helix-8 lysine residues were important in mediating

GRK interaction and C-tail phosphorylation of the receptors. Mutation of TRH_1R Helix-8 Lys^{326} was found to significantly reduce C-tail phosphorylation and receptor internalization, which could be partially overcome with overexpression of G-protein receptor kinase 2 (GRK2) (59). Similarly, Helix-8 lysine mutation to proline in B_2R ($Lys^{315/8.53}$; analogous to $Lys^{350/8.53}$ residue in PAR4) decreased agonist-stimulated C-tail phosphorylation and agonist-dependent internalization, which could be recovered in part by overexpression of GRK2 or GRK3 (33). Thus, alterations in GRK-mediated receptor phosphorylation may be responsible for the reductions observed with Lys^{350} mutation and should be investigated in future studies.

$DPxxYx_6F$ motif

Many Class A GPCRs possess a canonical $NPxxYX_{5,6}F$ motif/domain, spanning TM7 and Helix-8, including $Asn^{7.49}$, $Pro^{7.50}$, $Tyr^{7.53}$, and Helix-8 $Phe^{8.50}$. This motif is thought to be involved in stabilizing the inactive state of Class A GPCRs. In crystal structures of inactive state GPCRs, the side chain of $Tyr^{7.53}$ points towards helices I, II, or VIII, whereas, structures of the active state have $Tyr^{7.53}$ changing rotamer conformation to face the interior of the transmembrane bundle, pointing towards helices VI and III (60). Additionally, an inactive-state stabilizing water molecule network involving the TM7 NPxxY, TM3 E/DRY, and TM6 WXPF/Y motifs may be partially constituted by $Tyr^{7.53}$ (35). Previous studies of rhodopsin and the β_2-adrenergic receptor have demonstrated that mutations in this motif alter ligand affinity, receptor plasma membrane expression, G-protein coupling, and interactions with small G-proteins, such as RhoA, dependent on the receptor studied (34, 61–63). In our mutational study, we observed a complete ablation of $G\alpha_{q/11}$ signalling with both Tyr^{340}Ala and Phe^{347}Ala mutations despite appropriate cell membrane localization (Supplementary Figure 4.1). Functional studies have highlighted that the absence of side-chain interaction between $Tyr^{7.53}$ and $Phe^{8.50}$ increases the population of active rhodopsin (Meta II state) with no concomitant increase in transducin ($G\alpha_t$) activation (34, 35). Further, these studies show that hydrophobic side chain interaction between $Tyr^{7.53}$ and $Phe^{8.50}$ constitutes a constraint that becomes necessarily perturbed during receptor interaction to allow for conformational rearrangement of Helix-8 and G-protein binding (34, 35). Mutation of rhodopsin Helix-8 Phe^{313} (8.50) to alanine

caused a corresponding loss of 80-90% of $G\alpha_t$ activation with rhodopsin (34, 64). Further, perturbation of this interaction, as well an interaction between TM3 3.46 and TM6 6.37 residues, enables $Tyr^{7.53}$ to make a new contact with TM6 6.37 residue and form an interaction with the α5 helix of the G-protein, which has been demonstrated in five Class A GPCRs (rhodopsin, M2R, μOR, β_2AR, and A_{2A}R) (65). Mutation of $Tyr^{7.53}$ in the V2 vasopressin receptor (V2R) significantly reduces the receptor-mediated activation of both $G\alpha_s$ and $G\alpha_q$ (65). While it is not possible in this study to resolve if a change in the active-state population of PAR4 or a perturbation in the conformational rearrangement of TM7/Helix-8 interaction is responsible for the loss of calcium signalling observed, it is clear that these residues have a role in $G\alpha_{q/11}$-mediated calcium signalling.

In addition to abrogation of $G\alpha_{q/11}$-mediated calcium signalling, we observed significant decreases in both thrombin- and peptide-stimulated recruitment of β-arrestin-1/-2 to PAR4 DPxxYx_6F mutants, Tyr^{340}Ala and Phe^{347}Ala. The NPxxY$x_{5,6}$F motif has been shown for several Class A GPCRs to be involved in interactions with β-arrestins. Mutations of this motif are thought to perturb GRK interactions with the GPCR and thus decrease GRK-mediated phosphorylation (28–30). In studies of the β_2-adrenergic receptor (β_2AR), mutation of TM7 Tyr^{326} (7.53) decreased GRK-mediated phosphorylation and receptor sequestration, which was reversible through overexpression of GRKs 2-6 (61, 66, 67). As we observed in the PAR4 Tyr^{340}Ala and Phe^{347}Ala mutations, β-arrestin recruitment has also been reported to be significantly reduced in both β_2AR and α_{1B}AR receptors with TM7 $Tyr^{7.53}$ mutations in (68). Whether changes in GRK-mediated receptor phosphorylation of PAR4 accounts for the reduction in β-arrestin recruitment observed with Tyr^{340}Ala and Phe^{347}Ala mutations should be the focus of further study.

Phosphorylation-site mutations

A role for phosphorylation-dependent GPCR-mediated recruitment of β-arrestins is well established (36, 37). The importance of a phosphorylation barcode motif in β-arrestin

binding and signalling has also been demonstrated for many GPCRs including the β2-adrenergic receptor, rhodopsin receptor, chemokine receptors 4 & 7, vasopressin, and angiotensin II receptor type 1 receptors (38–41). It has been reported that 52.3% of Class A GPCRs possess either a full or partial phosphorylation barcode (42). Class A GPCRs can be further divided into two "classes" (distinct from GPCR class; beta-arrestin-binding class shown as lowercase letters) based on their β-arrestin-1 and -2 binding – "class a" GPCRs bind β-arrestin-2 more tightly than β-arrestin-1 (such as α1- and β2-adrenergic, μ-opioid, and dopamine D_1A receptors), and "class b" GPCRs bind β-arrestins-1/-2 as well as visual arrestin (e.g. angiotensin II type 1A receptor, neurotensin receptor 1, vasopressin-2 receptor, thyrotropin-releasing hormone receptor, and substance P receptor) (69). All "class a" β-arrestin-binding GPCRs have, at most, one complete phosphorylation barcode (PxxPxxP, as previously defined) (42). Interestingly, our data consistently show more robust recruitment of β-arrestin-2 versus β-arrestin-1 and the PAR4 C-tail possesses only one complete phosphorylation barcode. Thus, PAR4 may be considered a "class a" β-arrestin-binding GPCR. Further, when the complete phosphorylation barcode is mutated (Thr^{363}Ala/Ser^{366}Ala/Ser^{369}Ala), we observe significantly reduced β-arresin-1/-2 recruitment in response to peptide- and thrombin activation of the receptor compared to wild-type receptor. However, given that β-arrestin recruitment still occurred, we examined β-arrestin recruitment to a phosphorylation-site-null PAR4 ($PAR4^{0P}$) to determine if recruitment was further reduced. While phosphorylation barcodes may play a role arrestin subtype-specificity and the recruitment of other downstream signalling partner (such as SNX27 for β_2AR) and may be the only mediator of high-affinity β-arrestin binding, other phosphorylated residues may be a part of β-arrestin recruitment to activated GPCRs (38, 39, 42, 70). Interestingly, only peptide-stimulated β-arrestin-2 recruitment was further reduced compared to Thr^{363}Ala/Ser^{366}Ala/Ser^{369}Ala mutation alone. Thus, these data support an important role for the complete phosphorylation barcode in β-arrestin recruitment to activated PAR4, while other phosphorylatable residues likely to contribute less meaningfully to recruitment to PAR4. When we evaluate the impact of reduced β-arrestin-1/-2 recruitment to PAR4 on calcium signalling, we observed no significant differences in

agonist-stimulated calcium signalling compared to wild-type receptor. This is in contrast to what we have observed with PAR2-mediated signalling in β-arrestin-deficient cells, wherein, maximal calcium signalling increases and demonstrates prolonged kinetics compared to β-arrestin-1/-2-expressing cells (20). These data are in agreement with previously published mutational studies of serine/threonine residues in the PAR4 C-tail which had no effect on increasing PAR4 G-protein signalling (49). While β-arrestin recruitment is reduced in the PAR4 phosphorylation barcode motif mutant, the level of recruitment may be sufficient to desensitize the calcium signalling pathway. Alternatively, there may be other mechanisms enabling PAR4 desensitization such as ubiquitination and internalization as observed with PAR1 and PAR2 (71). Given that PAR4, once cleaved, is irreversibly activated it follows that several mechanisms may be capable of receptor desensitization, however, a more thorough investigation of PAR4 signal regulation will need to be undertaken to support this hypothesis.

In some Class A GPCRs, Helix-8 and C-tail mutations analogous to those made in this study negatively impact cell surface expression. Mutation of Helix-8 lysine residues reduce membrane expression of both MCH_1R and B_2R (32, 33). Additionally, mutation of the highly-conserved $NPxxYx_{5,6}F$ motif in rhodopsin and β_2AR significantly affect cell surface expression of these receptors (34, 61–63). Previously, we demonstrated that Helix-8 $R^{352}AGLFQRS^{359}$ deletion did not impact appropriate cell membrane localization of PAR4 (22). Further, studies wherein the C-tail of PAR4 from Helix-8 Lys^{350} (ΔK350) or distal Lys^{367} (ΔK350) are truncated have previously reported appropriate cell membrane expression and agonist-dependent internalization (72). In the current study, we assess cell surface expression of PAR4 mutants and observed no deficits in expression. In the current study we confirmed the Helix-8 $R^{352}AGLFQRS^{359}$ sequence and C-tail Lys^{350}/Lys^{367} residues are not essential for appropriate membrane expression. Importantly, while we observed cell membrane expression of all mutant constructs studied, more thorough assessment of the impacts of these mutations on agonist-stimulated internalization and trafficking, should be undertaken. In previous studies, a role for β-arrestin-independent internalization of PAR4 has been reported (72, 73). In our hands, we find an essential role for β-arrestin in PAR4 internalization, wherein

CRISPR/Cas9 knockout of β-arrestin-1/-2 significantly reduces PAR4 internalization, which is rescued through reconstitution of β-arrestins into the knockout cells (data not shown). Future studies could utilize C-tail mutants with decreased β-arrestin recruitment described in this study to assist in dissecting the role of β-arrestins in agonist-stimulated receptor internalization of PAR4.

Together, the data herein begin to provide insights into the molecular mechanisms underscoring PAR4 $G\alpha_{q/11}$ and β-arrestin-1/-2 signalling and regulation. Further, these data highlight important divergences in the relative importance of Helix-8 and C-tail residues on PAR4 signalling, dependent on peptide- or enzyme-activation of PAR4. Further, unraveling the differential contributions of the residues in signalling and regulation downstream of either peptide activation or proteolytic cleavage provides insight into how these two different modes of activation may differentially regulate these interactions. Ultimately, understanding the molecular mechanisms governing effector interactions, signalling, and signal regulation at PAR4 provides novel insights into how this receptor functions and may aid in the development of novel therapeutics targeting PAR4.

4.5 References

1. Fredriksson, R., and Schioth, H. B. (2005) The repertoire of G-protein-coupled receptors in fully sequenced genomes. *Molecular pharmacology*. **67**, 1414–1425

2. Fredriksson, R., Lagerström, M. C., Lundin, L.-G., and Schiöth, H. B. (2003) The G-Protein-Coupled Receptors in the Human Genome Form Five Main Families. Phylogenetic Analysis, Paralogon Groups, and Fingerprints. *Mol Pharmacol*. **63**, 1256–1272

3. Adams, M. N., Ramachandran, R., Yau, M.-K., Suen, J. Y., Fairlie, D. P., Hollenberg, M. D., and Hooper, J. D. (2011) Structure, function and pathophysiology of protease activated receptors. *Pharmacology & therapeutics*. **130**, 248–282

4. Ramachandran, R., Noorbakhsh, F., Defea, K., and Hollenberg, M. D. (2012) Targeting proteinase-activated receptors: therapeutic potential and challenges. *Nature reviews. Drug discovery*. **11**, 69–86

5. Heuberger, D. M., and Schuepbach, R. A. (2019) Protease-activated receptors (PARs): mechanisms of action and potential therapeutic modulators in PAR-driven inflammatory diseases. *Thromb J*. 10.1186/s12959-019-0194-8

6. Chen, J., Bernstein, H. S., Chen, M., Wang, L., Ishii, M., Turck, C. W., and Coughlin, S. R. (1995) Tethered ligand library for discovery of peptide agonists. *The Journal of biological chemistry*. **270**, 23398–23401

7. Faruqi, T. R., Weiss, E. J., Shapiro, M. J., Huang, W., and Coughlin, S. R. (2000) Structure-function analysis of protease-activated receptor 4 tethered ligand peptides. Determinants of specificity and utility in assays of receptor function. *The Journal of biological chemistry*. **275**, 19728–19734

8. Kawabata, A., Kanke, T., Yonezawa, D., Ishiki, T., Saka, M., Kabeya, M., Sekiguchi, F., Kubo, S., Kuroda, R., Iwaki, M., Katsura, K., and Plevin, R. (2004) Potent and metabolically stable agonists for protease-activated receptor-2: evaluation of activity in multiple assay systems in vitro and in vivo. *The Journal of pharmacology and experimental therapeutics*. **309**, 1098–1107

9. Hollenberg, M. D., Saifeddine, M., Al-Ani, B., and Kawabata, A. (1997) Proteinase-activated receptors: structural requirements for activity, receptor cross-reactivity, and receptor selectivity of receptor-activating peptides. *Can J Physiol Pharmacol*. **75**, 832–841

10. Vretenbrant, K., Ramström, S., Bjerke, M., and Lindahl, T. L. (2007) Platelet activation via PAR4 is involved in the initiation of thrombin generation and in clot elasticity development. *Thromb. Haemost.* **97**, 417–424

11. Vandendries, E. R., Hamilton, J. R., Coughlin, S. R., Furie, B., and Furie, B. C. (2007) Par4 is required for platelet thrombus propagation but not fibrin generation in a mouse model of thrombosis. *Proceedings of the National Academy of Sciences*. **104**, 288–292

12. Sambrano, G. R., Weiss, E. J., Zheng, Y. W., Huang, W., and Coughlin, S. R. (2001) Role of thrombin signalling in platelets in haemostasis and thrombosis. *Nature*. **413**, 74–78

13. Thibeault, P. E., LeSarge, J. C., Arends, D., Fernandes, M., Chidiac, P., Stathopulos, P. B., Luyt, L. G., and Ramachandran, R. (2019) Molecular basis for activation and biased signalling at the thrombin-activated GPCR Proteinase Activated Receptor-4 (PAR4). *J. Biol. Chem.* 10.1074/jbc.RA119.011461

14. Holinstat, M., Voss, B., Bilodeau, M. L., McLaughlin, J. N., Cleator, J., and Hamm, H. E. (2006) PAR4, but not PAR1, signals human platelet aggregation via Ca2+ mobilization and synergistic P2Y12 receptor activation. *The Journal of biological chemistry*. **281**, 26665–26674

15. Bilodeau, M. L., and Hamm, H. E. (2007) Regulation of Protease-Activated Receptor (PAR) 1 and PAR4 Signaling in Human Platelets by Compartmentalized Cyclic Nucleotide Actions. *The Journal of pharmacology and experimental therapeutics*. **322**, 778–788

16. Coughlin, S. R. (2000) Thrombin signalling and protease-activated receptors. *Nature*. **407**, 258–264

17. Voss, B., McLaughlin, J. N., Holinstat, M., Zent, R., and Hamm, H. E. (2007) PAR1, but not PAR4, activates human platelets through a Gi/o/phosphoinositide-3 kinase signaling axis. *Molecular pharmacology*. **71**, 1399–1406

18. Kim, S., Foster, C., Lecchi, A., Quinton, T. M., Prosser, D. M., Jin, J., Cattaneo, M., and Kunapuli, S. P. (2002) Protease-activated receptors 1 and 4 do not stimulate G(i) signaling pathways in the absence of secreted ADP and cause human platelet aggregation independently of G(i) signaling. *Blood*. **99**, 3629–3636

19. Nylander, S., Mattsson, C., Ramström, S., and Lindahl, T. L. (2003) The relative importance of the ADP receptors, P2Y12 and P2Y1, in thrombin-induced platelet activation. *Thrombosis Research*. **111**, 65–73

20. Thibeault, P. E., and Ramachandran, R. (2020) Role of the Helix-8 and C-Terminal Tail in Regulating Proteinase Activated Receptor 2 Signaling. *ACS Pharmacol. Transl. Sci.* 10.1021/acsptsci.0c00039

21. Vanderboor, C. M., Thibeault, P. E., Nixon, K. C., Gros, R., Kramer, J. M., and Ramachandran, R. (2020) Proteinase-Activated Receptor 4 (PAR4) Activation Triggers Cell Membrane Blebbing through RhoA and β-arrestin. *Mol Pharmacol*. 10.1124/mol.119.118232

22. Ramachandran, R., Mihara, K., Thibeault, P., Vanderboor, C. M., Petri, B., Saifeddine, M., Bouvier, M., and Hollenberg, M. D. (2017) Targeting a Proteinase-Activated Receptor 4 (PAR4) Carboxyl Terminal Motif to Regulate Platelet Function. *Molecular pharmacology*. **91**, 287–295

23. Mihara, K., Ramachandran, R., Saifeddine, M., Hansen, K. K., Renaux, B., Polley, D., Gibson, S., Vanderboor, C., and Hollenberg, M. D. (2016) Thrombin-Mediated Direct Activation of Proteinase-Activated Receptor-2: Another Target for Thrombin Signaling. *Molecular pharmacology*. **89**, 606–614

24. Vanderboor, C. M., Thibeault, P. E., Nixon, K. C., Gros, R., Kramer, J., and Ramachandran, R. (2019) *Proteinase-Activated Receptor 4 (PAR4) Activation Triggers Cell Membrane Blebbing through RhoA and β-arrestin*, Pharmacology and Toxicology, 10.1101/746677

25. Ramachandran, R., Mihara, K., Chung, H., Renaux, B., Lau, C. S., Muruve, D. A., DeFea, K. A., Bouvier, M., and Hollenberg, M. D. (2011) Neutrophil elastase acts as a biased agonist for proteinase-activated receptor-2 (PAR2). *The Journal of biological chemistry*. **286**, 24638–24648

26. Mihara, K., Ramachandran, R., Renaux, B., Saifeddine, M., and Hollenberg, M. D. (2013) Neutrophil elastase and proteinase-3 trigger G protein-biased signaling through proteinase-activated receptor-1 (PAR1). *The Journal of biological chemistry*. **288**, 32979–32990

27. Kim, B. H., Wang, F. I., Pereverzev, A., Chidiac, P., and Dixon, S. J. (2019) Toward Defining the Pharmacophore for Positive Allosteric Modulation of PTH1 Receptor Signaling by Extracellular Nucleotides. *ACS Pharmacol. Transl. Sci.* **2**, 155–167

28. Sato, T., Kawasaki, T., Mine, S., and Matsumura, H. (2016) Functional Role of the C-Terminal Amphipathic Helix 8 of Olfactory Receptors and Other G Protein-Coupled Receptors. *Int J Mol Sci*. 10.3390/ijms17111930

29. Scheerer, P., and Sommer, M. E. (2017) Structural mechanism of arrestin activation. *Current Opinion in Structural Biology*. **45**, 160–169

30. Hu, J., Wang, Y., Zhang, X., Lloyd, J. R., Li, J. H., Karpiak, J., Costanzi, S., and Wess, J. (2010) Structural basis of G protein–coupled receptor–G protein interactions. *Nature Chemical Biology*. **6**, 541–548

31. Sato, T. (2019) Conserved 2nd Residue of Helix 8 of GPCR May Confer the Subclass-Characteristic and Distinct Roles through a Rapid Initial Interaction with Specific G Proteins. *International Journal of Molecular Sciences*. **20**, 1752

32. Tetsuka, M., Saito, Y., Imai, K., Doi, H., and Maruyama, K. (2004) The Basic Residues in the Membrane-Proximal C-Terminal Tail of the Rat Melanin-

Concentrating Hormone Receptor 1 Are Required for Receptor Function. *Endocrinology*. **145**, 3712–3723

33. Feierler, J., Wirth, M., Welte, B., Schüssler, S., Jochum, M., and Faussner, A. (2011) Helix 8 Plays a Crucial Role in Bradykinin B2 Receptor Trafficking and Signaling. *J. Biol. Chem.* **286**, 43282–43293

34. Fritze, O., Filipek, S., Kuksa, V., Palczewski, K., Hofmann, K. P., and Ernst, O. P. (2003) Role of the conserved NPxxY(x)5,6F motif in the rhodopsin ground state and during activation. *Proc Natl Acad Sci U S A.* **100**, 2290–2295

35. Angel, T. E., Chance, M. R., and Palczewski, K. (2009) Conserved waters mediate structural and functional activation of family A (rhodopsin-like) G protein-coupled receptors. *Proceedings of the National Academy of Sciences*. **106**, 8555–8560

36. Shukla, A. K., Xiao, K., and Lefkowitz, R. J. Emerging paradigms of beta-arrestin-dependent seven transmembrane receptor signaling. *Trends in Biochemical Sciences*. **36**, 457–469

37. Lefkowitz, R. J., and Shenoy, S. K. (2005) Transduction of receptor signals by beta-arrestins. *Science*. **308**, 512–517

38. Liggett, S. B. (2011) Phosphorylation Barcoding as a Mechanism of Directing GPCR Signaling. *Sci. Signal.* **4**, pe36–pe36

39. Nobles, K. N., Xiao, K., Ahn, S., Shukla, A. K., Lam, C. M., Rajagopal, S., Strachan, R. T., Huang, T.-Y., Bressler, E. A., Hara, M. R., Shenoy, S. K., Gygi, S. P., and Lefkowitz, R. J. (2011) Distinct phosphorylation sites on the β(2)-adrenergic receptor establish a barcode that encodes differential functions of β-arrestin. *Science Signaling*. **4**, ra51–ra51

40. Reiter, E., Ahn, S., Shukla, A. K., and Lefkowitz, R. J. (2012) Molecular Mechanism of β-Arrestin-Biased Agonism at Seven-Transmembrane Receptors. *Annual Review of Pharmacology and Toxicology*. **52**, 179–197

41. Ostermaier, M. K., Peterhans, C., Jaussi, R., Deupi, X., and Standfuss, J. (2014) Functional map of arrestin-1 at single amino acid resolution. *PNAS*. **111**, 1825–1830

42. Zhou, X. E., He, Y., Waal, P. W. de, Gao, X., Kang, Y., Eps, N. V., Yin, Y., Pal, K., Goswami, D., White, T. A., Barty, A., Latorraca, N. R., Chapman, H. N., Hubbell, W. L., Dror, R. O., Stevens, R. C., Cherezov, V., Gurevich, V. V., Griffin, P. R., Ernst, O. P., Melcher, K., and Xu, H. E. (2017) Identification of Phosphorylation Codes for Arrestin Recruitment by G Protein-Coupled Receptors. *Cell*. **170**, 457-469.e13

43. Stalheim, L., Ding, Y., Gullapalli, A., Paing, M. M., Wolfe, B. L., Morris, D. R., and Trejo, J. (2005) Multiple independent functions of arrestins in the regulation of

protease-activated receptor-2 signaling and trafficking. *Molecular pharmacology*. **67**, 78–87

44. DeFea, K. (2008) Beta-arrestins and heterotrimeric G-proteins: collaborators and competitors in signal transduction. *Br J Pharmacol*. **153 Suppl 1**, S298–309

45. Ferguson, S. S. (2001) Evolving concepts in G protein-coupled receptor endocytosis: the role in receptor desensitization and signaling. *Pharmacol Rev*. **53**, 1–24

46. Ahn, S., Nelson, C. D., Garrison, T. R., Miller, W. E., and Lefkowitz, R. J. (2003) Desensitization, internalization, and signaling functions of beta-arrestins demonstrated by RNA interference. *Proceedings of the National Academy of Sciences*. **100**, 1740–1744

47. Ricks, T. K., and Trejo, J. (2009) Phosphorylation of protease-activated receptor-2 differentially regulates desensitization and internalization. *The Journal of biological chemistry*. **284**, 34444–34457

48. DeFea, K., Schmidlin, F., Dery, O., Grady, E. F., and Bunnett, N. W. (2000) Mechanisms of initiation and termination of signalling by neuropeptide receptors: a comparison with the proteinase-activated receptors. *Biochemical Society transactions*. **28**, 419–426

49. Shapiro, M. J., Weiss, E. J., Faruqi, T. R., and Coughlin, S. R. (2000) Protease-activated receptors 1 and 4 are shut off with distinct kinetics after activation by thrombin. *The Journal of biological chemistry*. **275**, 25216–25221

50. García-Nafría, J., and Tate, C. G. (2019) Cryo-EM structures of GPCRs coupled to Gs, Gi and Go. *Molecular and Cellular Endocrinology*. **488**, 1–13

51. Kim, K., Che, T., Panova, O., DiBerto, J. F., Lyu, J., Krumm, B. E., Wacker, D., Robertson, M. J., Seven, A. B., Nichols, D. E., Shoichet, B. K., Skiniotis, G., and Roth, B. L. (2020) Structure of a Hallucinogen-Activated Gq-Coupled 5-HT2A Serotonin Receptor. *Cell*. **182**, 1574-1588.e19

52. Yang, H.-S., Sun, N., Zhao, X., Kim, H. R., Park, H.-J., Kim, K.-M., and Chung, K. Y. (2019) Role of Helix 8 in Dopamine Receptor Signaling. *Biomol Ther (Seoul)*. **27**, 514–521

53. Swift, S. (2006) Role of the PAR1 Receptor 8th Helix in Signaling: THE 7-8-1 RECEPTOR ACTIVATION MECHANISM. *Journal of Biological Chemistry*. **281**, 4109–4116

54. Natochin, M., Gasimov, K. G., Moussaif, M., and Artemyev, N. O. (2003) Rhodopsin Determinants for Transducin Activation: A GAIN-OF-FUNCTION APPROACH. *J. Biol. Chem.* **278**, 37574–37581

55. Ahn, K. H., Nishiyama, A., Mierke, D. F., and Kendall, D. A. (2010) Hydrophobic Residues in Helix 8 of Cannabinoid Receptor 1 Are Critical for Structural and Functional Properties. *Biochemistry*. **49**, 502–511

56. Lan, H., Liu, Y., Bell, M. I., Gurevich, V. V., and Neve, K. A. (2009) A dopamine D2 receptor mutant capable of G protein-mediated signaling but deficient in arrestin binding. *Mol. Pharmacol.* **75**, 113–123

57. Namkung, Y., Dipace, C., Javitch, J. A., and Sibley, D. R. (2009) G protein-coupled receptor kinase-mediated phosphorylation regulates post-endocytic trafficking of the D2 dopamine receptor. *J. Biol. Chem.* **284**, 15038–15051

58. Kirchberg, K., Kim, T.-Y., Möller, M., Skegro, D., Raju, G. D., Granzin, J., Büldt, G., Schlesinger, R., and Alexiev, U. (2011) Conformational dynamics of helix 8 in the GPCR rhodopsin controls arrestin activation in the desensitization process. *PNAS*. **108**, 18690–18695

59. Gehret, A. U., Jones, B. W., Tran, P. N., Cook, L. B., Greuber, E. K., and Hinkle, P. M. (2009) Role of Helix 8 of the Thyrotropin-Releasing Hormone Receptor in Phosphorylation by G Protein-Coupled Receptor Kinase. *Mol Pharmacol*. 10.1124/mol.109.059733

60. Katritch, V., Cherezov, V., and Stevens, R. C. (2013) Structure-function of the G protein-coupled receptor superfamily. *Annual Review of Pathology: Mechanisms of Disease*. **53**, 531–556

61. Barak, L. S., Ménard, L., Ferguson, S. S., Colapietro, A. M., and Caron, M. G. (1995) The conserved seven-transmembrane sequence NP(X)2,3Y of the G-protein-coupled receptor superfamily regulates multiple properties of the beta 2-adrenergic receptor. *Biochemistry*. **34**, 15407–15414

62. Prioleau, C., Visiers, I., Ebersole, B. J., Weinstein, H., and Sealfon, S. C. (2002) Conserved Helix 7 Tyrosine Acts as a Multistate Conformational Switch in the 5HT2C Receptor: IDENTIFICATION OF A NOVEL "LOCKED-ON" PHENOTYPE AND DOUBLE REVERTANT MUTATIONS. *J. Biol. Chem.* **277**, 36577–36584

63. Mitchell, R., McCulloch, D., Lutz, E., Johnson, M., MacKenzie, C., Fennell, M., Fink, G., Zhou, W., and Sealfon, S. C. (1998) Rhodopsin-family receptors associate with small G proteins to activate phospholipase D. *Nature*. **392**, 411–414

64. Swift, S., Leger, A. J., Talavera, J., Zhang, L., Bohm, A., and Kuliopulos, A. (2006) Role of the PAR1 Receptor 8th Helix in Signaling THE 7-8-1 RECEPTOR ACTIVATION MECHANISM. *J. Biol. Chem.* **281**, 4109–4116

65. Venkatakrishnan, A. J., Deupi, X., Lebon, G., Heydenreich, F. M., Flock, T., Miljus, T., Balaji, S., Bouvier, M., Veprintsev, D. B., Tate, C. G., Schertler, G. F.

X., and Babu, M. M. (2016) Diverse activation pathways in class A GPCRs converge near the G-protein-coupling region. *Nature*. **536**, 484–487

66. Ménard, L., Ferguson, S. S. G., Barak, L. S., Bertrand, L., Premont, R. T., Colapietro, A.-M., Lefkowitz, R. J., and Caron, M. G. (1996) Members of the G Protein-Coupled Receptor Kinase Family That Phosphorylate the β2-Adrenergic Receptor Facilitate Sequestration. *Biochemistry*. **35**, 4155–4160

67. Ferguson, S. S., Ménard, L., Barak, L. S., Koch, W. J., Colapietro, A. M., and Caron, M. G. (1995) Role of phosphorylation in agonist-promoted beta 2-adrenergic receptor sequestration. Rescue of a sequestration-defective mutant receptor by beta ARK1. *J. Biol. Chem.* **270**, 24782–24789

68. Ragnarsson, L., Andersson, Å., Thomas, W. G., and Lewis, R. J. (2019) Mutations in the NPxxY motif stabilize pharmacologically distinct conformational states of the a1B- and b2-adrenoceptors. *SCIENCE SIGNALING*

69. Oakley, R. H., Laporte, S. A., Holt, J. A., Caron, M. G., and Barak, L. S. (2000) Differential Affinities of Visual Arrestin, βArrestin1, and βArrestin2 for G Protein-coupled Receptors Delineate Two Major Classes of Receptors. *The Journal of biological chemistry*. **275**, 17201–17210

70. Yang, F., Yu, X., Liu, C., Qu, C.-X., Gong, Z., Liu, H.-D., Li, F.-H., Wang, H.-M., He, D.-F., Yi, F., Song, C., Tian, C.-L., Xiao, K.-H., Wang, J.-Y., and Sun, J.-P. (2015) Phospho-selective mechanisms of arrestin conformations and functions revealed by unnatural amino acid incorporation and (19)F-NMR. *Nat Commun*. **6**, 8202

71. Soh, U. J., Dores, M. R., Chen, B., and Trejo, J. (2010) Signal transduction by protease-activated receptors. *British journal of pharmacology*. **160**, 191–203

72. Smith, T. H., Coronel, L. J., Li, J. G., Dores, M. R., Nieman, M. T., and Trejo, J. (2016) Protease-activated Receptor-4 Signaling and Trafficking Is Regulated by the Clathrin Adaptor Protein Complex-2 Independent of β-Arrestins. *J. Biol. Chem.* **291**, 18453–18464

73. Smith, T. H., Li, J. G., Dores, M. R., and Trejo, J. (2017) Protease-activated receptor-4 and purinergic receptor P2Y12 dimerize, co-internalize, and activate Akt signaling via endosomal recruitment of β-arrestin. *The Journal of biological chemistry*. **292**, 13867–13878

4.6 Chapter 4 Supplementary Information

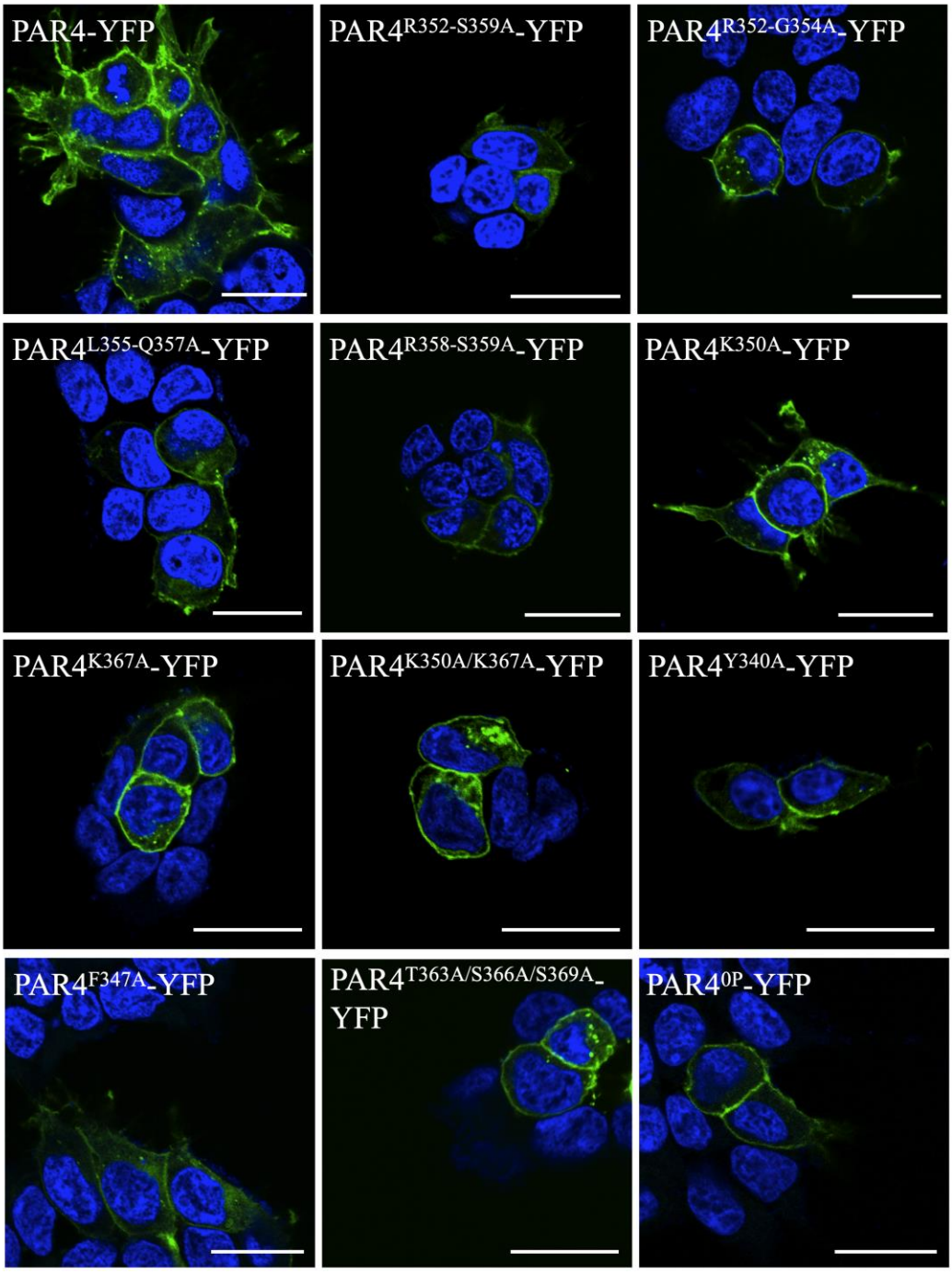

Supplementary Figure 4.1 Confocal micrographs of PAR4-YFP and mutant receptor cellular expression. Confocal microscopy was employed to determine appropriate cell membrane expression of wild-type PAR4-YFP and mutant PAR4

constructs. We observed membrane expression with wild-type and all mutant PAR4 receptor constructs. Scale bar is 20 μm. (*n = 3*)

Chapter 5

5 Summary and Discussion

5.1 Summary of Findings

The overall objective of my thesis was to improve our understanding of the molecular determinants of PAR4 activation, signalling, and signal regulation to further support drug discovery efforts and our understanding of this non-canonically-activated Class A GPCR. Further, my thesis work explored the potential for biased agonism of PAR4 in modulating PAR4 signalling in the platelet context (1). Additionally, I investigated the role of various receptor domains (Helix-8, C-tail) in enzyme- and peptide-stimulated PAR2 and PAR4 signalling and regulation to determine if some bias exists with canonical activators of PARs (2). First, I employed a structure activity relationship approach to determine what chemical and structural characteristics underscore activity of the PAR4 agonist peptide, AYPGKF-NH_2. In chapter 2, I determined requirements for agonist peptide residues in activity at PAR4 including chemical characteristics (such as hydrophobicity, stericity, and side chain properties) (3). Additionally, SAR findings indicated a structural role for some residues (including Pro^3) and thus prompted solution NMR studies to determine the structure of AYPGKF-NH_2. In collaboration, I discovered two distinct structures of the AYPGKF-NH_2 peptide, which constitute the first solved structures of a PAR-activating peptide. I also reported the first biased peptide ligands of the PAR4 receptor and demonstrated that biased agonism of PAR4 can be employed to modulate PAR4-mediated platelet activation and aggregation. Having assessed molecular determinants of PAR4 activation and signalling from the extracellular surface of the receptor, I next turned to investigating the role of two important intracellular domains on effector interactions. PAR4 lacks some canonical residues and motifs that have been shown to be important in G-protein binding and β-arrestin recruitment. PAR2 is activated similarly to PAR4 and signals through shared G-protein pathways, however, contains some of these more canonical residues, including a Helix-8 palmitoylated cysteine and C-tail serine/threonine residue clusters, that PAR4 lacks. In chapter 3, the importance of these G-protein and β-arrestin interacting residues/motifs was explored with PAR2 as an important PAR comparator for additional studies with PAR4 (2). I investigated the

contribution of Helix-8 cysteine and C-tail serine/threonine residues and determined a role for the Helix-8 and C-tail residues in G-protein signalling and β-arrestin recruitment. Interestingly, I also reported differential roles for these residues dependent on whether PAR2 was proteolytically-activated by trypsin or peptide activated. These data underscored the potential for differential and perhaps even biased signalling in PARs between their canonical protease, uncanonical proteases, and peptide or small molecule ligands. Thus, when investigating the role of Helix-8 and C-tail residues in PAR4 signalling and regulation, I determined the contribution of these residues in both thrombin-cleaved and peptide-stimulated receptor. In previously published work we demonstrated a role for the Helix-8 in PAR4 signalling (4). Further, we demonstrated that PAR4-mediated platelet activation could be inhibited by a palmitoylated peptide mimicking a sequence of the PAR4 Helix-8 (4). In chapter 4, I reported a requirement for these Helix-8 residues and several others in both G-protein signalling and β-arrestin recruitment. Further, I demonstrate an important role for a phosphorylation barcode in the PAR4 C-tail in mediating β-arrestin recruitment to activated PAR4. Finally, I report differential roles of PAR4 Helix-8 and C-tail residues dependent on which mode of activation was employed (cleaved/thrombin-activated vs. uncleaved/peptide-stimulated) and the potential for some of these residues to contribute to effector subtype selectivity.

PAR4 has been demonstrated to be a tractable and desirable receptor target for anti-platelet therapeutics (4, 5). Ultimately, I predict that the data and analyses generated by this thesis work will provide the necessary foundation on which to build future drug discovery efforts with PAR4 in developing improved anti-platelet therapeutics and PAR4-targetting ligands, including biased ligands. Further, we and others have demonstrated that PAR4 is able to bind to several G-protein subtypes ($G\alpha_{q/11}$, $G\alpha_{12/13}$, and $G_{\alpha i/o}$) although magnitude of these interactions and the potential interplay between these G-protein signalling pathways has been largely unexplored with PAR4 (3, 6–9). This thesis work demonstrates the necessity of evaluating all potential signalling and regulation consequences of ligands targeting PAR4 and PAR2.

5.1.1 Chapter 2 – Molecular basis for activation and biased signalling at the thrombin-activated GPCR Proteinase Activated Receptor-4 (PAR4)

In chapter 2, I investigated the chemical and structural characteristics of peptide ligands for PAR4 to determine which characteristics enable activation of PAR4. Further, I sought to develop biased peptide ligands of PAR4 and to provide proof of concept experiments demonstrating the utility of biased agonism in PAR4-targeted anti-platelet therapeutics. Previously, it was reported that an amidated and modified peptide of the rat PAR4 tethered ligand (GYPGKF), AYPGKF-NH_2, had activity similar to the thrombin-revealed tethered ligand of human PAR4 (9). While this landmark study provided us the PAR4-activitating peptide still used today, the study was limited by only investigating one G-protein-coupled pathway downstream of PAR4 activation. In chapter 2, I used a library of peptides in a SAR study to determine the effect of single amino acid substitutions in this canonical peptide and evaluated $G\alpha_{q/11}$ signalling, β-arrestin recruitment, and MAPK signalling (Figure 5.1); determined residues within the orthosteric binding site of PAR4 using homology modelling of the receptor and *in silico* peptide docking studies; determined the structure of AYPGKF-NH_2; and tested a subset of novel peptides in *ex vivo* platelet aggregation assays.

In the first SAR, I sought to identify if any one residue in the canonical peptide was wholly or largely responsible for agonist activity at PAR4 by individual substitution of residues 2-6 of the peptide with alanine. I observed shifts in the potency of $G\alpha_{q/11}$-mediated calcium signalling (except with AYPGAF-NH_2) and decreases in β-arrestin recruitment to PAR4 in all of the alanine substitutions made. Thus, I was able to determine that no one amino acid is wholly responsible for the activity observed at PAR4.

In a follow-up SAR using D-isomer residue substitutions for positions 1-3, 5, and 6 (glycine^4 has no D-isomer), I identified that the backbone conformation of all residues within the peptide, with the exception of phenylalanine^6, was critical to agonist activity in all pathways studied. Specifically, substitution of proline and tyrosine with their respective D-isomers (D-proline and D-tyrosine, respectively), was unable to stimulate

calcium signalling even at the highest concentrations tested. In a series of follow-up SAR studies evaluating each position and specifically modifying residue characteristics, we identified that unnatural amino acid substitution of proline with pipecolic acid, which is structurally similar to proline but has an increased steric bulk and backbone elongation provided by a six-membered ring, yielded modesty decreased efficacy and potency in calcium signalling and β-arrestin recruitment, however, maintained agonist properties at PAR4. Interestingly, substitution with a largely analogous unnatural amino acid to pipecolic, nipecotic acid which changes the peptide backbone direction (relative to pipecolic acid and proline), significantly abolished agonist activity at PAR4. Similarly, elongation of the backbone in position 4 (glycine in the parental agonist peptide) reduced agonist activity at PAR4.

Together, these data provided the impetus to explore solution NMR of AYPGKF-NH_2 to determine if the hexapeptide adopts a structure. Interestingly, while a hexapeptide would not be predicted to adopt a defined structural conformation, I identified two distinct conformations adopted by AYPGKF-NH_2, one in higher abundance ("major") and one in lower abundance ("minor"). These structures are the first reported structures of a PAR agonist peptide and further, in concert with our SAR data, reveal that there may be a structural component to peptide activation of PAR4. Additional peptides have been analyzed with NMR, including peptides with pipecolic acid and nipecotic acid substitution, to further determine if either of the two conformations adopted by AYPGKF-NH_2 is more analogous to the peptides with agonist activity or those without. These studies reveal a previously unanticipated role for ligand structure in activity at PAR4. Further, they highlight areas for further peptide modifications that would be tolerated structurally, or perhaps even to force a specific structure, in future drug discovery efforts with PAR4.

In several previously published works, we have observed (by BRET) that β-arrestin-1/-2 recruitment to PAR4 does not saturate with the canonical activating peptide (3, 4, 8). In this study, we demonstrated that several of our novel peptide ligands [(*N*-Me-A)-YPGKF-NH_2, AYPG-(N^{α}-Me-K)-F-NH_2, and AYPGK-(*N*-Me-F)-NH_2] were able to recruit β-arrestin-1/-2 to saturation. Further, two of these novel peptides [(*N*-Me-A)-

YPGKF-NH_2, AYPG-(N^{α}-Me-K)-F-NH_2] did not stimulate a $G\alpha_{q/11}$-mediated calcium signalling and thus were determined to be β-arrestin biased ligands. These β-arrestin-biased peptides are novel and exciting tool compounds with which to study the contributions of β-arrestins-1/-2 signalling in various tissue and cell contexts, such as the platelet, to determine the role of these scaffolding and signalling proteins in the PAR4 response.

Finally, the SAR studies revealed that side chain modifications to Tyr^2, Lys^5, and Phe^6 are largely well-tolerated provided certain chemical characteristics (like backbone conformation) are maintained. In the original SAR study by Faruqi and colleagues, as well as in this study, it was observed that substitutions in Tyr^2 and Phe^6 have a requirement of being aromatic residues (3, 9). Modifications to the side chain of Lys^5 are very well tolerated, however the side chain should remain positively charged. These findings together orient future drug discovery and SAR studies to residues within the PAR4 agonist peptide that are amenable to modification without sacrificing activity at the receptor. This amenability may be particularly useful in the generation of imaging agents as we have shown with collaborators for ligands of PAR2 and growth hormone secretagogue receptor 1a (GHSR1a) (10, 11).

When evaluating the downstream signalling MAPK pathway, I determined that PAR4-stimulated MAPK signalling is $G\alpha_{q/11}$ dependent using the selective inhibitor YM254890 which abolished ERK phosphorylation. As expected, peptides which were unable to stimulate $G\alpha_{q/11}$ signalling were similarly unable to stimulate ERK phosphorylation. Unexpectedly, β-arrestin biased compounds, that were also able to stimulate calcium signalling to varying degrees, dramatically increased ERK phosphorylation which may underscore a role for β-arrestin-assisted ERK phosphorylation as has been observed in PAR4-stimulated Akt phosphorylation, as well as, PAR2-stimulated ERK phosphorylation following cleavage with Neutrophil Elastase or Cathepsin-S (4, 12).

Following peptide SAR studies, I sought to identify residues within the PAR4 orthosteric binding site – where both tethered ligand and tethered ligand-mimicking peptides are expected to bind. Using homology modelling with the assistance of Dr. Peter B.

Stathopulos, I generated two homology models of PAR4 based on the known crystal structure coordinates of PAR1 and PAR2, which share high sequence identity with PAR4 (41% by Phyre2 analysis) (13). These homology models were used as an input for iterative peptide docking with GalaxyPepDock (14). This study revealed 17 predicted sites of interaction between the agonist peptide and receptor through 10 different models. Since the pose adopted by peptide in each model was different, I quantified the number of times a particular interaction was predicted to occur. Using site-directed mutagenesis (SDM) I tested the impact of mutations to three of the most highly predicted sites (His^{229}, Asp^{230}, Gln^{242}) and determined that Asp^{230}, in ECL2, is an integral residue in both peptide and tethered ligand activation of PAR4.

Finally, I evaluated the ability of some of the novel peptides uncovered by SAR to activate and aggregate platelets in an *ex vivo* platelet assay. Given the well-established role of PAR4-dependent calcium signalling in platelet activation I tested whether a peptide that was unable to stimulate calcium signalling but able to stimulate β-arrestin would stimulate platelet aggregation (Figure 5.1) (15–17). I observed that AyPGKF-NH_2, which was able to stimulate β-arrestin recruitment but not calcium signalling, did not cause platelet aggregation. Thus, as a proof of concept, β-arrestin biased ligands may be therapeutically beneficial as anti-platelet therapeutics. Further, the role of β-arrestins in the PAR4-platelet signalling axis is poorly understood (4, 18). Using another type of β-arrestin-biased ligand, AYPGRF-NH_2, that can equipotently signal calcium but has enhanced β-arrestin recruitment compared to the parental agonist peptide, I demonstrated a distinct role for β-arrestin signalling in PAR4-dependent platelet activation (Figure 5.1). PAR4-stimulated platelet aggregation following AYPGRF-NH_2 treatment enhanced platelet aggregation, beyond that typically observed with AYPGKF-NH_2 stimulation, to levels comparable to thrombin stimulation. Thus, biased ligands of PAR4 are indeed useful for determining the contributions of varied signalling pathways downstream of PAR4, including the novel ligands presented in my thesis for studying β-arrestins.

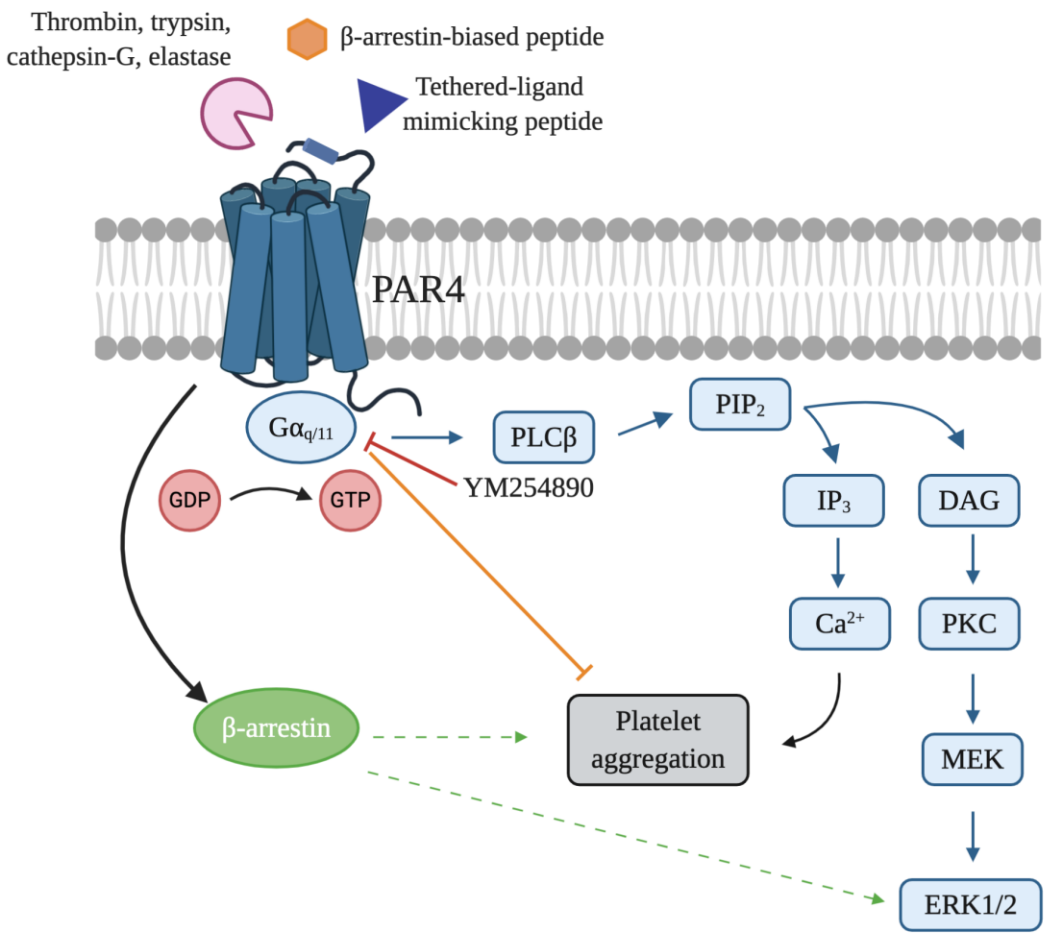

Figure 5.1 Summary of PAR4 signalling contributing to platelet activation and aggregation. PAR4 signalling contribution to PAR4-mediated platelet activation following stimulation with thrombin (pink), AYPGKF-NH_2 (purple, triangle), or β-arrestin-biased peptides (orange, hexagon). Following stimulation with thrombin or peptide, PAR4 signals through $G\alpha_{q/11}$ and β-arrestin which leads to platelet activation and aggregation. Application of β-arrestin-biased ligand AYPGRF-NH_2 enhances PAR4-mediated platelet aggregation and ERK signalling, revealing a role for β-arrestin-dependent signalling in platelet activation and downstream PAR4 signalling. Application of β-arrestin-biased peptide, AyPGKF-NH_2, which does not stimulate $G\alpha_{q/11}$ signalling, effectively inhibits PAR4-mediated platelet activation. Created with BioRender.com

5.1.2 Chapter 3 – Role of the Helix-8 and C-terminal tail in regulating Proteinase Activated Receptor 2 (PAR2) signalling

In chapter 3, I investigated the role of residues that are common to Class A GPCRs on the signalling and regulation of PAR2. PAR2 contains several such residues, including a Helix-8 cysteine and C-tail serine/threonine clusters, which PAR4 lacks (Figure 5.2). Given that PARs are non-canonically activated, I studied the role of these residues in PAR2 regulation as a PAR comparator to residues regulating signalling in PAR4 (Chapter 4). I employed site-directed mutagenesis to create mutants to probe the impact of loss of these residues on signalling and regulation. Interestingly, few studies have probed whether these sites of regulation differ between enzyme- or peptide-activated receptor. Therefore, I evaluated impact of these mutations in both enzyme- and peptide-stimulated PAR2. First, I evaluated the role of β-arrestins on regulation of PAR2-mediated calcium signalling. I determined that in the absence of β-arrestins, through CRISPR/Cas9 knockout, PAR2-mediated calcium signalling was significantly increased in both maximal calcium signal and the duration of signalling in response to either trypsin cleavage or peptide stimulation of the receptor. Interestingly, I also observed an increase in $G\alpha_{q/11}$-dependent ERK phosphorylation in β-arrestin-1/-2 knockout cells. Thus, β-arrestins are important for desensitizing the $G\alpha_{q/11}$ calcium and ERK signalling of PAR2.

A role for Helix-8 cysteine palmitoylation has been demonstrated with a number of Class A GPCRs including PAR1, β2-adrenergic, M1 and M2 muscarinic acetylcholine, glucagon-like peptide-1 receptor, 5-hydroxytryptamine (1A) receptor, CCR2 receptors, and some odorant receptors (19–26). Like many of these GPCRs, it has been demonstrated that a cysteine in the Helix-8 of PAR2 undergoes palmitoylation, leading to insertion of the palmitoyl moiety into the cell membrane and subsequent stabilization of the Helix-8 (27, 28). Loss of Helix-8 Cys^{361} was determined to have an effect on both SLIGRL-NH_2- and trypsin-stimulated calcium signalling. Thus, we showed that this Helix-8 residue, which undergoes palmitoylation, is necessary for appropriate PAR2-mediated calcium signalling. SLIGRL-NH_2-stimulated β-arrestin-1/-2 recruitment was also significantly reduced to the Cys^{361}Ala mutant, however, was only decreased in β-

arrestin-1 recruitment to trypsin-activated PAR2. This may represent some agonist-dependent differences in the importance of this residue in β-arrestin recruitment to PAR2 (Figure 5.2). PAR4 lacks both Helix-8 cysteine and instead contains a glutamine residue which when mutated to cysteine leads to improved recruitment of β-arrestins (4).

The C-tail of PAR2 contains clusters of serine and threonine residues which have been shown to important sites of β-arrestin recruitment following phosphorylation in many receptors including PAR2 (29–31). PAR4 lacks comparable clusters of serine and threonine residues in the C-tail. The PAR2 C-tail contains two serine/threonine clusters. To determine if each of these clusters contributes to β-arrestin recruitment, and therefore regulation of PAR2 we generated mutants lacking portions of these residue clusters. Interestingly, mutation of a cluster of serine residues ($Ser^{383-395}Ala$) significantly reduced β-arresin-1 recruitment to trypsin-stimulated PAR2 but increased recruitment to peptide-stimulated PAR2. Further, β-arrestin-2 recruitment was unaffected in this mutant revealing subtype-selective role for these residues in PAR2-β-arrestin interaction. Mutation of a cluster of serine/threonine residues (Ser^{387}-$Thr^{392}Ala$) reduced β-arrestin-1 and -2 recruitment to peptide activated PAR2, however, only reduced recruitment of β-arrestin-1 to trypsin-stimulated PAR2. Combined mutation of both of these residue clusters decreased β-arrestin-1 recruitment, independent of which agonist was used, however only decreased β-arrestin-2 recruitment to peptide-stimulated PAR2. Thus, it is clear that additional residues must be involved in β-arrestin-2 recruitment to trypsin-stimulated PAR2 (Figure 5.2).

In both of the individual cluster mutations, as well as the combined Ser/Thr mutations, calcium signalling was decreased. Interestingly, only combined mutation ($Ser^{383-385}Ala$/Ser^{387}-$Thr^{392}Ala$) resulted in increased ERK signalling. These data may indicate that despite the apparent decrease in β-arrestin recruitment to these mutants the quanta of β-arrestin recruited may be sufficient to inhibit $G\alpha_{q/11}$-stimulated MAPK signalling or that the level of $G\alpha_{q/11}$-activation downstream of mutant receptor activation is insufficient to lead to MAPK signalling at the concentrations evaluated. Alternatively, these data may illustrate a switch between β-arrestin-dependent/G-protein-independent and G-protein-

dependent/β-arrestin-independent ERK phosphorylation, as has been observed with the β_2AR (32, 33).

In this study, I uncovered evidence of agonist-dependent differential roles for C-tail residues. This necessarily prompts further study to determine what the molecular determinants of these differences are between enzyme-activated or peptide-stimulated PAR2. Further, I demonstrated that C-tail Ser/Thr clusters differentially regulate the recruitment of β-arrestin-1 and -2, which has been shown with other GPCRs such as the β_2AR and V2R receptors (34–36).

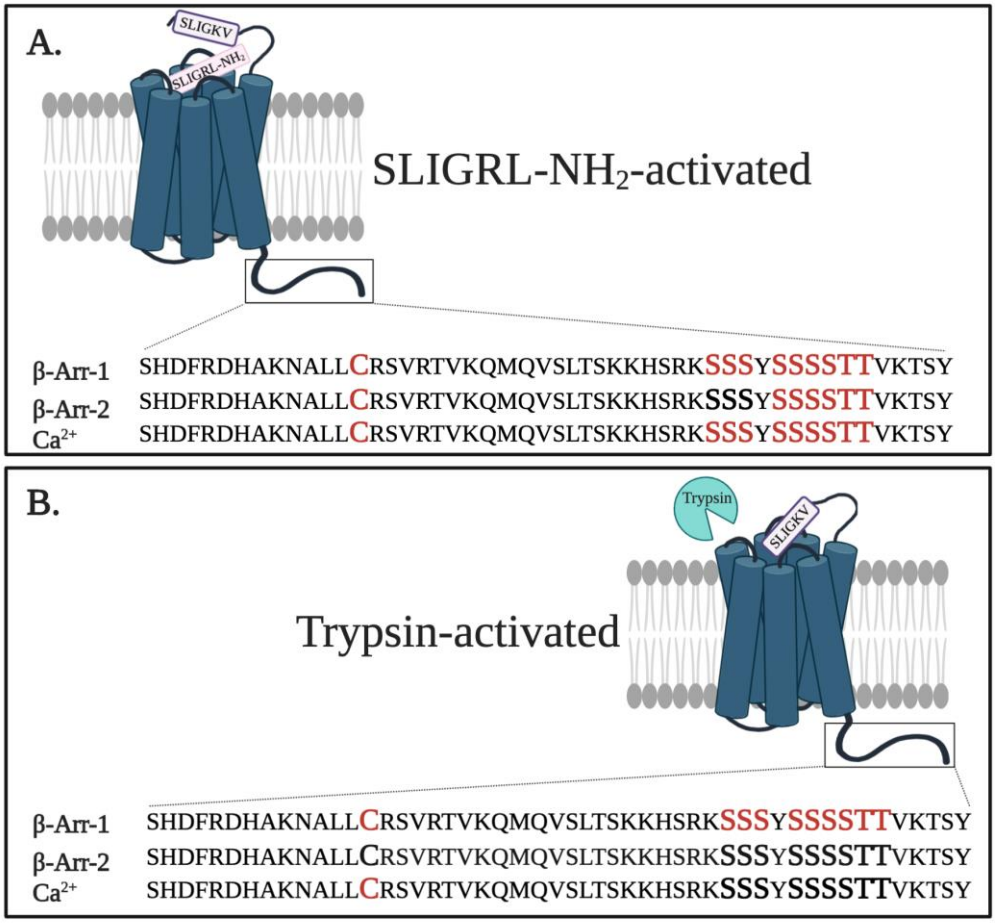

Figure 5.2 Summary of residue contribution to PAR2-mediated calcium signalling and β-arrestin-1/-2 recruitment. Residues studied (bold) are shown with their relative contribution to peptide- (A) and trypsin-stimulated (B) PAR2-mediated calcium signalling and β-arrestin recruitment. Residues that decreased PAR2-mediated signalling and recruitment are shown in red, while residues that when mutated to alanine increased signalling are shown in green. Created with BioRender.com

5.1.3 Chapter 4 - Differential Role of Helix-8 and C-terminal Tail Residues in Signalling and Regulation of peptide- and thrombin-activated Proteinase Activated Receptor 4 (PAR4)

In chapter 2, I determined molecular mechanisms of PAR4 activation. In chapter 3, I reported a role for canonical motifs in PAR2 signalling and regulation. In chapter 4, I turned my attention back to PAR4 and evaluated the contribution of various PAR4 Helix-8 and C-tail on signalling and signalling regulation. Helix-8 and C-terminal tail residues have been shown for many Class A GPCRs to be involved in both interactions with β-arrestins and G-proteins and changes in the activation state of the GPCR (37–39). Given that PAR4 lacks certain canonical Class A GPCR residues, such as Helix-8 and C-tail serine/threonine clusters, we hypothesized that other residues must be responsible for mediating these effector interactions and signalling.

Previously, we demonstrated that deletion of an eight amino acid motif within the PAR4 Helix-8, R^{352}AGLFQRS^{359}, is necessary for $G\alpha_{q/11}$-mediated calcium signalling and β-arrestin recruitment (4). Further, we demonstrated that a palmitoylated-peptide (pepducin) of this Helix-8 sequence (palmitoyl-RAGLFQRS-NH_2) acts as an antagonist of $G\alpha_{q/11}$-mediated calcium signalling and β-arrestin recruitment, and further, inhibits PAR4-mediated Akt signalling and platelet aggregation (4). In chapter 4, I probed this sequence further through mutational studies to determine 1) if our the loss of function observed in R^{352}AGLFQRS^{359} deletion is recapitulated through alanine mutation and, 2) if I could determine which residues in this sequence, if not all, are responsible for the loss of signalling we previously reported. First, I determined that mutation of R^{352}AGLFQRS^{359}Ala mirrored the loss of $G\alpha_{q/11}$-mediated calcium signalling and β-arrestin recruitment to PAR4 that we observed in the previous deletional study. Further, I discovered that the loss of function could be recapitulated through mutation of Leu^{355}-Gln^{357} to alanine. This mutation leads to abrogation of calcium signalling as well as significantly decreases β-arrestin recruitment in response to both peptide- and thrombin-stimulated PAR4. Since I did not observe a total loss of β-arrestin recruitment with this mutation, additional site-directed mutagenesis was done to determine the impact of lysine

residues, the DPxxYx_6F motif, and serine/threonine phosphorylation-sites on β-arrestin recruitment and G-protein signalling.

In chapter 4, I report that Helix-8 Lys^{350} is necessary for both peptide- and thrombin-stimulated calcium signalling and β-arrestin recruitment. Previously published studies have shown a role for Helix-8 lysine residues mediating G-protein recruitment, interaction, and signalling with M3R, μOR, and MCH_1R receptors (37, 39, 40). Additionally, experiments with thyrotropin-releasing hormone (TRH) receptor (TRH_1R) and B_2R have shown that Helix-8 lysine residues were important in mediating GRK interaction and C-tail phosphorylation of these receptors, and ultimately, β-arrestin recruitment (41, 42). Further, I demonstrated that mutation of either Tyr^{340} (TM7) or Helix-8 Phe^{347} abolished calcium signalling and significantly reduced β-arrestin recruitment to PAR4. These effects are likely mediated through a loss of interaction between $Tyr^{7.53}$/$Phe^{8.50}$, which has been demonstrated in a number of Class A GPCRs to be an important motif in activation and signalling (43, 44).

A role for phosphorylation-dependent GPCR-mediated recruitment of β-arrestins is well established (45, 46). As previously mentioned, the PAR4 C-tail lacks clusters of serine/threonine residues, common among Class A GPCRs, and PAR4 phosphorylation is nearly undetectable(47). Thus, I sought to determine a role for serine/threonine phosphorylation-sites in PAR4 signalling and regulation. I determined that a so-called "phosphorylation barcode" motif in the PAR4 C-tail is necessary for both peptide- and thrombin-simulated β-arrestin-1/-2 recruitment. Given that I still observed some β-arrestin recruitment following mutation of the barcode motif, I generated a PAR4 receptor that lacks serine/threonine residues. Interestingly, these additional mutations only further decreased peptide-stimulated β-arrestin-2 recruitment, which may indicate a role for these sites in arrestin subtype-selectivity. Finally, unlike what I observed with mutation of phosphorylation sites in PAR2 (Chapter 3), I report no significant increase in calcium signalling in either the phosphorylation barcode mutant PAR4 or the complete C-tail serine/threonine-alanine mutant PAR4. These data are consistent with previously published reports that mutation of serine/phosphorylation sites does not increase PAR4-mediated signalling (47).

This summary provided highlights the major sites important in signalling and signal regulation, however, the data are more nuanced and have revealed both agonist- and subtype-dependent roles for Helix-8 and C-tail residues in PAR4. Thus, I have been able to generate a “thumbprint” of residues important in peptide- (Figure 5.3A) versus enzyme-stimulated (Figure 5.3B) PAR4, as well as, a role for various residues in β-arrestin-1 versus -2 recruitment.

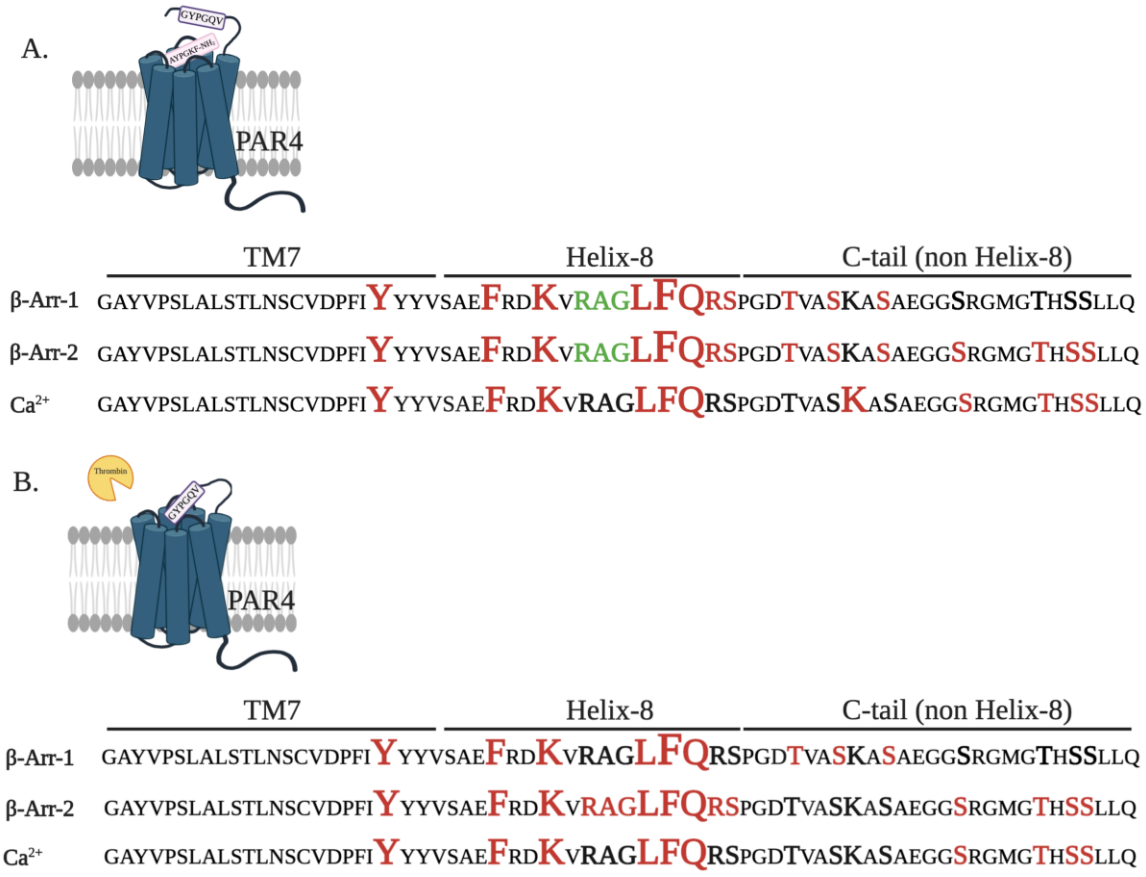

Figure 5.3 Summary of residue contributions to PAR4 peptide- and thrombin-stimulated calcium signalling and β-arrestin recruitment. Residues studied (bold) are shown with their relative contribution to peptide- (A) and thrombin-stimulated (B) PAR4-mediated calcium signalling and β-arrestin recruitment. Residue size is increased with magnitude of detriment from mutation to alanine. Residues that decreased signalling and recruitment are shown in red, while residues that when mutated to alanine increased signalling are shown in green. Created with BioRender.com

5.2 Clinical Significance

Despite promising advances in therapeutically targeting PAR4 as an anti-platelet target, there remains the question of whether a complete inhibition of PAR4 will also lead to deleterious side effects as observed with the PAR1 anti-platelet therapeutic voropaxar. PAR4 can activate multiple signalling pathways through coupling to $G\alpha_{q/11}$, $G\alpha_{12/13}$, and β-arrestin (4, 8, 48). Throughout this thesis, I demonstrate that different pathways can be regulated by ligands, which opens up the possibility to selectively probe which pathways are deleterious and avoiding activating those as a target for therapy. PAR4 signalling, through biased agonism, is of great interest and a viable strategy for obtaining therapeutically superior drugs to target PAR4. Modern drug discovery efforts rely on inputs from both the extracellular, ligand-binding surface of the receptor, as well as, a detailed understanding of receptor signalling and regulation. To address the dearth of this information with PAR4, this thesis furthers our knowledge of PAR4 agonism and presents the first evidence of biased agonism and its potential relevance with PAR4 therapeutics. These novel peptides for PAR4 enable dissection of β-arrestin signalling contributions in physiologically relevant systems, such as platelets. Further, I established unique residues involved in PAR4 $G\alpha_{q/11}$-mediated calcium signalling and β-arrestin recruitment. Finally, this thesis demonstrates the necessity of evaluating signalling and regulation of PAR4 downstream of PAR4 agonists and antagonists, beyond the classical focus of $G\alpha_{q/11}$ coupling and signalling.

5.3 Limitations and Future Directions

While this thesis makes significant contributions to our understanding of the molecular mechanisms of PAR4 activation and signal, there are a few notable limitations to the studies presented. First, most experiments were conducted in HEK-293 cells with overexpression of PAR2 or PAR4. HEK-293 cells are utilized as a cell system in many GPCR pharmacology studies, as they are very amenable to transfection and contain many of the necessary signalling effectors GPCRs signal to (49, 50). For these reasons, we chose HEK-293 cells for our pharmacology studies. HEK-293 cells are not a physiologically relevant cell line, especially since they do not endogenously express

PAR4, therefore we have shown in both platelet and vascular smooth muscle cells that our findings in HEK-293 cells are consistent with our findings in physiologically-relevant systems (3, 8). Future studies should endeavor to recapitulate the pharmacology studies conducted throughout with lead compounds in additional physiologically relevant systems. Additionally, overexpression of proteins provides an excellent opportunity to study signalling, however, may not be representative of the signal magnitude and utility of activating compounds in physiological systems.

PAR4 signals to several G-protein subtypes including $G\alpha_{q/11}$, $G\alpha_{12/13}$, and has even been shown to couple $G\alpha_{i/o}$ in some cellular contexts (3, 6, 7, 51–53). The studies presented primarily assess the impact of novel peptides or mutations on $G\alpha_{q/11}$-mediated signalling and β-arrestin recruitment, therefore, additional studies evaluating some of PAR4's other G-protein signalling pathways is warranted. Until recently, the lab did not possess an adequate means to directly assess activation of $G\alpha_{12/13}$. In May of 2020, an open-source biosensor BRET platform, called TRUPATH, was released. This platform enables evaluation of 15 G-protein subtypes (54). Our laboratory obtained this biosensor platform and begun experiments assessing the impact of PAR4 Helix-8 and C-tail mutations on these additional G-protein subtypes. These ongoing and future studies will be informative to determine whether the novel biased peptides presented herein are also G-protein biased for additional subtypes. Further, mutational studies with additional G-protein subtypes may reveal novel roles for the Helix-8 and C-tail domains between subtypes.

In this thesis I have demonstrated the potential for biased ligands of PAR4 in modulating signalling with therapeutic intention. While these foundational studies have been very informative, further SAR is necessary to optimize biased signalling and enhance affinity for the receptor. Future studies should assess combination substitutions in the PAR4 agonist peptide that may improve the pharmacological profile of the ligands presented herein. For therapeutic purposes, a peptide ligand of PAR4 is an unlikely goal. Therefore, using the chemical and structural determinants for agonism discussed in this thesis, in combination with homology modelling, database screening for novel PAR4-targetting small molecules capable of biasing PAR4 signalling should be undertaken.

5.4 References

1. Thibeault, P. E., and Ramachandran, R. (2020) Biased signalling in platelet G-protein-coupled receptors. *Can. J. Physiol. Pharmacol.* 10.1139/cjpp-2020-0149

2. Thibeault, P. E., and Ramachandran, R. (2020) Role of the Helix-8 and C-Terminal Tail in Regulating Proteinase Activated Receptor 2 Signaling. *ACS Pharmacol. Transl. Sci.* 10.1021/acsptsci.0c00039

3. Thibeault, P. E., LeSarge, J. C., Arends, D., Fernandes, M., Chidiac, P., Stathopulos, P. B., Luyt, L. G., and Ramachandran, R. (2019) Molecular basis for activation and biased signalling at the thrombin-activated GPCR Proteinase Activated Receptor-4 (PAR4). *J. Biol. Chem.* 10.1074/jbc.RA119.011461

4. Ramachandran, R., Mihara, K., Thibeault, P., Vanderboor, C. M., Petri, B., Saifeddine, M., Bouvier, M., and Hollenberg, M. D. (2017) Targeting a Proteinase-Activated Receptor 4 (PAR4) Carboxyl Terminal Motif to Regulate Platelet Function. *Molecular pharmacology*. **91**, 287–295

5. Ramachandran, R., Noorbakhsh, F., Defea, K., and Hollenberg, M. D. (2012) Targeting proteinase-activated receptors: therapeutic potential and challenges. *Nature reviews. Drug discovery*. **11**, 69–86

6. Nylander, S., Mattsson, C., Ramström, S., and Lindahl, T. L. (2003) The relative importance of the ADP receptors, P2Y12 and P2Y1, in thrombin-induced platelet activation. *Thrombosis Research*. **111**, 65–73

7. Kim, S., Foster, C., Lecchi, A., Quinton, T. M., Prosser, D. M., Jin, J., Cattaneo, M., and Kunapuli, S. P. (2002) Protease-activated receptors 1 and 4 do not stimulate G(i) signaling pathways in the absence of secreted ADP and cause human platelet aggregation independently of G(i) signaling. *Blood*. **99**, 3629–3636

8. Vanderboor, C. M., Thibeault, P. E., Nixon, K. C., Gros, R., Kramer, J. M., and Ramachandran, R. (2020) Proteinase-Activated Receptor 4 (PAR4) Activation Triggers Cell Membrane Blebbing through RhoA and β-arrestin. *Mol Pharmacol*. 10.1124/mol.119.118232

9. Faruqi, T. R., Weiss, E. J., Shapiro, M. J., Huang, W., and Coughlin, S. R. (2000) Structure-function analysis of protease-activated receptor 4 tethered ligand peptides. Determinants of specificity and utility in assays of receptor function. *The Journal of biological chemistry*. **275**, 19728–19734

10. Lalonde, T., Fowkes, M. M., Hou, J., Thibeault, P. E., Milne, M., Dhanvantari, S., Ramachandran, R., and Luyt, L. G. (2019) Single Amino Acid Replacement in G-7039 Leads to a 70-fold Increase in Binding toward GHS-R1a. *ChemMedChem*. **14**, 1762–1766

11. LeSarge, J. C., Thibeault, P., Milne, M., Ramachandran, R., and Luyt, L. G. (2019) High Affinity Fluorescent Probe for Proteinase-Activated Receptor 2 (PAR2). *ACS Med. Chem. Lett.* **10**, 1045–1050

12. Ramachandran, R., Mihara, K., Chung, H., Renaux, B., Lau, C. S., Muruve, D. A., DeFea, K. A., Bouvier, M., and Hollenberg, M. D. (2011) Neutrophil elastase acts as a biased agonist for proteinase-activated receptor-2 (PAR2). *Journal of Biological Chemistry*. **286**, 24638–24648

13. Kelley, L. A., Mezulis, S., Yates, C. M., Wass, M. N., and Sternberg, M. J. E. (2015) The Phyre2 web portal for protein modeling, prediction and analysis. *Nature Protocols*. **10**, 845–858

14. Lee, H., Heo, L., Lee, M. S., and Seok, C. (2015) GalaxyPepDock: a protein–peptide docking tool based on interaction similarity and energy optimization. *Nucleic Acids Res*. **43**, W431–W435

15. French, S. L., and Hamilton, J. R. (2016) Protease-activated receptor 4: from structure to function and back again. *Br J Pharmacol*. **173**, 2952–2965

16. Tourdot, B. E., Stoveken, H., Trumbo, D., Yeung, J., Kanthi, Y., Edelstein, L. C., Bray, P. F., Tall, G. G., and Holinstat, M. (2018) Genetic Variant in Human PAR (Protease-Activated Receptor) 4 Enhances Thrombus Formation Resulting in Resistance to Antiplatelet Therapeutics. *Arterioscler. Thromb. Vasc. Biol.* **38**, 1632–1643

17. Edelstein, L. C., Simon, L. M., Lindsay, C. R., Kong, X., Teruel-Montoya, R., Tourdot, B. E., Chen, E. S., Ma, L., Coughlin, S., Nieman, M., Holinstat, M., Shaw, C. A., and Bray, P. F. (2014) Common variants in the human platelet PAR4 thrombin receptor alter platelet function and differ by race. *Blood*. **124**, 3450–3458

18. Khan, A., Li, D., Ibrahim, S., Smyth, E., and Woulfe, D. S. (2014) The Physical Association of the P2Y12 Receptor with PAR4 Regulates Arrestin-Mediated Akt Activation. *Molecular pharmacology*. **86**, 1–11

19. Swift, S. (2006) Role of the PAR1 Receptor 8th Helix in Signaling: THE 7-8-1 RECEPTOR ACTIVATION MECHANISM. *Journal of Biological Chemistry*. **281**, 4109–4116

20. O'Dowd, B. F., Hnatowich, M., Caron, M. G., Lefkowitz, R. J., and Bouvier, M. (1989) Palmitoylation of the human beta 2-adrenergic receptor. Mutation of Cys341 in the carboxyl tail leads to an uncoupled nonpalmitoylated form of the receptor. *J. Biol. Chem.* **264**, 7564–7569

21. Mouillac, B., Caron, M., Bonin, H., Dennis, M., and Bouvier, M. (1992) Agonist-modulated palmitoylation of beta 2-adrenergic receptor in Sf9 cells. *J. Biol. Chem.* **267**, 21733–21737

22. Hayashi, M. K., and Haga, T. (1997) Palmitoylation of muscarinic acetylcholine receptor m2 subtypes: reduction in their ability to activate G proteins by mutation of a putative palmitoylation site, cysteine 457, in the carboxyl-terminal tail. *Arch Biochem Biophys*. **340**, 376–382

23. Vázquez, P., Roncero, I., Blázquez, E., and Alvarez, E. (2020) Substitution of the cysteine 438 residue in the cytoplasmic tail of the glucagon-like peptide-1 receptor alters signal transduction activity. *Journal of Endocrinology*. **185**, 35–44

24. Papoucheva, E., Dumuis, A., Sebben, M., Richter, D. W., and Ponimaskin, E. G. (2004) The 5-Hydroxytryptamine(1A) Receptor Is Stably Palmitoylated, and Acylation Is Critical for Communication of Receptor with Gi Protein. *J. Biol. Chem.* **279**, 3280–3291

25. Markx, D., Schuhholz, J., Abadier, M., Beier, S., Lang, M., and Moepps, B. (2019) Arginine 313 of the putative 8th helix mediates Gαq/14 coupling of human CC chemokine receptors CCR2a and CCR2b. *Cell. Signal.* **53**, 170–183

26. Kawasaki, T., Saka, T., Mine, S., Mizohata, E., Inoue, T., Matsumura, H., and Sato, T. (2015) The N-terminal acidic residue of the cytosolic helix 8 of an odorant receptor is responsible for different response dynamics via G-protein. *FEBS Lett.* **589**, 1136–1142

27. Botham, A., Guo, X., Xiao, Y. P., Morice, A. H., Compton, S. J., and Sadofsky, L. R. (2011) Palmitoylation of human proteinase-activated receptor-2 differentially regulates receptor-triggered ERK1/2 activation, calcium signalling and endocytosis. *Biochem. J.* **438**, 359–367

28. Adams, M. N., Christensen, M. E., He, Y., Waterhouse, N. J., and Hooper, J. D. (2011) The role of palmitoylation in signalling, cellular trafficking and plasma membrane localization of protease-activated receptor-2. *PLoS ONE*. **6**, e28018

29. Luttrell, L. M., and Lefkowitz, R. J. (2002) The role of beta-arrestins in the termination and transduction of G-protein-coupled receptor signals. *J Cell Sci*. **115**, 455–465

30. Peterson, Y. K., and Luttrell, L. M. (2017) The Diverse Roles of Arrestin Scaffolds in G Protein-Coupled Receptor Signaling. *Pharmacol Rev*. **69**, 256–297

31. Ricks, T. K., and Trejo, J. (2009) Phosphorylation of protease-activated receptor-2 differentially regulates desensitization and internalization. *The Journal of biological chemistry*. **284**, 34444–34457

32. Luttrell, L. M., Wang, J., Plouffe, B., Smith, J. S., Yamani, L., Kaur, S., Jean-Charles, P.-Y., Gauthier, C., Lee, M.-H., Pani, B., Kim, J., Ahn, S., Rajagopal, S., Reiter, E., Bouvier, M., Shenoy, S. K., Laporte, S. A., Rockman, H. A., and Lefkowitz, R. J. (2018) Manifold roles of β-arrestins in GPCR signaling elucidated with siRNA and CRISPR/Cas9. *Sci. Signal.* 10.1126/scisignal.aat7650

33. O'Hayre, M., Eichel, K., Avino, S., Zhao, X., Steffen, D. J., Feng, X., Kawakami, K., Aoki, J., Messer, K., Sunahara, R., Inoue, A., Zastrow, M. von, and Gutkind, J. S. (2017) Genetic evidence that β-arrestins are dispensable for the initiation of β2-adrenergic receptor signaling to ERK. *Sci. Signal.* 10.1126/scisignal.aal3395

34. Liggett, S. B. (2011) Phosphorylation Barcoding as a Mechanism of Directing GPCR Signaling. *Sci. Signal.* **4**, pe36–pe36

35. Nobles, K. N., Xiao, K., Ahn, S., Shukla, A. K., Lam, C. M., Rajagopal, S., Strachan, R. T., Huang, T.-Y., Bressler, E. A., Hara, M. R., Shenoy, S. K., Gygi, S. P., and Lefkowitz, R. J. (2011) Distinct phosphorylation sites on the β(2)-adrenergic receptor establish a barcode that encodes differential functions of β-arrestin. *Science Signaling*. **4**, ra51–ra51

36. Yang, F., Yu, X., Liu, C., Qu, C.-X., Gong, Z., Liu, H.-D., Li, F.-H., Wang, H.-M., He, D.-F., Yi, F., Song, C., Tian, C.-L., Xiao, K.-H., Wang, J.-Y., and Sun, J.-P. (2015) Phospho-selective mechanisms of arrestin conformations and functions revealed by unnatural amino acid incorporation and (19)F-NMR. *Nat Commun*. **6**, 8202

37. Sato, T., Kawasaki, T., Mine, S., and Matsumura, H. (2016) Functional Role of the C-Terminal Amphipathic Helix 8 of Olfactory Receptors and Other G Protein-Coupled Receptors. *Int J Mol Sci*. 10.3390/ijms17111930

38. Scheerer, P., and Sommer, M. E. (2017) Structural mechanism of arrestin activation. *Current Opinion in Structural Biology*. **45**, 160–169

39. Hu, J., Wang, Y., Zhang, X., Lloyd, J. R., Li, J. H., Karpiak, J., Costanzi, S., and Wess, J. (2010) Structural basis of G protein–coupled receptor–G protein interactions. *Nature Chemical Biology*. **6**, 541–548

40. Tetsuka, M., Saito, Y., Imai, K., Doi, H., and Maruyama, K. (2004) The Basic Residues in the Membrane-Proximal C-Terminal Tail of the Rat Melanin-Concentrating Hormone Receptor 1 Are Required for Receptor Function. *Endocrinology*. **145**, 3712–3723

41. Feierler, J., Wirth, M., Welte, B., Schüssler, S., Jochum, M., and Faussner, A. (2011) Helix 8 Plays a Crucial Role in Bradykinin B2 Receptor Trafficking and Signaling. *J. Biol. Chem.* **286**, 43282–43293

42. Gehret, A. U., Jones, B. W., Tran, P. N., Cook, L. B., Greuber, E. K., and Hinkle, P. M. (2009) Role of Helix 8 of the Thyrotropin-Releasing Hormone Receptor in Phosphorylation by G Protein-Coupled Receptor Kinase. *Mol Pharmacol*. 10.1124/mol.109.059733

43. Fritze, O., Filipek, S., Kuksa, V., Palczewski, K., Hofmann, K. P., and Ernst, O. P. (2003) Role of the conserved NPxxY(x)5,6F motif in the rhodopsin ground state and during activation. *Proc Natl Acad Sci U S A*. **100**, 2290–2295

44. Angel, T. E., Gupta, S., Jastrzebska, B., Palczewski, K., and Chance, M. R. (2009) Structural waters define a functional channel mediating activation of the GPCR, rhodopsin. *Proceedings of the National Academy of Sciences*. **106**, 14367–14372

45. Lefkowitz, R. J., and Shenoy, S. K. (2005) Transduction of receptor signals by beta-arrestins. *Science*. **308**, 512–517

46. Shukla, A. K., Xiao, K., and Lefkowitz, R. J. (2011) Emerging paradigms of β-arrestin-dependent seven transmembrane receptor signaling. *Trends Biochem Sci*. **36**, 457–469

47. Shapiro, M. J., Weiss, E. J., Faruqi, T. R., and Coughlin, S. R. (2000) Protease-activated receptors 1 and 4 are shut off with distinct kinetics after activation by thrombin. *The Journal of biological chemistry*. **275**, 25216–25221

48. Li, D., D'Angelo, L., Chavez, M., and Woulfe, D. S. (2011) Arrestin-2 Differentially Regulates PAR4 and ADP Receptor Signaling in Platelets. *J. Biol. Chem.* **286**, 3805–3814

49. Lin, Y.-C., Boone, M., Meuris, L., Lemmens, I., Van Roy, N., Soete, A., Reumers, J., Moisse, M., Plaisance, S., Drmanac, R., Chen, J., Speleman, F., Lambrechts, D., Van de Peer, Y., Tavernier, J., and Callewaert, N. (2014) Genome dynamics of the human embryonic kidney 293 lineage in response to cell biology manipulations. *Nature Communications*. **5**, 4767

50. Graham, F. L., Smiley, J., Russell, W. C., and Nairn, R. (1977) Characteristics of a Human Cell Line Transformed by DNA from Human Adenovirus Type 5. *Journal of General Virology,*. **36**, 59–72

51. Vanderboor, C. M., Thibeault, P. E., Nixon, K. C., Gros, R., Kramer, J. M., and Ramachandran, R. (2020) Proteinase-Activated Receptor 4 (PAR4) Activation Triggers Cell Membrane Blebbing through RhoA and β-arrestin. *Mol Pharmacol*. 10.1124/mol.119.118232

52. Rwibasira Rudinga, G., Khan, G. J., and Kong, Y. (2018) Protease-Activated Receptor 4 (PAR4): A Promising Target for Antiplatelet Therapy. *Int J Mol Sci*. 10.3390/ijms19020573

53. Offermanns, S., Laugwitz, K. L., Spicher, K., and Schultz, G. (1994) G proteins of the G12 family are activated via thromboxane A2 and thrombin receptors in human platelets. *Proceedings of the National Academy of Sciences of the United States of America*. **91**, 504–508

54. Olsen, R. H. J., DiBerto, J. F., English, J. G., Glaudin, A. M., Krumm, B. E., Slocum, S. T., Che, T., Gavin, A. C., McCorvy, J. D., Roth, B. L., and Strachan, R. T. (2020) TRUPATH, an open-source biosensor platform for interrogating the GPCR transducerome. *Nature Chemical Biology*. **16**, 841–849

6 Appendices

Appendix 1 Analytical RP-HPLC UV detection chromatograms of synthesized peptides (Chapter 2). Purity of all peptides are > 95% as determined by analytical RP-HPLC UV detection (see traces below).

Ac-AYPGKF-NH_2:

t_R = 10.50 min; gradient = 10% to 50% (solvent A in solvent B, 0 to 10 min)

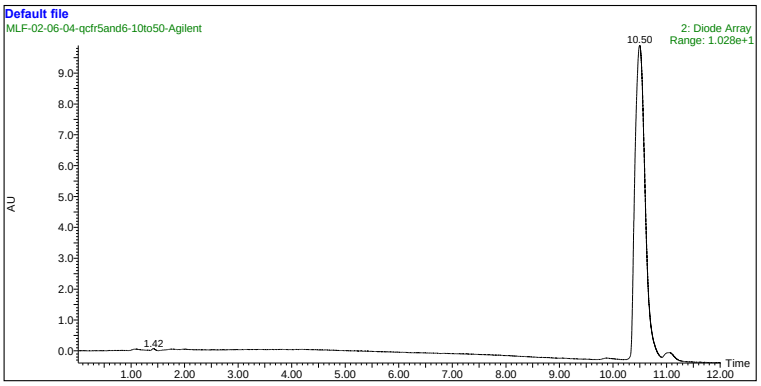

AAPGKF-NH_2:

t_R = 8.08 min; gradient = 10% to 70% (solvent A in solvent B, 0 to 10 min)

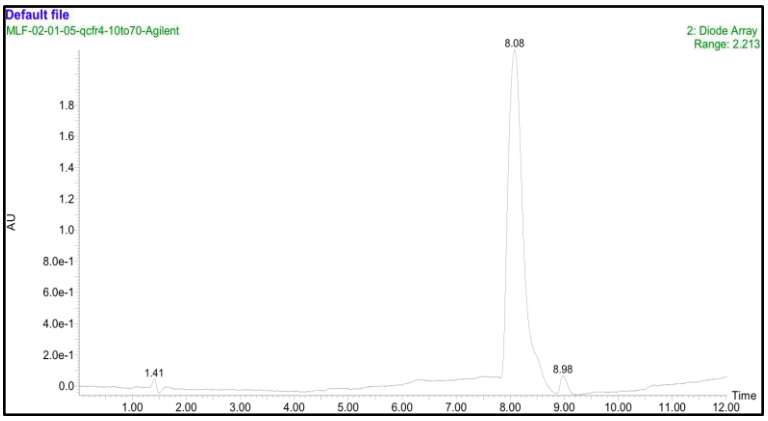

AYAGKF-NH_2:

t_R = 9.14 min; gradient = 10% to 60% (solvent A in solvent B, 0 to 10 min)

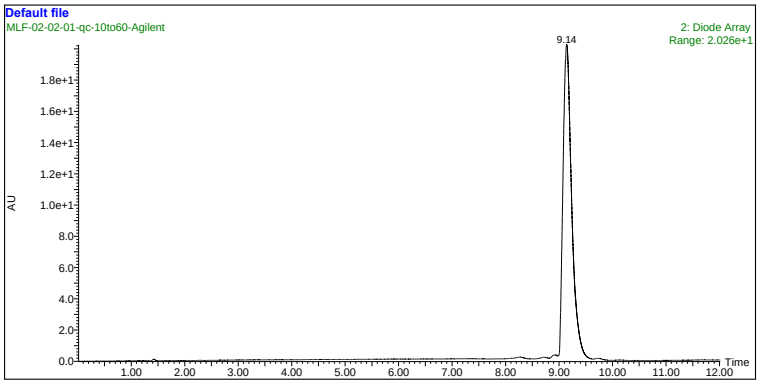

AYPAKF-NH_2:

t_R = 10.53 min; gradient = 10% to 50% (solvent A in solvent B, 0 to 10 min)

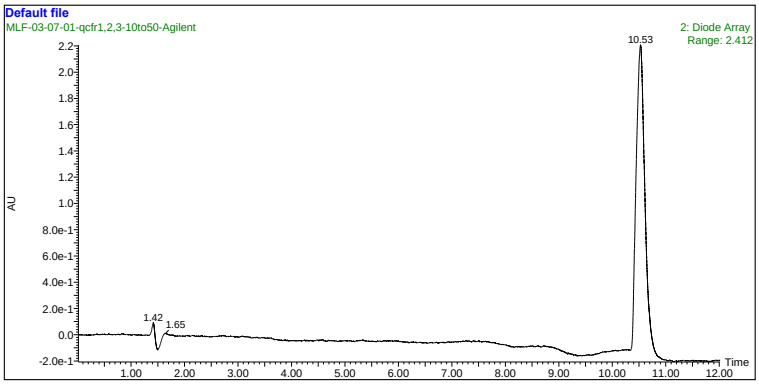

AYPGAF-NH_2:

t_R = 10.83 min; gradient = 10% to 50% (solvent A in solvent B, 0 to 10 min)

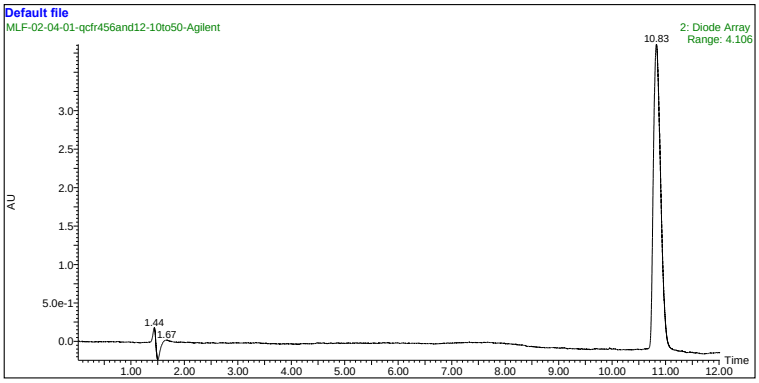

AYPGKA-NH_2:

t_R = 9.71 min; gradient = 5% to 30% (solvent A in solvent B, 0 to 10 min)

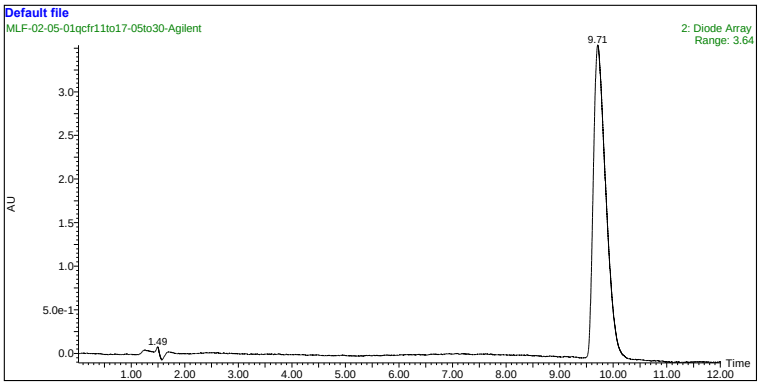

aYPGKF-NH_2:

t_R = 10.06 min; gradient = 10% to 50% (solvent A in solvent B, 0 to 10 min)

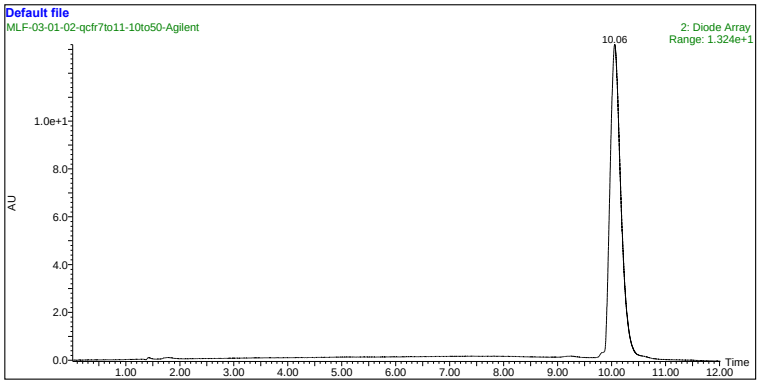

AyPGKF-NH_2:

t_R = 9.49 min; gradient = 15% to 50% (solvent A in solvent B, 0 to 10 min)

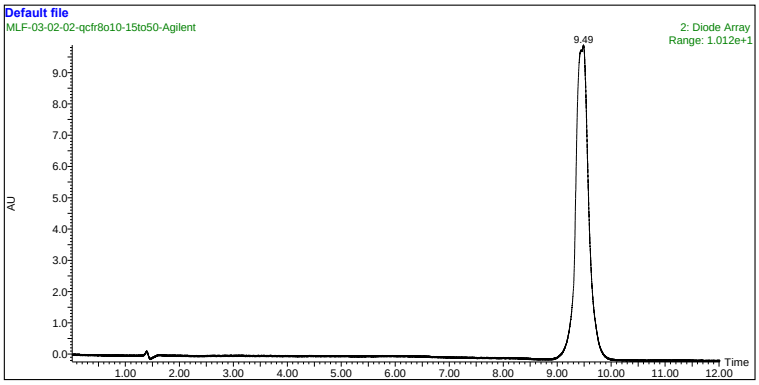

AYPGkF-NH_2:

t_R = 9.17 min; gradient = 10% to 70% (solvent A in solvent B, 0 to 10 min)

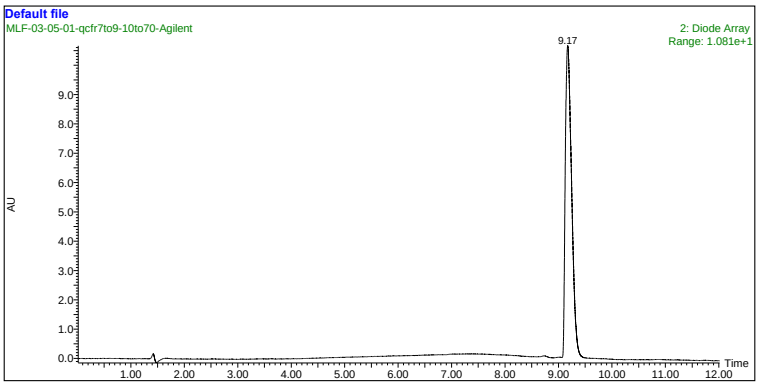

AYPGKf-NH_2:

t_R = 9.04 min; gradient = 10% to 70% (solvent A in solvent B, 0 to 10 min)

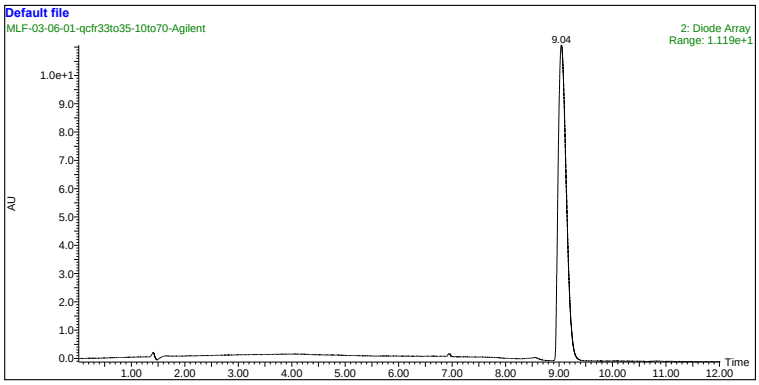

Aib-YPGKF-NH_2:

t_R = 9.35 min; gradient = 10% to 70% (solvent A in solvent B, 0 to 10 min)

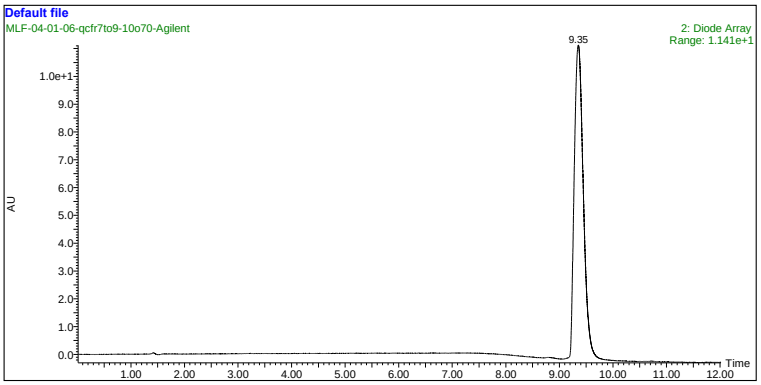

Sar-YPGKF-NH_2:

t_R = 9.23 min; gradient = 10% to 70% (solvent A in solvent B, 0 to 10 min)

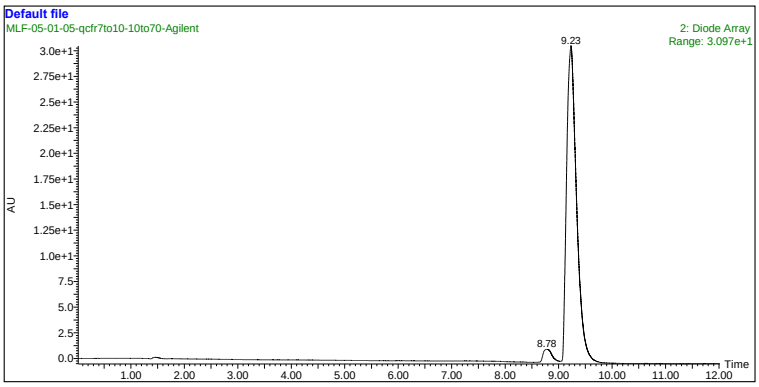

Inp-YPGKF-NH_2:

t_R = 9.26 min; gradient = 10% to 70% (solvent A in solvent B, 0 to 10 min)

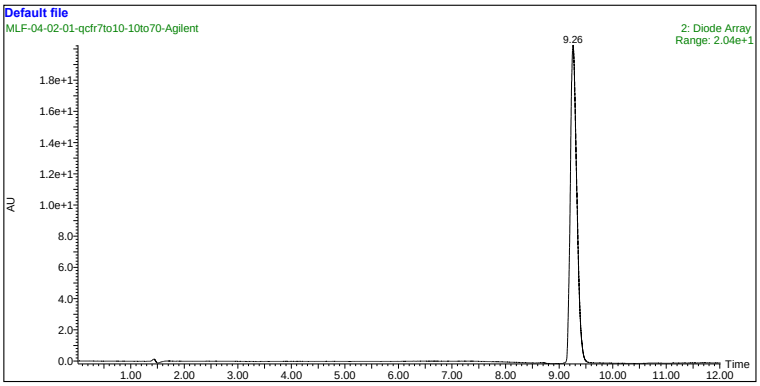

betaAla-YPGKF-NH_2:

t_R = 9.34 min; gradient = 10% to 70% (solvent A in solvent B, 0 to 10 min)

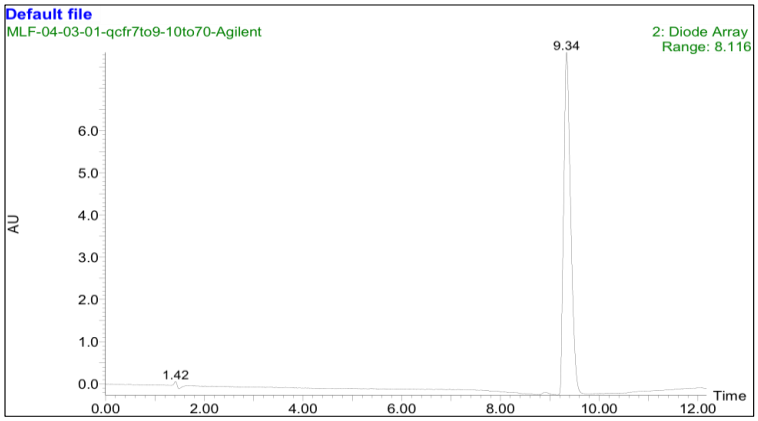

A-Tyr(Me)-PGKF-NH_2:

t_R = 9.57 min; gradient = 13% to 70% (solvent A in solvent B, 0 to 10 min)

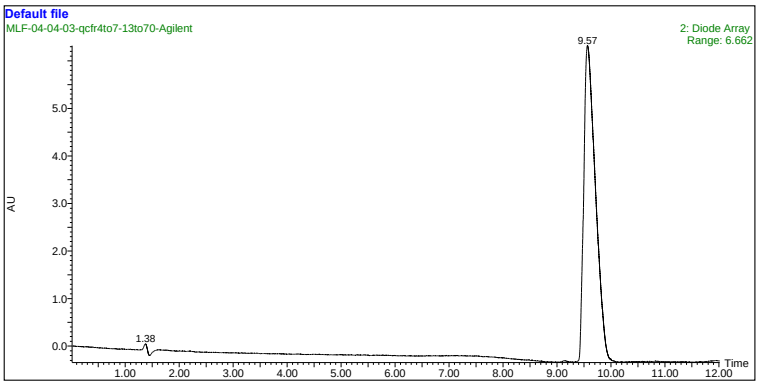

A-F(4-fluoro)-PGKF-NH_2:

t_R = 9.63 min; gradient = 13% to 70% (solvent A in solvent B, 0 to 10 min)

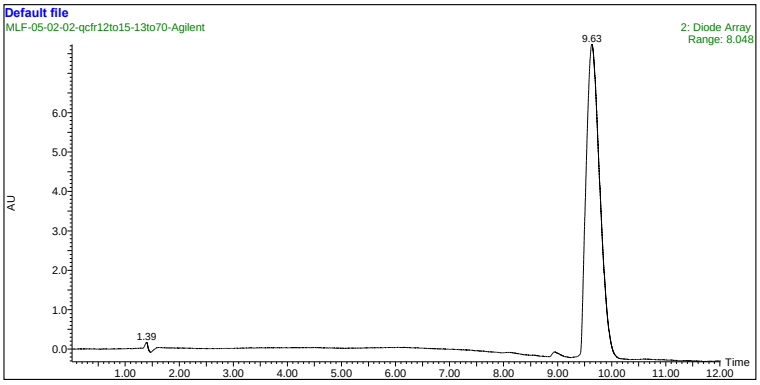

AY-Pip-GKF-NH_2:

t_R = 9.25 min; gradient = 13% to 70% (solvent A in solvent B, 0 to 10 min)

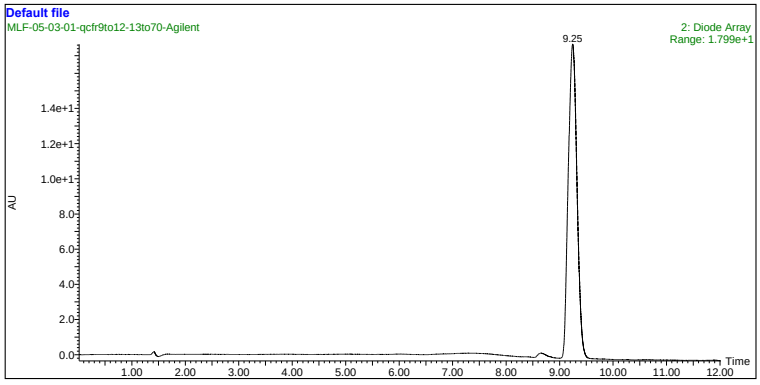

AY-Nip-GKF-NH_2:

t_R = 8.77 min; gradient = 13% to 70% (solvent A in solvent B, 0 to 10 min)

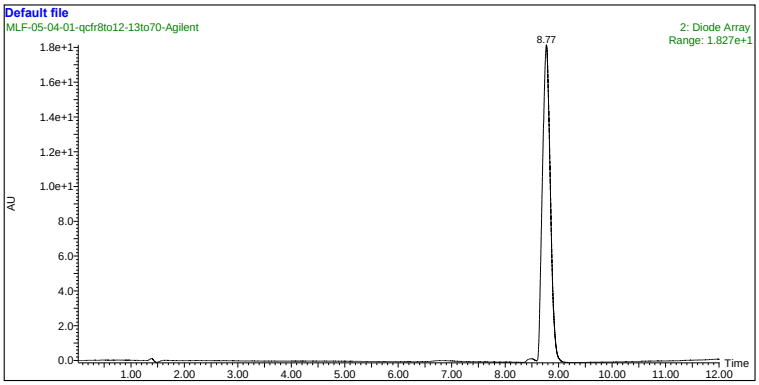

AYP-Sar-KF-NH_2:

t_R = 9.56 min; gradient = 10% to 60% (solvent A in solvent B, 0 to 10 min)

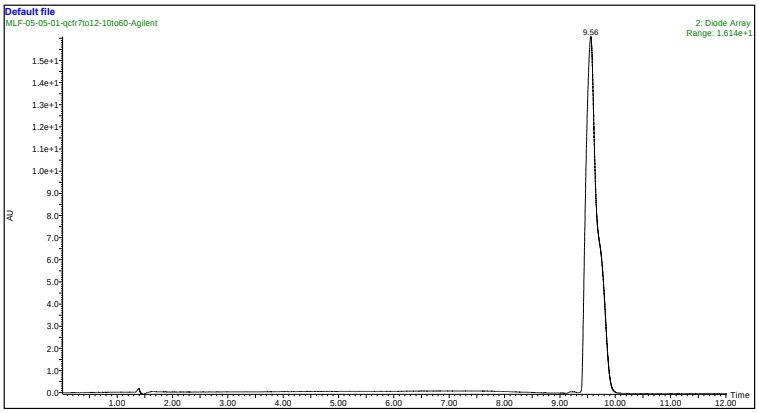

AYP-betaAla-KF-NH_2:

t_R = 9.38 min; gradient = 10% to 70% (solvent A in solvent B, 0 to 10 min)

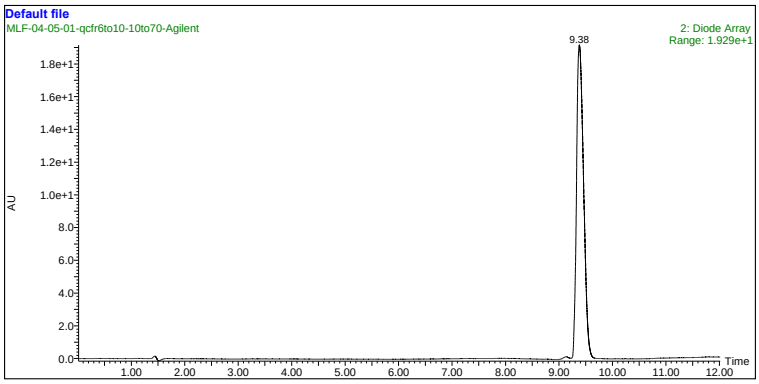

AYPGK-1Nal-NH_2:

t_R = 9.71 min; gradient = 13% to 70% (solvent A in solvent B, 0 to 10 min)

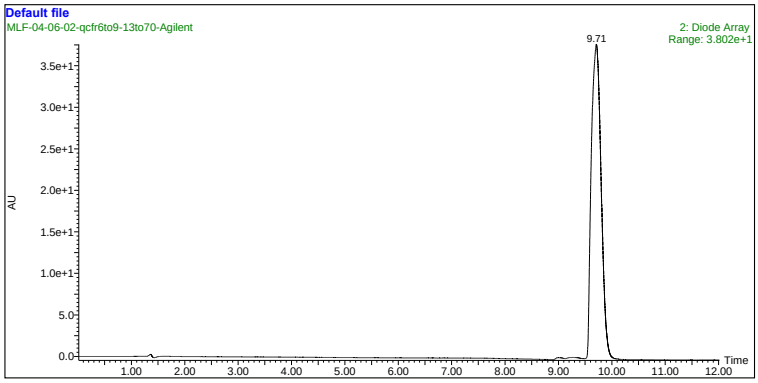

AYPGK-2Nal-NH_2:

t_R = 9.72 min; gradient = 13% to 70% (solvent A in solvent B, 0 to 10 min)

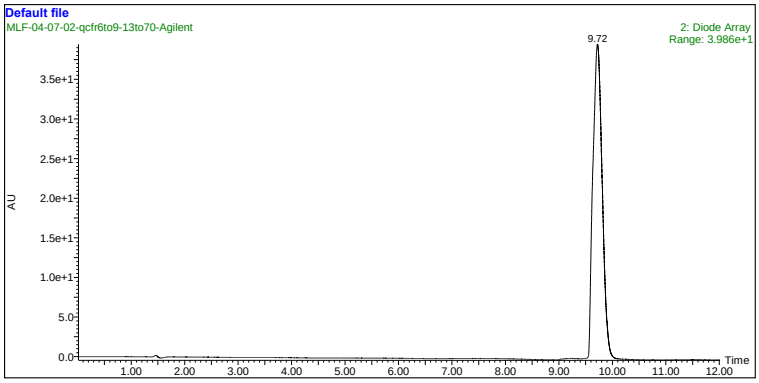

AYPGK-F(4-fluoro)-NH_2:

t_R = 8.91 min; gradient = 13% to 70% (solvent A in solvent B, 0 to 10 min)

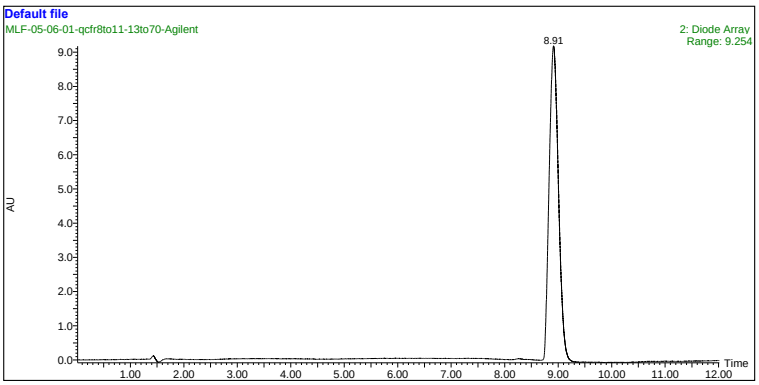

AYPGK-F(4-Me)-NH_2:

t_R = 9.32 min; gradient = 13% to 70% (solvent A in solvent B, 0 to 10 min)

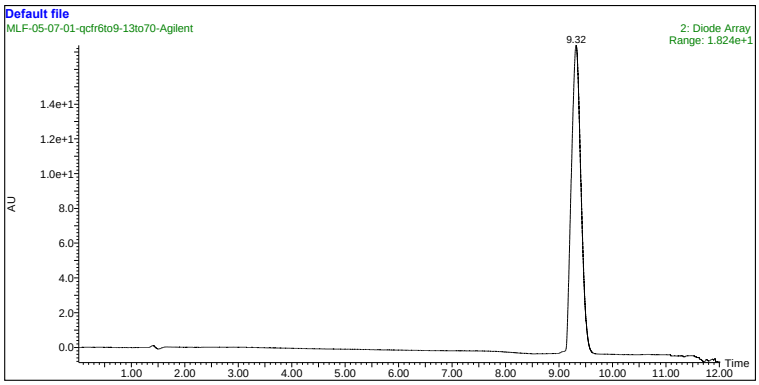

AYpGKF-NH_2:

t_R = 9.02 min; gradient = 12% to 75% (solvent A in solvent B, 0 to 10 min)

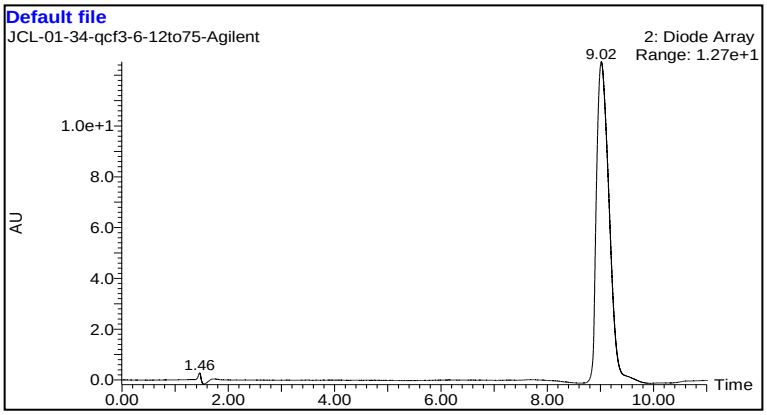

AYPGK-(*N*-Me-F)-NH_2:

t_R = 8.73 min; gradient = 12% to 80% (solvent A in solvent B, 0 to 10 min)

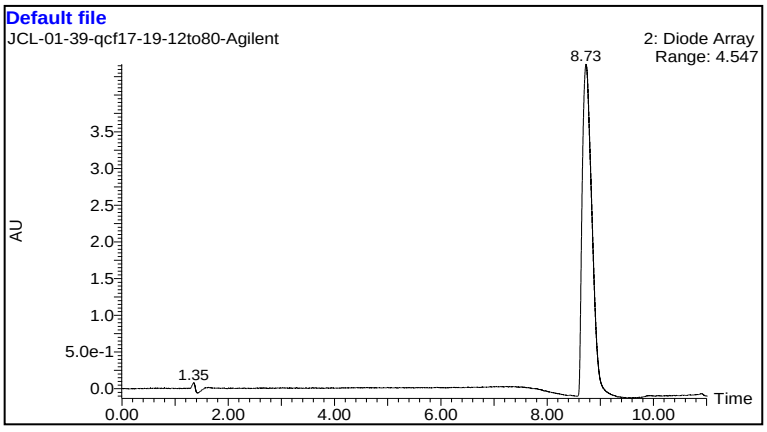

AYPG-(N_α-Me-K)-F-NH_2:

t_R = 8.33 min; gradient = 15% to 70% (solvent A in solvent B, 0 to 10 min)

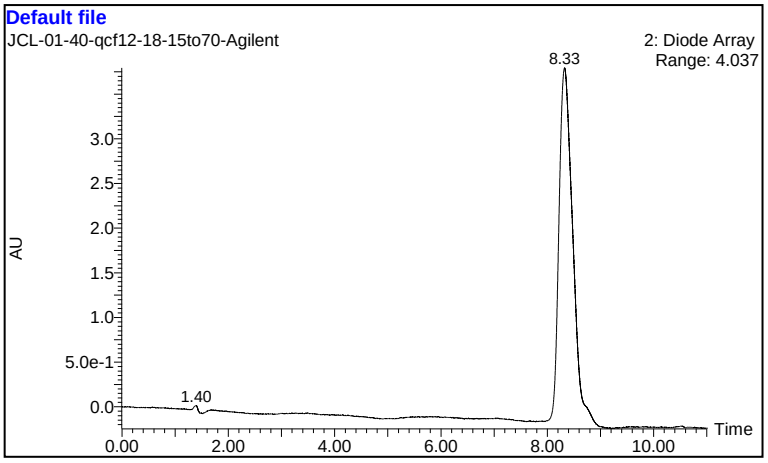

A-(*N*-Me-Y)-PGKF-NH_2:

t_R = 8.74 min; gradient = 12% to 70% (solvent A in solvent B, 0 to 10 min

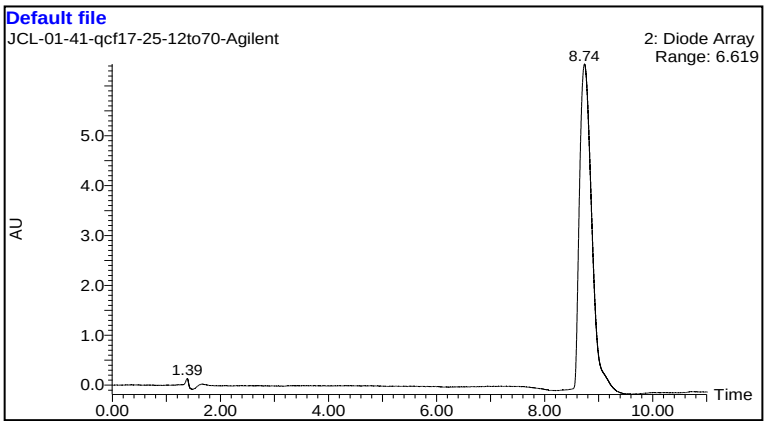

(*N*-Me-A)-YPGKF-NH_2:

t_R = 8.88 min; gradient = 12% to 70% (solvent A in solvent B, 0 to 10 min)

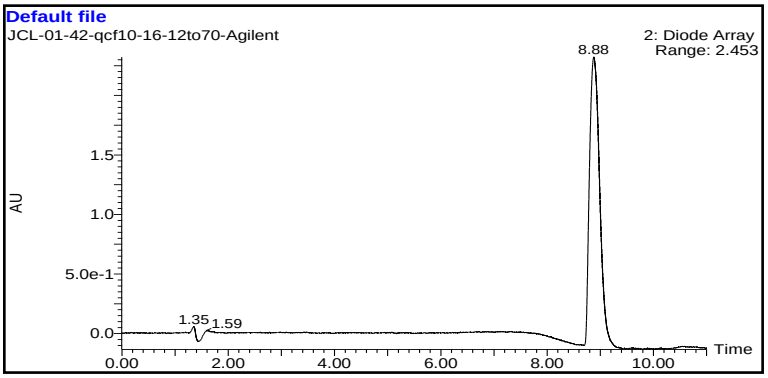

VYPGKF-NH_2:

t_R = 8.90 min; gradient = 12% to 70% (solvent A in solvent B, 0 to 10 min)

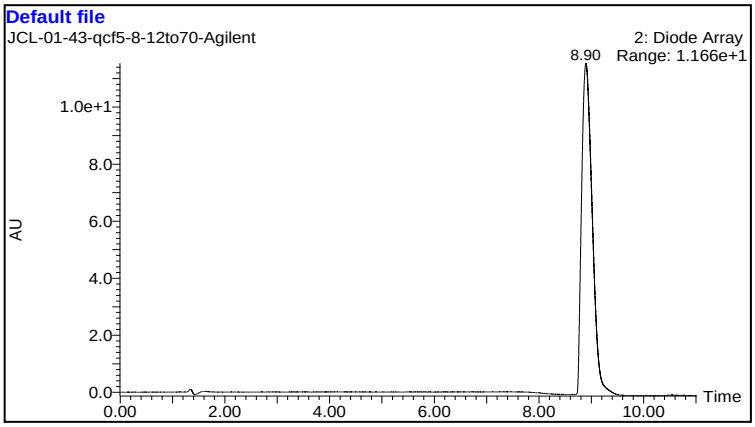

(*N*-Me-S)-YPGKF-NH_2:

t_R = 9.00 min; gradient = 13% to 70% (solvent A in solvent B, 0 to 10 min)

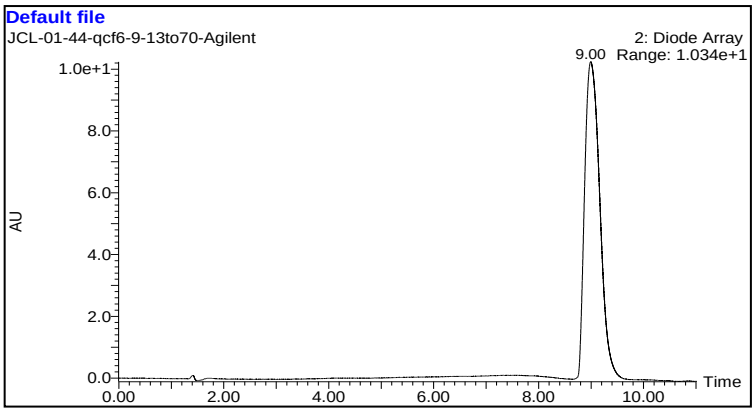

Nle-YPGKF-NH_2:

t_R = 8.88 min; gradient = 15% to 70% (solvent A in solvent B, 0 to 10 min)

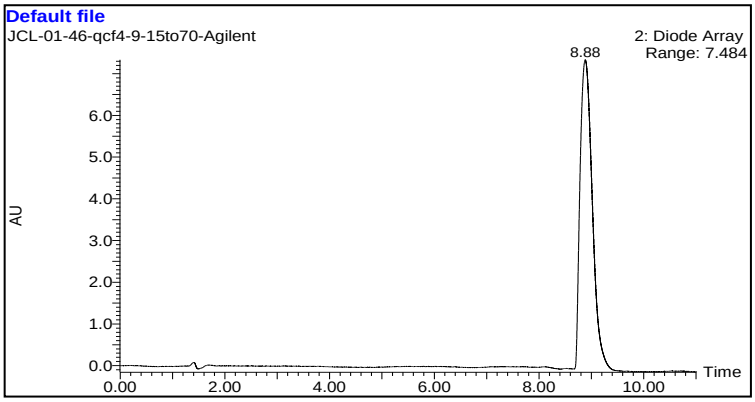

AYPGRF-NH_2:

t_R = 8.73 min; gradient = 13% to 70% (solvent A in solvent B, 0 to 10 min)

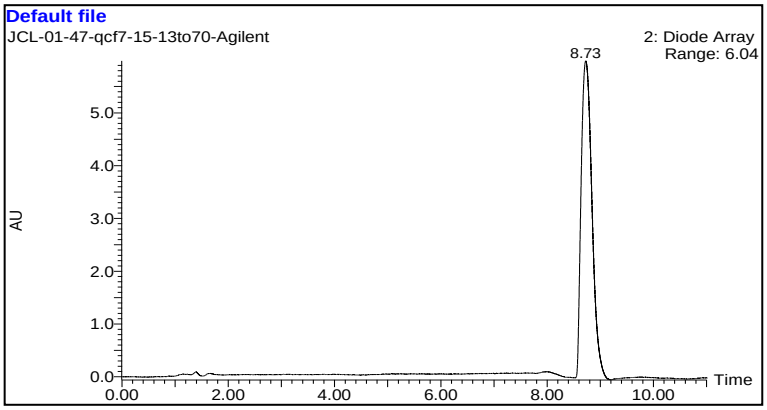

AYPGOF-NH_2:

t_R = 9.16 min; gradient = 12% to 80% (solvent A in solvent B, 0 to 10 min)

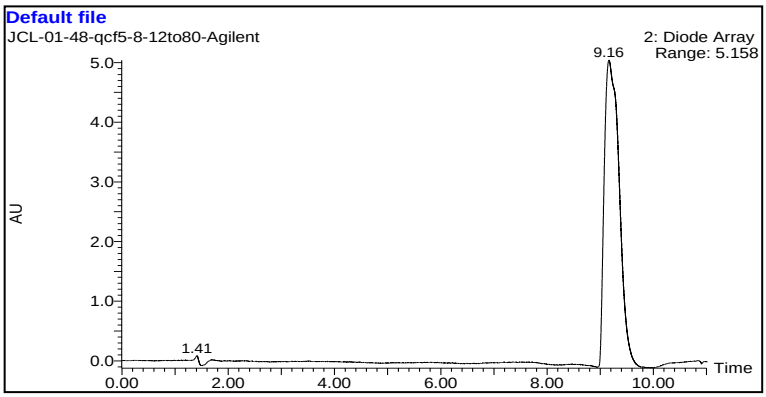

AYPG-Cit-F-NH_2:

t_R = 8.82 min; gradient = 13% to 80% (solvent A in solvent B, 0 to 10 min)

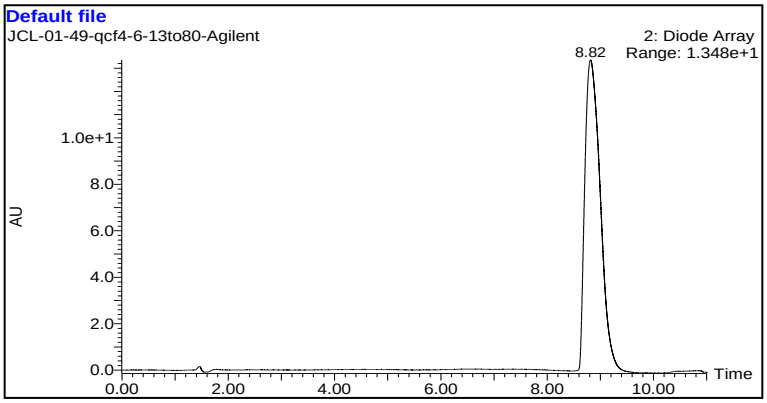

AYPG-(N_ε-Me-K)-F-NH_2:

t_R = 8.74 min; gradient = 12% to 70% (solvent A in solvent B, 0 to 10 min)

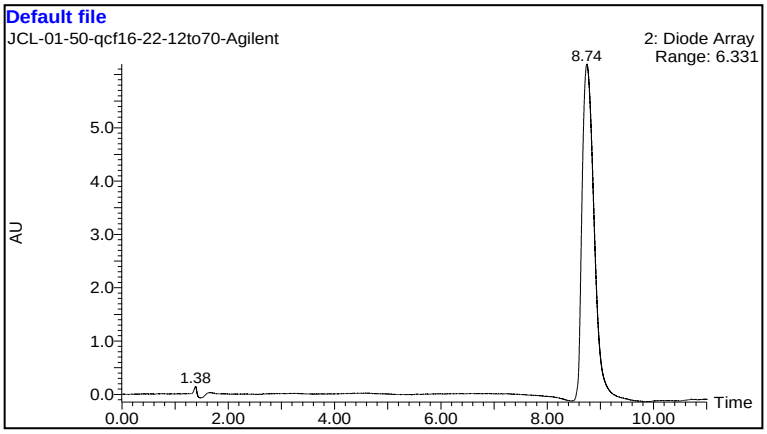

AYPGKY-NH_2:

t_R = 8.88 min; gradient = 8% to 80% (solvent A in solvent B, 0 to 10 min)

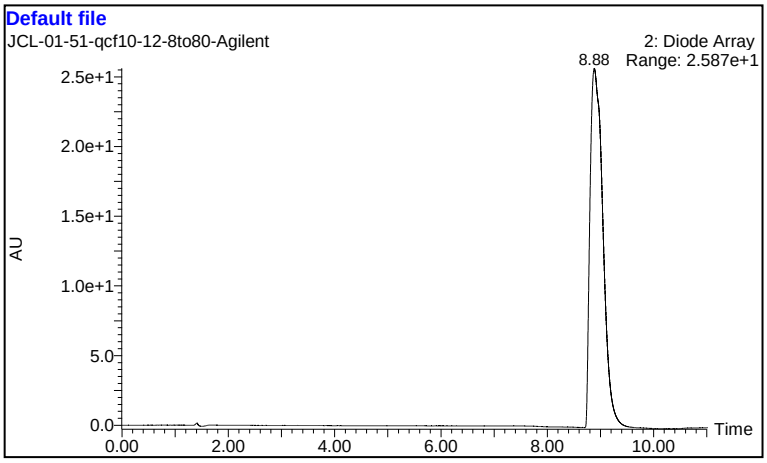

Appendix 2 Curriculum Vitae

EDUCATION

PhD Physiology and Pharmacology (2020), University of Western Ontario

BSc. Honours Medical Science (Honours, 2015), Brock University

Diploma in Music and Musical Theory (2009), Faith College International

PUBLICATIONS

Thibeault, P. E., and Ramachandran, R. (2020) Biased signalling in platelet G-protein-coupled receptors. *Can. J. Physiol. Pharmacol.* 10.1139/cjpp-2020-0149

Thibeault, P. E., and Ramachandran, R. (2020) Role of the Helix-8 and C-Terminal Tail in Regulating Proteinase Activated Receptor 2 Signaling. *ACS Pharmacol. Transl. Sci.* 10.1021/acsptsci.0c00039

Vanderboor, C. M.[1], **Thibeault, P. E.**[1], Nixon, K. C., Gros, R., Kramer, J. M., and Ramachandran, R. (2020) Proteinase-Activated Receptor 4 (PAR4) Activation Triggers Cell Membrane Blebbing through RhoA and β-arrestin. *Mol. Pharmacol.* 10.1124/mol.119.118232 ([1]co-first author)

Thibeault, P. E., LeSarge, J. C., Arends, D., Fernandes, M., Chidiac, P., Stathopulos, P. B., Luyt, L. G., and Ramachandran, R. (2019) Molecular basis for activation and biased signalling at the thrombin-activated GPCR Proteinase Activated Receptor-4 (PAR4). *J. Biol. Chem.* 10.1074/jbc.RA119.011461

Lalonde, T., Hou, J., **Thibeault, P. E.**, Milne, M., Dhanvantari, S., Ramachandran, R., & Luyt, L. G. (2019). Single amino acid replacement in G-7039 leads to a 70-fold increase in binding towards GHS-R1a. *ChemMedchem*, doi:10.1002/cmdc.201900466

LeSarge, J. C., **Thibeault, P.**, Milne, M., Ramachandran, R., & Luyt, L. G. (2019). High affinity fluorescent probe for proteinase-activated receptor 2 (PAR2). *ACS Medicinal Chemistry Letters*, 10(7), 1045-1050. doi:10.1021/acsmedchemlett.9b00094

Ramachandran, R., Mihara, K., **Thibeault, P.**, Vanderboor, C. M., Petri, B., Saifeddine, M., Bouvier, M., & Hollenberg, M. D. (2017). Targeting a proteinase-activated receptor 4 (PAR4) carboxyl terminal motif to regulate platelet function. *Molecular Pharmacology*, 91(4), 287-295. doi:10.1124/mol.116.106526

PUBLICATIONS - ACADEMIC SCHOLARSHIP

Thibeault, P. E., Hollenberg, M. D., & Ramachandran, R. (2020). Proteinase Activated Receptors. *Encyclopedia of Biological Chemistry, 3rd Edition*

Thibeault, P. (2018). Promoting Active Learning in Physiology Lectures Through Student Response Systems: To Click or Not to Click. *Teaching Innovation Projects*, 8(1). https://doi.org/10.5206/tips.v8i1.6220

GRANTS AND AWARDS

- *Canadian Society of Pharmacology and Therapeutics/American Society of Pharmacology and Experimental Therapeutics inaugural travel award ($1600, June 2020)*
- *George W. Stavraky Teaching Award ($1,900; October 2019)*
- *Canadian Society of Pharmacology and Therapeutics Travel award ($350; June 2019)*
- *Queen Elizabeth II, Ontario Graduate Scholarship ($15,000; 2019-2020)*
- *Hari and Gudrun Sharma Graduate Award ($1900; October 2018)*
- *Poster award - Basic and Clinical Pharmacology ($200; October 2018)*
- *World Congress of Pharmacology conference bursary for oral presenters (50,000 JPY; July 2018)*
- *American Society of Pharmacology and Experimental Therapeutics Trainee Travel Award ($3000 USD; July 2018)*
- *K.M. Piafsky Trainee Presentation Award ($400; May 2018)*
- *Canadian Society of Pharmacology and Therapeutics Travel award ($350; May 2018)*
- *Peter Dresel Trainee Presentation Award ($400; May 2017)*
- *Canadian Society of Pharmacology and Therapeutics Travel award ($450; May 2017)*
- *Queen Elizabeth II, Ontario Graduate Scholarship ($15,000; 2017-2018)*
- *Western Graduate Research Scholarship (2015-Present)*

TEACHING EXPERIENCE

Teaching Assistant Roles

- MEDSCIEN 4931G, Summer 2020 – Selected Topics in Medical Sciences (online)
- PHYS 1020, Fall/Winter 2019-2020 – Human Physiology (blended)
- MEDSCIEN 4931G, Summer 2019 – Selected Topics in Medical Sciences (online)
- PHYS 1020, Fall/Winter 2018-2019 – Human Physiology (blended)
- MEDSCIEN 4931G, Summer 2018 – Selected Topics in Medical Sciences (online)
- PHYS 1020, Fall/Winter 2017-2018 – Human Physiology (blended)
- MEDSCIEN 4931G, Summer 2017 – Selected Topics in Medical Sciences (online)
- PHYS 1020, Fall/Winter 2016-2017 – Human Physiology (blended)
- PHYS 3130Z, Fall/Winter 2015-2016 – Physiology Laboratory

Assessment-Only Roles

[MEDICINE, Undergraduate Medical Education; second number denotes medical school year (i.e. 51xx, year 1; 52xx, year 2, etc.); typical enrollment 170 students]

- MEDICINE 5402, Summer 2020 – Integration and Transition
- MEDICINE 5250, Fall/Winter 2019-2020 – Medical Ethics
- MEDICINE 5210S, Fall/Winter 2019-2020 – Key Topics in Family Medicine
- MEDICINE 5402, Fall/Winter 2019-2020 – Integration and Transition
- *MEDICINE 5210S, Fall/Winter 2018-2019 – Key Topics in Family Medicine*
- *MEDICINE 5250, Fall/Winter 2018-2019 – Medical Ethics*
- *MEDICINE 5402, Fall/Winter 2018-2019 – Integration and Transition*
- *MEDICINE 5210S Fall/Winter 2017-2018 – Key Topics in Family Medicine*
- *MEDICINE 5250 Fall/Winter 2017-2018 – Medical Ethics*
- *MEDICINE 5151 Fall/Winter 2016-2017 – Social Medicine*
- *MEDICINE 5475 Fall/Winter 2015-2016 – Clinical Clerkship*
- *MEDICINE Principals of Medicine I*

LEADERSHIP EXPERIENCE

Chair, Grad Club Committee, Society of Graduate Students *2018-2020*

Research Committee, Graduate Student Representative *2017-2020*

Society of Graduate Students, Physiology & Pharmacology Councillor *2018-2020*

Chair, Financial Assistance Committee, PSAC 610 *2018-2020*

Member, Grad Club Committee, Society of Graduate Students *2016-2018*

Brock University Student Administrative Council, Councillor F.A.H.S. *2014-2015*

PRESENTATIONS

- National Conference: "Functional role of C-terminal tail and Helix-8 residues on signalling and regulation of the thrombin-activated GPCR, Proteinase Activated Receptor 4 (PAR4)" (virtual poster), "Canadian Society of Pharmacology and Therapeutics Annual Meeting". June 10-12, 2020
- International Conference: "Molecular Basis for Activation and Biased Signalling at the Platelet Thrombin Receptor Proteinase Activated Receptor-4 (PAR4) (poster), "20th Annual Great Lakes GPCR Retreat", Bromont, QC, Canada. September 26-28, 2019
- National Conference: "Proteinase Activated Receptor 4 (PAR4) agonist peptide structure and dynamics elucidated by solution NMR and computational simulations" (poster), "Canadian Society of Pharmacology and Therapeutics Annual Meeting", Calgary, Alberta, Canada. June 12-14, 2019
- International Conference: "Determination of the Proteinase Activated Receptor 4 (PAR4) agonist binding site through in-silico modeling and site directed mutagenesis." (Invited oral presentation and poster), "19th Annual Great Lakes GPCR Retreat", Detroit, Michigan, USA. October 25-27, 2018
- International Conference: "Insights into Proteinase Activated Receptor 4 (PAR4) Trafficking, Signalling, and Biased Agonism" (Invited oral presentation), "World Congress of Pharmacology", Kyoto, Japan. July 1-6, 2018
- National Conference: "Insights into Proteinase Activated Receptor 4 (PAR4) Trafficking and Biased Agonism" (Invited oral presentation and poster), "Joint Annual Meeting of the Canadian Society of Pharmacology and Therapeutics (CSPT), The Canadian Society of Pharmaceutical Sciences (CSPS), and Canadian Chapter of the Controlled Release Society (CC-CRS)", Toronto, ON, Canada. May 22-25, 2018
- International Conference: "Proteinase Activated Receptor 4 (PAR4) Biased Agonism" (poster), "18th Annual Great Lakes GPCR Retreat ", Ottawa, ON, Canada. October 19-21, 2017
- Departmental research focus group "Proteinase Activated Receptor 4 (PAR4): Characterizing a non-canonical GPCR" (invited oral presentation), Cardiovascular Journal Club, London, ON, Canada. September 27, 2017
- National Conference: "Role of the C-terminal tail in regulating Proteinase Activated Receptor (PAR)-2 signalling" (poster), "Canadian Society of Pharmacology and Therapeutics Annual Meeting", Halifax, N.S., Canada. June 14-16, 2017
- Local Conference: "Proteinase Activated Receptor 4 (PAR4) Internalization and Trafficking" (platform presentation), London Health Research Day, London, Ontario, March 28, 2017
- International Conference: "Internalization and Trafficking of Proteinase Activated Receptor 4 (PAR4) by clathrin-mediated endocytosis" (poster), "Pharmacology 2016", London, England, U.K. December 13-15, 2016

- Institutional Conference: "Proteinase Activated Receptor 4 (PAR4) Internalization- Role for C-terminal tail motifs and beta-arrestin recruitment" (poster), PHYS/PHARM Research Day, London, ON, Canada. November 1, 2016
- International Conference: "Proteinase Activated Receptor 4 (PAR4) Internalization- Role for C-terminal tail motifs and beta-arrestin recruitment" (poster), "17th Annual Great Lakes GPCR Retreat", Chicago, IL, USA. October 13-16, 2016
- Local Conference: "Investigating the role of Beta-arrestin1/2 in Proteinase Activated Receptor 4 (PAR4) Internalization" (Top 100 poster), London Health Research Day, London, ON, Canada. March 29, 2016

CONFERENCE ATTENDANCE

- Annual Meeting 2020, Canadian Society of Pharmacology and Therapeutics, Virtual
- Great Lakes G-protein coupled receptor Retreat 2019, Bromont, QC., Canada
- Annual Meeting 2019, Canadian Society of Pharmacology and Therapeutics, Calgary, AB., Canada
- London Health Research Institute- Research Day 2019 (judge)
- Great Lakes G-protein coupled receptor Retreat 2018, Detroit, MI., U.S.A
- World Congress of Pharmacology 2016, Kyoto, Japan
- CSPT, CSPS, and CC-CRS Joint Annual Meeting 2018, Toronto, ON, Canada
- London Health Research Institute- Research Day 2018 (judge)
- Great Lakes G-protein coupled receptor Retreat 2017, Ottawa, ON., Canada
- Annual Meeting 2017, Canadian Society of Pharmacology and Therapeutics, Halifax, Canada
- London Health Research Institute- Research Day 2017
- Pharmacology 2016, British Pharmacological Society, London, England, U.K.
- Great Lakes G-protein coupled receptor Retreat 2016, Chicago, IL., U.S.A.
- London Health Research Institute- Research Day 2016
- Great Lakes G-Protein Coupled Receptor Retreat 2015, Mono, ON., CAN.

PROFESSIONAL DEVELOPMENT

- Certificate in Undergraduate Teaching and Learning (University of Western Ontario)
- Graduate Program Review (Microbiology and Immunology)- Invited graduate member